New Concepts in Polymer Science

Thermal Stability of Engineering Heterochain Thermoresistant Polymers

E.V. Kalugina, K.Z. Gumargalieva and G.E. Zaikov

///VSP///

UTRECHT • BOSTON - 2004

VSP
an imprint of Brill Academic Publishers
P.O. Box 346
3700 AH Zeist
The Netherlands

Tel: +31 30 692 5790
Fax: +31 30 693 2081
vsppub@brill.nl
www.vsppub.com
www.brill.nl

First published in 2004

ISBN 90-6764-417-X

Library of Congress Cataloging-in-Publication Data

A CIP record for this book is available from the Library of Congress

Printed in The Netherlands by Ridderprint bv, Ridderkerk.

CONTENTS

INTRODUCTION

The development of special machinery, aircraft and missile engineering, and automotive industry brought up the task of creating heat-resistant polymeric materials before chemistry of high-molecular compounds. By now manufacturing of articles by press molding or extrusion is one of the most effective and progressive methods. Therefore, polymeric materials must possess thermoplastic property.

In recent decades, the achievements in chemistry of high-molecular compounds are associated with creation of several polycondensation polymers, which combine aromatic, carbo- and heterochain groups with aliphatic branches in their structure. On the one hand, high softening temperatures which usually fall above 250 – 350°C represent an important positive feature of these compounds. It indicates the shape stability of even unfilled polymers in articles up to 200 - 300°C or even higher. On the other hand, closeness of the melting point and the start of degradation hamper processing of these materials. Therefore, of importance becomes stabilization of heat-resistant polymers at increased processing temperatures, usually falling in the range of 300 - 400°C. Hence, the traditional task of polymer stabilization during long-term operation (currently, also at increased temperatures) is actual still. Development of these tasks requires implementation of a set of studies which include:

- Detection of thermally labile or defect structures in macromolecules;
- Determination of acceptable content of primary and process additives in the polymer;
- Setting the upper temperature border of processing, above which degradation makes problems with the final product quality or abruptly decreases sanitary-hygienic conditions of processing;
- A set of data for making sanitary-chemical passports for processing of polymeric materials: identification and quantitative analysis of volatile products extracted in the processing cycle;
- Estimation of operation property changes of polymeric materials at aging and forecasting of temperature-time criteria of operation (durability).

Such applied setting of the problem allows posing of definite requirements to raw materials and production process, which provide the

complex of properties or the "quality" of the polymeric material, and setting the operational life of the articles. Hence, more detailed approach to the problem is possible: thermal transformations are based on chemical reactions of macromolecules initiated by heat and active chemical agents present in the environment, mainly, air oxygen (a special case, the so-called physical aging). The study of chemistry (the mechanism) of thermal transformations of macromolecules is not the point of fundamental sciences. They are highly applicable, because understanding of the mechanism defines the possibility of effect or control – currently, deceleration (stabilization) or acceleration (ecological self-elimination or industrial processing of polymeric waste) of polymer destruction. Of high importance are hydrocarbon (carbochain) and vinyl chloride derived polymers. The fundamental studies of degradation of these polymers, developed in the framework of chemical kinetics [1 – 5] and united in monographs [4 – 22], have indicated the methods of thermal and thermal oxidative stabilization, mostly using additives. For the main elementary reactions, the classical kinetic problem of the "structure – reactivity" type is solved via additives inhibiting the radical-chain process. This created a wide range of effective stabilizers for polyolefins and PVC in the world industrial production scope equal hundred thousand tons at 5% annual increase of production [23]. The modern stabilizing compositions have drastically improved stability of carbochain polymers and PVC at processing that allowed realization of highly effective processing modes and significant increase of the operational life of polymeric materials in articles.

The new phase in studying degradation and stabilization of polymers was started over 20 years ago. Primarily, it concerned the so-called engineering or construction thermoplastic polymers (thermoplasts), the overwhelming majority of which represent heterochain polymers. Since 1985 till 2000, the part of these polymers in the total volume of materials, including metals, increased from 5 to 20%, which may potentially increase to 40% [24]. The most rapid development is observed for the so-called high-temperature or heat-resistant polymers, the production scope of which in the period of 1986 – 2002 was increased by 14%. The highest raise was observed for polyester ketones – 27%, polyester sulfones, polysulfones and polyester imides – 21%, liquid-crystal polymers – 25%, aromatic and aliphatic-aromatic polyamides – 7%. Up to 60% of high-temperature engineering plastics are applied in hi-tech branches of industry - electronics and aerospace industry. For instance, the Boeing Company experts estimated reduction of the cost price by 90% weight of articles by 30% as replacing aluminum by modern composites (the so-called advanced polymer composites – APC) in the aircraft building industry.

Engineering polymers are subject to thermal impacts during their life: short-term when synthesized and processed and long-term during operation. Seemingly, the situation is similar to the well-known polyolefins, styrene, acrylic and vinylchloride polymers. However, thermal loads on technological polymers in both phases are much higher, which is illustrated in Figure 1. Here the abscissa axis represents processing temperature of polymer molding or extrusion, and the axis of ordinates gives temperature resource of polymer work capacity, characterized by the known UL parameter (where UL is the Temperature Index) [25]. Therefore, the following tendency is obvious: polymers with higher UL-indices are usually processes at higher temperatures. The formal tendency indicates the fundamental dependence of thermal stability on structure: the more rigid aromatic structure of a polymer is, the higher its thermal stability is. The fundamental experience obtained in the science (chemical physics) on the polymer aging at the previous stage of studying mostly hydrocarbon polymers prompts a complex of interrelated physical and chemical mechanisms defining kinetics of degradation of solid and melted aromatic polymers.

However, mechanical transfer of the known degradation schemes, for example, thermal oxidation, on aromatic polymers is not unambiguous: π- and n,π-systems differ from σ-systems in their electrical and magnetic properties, and electron excitation levels in them are much lower. It is commonly known from the classical kinetics [1] that differences in electron structures affect reactivity of aromatic and aliphatic molecules both qualitatively (different mechanisms) and quantitatively (kinetically). Therefore, further development of science on degradation and stabilization requires experimental study of degradation behavior of new polymeric structures. Naturally, there are also purely applied reasons for such investigations.

Technological polymers may conditionally be divided into two groups.

The first group is represented by heterochain aliphatic and aromatic polymers with relatively low processing and operation temperatures: polyacetals, aliphatic polyamides, PET, poly(butylene terephthalate), polycarbonate. The phenomenology of thermal and thermal oxidative degradation of these polymers is studied quite well. The applied thermal stabilization of these polymers is definitely different from classical antioxidant compositions; therefore, its successful development is generally based on the empirical experience rather than on the understanding of the degradation and inhibition mechanism.

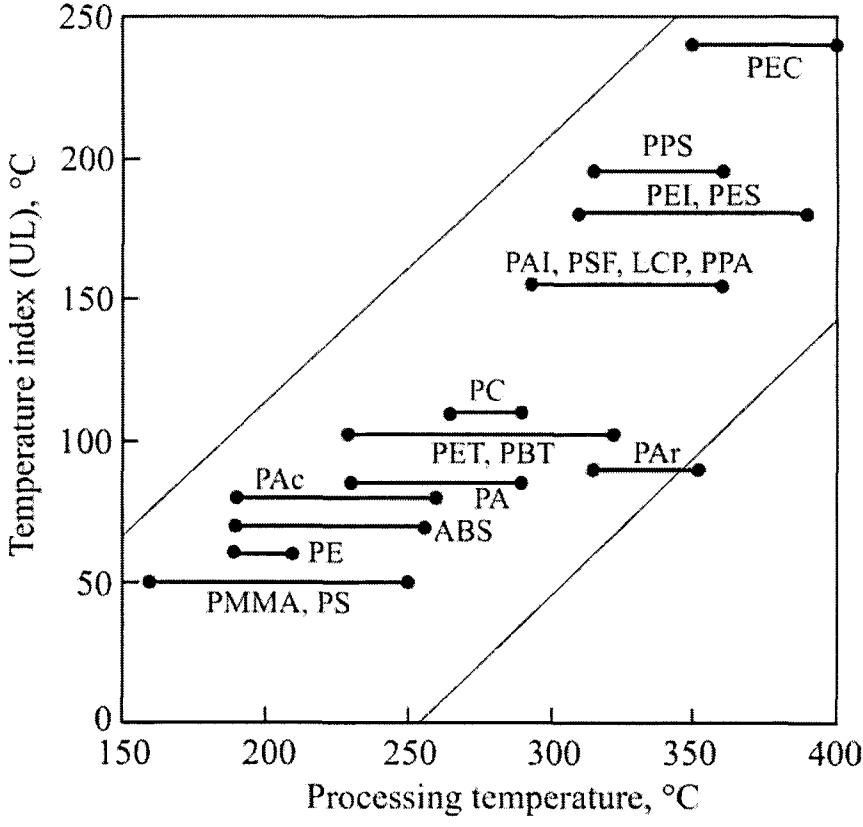

Figure 1. The upper temperature boundary of long-term operation (according to UL temperature indices [25]) and temperatures of polymer processing (beside the known abbreviations PA, PMMA and PE, the following are used: PSF – polysulfones; PPS – polyphenylene sulfide; PEK – polyester ketone; PAI – polyalkanimide; PEI – polyester imide; PES – polyester sulfone; PBT – poly(butylene terephthalate); PAr – polyarylates; PAc – polyacetals; LCP – liquid-crystal polyesters; PPA – polyphthalamides; etc.)

The second group is composed of the so-called heat resistant and high-heat-resistant polymers – polysulfones, polyester ketones, liquid-crystal aromatic polyesters, fatty-aromatic and aromatic polyimides and polyamides, polyester imides, and other polyheteroarylenes. These polymers are processed under rigid temperature conditions (300 - 400°C) and long operated at 150 – 300°C with respect to the structure type. Intense studies of thermal behavior of

polyheteroarylenes were initiated in 1970's – the early 1980's [25 – 28]. Apparently, this was associated with intensive introduction of these polymers in aerospace technologies. Though degradation transformation mechanisms in aromatic systems are still ambiguous, high-temperature antioxidant stabilization of some polyheteroarylenes was successfully realized [26, 29 – 32], and even hypotheses were advanced about the stabilizing action mechanism, principally different from the mechanism of non-chain inhibition [33] considered as the universal mechanism of high-temperature stabilization.

However, degradation behavior of the group of thermoplasts, usually named as heat-resistant engineering polymers (HRP) - polysulfones and polyester sulfones, fatty-aromatic polyimides and polyester imides, polyester ketones, and liquid-crystal polymers, etc. – is not well studied yet. These polymers are designed as hi-tech construction materials, mostly for electronics, energy and vehicle machine industry [34]. Though temperature boundary for long-tern operation of these polymers (about 200 - 250°C) is not so high as for fully aromatic polyheteroarylenes, increased thermal stability and other properties, as well as relative (compared with polyheteroarylenes) economical efficiency of manufacturing and processing form the optimal set of properties, owing to which HRP are intensively developed at present and will being developed in future. Nevertheless, problems of HRP thermal stability, specifically during processing, when the material "quality" is established, are of particular character due to developing technology of HRP manufacturing. This circumstance as well as the deficiency of information about thermal transformations of HRP in the literature stimulated writing of this monograph.

The book is intended to cover questions interesting to a wide range of specialists working in the branch of synthesis, processing and application of plastics.

Chapter 1. Degradation of aliphatic-aromatic polyimides – polyalkanimides

Polyalkanimides (PAI) are fatty-aromatic polymers derived from aliphatic, usually linear diamines and tetracarboxylic aromatic acids.

For the first time PAI were synthesized in 1955 by polycondensation in melt of pyromellitic acid and C_7 and C_9 diamines [36]. In the former USSR, Academician V.V. Korshak *et al.* were the first who synthesized PAI by the one-stage high-temperature polycondensation in solution [37]. The studies of PAI properties, derived from 3,3'4,4'-diphenyl tetracarboxylic, 3,3'4,4'-diphenyloxide tetracarboxylic, and 3,3'4,4'-diphenylsulfone tetracarboxylic acids, as well as on pyromellitic acid and C_6 and C_8 diamines indicated the prospect of PAI application as heat-resistant construction fiber polymers and the binder for abrasion tools.

Industrial development of PAI was determined by the increase of industrial demand in heat-resistant wire insulation. Experts of Raychem Company tested many polymers, including polycarbonate and polysulfone. The results of these investigations gave raise to design of technology and organization of manufacturing PAI derived from pyromellitic anhydride and dodecamethylene diamines or tridecamethylene diamines. These PAI possess high hardness number at room temperature, are strong at temperatures above 150°C, and may be effectively processed by extrusion. In 1970's, Raychem Company already produced a great variety of wires with insulation from PAI [38 – 40], PAI-based films and fibers, and construction materials of *Polyimidal* and *Poly-X* trademarks for the automobile industry. Rohm und Haas GmbH produces PAI derived from dodecamethylene diamine under *Kamax 201* and *Kamax 301* trademarks [43]. In Russia, pilot production of PAI and composite glass-filled materials derived from them is also realized.

Chemical structure of PAI with variable fatty chain length is the following:

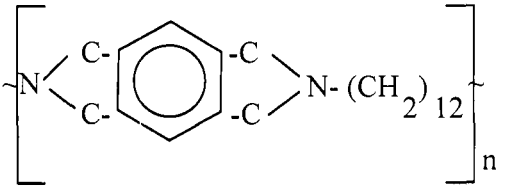

It provides the variety of macromolecule packing in polymeric body; therefore, homological sequences of PAI became the object of many X-ray diffraction studies which, besides works on synthesis, gave a large volume of fundamental publications on PAI also concerning degradation transformations [37, 44, 45, 47 – 49].

From applied positions, in the PAI family polydodecamethylene pyromellitimide (PAI-12) attracts attention due to its excellent physical and mechanical, heat physical and dielectric properties [50 – 52]. In the sequence of engineering thermoplasts, PAI-12 is considered as material for electrotechnical purposes, having the working temperature range of 150 - 200°C. As is indicated by "UL – temperature indices", PAI are present in the same sequence with polysulfones.

PAI-12 (hereinafter, PAI, if not compared with different polyalkanimides) is synthesized in sequence by polycondensation of dodecamethylene diamine and pyromellitic dianhydride in N-methylpyrrolidone solutions at 40 - 50°C, further polyamidoacid cyclization at 150°C, separation of precipitated polymer with the cyclization degree over 90% (IR-spectroscopy data on the ratio of absorption bands at 1780 and 1720 cm^{-1}), and then powder washing and drying.

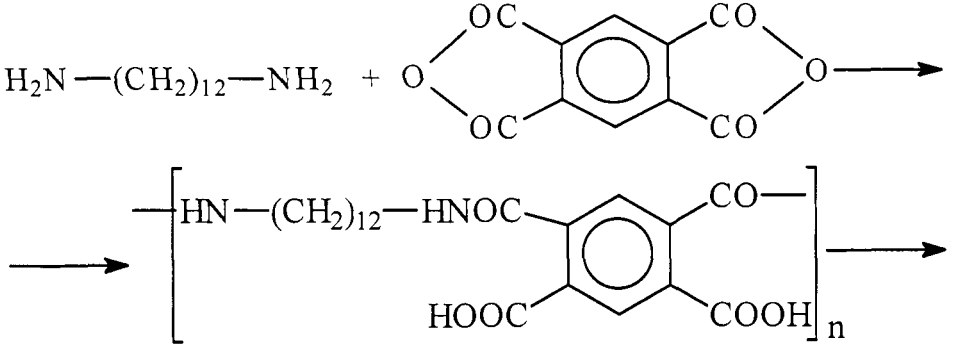

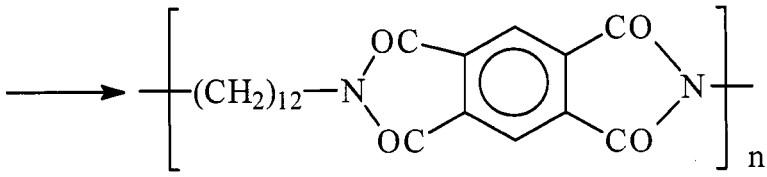

Polycondensation in amide solvent proceeds through formation of intermediate salts of the following structure:

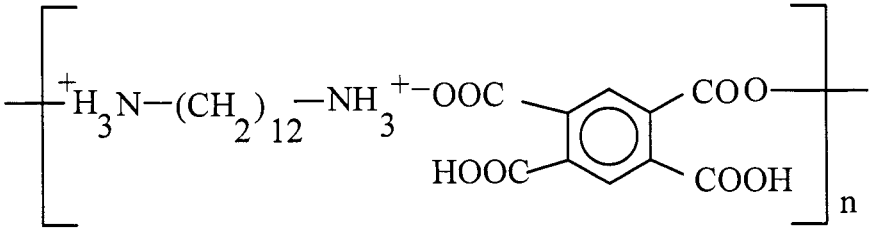

which was determined with the help of IR-spectra and potentiometric titration technique [54]. Studies of condensation in model systems, for example, phthalic anhydride – lauryl amine or pyromellitic acid – lauryl amine ones, also indicated possible formation of di-, tri- and tetrasalts at a single aromatic ring which, in turn, indicated quite high reactivity of all carboxylic groups at the aromatic ring. At polycondensation appropriate group reactions must lead to branching of macrochains, which is the apparent reason for low gel-fraction concentration (below 5 wt.%) in the marketable end PAI. Low defectiveness of the structure is also indicated by comparison of calculated ([C] = 69.1%, [H] = 6.8%, [N] = 7.3%, [O] = 16.8%) and experimental ([C] = 69.0%, [H] = 7.5%, [N] = 7.1%, [O] = 15.4%) of PAI elemental composition.

End groups significantly affect thermal oxidative stability of PAI. In PAI synthesis pyromellitic dianhydride is taken in some excess that defines predominance of carboxylic end groups in macromolecules compared with amine ones or blockade of amino groups by acetic anhydride. Marketable end PAI are have the melt viscosity equal 10^3 - 5×10^5 P or η_{sp} = 0.8 – 1.5 (0.5% solution of *m*-cresol – tetrachloroethane mixture). According to X-ray diffraction data [46, 47] PAI has 40 - 60% crystallinity degree, and the chain conformation of the polymer extracted from the reaction mixture is coiled in the amine component. At temperature about 270°C, resulting conformation transformation, the chain is straightened and becomes bladed; PAI melting point is 285°C with the maximum of appropriate endothermic DSC peak at 298°C.

The following production phase – extrusion, is used either for powder pelletization or obtaining composite materials (glass-, mineral-, etc. filled), derived from PAI. The temperature mode by zones is 270 - 330°C. The mass was press molded at 330 ± 10°C to a mold, heated up to 150 - 180°C. These stages are the most temperature aggressive for the polymer. That is why the study of degradation transformations in the melt is the urgent problem.

POLYALKANIMIDE DEGRADATION IN MELT

Thermal degradation

Chemical instability of PAI macromolecules in melt becomes noticeable already at 300°C due to the increase of gel-fraction content and decrease of specific viscosity in solution (Figure 2). The processes are speeded up with temperature, and the effective activation energy of PAI gel formation in the temperature range of 300 - 450°C equals (50 ± 10) kJ/mol.

Judging by kinetics of mass losses and $C_1 - C_3$ hydrocarbon extraction (Figures 3 and 4), pyrolytic reactions in PAI are detected already at 300°C, though after tens of hours of heating are required for detection. At the initial stage, the seeming zero order of kinetics of mass losses and hydrocarbon extraction is determined by transformations degrees, negligible even at 400°C. The effective activation energy of mass losses, equal (232 ± 20) kJ/mol, correlates with E_a values for release of methane, ethylene, ethane and propane equal (192 ± 15), (160 ± 15), (238 ± 15) and (170 ± 15) kJ/mol, respectively.

PAI pyrolysis at 300°C proceeds with release of light (volatile) hydrocarbons only; at 350°C or higher carbon oxides and low-volatile products are also released from PAI. The latter precipitate near the hot zone, shaped as yellow-brown oil-like blushes and light crystals.

According to ^{13}C NMR-spectroscopic and mass-spectroscopic data, this oil-like blush is formed by the following homologues of phthalamide, nitrile phthalamide and pyromellite diimide:

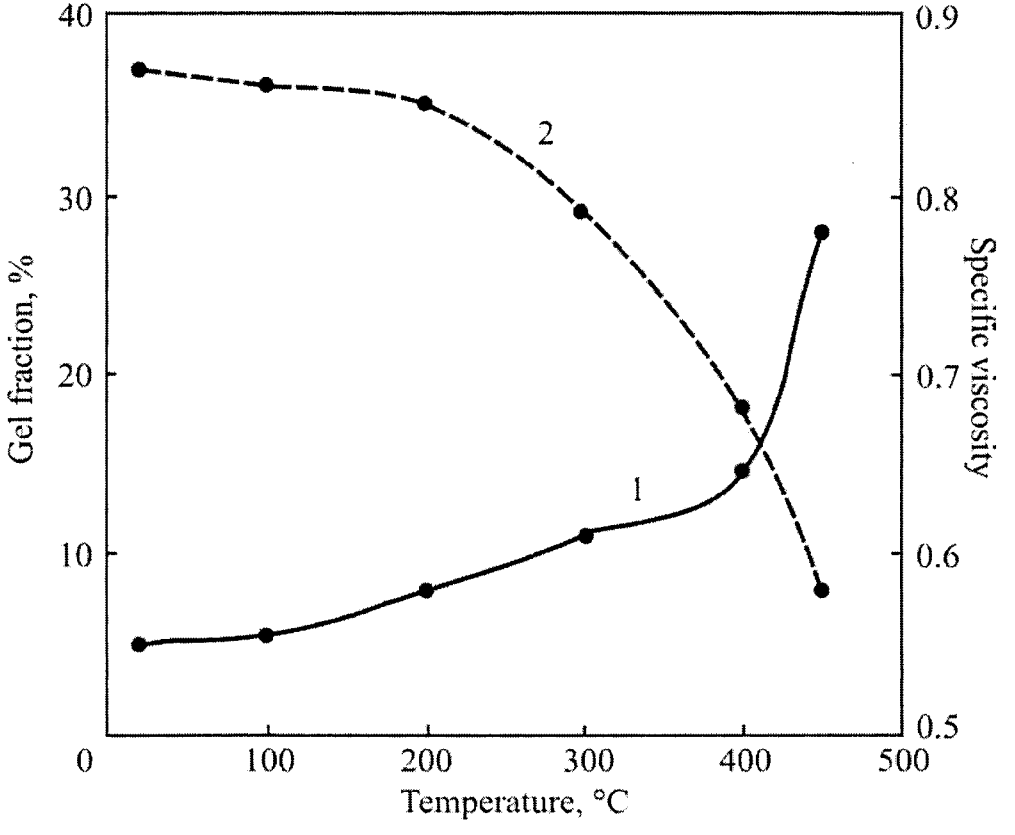

Figure 2. Kinetics of gel-fraction accumulation (1) and sol fraction viscosity variation (2) at PAI degradation in vacuum

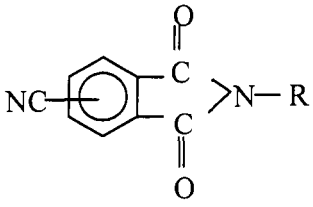

R= CH_3, $C_{11}H_{23}$, $C_{12}H_{25}$

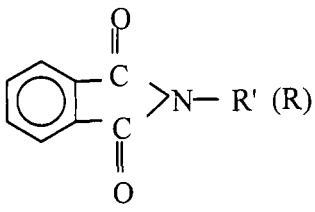

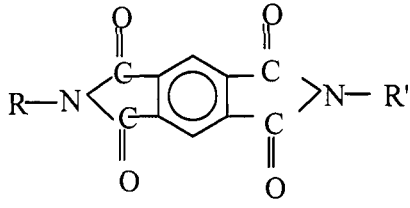

R= CH_3-$(CH_2)_n$, R'= $(CH_2)_n$-CH=CH_2

Homological sequences are traced well by mass-spectra of degradation products measured at low ionization potential with sequences of molecular ions, differed by 14 wt. units:

(CH_2) – 217 – 231 – 245 – 259 – 273 – 267 – 301 – 315;
201 – 215 – 229 – 243 – 257 – 271 – 285 - 299 – 313 – 327 – 341;
230 – 244 – 258 – 272 – 286 – 300 – 314 – 328 – 342 – 356 – 370 – 384 – 398 – 412 – 426 – 440 – 454 – 468 – 482 – 496 – 510 – 524 - 538.

Natural fractionation of the products with respect to distance from the hot zone and determination of mass-spectra at programmed heating allow detection of the yield distribution in homological sequences. This distribution indicates preferable breaks of methylene chains at their ends (a great amount of methyl phthalimide is formed) or almost at the middle of them.

A low volatile product precipitating as crystals (judging by IR-spectra of crystals and ethanol [136]) represents ammonium bicarbonate, the formation of which during PAI pyrolysis is possible at the interaction of primary products (ammonia and CO_2) in the hot zone, i.e. NH_4HCO_3 is the secondary product.

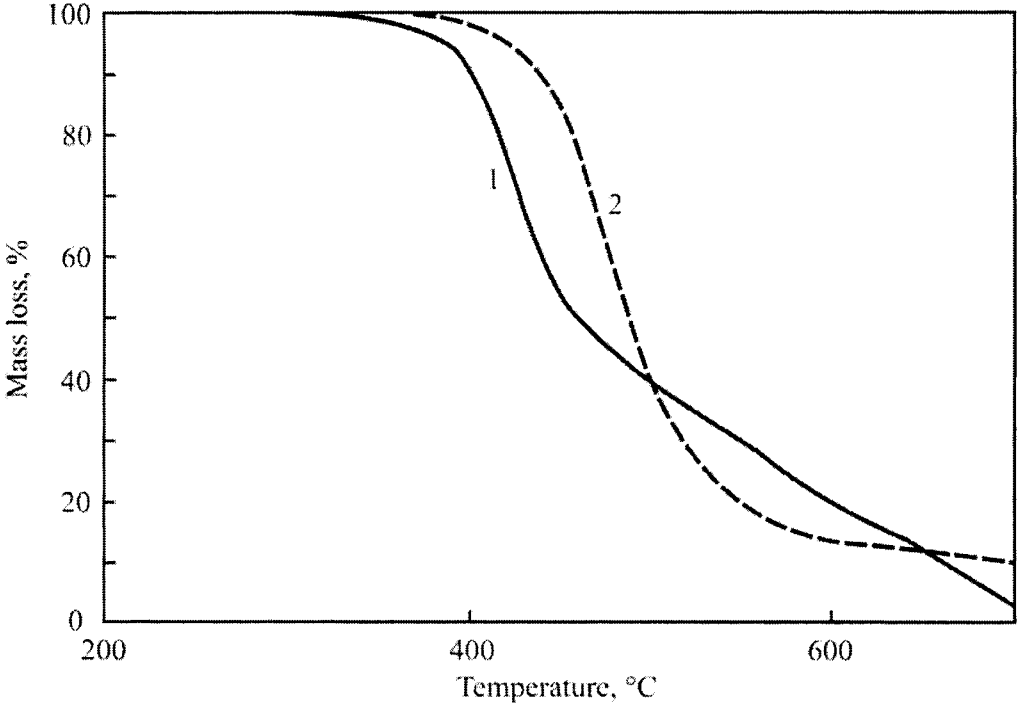

Figure 3. Thermogravimetric analysis (TGA) of PAI at the heating rate of 5 deg/min in air (1) and argon flow (2)

As the initial chemical structure and chemical structures of the products are compared, it is indicated that pyrolytic transformations of PAI proceed in two directions: by methylene chains and heterocycles. Being the most thermally labile fragments of PAI macrostructure, ethylene chains begin degrading at a noticeable rate when polymer melts, i.e. at 300°C, approximately, though even at this temperature the pyrolysis rate is also negligibly low (judging by total yield of hydrocarbons): about 0.1% of methylene chains per hour are damaged.

At 350°C, products of heterocycle decomposition occur: carbon oxides, phthalimide and nitrile phthalimidestructures, but the yield of these products is very low yet. For example, the release rate of CO_2 – the main product (by yield) of heterostructure degradation - is by one and half orders of magnitude lower than hydrocarbon release rate, not even taking into account the release of oligomeric fractures with residues of broken methylene chains. However, heterocycle pyrolysis becomes clearer with temperature increase. At 400 –

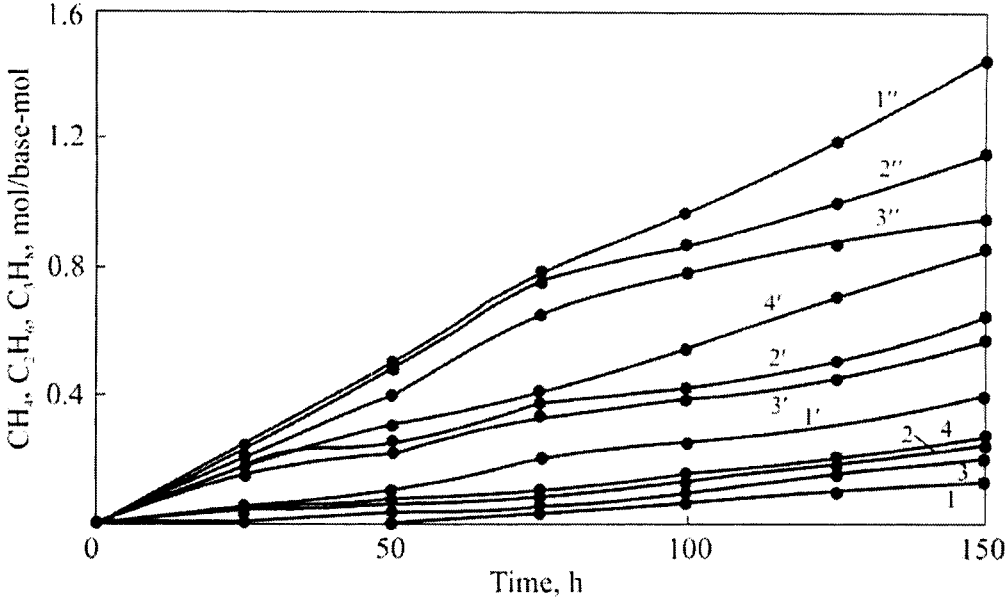

Figure 4. Extraction kinetics of CH_4 (1, 1',1"), C_2H_4 (2, 2', 2") and C_2H_6 (3, 3', 3") at 300, 350 and 450°C, respectively, and C_3H_8 (4, 4') at 350 and 400°C at PAI degradation in vacuum

450°C IR-spectra display the progressive degradation of heterocycles, first, by a decrease and then full disappearance of absorption bands at 1720 and 1780 cm^{-1}, related to ν_s(C=O) and ν_{as}(C=O) of the imide cycle [137], respectively. One more sign of this degradation is occurrence and intensification, and then full dominance (at 450°C or higher) of ν(C=N) absorption band of nitrile groups [138]. Aliphatic structure degradation leads to the conjugation system increase in pyrolyzate, detected by intensive coloring of the coke residue and paramagnetic manifestations (ESR signal represents a singlet with *g*-factor equal to free electron). The analysis of polymer degradation always implies two points of view on this process. From practical positions, purely thermal (pyrolytic) reactions must not make obstacles at normal cycle of PAI processing lasting several minutes. However, thermally, PAI is not absolutely inert in the temperature range of processing. Though the pyrolysis rate is still negligibly low, at overheatings and long stay of the material in dead volumes pyrolytic reactions will cause serious damages of chemical structure of macromolecules and, correspondingly, a decrease of polymeric material quality.

Moreover, thermal transformations in PAI are of definite scientific interest. The structure of PAI which represents (very simply) a hybrid of polyethylene and polyimide has not ever been considered in terms of reactivity in thermal reactions. Basing on the previous experience in the polymer science, it might be instinctively forecasted that methylene chains are thermally stable compared with cycloarylene structure, but the experiment is the only think that may determine the features of flexible and rigid fragment reaction in the chemical structure and, apparently, their interrelations.

Let us start from low temperatures (300°C), when methylene chains break and heterocycle is stable still. Typical feature of this process is rather narrow selection of C_1-C_3 hydrocarbons – the degradation products. Random breaks would cause occurrence of wide selection of products from methane to dodecane and release of alkylpyromellitimide oligomers. In the sensitivity range of modern instrumental techniques of analysis (GLC, mass-spectroscopy) the attempts to detect these substances failed. This means that either these substances do not occur at all or, which is most probable, their synthesis rate is negligibly low versus light hydrocarbons. As a consequence, methylene chain breaks in PAI have some specificity.

It is common knowledge that similar to cracking of alkanes, pyrolysis of PE and other hydrocarbon polymers is the radical-chain process [82]. The signs of radical process are observed for pyrolysis of methylene chains in PAI, which are high activation energies and synthesis of not single but several unitypical products (hydrocarbons up to C_3) with approximately similar yields. Finally, of great importance is the similarity principle concluded in equal structure (methylene chains) and equal chemistry. The chain type of the process is determined directly by chain initiation and propagation rate changes. This was made at the study of hydrocarbon cracking, when the origin of one product or another in one elementary reaction or another may be simply determined. At polymer pyrolysis direct proofs of the chain process proceeding are not obtained. Indirect proofs are used: correlation of effective activation energies with C-C bond strength and identification of products, which synthesis might be explained as the consequence of the chain transfer reaction.

These signs are also displayed by pyrolysis of PAI methylene chains: effective activation energies of C_1-C_3 hydrocarbon release fall within the range of 160 - 240 kJ/mol, which is much lower than any estimations of C-C-bond energy both in purely carbon surrounding (330 - 360 kJ/mol) and nearby the heteroatom (290 – 330 kJ/mol) [78]. Homolytical break of α-C-C-bond happens simpler compared with more distant bonds. Single O and N atoms in the chain

reduce α-C-C-bond strength by 12 – 20 kJ/mol [139]. High delocalizing ability is displayed by aromatic ring: delocalization energy of benzene radical equals 30 - 40 kJ/mol [115]. Following the additivity concept in chemistry, one would expect an analogous effect for pyromellitimide fragment. The authors of the current monograph have calculated molecular diagrams for methyl phthalimide and dimethyl pyromellite diimide – compounds modeling the boundary fragment of the elementary unit of PAI – by CNDO/2 technique using the software developed in L.Ya. Karpov Research Institute of Physical Chemistry. The geometry of molecules is shown in [140]. Diagrams in Figure 5 show charge distribution on atoms of the models.

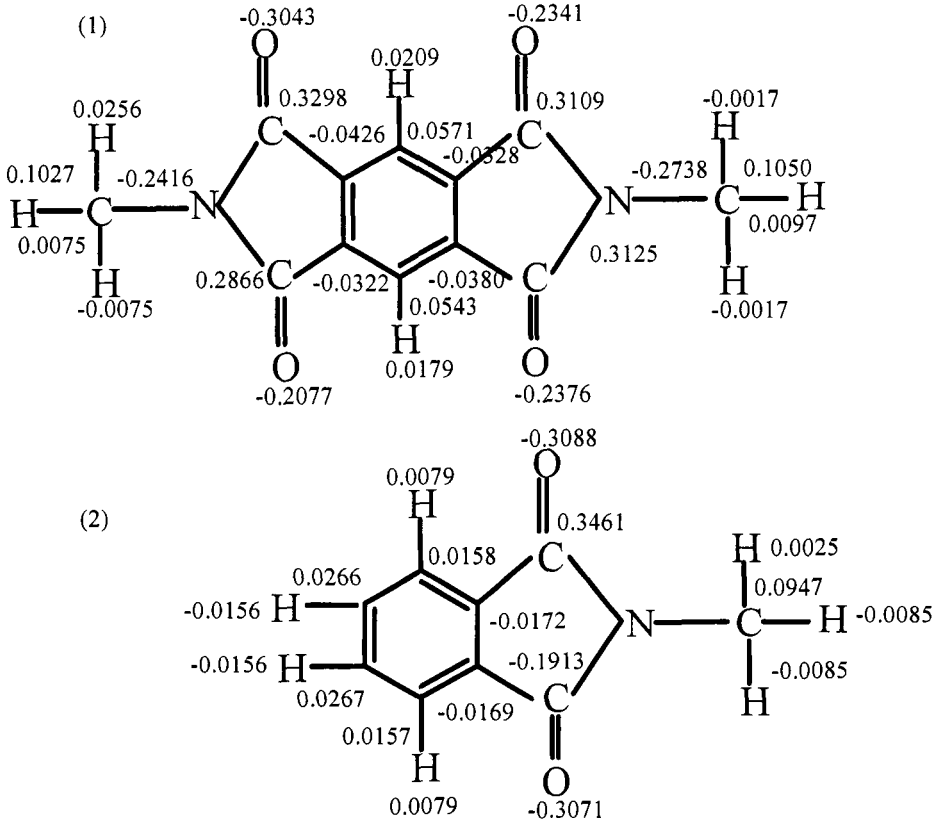

Figure 5. Molecular diagrams of PAI model compounds: dimethyl pyromellite diimide (1) and methylphthalimide (2)

The calculations show development of π-electron system in the model, which also affects alkyl substituting groups, to higher extent at α-C atom rather than at a distant one. Valent π-electron released from α-C atom at homolytical break of C-C and C-H bond is engaged in the π-system of arimide cycle, e.g. delocalization energy is released, by the value of which the strength of α-C atom bonding in alkyl substituting group is reduced.

Therefore, since strength of aliphatic C-H-bonds is much higher than that of C-C-bonds [78], the most probable initiation act is the weakest α-C-C bond break in the methylene chain:

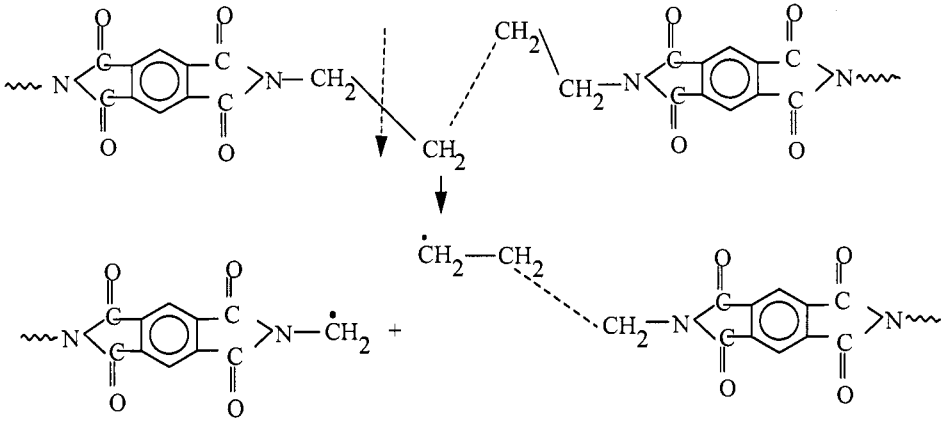

I II

Though the end alkyl macroradical I is stabilized by the arimide structure, it dies eventually, most likely, by detachment of H-atom and sequential formation of methyl pyromellitimide end group. End macroradical II of quite long methylene chain is quite reactive, especially in the polymer melt. Actually, macroradical II is identical to corresponded macroradical of methylene chain in PE.

The situation becomes more similar due to close viscosities of the melts of marketable end PAI and common PE trademarks (up to 10^5 P). This definitely indicates equal molecular mobility in melts. The probability of two subsequent breaks in the same methylene chain of limited length is low. Therefore, long hydrocarbons are not detected in products of PAI pyrolysis at 300°C. More probable is depolymerization of macroradical II with ethylene detachment, which is the main product by output at 300 - 350°C.

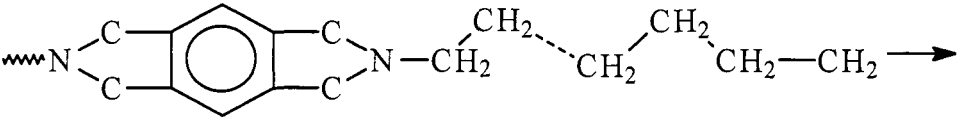

$\longrightarrow C_2H_4 + II$

Ethylene polymerization heat known from the literature [141] equals 121 kJ/mol, which correlates well with experimentally determined activation energy of ethylene release at PAI pyrolysis (158 ± 12 kJ/mol). End macroradicals of type II are capable of realizing the chain transfer by detaching H atom from CH_2-group in intermolecular or intramolecular reactions. Intramolecular detachment of H atom as a monomolecular reaction is kinetically more profitable than the interchain exchange [1], if nonstressed transition complexes are synthesized. This possibility of macroradical II isomerization through six-term transition complex formation leads to detachment of C_3H_7 radical then formation of C_3H_8 and end allyl groups:

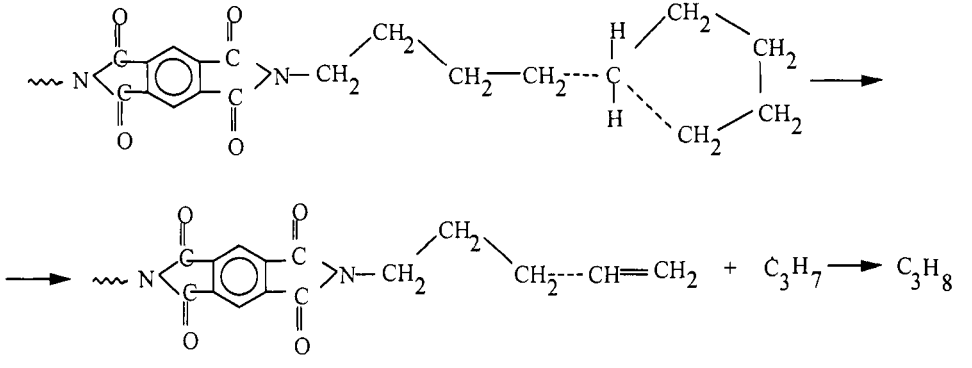

Compared to other hydrocarbons, besides ethylene, relatively low effective activation energy of propane release which equals (170 ± 14) kJ/mol correlates with suggested mechanism of its formation in specific reaction of radical isomerization. As temperature increases, differences in the reaction energy becomes smoother, and already at 350°C products of PAI pyrolysis possess compounds of oligomeric type with full selection of lengths of methylene chains.

Thermal instability of the imide cycle is observed already at 350°C, when products of its decomposition – carbon oxides, phthalimide and nitrile

phthalimide structures – are primarily detected (formed). Schemes of pyrolytic reactions of polymellitimide cycle are widely discussed in the literature, devoted to degradation problems of classical aromatic polyimides [28]. Generally, these schemes are unambiguous, but some reactions - imide-isoimide regrouping, in particular, which leads to formation of a "crude" for CO_2 (one of the main products) – are unique:

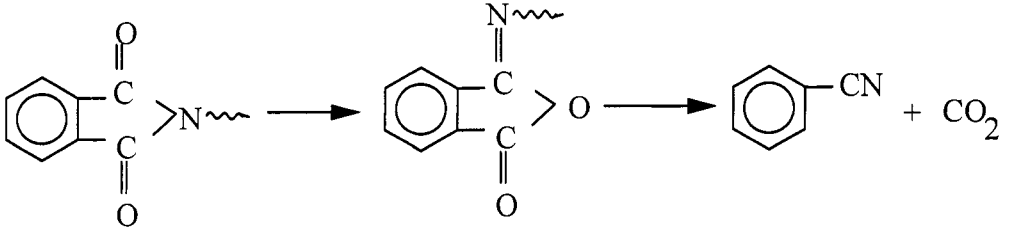

This reaction explains the occurrence of both CO_2 and nitrile phthalimide homologues in PAI pyrolysis products with some molecular ions in the following mass-spectrum: 201 – 215 – 229 – 257 – 271 - 285.

The only way for CO formation is direct break of isoimide cycle and its decomposition. Besides molecular hydrogen release, some products may be hydrogenated at high temperature in hydrogen-fertile systems (which are PAI) with active transfer of H atoms from methylene chains. This is confirmed experimentally by detection of ammonium bicarbonate (the "witness" of ammonia presence in the system) in the pyrolysis products:

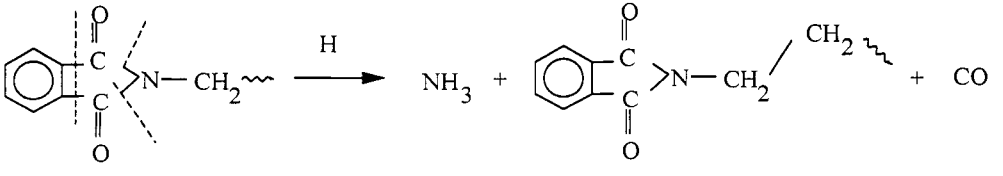

The set of heterocycle pyrolysis products in PAI conforms to that of polypyromellitimide derived from 4,4'-diaminodiphenyl ester of the Kapton type - the representative of aromatic polyimide family, most well known and studied.

Of interest is another thing: if the radical process of methylene chain degradation in PAI affects stability of heterocycles in its structure compared with classical polyimides, in which chain type of the process is rather

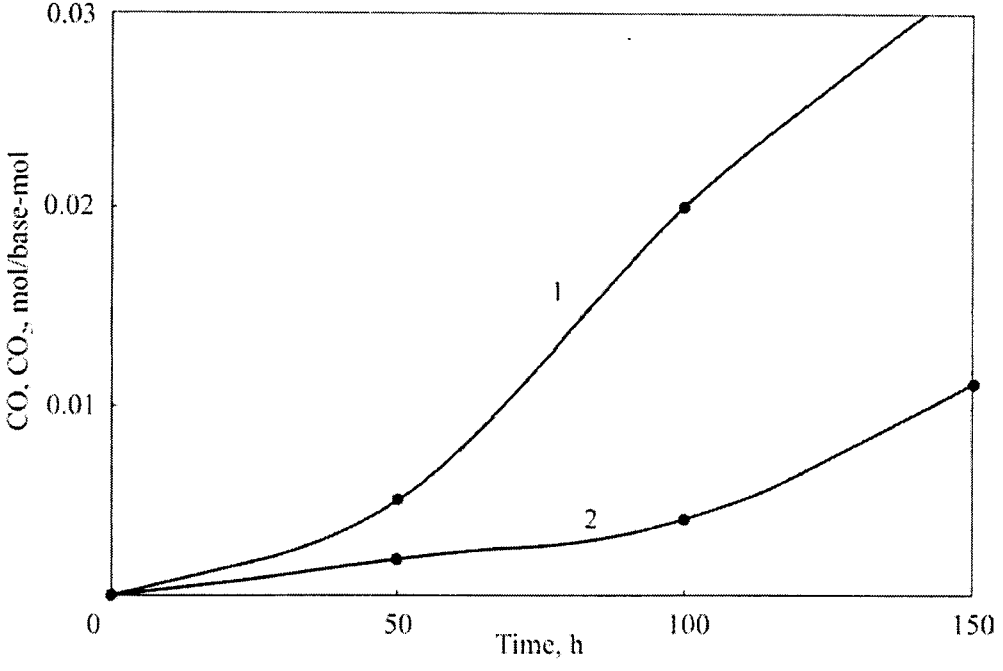

Figure 6. Kinetic curves of CO (1) and CO_2 (2) release at PAI degradation in vacuum at 350°C

ambiguous at low temperatures, when direct detachment of H atom from the ring is thermally hampered still. Among organic compounds, the strength of $C_{aromatic}$-H-bonds is maximal [78]. Figure 6 shows kinetic curves of carbon oxides release during PAI thermal degradation at 350°C. There are no data in the literature on transformations of aromatic polyimides under current conditions. Therefore, these products obtained at pyrolysis of fatty-aromatic and fully aromatic polyimides may not be accurately compared. It has been shown [142] that thermal processing of aromatic polyimide PM proceeding during 2 hours at 485°C in the oxygen-free environment releases 0.15 and 0.3 mol/base-mol of CO_2 and CO, respectively. Even a rough comparison of total yields of these products shows much lower stability of the heterocycle in fatty-aromatic polyimide. Apparently, chemical structure of PAI represents one more example of interrelation and agreement of structural components, absolutely different in their structure. Elementary unit of the macromolecule is presented by an entire construction. Some elements of the structure are displayed under some conditions, and the rest elements - under other conditions, but signs of

nonadditivity will always be found in the behavior, indicating the interaction of elements. The concept of additivity is a suitable tool of investigation, which gives an opportunity to assess the system response. Therefore, real deviations from additivity create a broad palette of reactivity and properties observed for polymers, which macromolecules are "built up" from the same "bricks".

Thus, in the temperature range of PAI processing, its pyrolytic transformations, generally associated with degradation of methylene chains, is possible. Since high-temperature inhibition of alkyl radicals, for instance, such radical "traps" as conjugation systems or stable radicals, is low effective, the processing mode must be strictly observed and overheatings avoided.

Heating in air is of greater danger for PAI, because its degradation is sharply intensified due to oxidation.

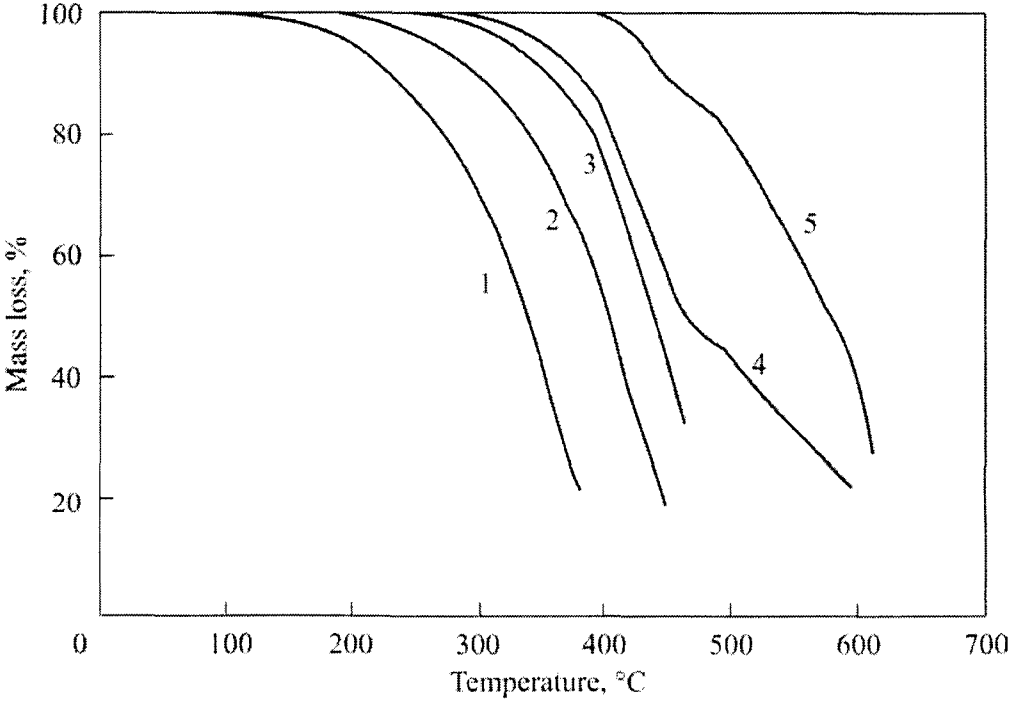

Figure 7. TGA curves for PE (1), PA-12 (2), PA-6 (3), PAI (4), and PI (5), in air at 5 deg/min heating rate

Thermal oxidative degradation

The formal assessment by TGA technique in air (Figure 7) shows that among other polymers with one or another PAI fragments in the structure (namely, aliphatic polyamide derived from dodecalactam (PA-12) and polypyromellitimide derived from 4,4'-diaminodiphenyl ester (polyimide PM-1 or *Kapton*), thermal oxidative stability of PAI is medium. Figure 7 also shows TGA curves for high density polyethylene (HDPE), which structure models very long methylene chain (3 – 6 branches and 0.6 – 0.8 unsaturated bonds per 1000 C atoms in the methylene chain) [143], and polycaproamide (PA-6) – the polymer with relatively short methylene chain.

It is clear why thermal stability of PAI in air is lower compared with aromatic polyimide. The whole experimental experience in questions of oxidation of hydrocarbons, hydrocarbon and heterochain polymers [1, 8] testifies about higher reactivity of aliphatic structures in thermal oxidation reactions, which confirmed by well-developed theory of gas- and liquid-phase oxidation [2, 8]. This theory associates kinetics of oxidative reactions with C-H bond strength, chain process specificity, and the presence of intermediate products which branch the kinetic chain. *Apriori* thermal oxidative degradation of PAI is developed in the aliphatic chain. PAI possesses higher thermal oxidative stability compared with other polymers of similar structure, specifically with the closest analogue – PA-12. Judging by kinetics of H atom detachment by nitroxyl radical in heptane, pentane and linear PE [144], the strength of C-C and C-H-bonds changes weakly along the methylene chain. The energy of middle C-C-bond breaks in $C_{12}H_{26}$ and C_6H_{14} equal 334 kJ/mol. approximately [78]. The bond strength in alkanes increases by 10% approaching the chain end [78]. On the contrary, C-C- and C-H-bond strengths in nitrogen-containing aliphatic compounds are reduced by 8 - 20 kJ/mol compared with methylene groups more remote from the heteroatom [139]. Similar effect of another heteroatom (oxygen) on thermal oxidation kinetics of polyethers and strengths of appropriate bonds was shown before [139]. Calculations and experimental determination of C-H-bond strengths in individual compounds are confirmed by studies of thermal oxidative degradation of aliphatic polyamides, for which the primary attack of oxygen on α-methylene group was shown [26]. The above-shown results of quantum-chemical calculations of the models indicate delocalizing ability of the arimide fragment even in relation to valent σ-electrons of methylene C atom. Therefore, from positions of pure chemistry, one would hardly expect any advantage in thermal oxidative stability, which really exists in PAI compared with the analogues – aliphatic polyamides.

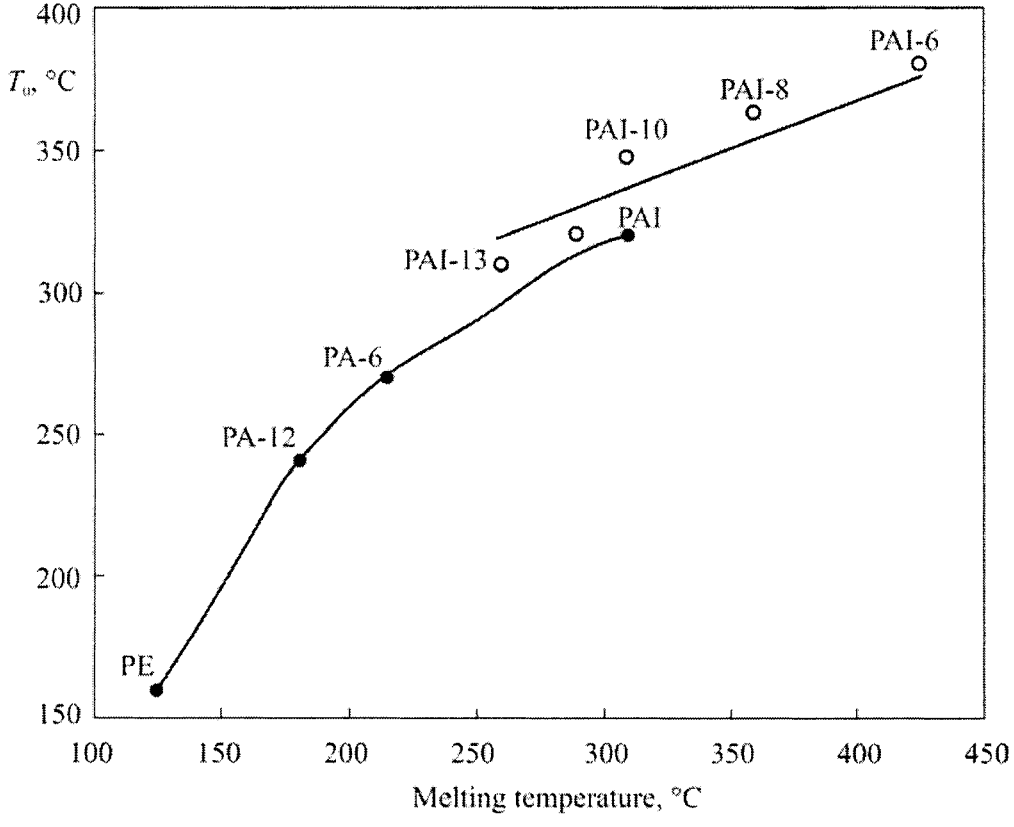

Figure 8. Dependencies of melting point and initial degradation temperature (T_0) according to TGA data on PE, PA-12, PA-6, PAI (1) and polyalkanimides (2) at the heating rate 5°/min in air

The modern concept of solid-phase degradation reactions [9] is illustrated by the dependence of almost all elementary reactions of chain oxidation, O_2 and degradation product transport due to molecular movements in the polymeric body. Even the initial mass loss temperature (T_0) – the gross parameter of thermal oxidative stability – in the sequence of polymers having similar chemical structure of the elementary unit is bound to macrochain mobility, estimated by melting points of the polymers. The polymers in the following sequence: PE, PA-12, PA-6 and PAI, possess melting points equal 125, 181, 215 and 298°C and T_0 equal 60, 240, 270 and 320°C, respectively. As is obvious, both parameters display almost linear dependence (Figure 8). Similar dependence was also observed for some polyalkanimides with

methylene chain from 6 to 13 carbon atoms long: PAI-6, PAI-8, ..., PAI-13, correspondingly (Figure 9).

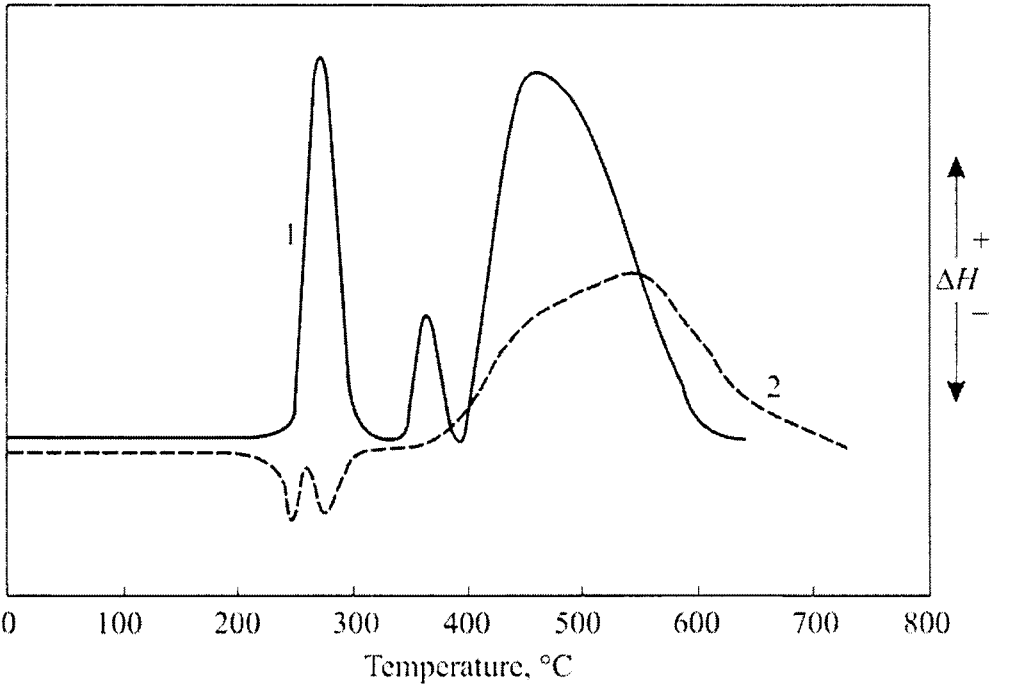

Figure 9. DTA curves for PAI in air (1) and argon flow (2). The heating rate is 5°/min

The thermogram of PAI in air (Figure 9) possesses high intensity exothermal DTA peak with the maximum at 290°C and two less intensive exothermal peaks with maximums at 350 and 450°C. The first peak corresponds to temperatures approaching the initial mass loss temperature, whereas other peaks correspond to advanced PAI degradation. A thermogram, recorded in the absence of O_2, possesses a split up endothermic peak, related [47] to the phase transition of PAI (279°C), at the place of the first exothermal DTA peak location.

The exothermal effect associated with O_2 presence fully masks endothermic effects of both phase transitions.

Similar situation is observed for other polyalkane pyromellitimides - PAI-6, PAI-8, PAI-9, PAI-10, PAI-11, and PAI-13 – for which the intensive

exothermal peak masks endothermic peaks of phase transitions and melting. The dependence of PAI chain conformation features on the evenness (the number of C atoms) of the methylene chain is considered [47]. It is proved that contrary to PAI with even number of methylene groups (except for PAI-6), a spiral twofold axis is typical of uneven aliphatic chains of PAI and PAI-6. In the case of massive framing (heterocycle), this axis prevents chain packing e.g. crystallization. PAI with even chains are highly crystalline polymers, and uneven ones are liquid-crystal with the long-range order along the chain and short-range order in the chain location plane [47]. The phase transition of primarily coiled structure to more stretched one is absent in uneven PAI and PAI-6, whereas in even PAI it is prior to melting.

Table 1

Temperature transitions and heat effects in PAI

Polymer	Phase transition temperature, °C [47]	Melting point, °C (by DTA peak maximum) [47]	DTA effect*, kJ/base-mol		
			Phase transitions (total)	Initial oxidation (1st DTA exopeak)	Exoeffect correction with respect to phase transition heats
PAI-6	-	430	10.3	139.1	149.4
PAI-9	-	303	23.3	76.1	99.4
PAI-11	-	292	23.4	77.0	100.4
PAI-13	-	263	24.6	107.9	132.5
PAI-8	349	362	18.5	190.3	208.8
PAI-10	308	318	26.9	191.9	218.8
PAI-12	279	298	31.0	203.5	234.5

Note: * According to known data from the literature, thermoanalyzer is calibrated by $NaNO_3$ and $AgNO_3$ standard substances, which melting temperatures fall within the range of PAI phase transition temperatures. Calibration check of PET melting heat gave (40.6 ± 4) kJ/mol, which correlated well with literary data [145] - 47.3 kJ/mol.

Therefore, the connection of exothermal DTA peak in the presence of O_2 in the system and its location near the initial mass loss (intensive PAI degradation) in the temperature field indicates its oxidative origin. Putting the

mechanism of PAI interaction with O_2 aside, note that the process in even PAI is characterized by almost twice higher hear release rather than in uneven PAI and PAI-6 (Table 1). This shows obvious correlation between thermal oxidation kinetics and morphological features of PAI structure.

Since the rate of heat release correlates with thermal oxidation rate, at molecular mobility defrost (1^{st} phase transition) and further melting the oxidation rate of even, highly crystalline PAI is twice higher compared with uneven, liquid-crystal PAI. NMR wide bands of uneven PAI also display a narrow component indicating the presence of non-crystalline domains. For more details on the liquid-crystal structure formation in uneven PAI, refer to X-ray diffraction analysis results [47].

At dynamic heating, a rigid, low mobile structure of even PAI somewhat stabilizes the polymer. Methylene chains in PAI, thermodynamically labile at high temperatures (in PE, these methylene chains are intensively oxidized and break at these temperatures), are kinetically unable to overcome the activation barrier of unfavorable (possibly for propagation and kinetic chain branching reactions) morphological structures. The polymer is somewhat "overheated", which promotes similarity with the idea of "explosive" depolymerization, put forward [146] in the analysis of TGA data on depolymerizing polymers at extremely high heating rates (over 200°/s). The authors [146] suggested characterize degradation by critical temperature, at which intermolecular links preventing emission of products – backbone fractures somewhat break at ones, and the polymer "explosion-like" degrades.

In PAI hydrogen bonds are absent [47]. Therefore, thermal oxidation kinetics is limited by dormancy of molecular motions in macrochains. We are not to discuss the mechanism of morphology effect on kinetics of PAI thermal oxidation in the radical-chain process. One may refer to the famous monograph written by Buchachenko and Emanuel [9], where this question is thoroughly discussed on the example of solid polyolefins. The oxidation chemistry of these substances and their low-molecular analogues – liquid hydrocarbons, is studied quite well. The following different thing is of importance in the context of the current monograph. The intense oxidation during a short time (within the 1^{st} exothermal peak at the thermogram – 10 min or less) leads to noticeable degradation-induced changes, increasing in the polymer symbate with oxidation proceeding (traced by the DTA curve run, Figure 10). The gel-fraction content in PAI within exothermal peak of oxidation is auto-excited accelerated up to 15%, and specific viscosity of the sol-fraction decreases from 0.88 to 0.52 dl/g.

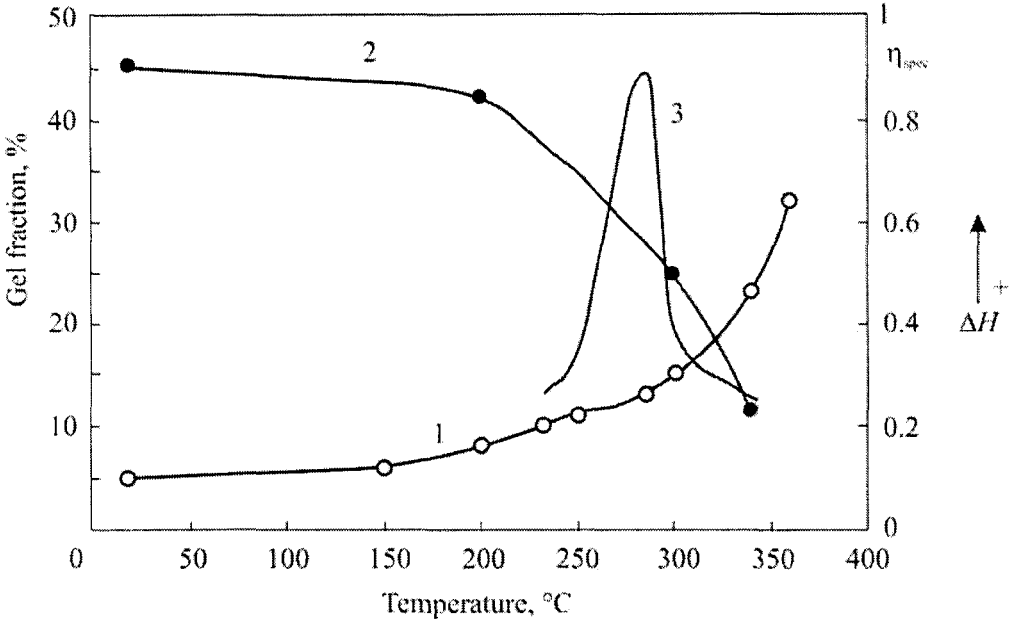

Figure 10. Gel-fraction content (1) and sol-fraction viscosity (2) in exothermal DTA peak for PAI (3) in air (the heating rate 5°/min)

The first stage of PAI-12 powder processing (extrusion, compounding) is similar to thermal analysis, and the sample is subject to dynamic heating in both cases. At initial stages of vacuum extruder the residual pressure equals 30 – 50 mm, e.g. oxygen is always present in the system, even not taking into account oxygen dissolved in the polymer. The gross heat release corresponded to the 1st exothermal DTA peak increases from 203.5 to 277.8 kJ/mol with the heating rate of 5°/min. As a consequence, in contrast with the extremely short range of dynamic heating (320 - 350°C) at vacuum extrusion of the powder, danger of PAI-12 thermal oxidation is significant at polymer melting. This is confirmed by difficulties in its processing into articles and problems with granular material quality.

Hindered PAI oxidation at low temperatures (below 250°C) does not show its full absence. For example, PAI heated in air at 200°C during 100 hours absorbs more than 1 O_2 mol/base-mol. The 1st exothermal peak is absent on the thermogram. It is replaced by an endothermic peak associated with melting of the polymer. On the thermogram of oxidized sample the first exothermal peak is

absent, and an endothermic peak associated with the polymer melting occurs at its place. The first exothermal peak is a suitable index of PAI-12 oxidation degree, if O_2 diffusion into the sample is free. For example, if a bulky sample melted in air is grinded, the powder thermogram possesses oxidation exotherm at the place of endotherm of melting.

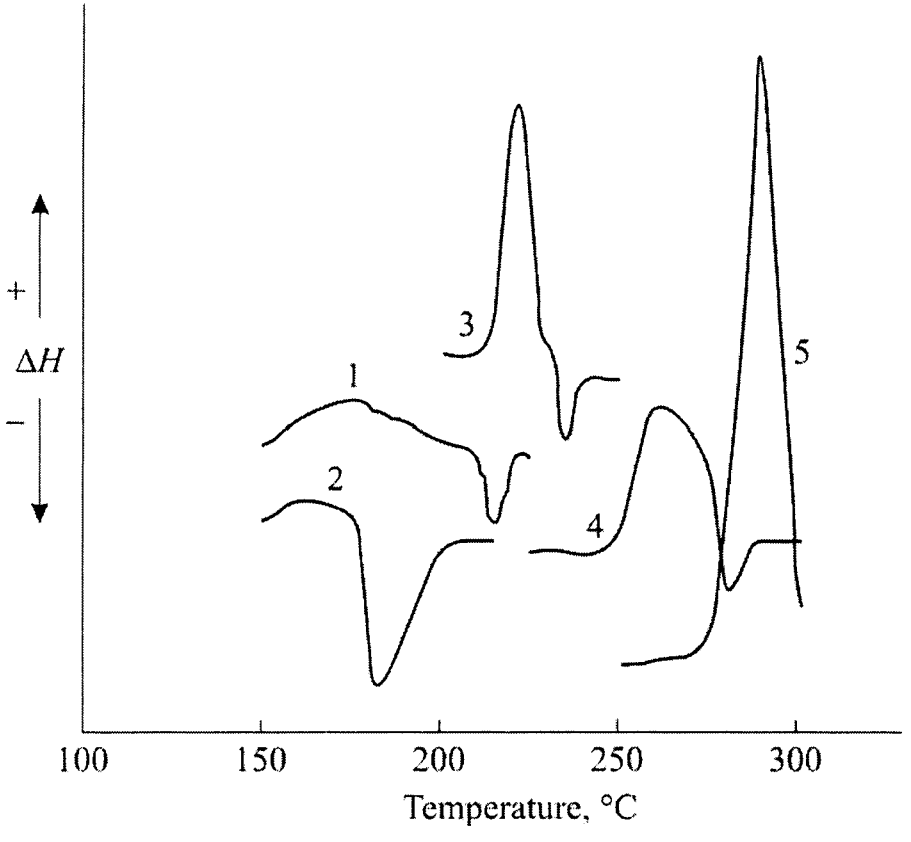

Figure 11. DTA curves for PA-6 (1), PA-12 (2), PBT (3), PET (4), and PAI-12 (5) heated in air (heating rate 5°/min)

The phase transition effect on exothermal DTA peak, similar to PAI, is observed for PET and specifically for poly(butylene terephthalate) (PBT). These are crystalline polymers with chemical structure affined to PAI, namely, by combined methylene chains and aromatic rings (Figure 11). Judging by significant intensity of exothermal peaks preceding endothermic melting peaks

on DTA curves, oxidation processes, primarily hindered due to the structure rigidity, are sharply intensified at pre-melting of these polyolefins. On the contrary, oxidation of aliphatic PA is described by a fuzzy exothermal peak. As shown in the thermogram, it begins at temperatures much below PA melting point (Figure 11). Exothermal PA peaks are symbate to weight increment due to atmospheric oxygen binding. No weight increments at PAI, PET and PBT heating are observed. DTA curves illustrate the difference in thermal oxidation kinetics for crystalline polymers having methylene chains in their structure. Purely aliphatic polymers with highly developed molecular motion in the solid phase are simply oxidized at dynamic heating at temperatures much below their melting points. Solid oxidation of fatty aromatic polymers is hindered, but becomes intensive at phase transition temperatures. DTA data is sufficient for thermal stabilization of engineering polymers. For example, for aliphatic PA, these data currently indicate the necessity in protection of polymers both at processing and operation, whereas PAI and aromatic polyester should be stabilized at processing only. However, the final decision about thermal stabilization at particular stages of polymer "life" may be made on basis of comprehensive study of polymer features concerning its thermal behavior in temperature intervals of material processing and operation.

When heated, PAI absorb O_2 and release carbon oxides, water and formaldehyde (Figure 12). Thermal oxidation kinetics (with eliminated diffusion hindrances) is at first glance of the breakthrough type typical of high temperature oxidation of hydrocarbon polymers [147]. At 250 - 300°C during initial 5 - 20 hours, PAI absorb up to 8 O_2 mol/base-mol. Further on, the process is abruptly slowed down, but the polymer manages to absorb more 2 O_2 mol/base-mol during next 100 - 200 hours. The two-stage type of thermal oxidation process is clearly observed at 350°C, when the first fast stage is finished by absorption of 8 O_2 mol/base-mol during last 2 hours, and then the second, slow stage with almost linear dependence of O_2 absorption rate lasts for hours. At low temperature oxidation of PAI (250°C or lower) the second stage is not observed. As transferred to semi-logarithmic coordinates, corresponded kinetic curves of O_2 absorption and those describing the first stage of high-temperature oxidation are transferred to lines that formally indicate the first kinetic order. The Arrhenius temperature dependence of O_2 absorption initial rate constants does not fit a straight line, but displays a break in the temperature range of phase transitions in PAI (Figure 13).

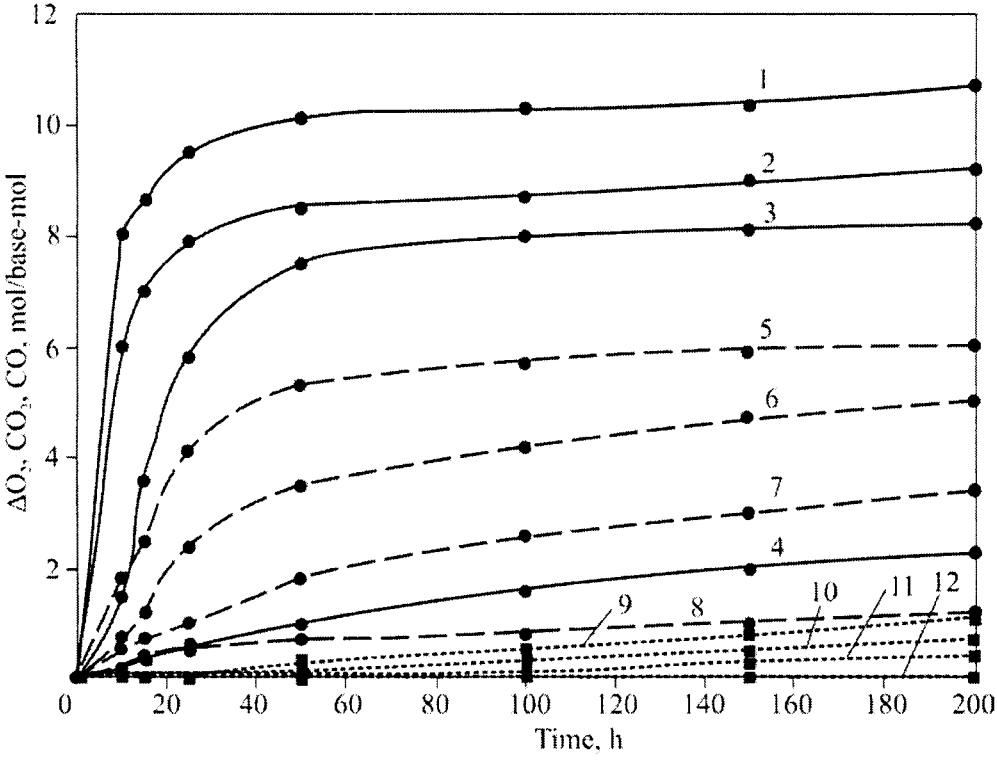

Figure 12. Kinetics of O_2 absorption (1 – 4), CO_2 (5 – 8) and CO (9 – 12) release at thermal oxidation of PAI in air at 350, 300, 250 and 200°C, respectively

Kinetics of carbon oxide release is identical to O_2 absorption kinetics. Effective activation energies of CO and O_2 release at PAI thermal oxidation in melt equal (163 ± 10) and (135 ± 10) kJ/mol.

The two stage kinetics of high temperature oxidation of aromatic polybenzoxazole containing the methylene bridge in the diamine component is described in the literature [148]. The first, fast stage is associated with aliphatic fragment oxidation, and the second, slow one – with oxidation of the aromatic structure. The case is similar for PAI. The below IR-spectroscopy and mass-spectrometry data indicate that methylene chains are primarily oxidized both at low temperature of PAI oxidation (the operation temperature range and close temperatures) and high temperature oxidation (temperature of processing)with exposures correlating with the processing cycle duration. Therefore, aromatic

structure is not practically touched. At processing temperature the rate of aromatic structure oxidative degradation is, at least, two orders of magnitude lower than the methylene chain oxidation rate, i.e. choosing the way of PAI thermal stabilization one may neglect oxidation of the aromatic structure.

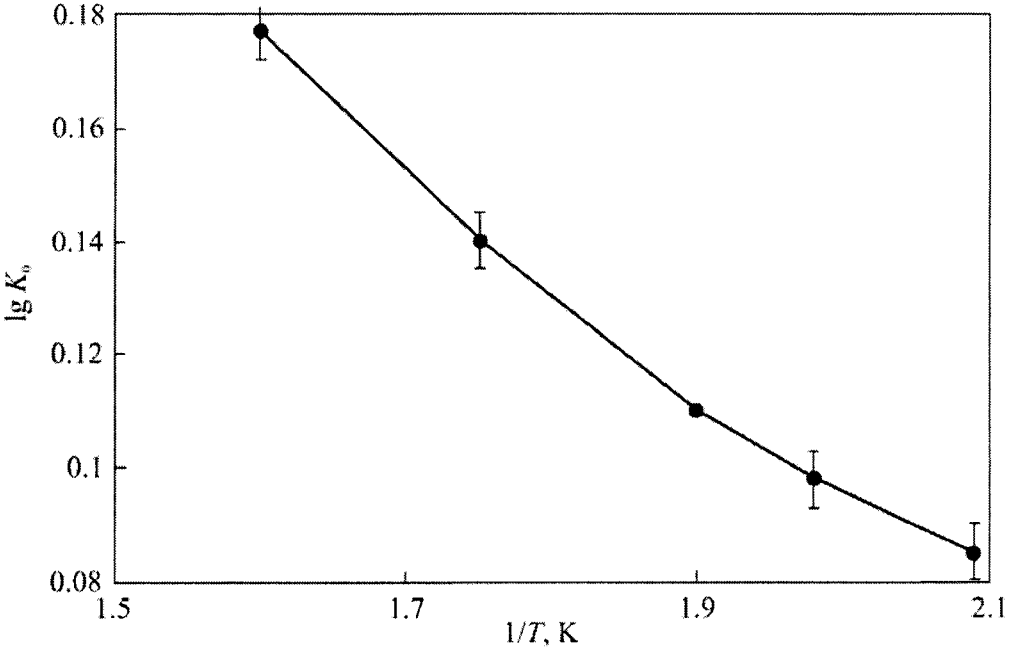

Figure 13. The Arrhenius dependence of initial rate constants K_0 of O_2 absorption on temperature of PAI thermal oxidation in air

The quantity of oxygen released from PAI at thermal oxidation (at the 1st stage), totally with carbon oxides, water and formaldehyde equals a half (molar) of O_2 absorbed by the polymer from the gas phase (Table 2).

Table 2

Oxygen balance at PAI thermal oxidation

Exposure conditions*	O_2 absorption, mol/base-mol	Total oxygen amount released with CO_2, CO, H_2O, CH_2O, mol/base-mol
350°C, 1 h	2.4	1.1
300°C, 2 h	3.3	1.5
250°C, 5 h	1.4	0.7
200°C, 50 h	0.9	0.5

Note: * Different exposure times are caused by the process kinetics at the mentioned temperatures. The data relate to the 1st oxidation stage.

Though the release of carbon oxides possesses quite high temperature coefficient: E_a = (134 – 163) ± 10 kJ/mol, temperature increase to 350°C leads to a noticeable reduction of the part of these products in the oxygen balance. Moreover, the release ratio of CO_2 and CO changes with temperature: it is 10:1 (molar) at temperature below 300°C, and 6:1 at 350°C. The increase of CO release is associated with heterocycle decay. As shown above, heterocycles participate in PAI pyrolysis at 350°C. The rate of these decays is low compared with methylene chain breaks. Moreover, as observed from mass losses, the gross rate of PAI pyrolysis at 350°C is by an order of magnitude lower than thermal oxidation rate. Therefore, a noticeable increase of CO output is explained by oxidative pyrolysis of heterocycles. Previously, using an isotope label in O_2, it is shown [149] that at temperatures of full thermal stability of imide cycles oxygen activates purely thermal reactions of heterocycles in aromatic polyimide.

As PAI oxidizes, relatively low amount of H_2O is released (2 – 5% of CO_2 release), whereas H_2O is the main product released at hydrocarbon polymer thermal oxidation, but in another temperature range (up to 200 - 220°C) [4, 28]. The variety of oxygen-containing organic oxidation products (aldehydes, ketones, alcohols, ethers, acids) is typical of thermal oxidation of polyolefins generally and methylene chain in PE specifically. Total output of these substances exceeds the release of carbon oxides [110]. The variety and output of these products at thermal oxidation of aliphatic PA is lower [26]. At temperatures up to 300°C, thermal oxidation of methylene chain in PAI leads to formaldehyde release and trace amounts of other aldehydes. At high temperatures, oxidative degradation of methylene chain in PAI in melt is clearly

displayed by sharp increase of formaldehyde output which, besides CO_2, becomes the basic volatile degradation product. According to ^1H NMR-spectra, PAI oxidation in melt gives various degradation products. The main contribution to the spectrum is belonged to aliphatic chain protons: signals with chemical shifts of 0.85 – 86 ppm correspond to end CH_3-groups; γ- and more remote CH_2-groups – 1.23-1.28 ppm; α- and β-CH_2-groups – 3.6 and 1.6-1.7 ppm, respectively; N-CH_3-groups – 3.2 ppm. Signal intensity integrals show the length of methylene chains in thermal oxidation products equal C_5-C_6 and, basing on the contributions from protons in N-CH_2-groups, about 20% of methylene chains are linked to imide cycles or other nitrogen-containing groups, amino groups, for example. The rest methylene chains (R) are distributed between the following structures: R-CH_2OC(O) – 4.0 – 4.1 ppm, and R-CH_2C(O) – 2.2 – 2.3 ppm. Signals with chemical shifts of 7.69 – 7.82, 7.93 and 8.24 ppm relate to phthalimide, nitrile phthalimide and pyromellitimide structures, respectively. In C NMR-spectrum, chemical shifts ranged within 132.3 – 133.8, 123.9 – 126.6 and 117.2 ppm correspond to the mentioned structures. Here, methylene chains are observed at 38.7 – 14.08 ppm at corresponded distance from nitrogen atom: for example, chemical shift of 38.7 - 38.1 ppm corresponds to α-CH_2 group, 27.0 – 26.8 ppm to β-CH_2 group, etc.

A lower amount of absorbed oxygen is released with volatile products. The rest oxygen is accumulated in the polymer (refer to Figure 14 showing temperature dynamics of changes in PAI elemental composition, induced by thermal oxidation at different temperatures). At 200°C, a noticeable oxygen accumulation in PAI takes about 1000 hours, whereas at 350°C change of the initial elemental composition C - 69.0%, H - 7.5%, N - 6.7%, O - 16.8% to 66.4, 6.0, 5.9 and 21.7%, respectively, takes 1 hour only.

Degradation changes in PAI are reflected by IR-spectra. The Fourier distribution IR-spectrum of initial PAI has the following absorption bands: a doublet at $\nu_{(C\text{-}H)arom}$ = 3038 and 3101 cm^{-1}; a doublet at $\nu_{(C\text{-}H)aliph}$ = 2848 and 2921 cm^{-1}; a doublet at ν_s = 1720 cm^{-1} and $\nu_{as(C=O)}$ = 1780 cm^{-1} of imide cycle, respectively [137]; and deformation oscillations of imide cycle at 728 cm^{-1} [138]. Intensive bands at 1122, 1157, 1367, 1397 and 1563 cm^{-1} are related to valence and deformation oscillations of bonds which form skeleton (backbone) of the macromolecule.

Compared with IR-spectrum of the initial polymer, spectra of PAI oxidized at high temperatures, but at low exposure at first glance display no significant differences, except for consecutive increase of the absorption band at

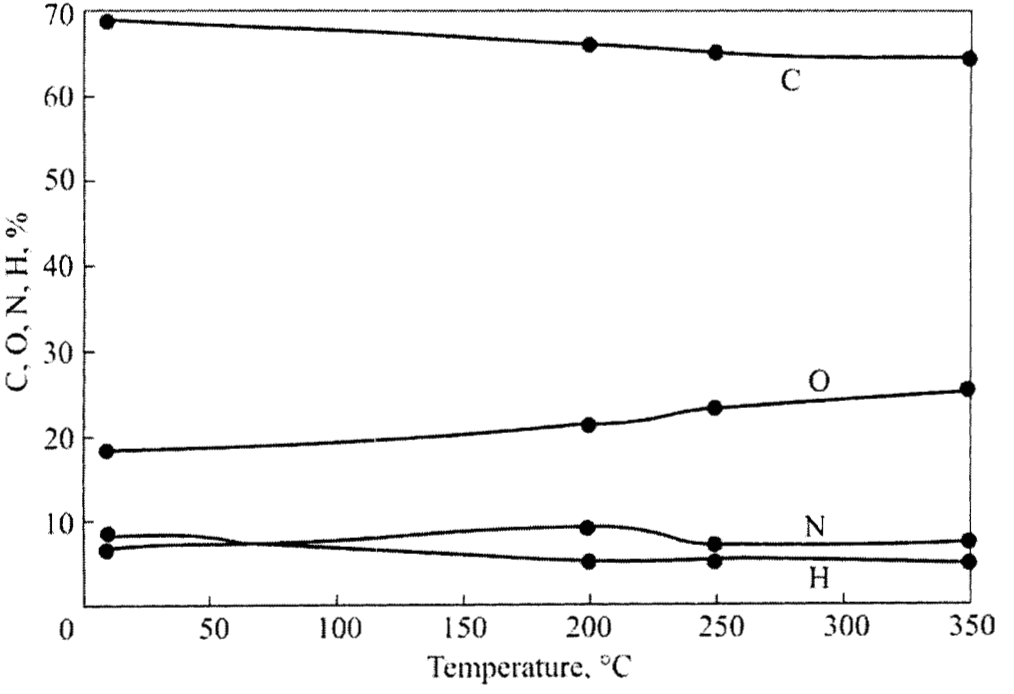

Figure 14. The change of PAI elemental composition at thermal oxidation in air: at 200, 250, 300 and 350°C and 500, 200, 10 and 1 hour exposure, respectively

3470 cm^{-1}, which relates to associated $\nu_{(OH)}$ [138], as well as broadening of the long-wave wing at 1720 cm^{-1} band base and occurrence of a bending at 1620 cm^{-1}. Computer treatment of degraded PAI spectrum and its comparison with the library of Fourier distribution IR-spectra, measured on Perkin-Elmer 1710 FTIR spectrophotometer has given a formal evidence of possible presence of the following structures: aromatic imide, for example, phthalimide, maleimide or glutimide, ureal and carbamate, and various linear or cyclic carbonyl groups. Obviously the first evidence of aromatic imides, currently pyromellitimide group, is unambiguous. Therefore, since computer searches by the most intensive bands in decodable spectrum, the rest structures suggested should be taken into consideration, and new evidences of their occurrence must be searched for.

Quantitatively, changes in optical densities of basic spectrum bands were estimated using the band of 728 cm^{-1} (Table 3).

Table 3

Relative optical densities $\frac{D_x}{D_{728}}$ of absorption bands in IR-spectra of oxidized PAI (at 1 h exposure)

Temperature, °C	$\frac{D_x}{D_{728}}$ at x equal:			
	2921 cm^{-1}	2848 cm^{-1}	1720 cm^{-1}	1780 cm^{-1}
Before oxidation	1.2	0.9	2.5	1.1
275	1.1	0.8	2.6	1.1
300	1.0	0.8	3.8	1.1
350	1.3	0.9	4.7	1.3

The band intensity at 1720 cm^{-1} regularly increases with thermal oxidation which is illustrated by differential IR-spectra. No regularity is observed in changes of other bands. These IR-spectroscopy data contradict to the hypothesis of primary oxidation of methylene chains in PAI. Actually, thermal oxidation of PAI at 300 and 350°C during 1 hour results in absorption of 1.6 and 2.4 mol O_2/base-mol and release of 0.1 and 0.5 mol CO_2/base-mol (dominant output product), respectively. Thus resulting oxidation, the oxygen content in PAI becomes nearly twice higher, whereas methylene chain damages calculated by CO_2 as the degradation index in the carbon balance give 2%, approximately. One may make a different suggestion: in oxidized structures one oxygen atom substitutes two (ketone) or, most frequently, one (aldehydes, alcohol, ether) hydrogen atom. As a consequence, the mentioned level of O_2 absorption induces the loss of hydrogen from methylene groups equal 10 – 20%. The lower level falls within the error of IR-spectrum quantitative assessments, where 20% difference would be noticeable. IR-spectra do not allow methylene chain oxidation assessment, but clearly indicate the increase of carbonyl group content.

The Fourier IR-spectra in the range of 1650 – 1750 cm^{-1} observed at high resolutions (2 cm^{-1}) indicated identity of the band shape at 1720 cm^{-1} with the maximum at 1713 cm^{-1}, detected at sensitivity increase for the initial and oxidized PAI (Figure 15). Propagation of a new carbonyl band somehow from inside (to say "from the same root") of the initial one related to $\nu_{(C=O)}$ of the imide cycle. This may be dually explained. Primarily, thermal oxidation and degradation of methylene chains intensify symmetrical oscillations of the cycle by means of asymmetrical oscillations. This explanation is obeyed by the

above-mentioned increase of negligibly small damage of methylene chains, detected at the moment of spectrum record. Moreover, if judged by the area of bands within 1,650 – 1,800 cm^{-1}, at 1,720 and 1,790 cm^{-1} both the relation of optical densities changes and carbonyl absorption significantly increases. Secondly, it may be explained by occurrence of new C=O-groups as the oxidation product.

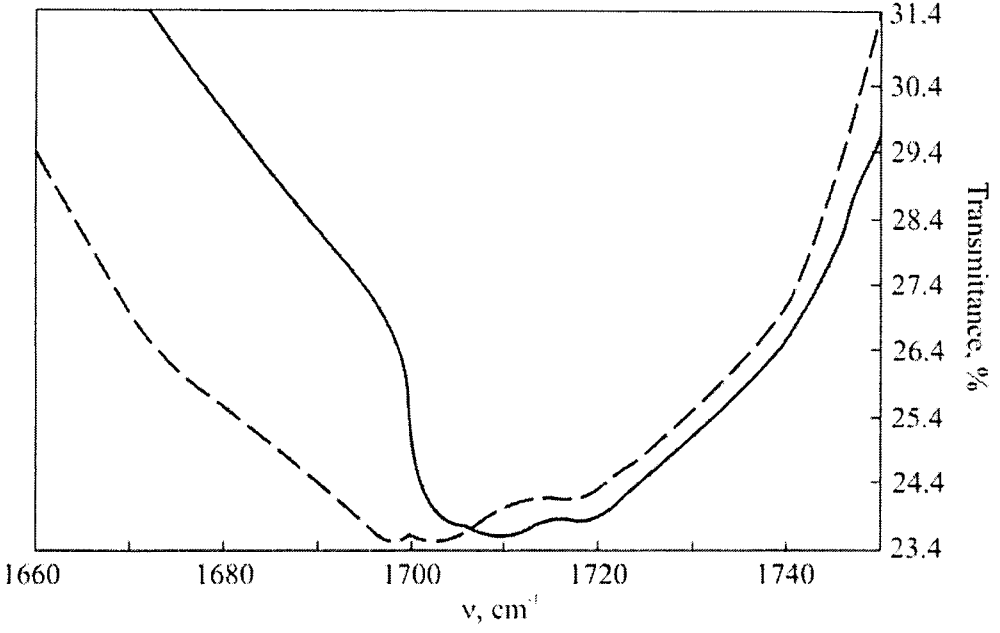

Figure 15. High resolution (2 cm^{-1}) Fourier IR-spectrum for PAI before (1) and after (2) thermal oxidation in air at 350°C during 1 hour

The literature shows investigations of aliphatic PA thermal oxidation by IR-spectroscopy [150]. The occurrence of new C=O-groups, resulted by low-temperature oxidation of PA-6, PA-66, PA-11, PA-12, and the so-called "soluble" N-methoxymethylated PA-6 is displayed in absorption increase in the range of 1700 – 1750 cm^{-1} at the short-wave wing of the initial amide band.

The authors have not performed the band separation, but, anyway, consider that the bending contains two maximums at 1715 - 1719 and 1731 - 1736 cm^{-1}, which they relate to a new imide structure, synthesized by α-CH_2-group oxidation.

For N-methoxymethylated PA-6, the most intensive, new carbonyl band in IR-spectrum is observed at 1719 cm^{-1}. As shown in the literature, the feature of oxidized PAI IR-spectra may be explained by occurrence of new α-C=O-group in the methylene chain. The alternative attack of molecular oxygen and preferable oxidation of internal methylene groups would form a situation similar to thermal oxidation of PE backbone, when a broad, multi-structural band occurs in the range of 1700 – 1800 cm^{-1} in IR-spectra of oxidized PE. Analysis of this multi-structural band has detected the contribution of aldehydes< ketone, ether, and carboxylic groups into $\nu_{(C=O)}$ [161].

Besides gaseous and polymeric products, PAI thermal oxidation produces low-volatile substances condensed near the hot zone. Natural fractioning of these products by the reaction chamber and programmed heating in the mass-spectrometric analysis with direct injection to the source of ions make mass-spectra, measured at low ionizing stress (12 – 20 eV) with mostly molecular ions fixed, simpler. These mass-spectra simply trace series of molecular ions with mass step of 14 mass units: 216-230-244-258-272-286-300-314-328-342-356-370-384-398-412 etc. to 552; 231-345-259-273-287-301-315; 243-257-271-285-299-313-327-341-355; 371-385-399-413-427-441-455-469-483-511-525-539; 543-557-571-585-599-613-641-655-669-683-698. Moreover, mass-spectra possess separate molecular ions either interfering into homological sequences, but being more intensive rather than the neighboring ones and all sequence members (for example, peaks with 160, 230 and 543 m.u.), or singles outside the sequence (for example, 73, 82, 214, 109 m.u.), or inside the sequence, not occupying a sequence member place (for example, 460 m.u.).

These peaks belong to substances with somewhat "economic" structure, e.g. the structure with no breaks of the methylene backbone with mostly arylene and heterocyclic end groups, as well as methylene or ethynyl products of heterocycle degradation. In mass-spectra of thermal oxidation products, homological sequences of molecular ions mainly correspond to analogous sequences in mass-spectra of PAI pyrolysis products. Initial two sequences with uneven values for molecular ions correspond to mass-spectra of pyrolysis products by both distribution and multiplicity (ions-satellites of sequence members with mass numbers $\pm(1 - 3)$). E.g. they respond to methylene backbone fractures having phthalimide end group, alkane phthalimides with end methyl or ethyl group. The rest two uneven sequences include higher order oligomers than these formed in pyrolysis. For example, molecular ion with 543 m.u. starts the following homological sequence:

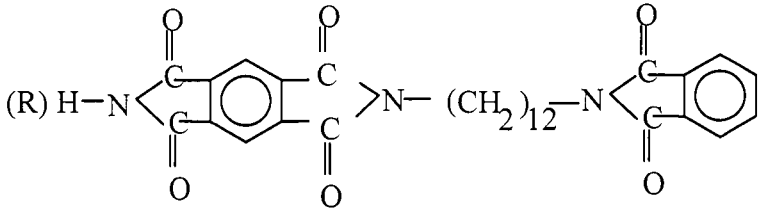

It is traced up to the last member of R = $C_{12}H_{25}$ sequence with the molecular weight 711. Therefore, thermal oxidation gives high yield of products representing the elementary unit fragment or fractures without methylene backbone fragments, or preserving it in full by means of end blockade similar to the above-mentioned product with molecular weight 543. Pyromellitimide and dodecamethylen diphthalimide are among these products.

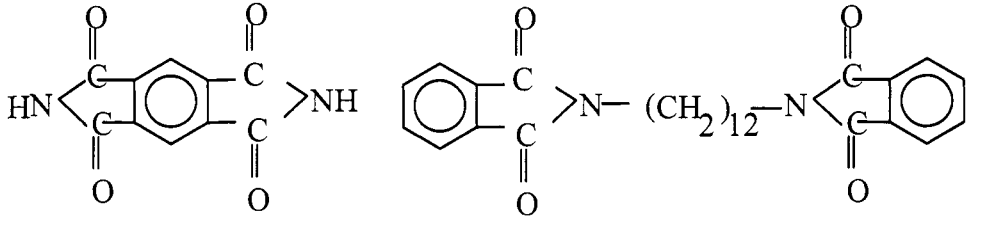

This molecular ion sharply interferes between alkane pyromellitimides. At thermal oxidation, homological sequence with even molecular ions is much longer than at pyrolysis. Tracing the intensity distribution and multiplicity, the second part of the sequence with molecular weights of 370 or higher is found analogous to some molecular ions of alkane pyromellitimide sequence formed at pyrolysis. The beginning of the even sequence of thermal oxidation products from 244 and 216 m.u. is not shown in mass-spectra of pyrolysis products. The intensity distribution in this half of the even sequence possesses the maximum at 230 m.u. Molecular ions in the first and the second half of the even sequence possess different multiplicities. Obviously, the even sequence is not a single homological sequence, but is formed by two independent sequences, one of which is represented by alkane pyromellitimides. Another sequence might be formed by oxidation products, containing C=O groups in the methylene backbone, for example:

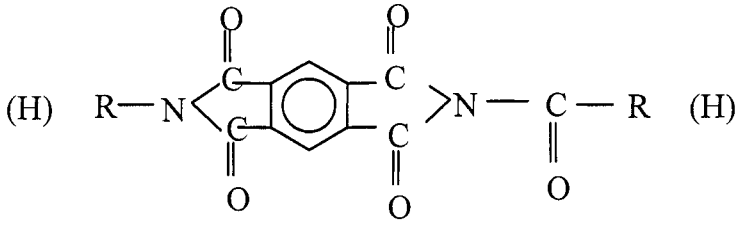

This oxygen-containing structure (possibly, an alternative of OH-containing structure) allows composing a sequence of homologues corresponded to experimentally obtained one. Enumeration of other alternatives does not give positive results, for example, nitrilephthalimide alkanes, which also form an even sequence. ^{1}H and ^{13}C NMR-spectroscopy data indicate the presence of carbonyl-containing aliphatic structures in thermal oxidation products.

Single, intensive molecular ions with 57, 73, 97 and 109 m.u. belong to nitrogen-containing products of pyromellitimide structure degradation. Comparison with the mass-spectra library shows that amides and pyrrolidone derivatives are most probable.

Judging by ^{13}C NMR-spectroscopy data, the part of polymelliiimide oligomers decreases with temperature in thermal oxidation products; vice versa, the contribution of phthalimide and substituted phthalimide oligomers, for example, nitrilephthalimide oligomers increases (Figure 16). These data allowed assessment of the mean molecular mass of thermal oxidation oligomeric products: 1,200 – 2,000 at 300 - 350°C and 350 – 700 at 400 - 450°C. Hence, the average length of methylene backbone twice decreases.

Finally, as PAI are subject to high-temperature thermal oxidation, the main degradation changes proceed in both methylene backbone and aromatic fragment, which is the imide cycle.

The unique property of PAI which differs it from the known polymeric materials, is high resistance to short-term (up to 30 s) thermal impact (260-280°C) without meltbacks and deformations that allows flow soldering of metal reinforcement [52].

Thermal aging (during 90 days) at 100 - 200°C [56] shows decrease of blow viscosity, stress at break and relative elongation of PAI at simultaneous change of polymer morphology (X-ray analysis and electron microscopy data). Thermal aging (1,000 hours at 170°C) and cycles of heating from -60 to +170°C

do not change the dielectric loss tangent and permeability, but an abrupt (almost by an order of magnitude) decrease of surface and volumetric electrical resistance is observed [52].

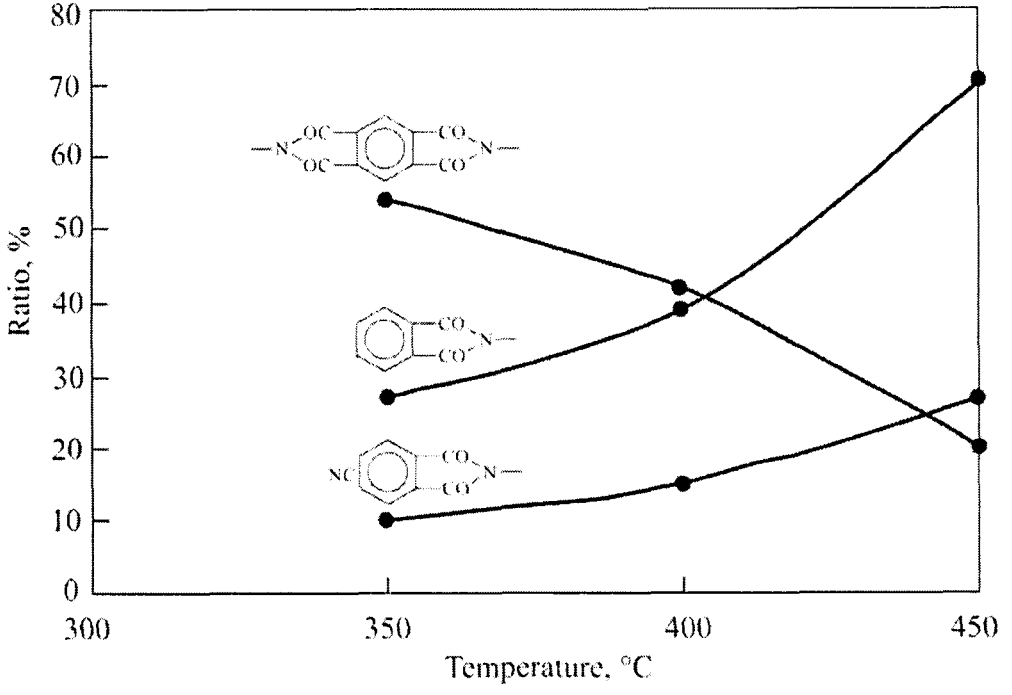

Figure 16. Changes in the ratio of structural fragments in oligomers at thermal oxidation of PAI (according to ^{13}C NMR-spectroscopy data)

Obviously, the mentioned macroscopic changes in PAI processing and operation temperatures are induced by definite changes in chemical structure of the polymer due to heat and oxygen effect.

Solid-phase oxidation

As obvious from IR-spectra of PAI subject to thermal oxidation at 200 - 250°C during 1,000 hours, the polymer, though slowly, is oxidized in the solid phase in the temperature range of operation: concentration of C=O-groups increases and methylene groups are clearly exhausted ($\nu_{(C\text{-}H)}$ bands at 2,800 –

2,900 cm^{-1}). Thermal oxidation during 1,000 hours at 250°C, i.e. under rigid operation conditions, leads to full burn off of methylene backbone and partial destruction of imide cycles (the occurrence and extension of $\nu_{(C-H)}$ band at 1,620 cm^{-1}). Similar observations were made [30, 32] at thermal oxidation of aromatic polypyromellitimide PM-1.

It is found that slow oxidation of aromatic nuclei happens already at 250°C. After several thousand hours, this process causes destruction of cycloarylene structure and the loss of macroscopic properties. Kinetics of O_2 absorption at 250°C (Figure 17) shows that thermal oxidation rate of fatty aromatic polyimide PAI is an order of magnitude higher than the oxidation rate of aromatic polyimide. Though in this case the main contribution is made by fatty chains, high reactivity is displayed by cycloaromatic structure in PAI should also be taken into account.

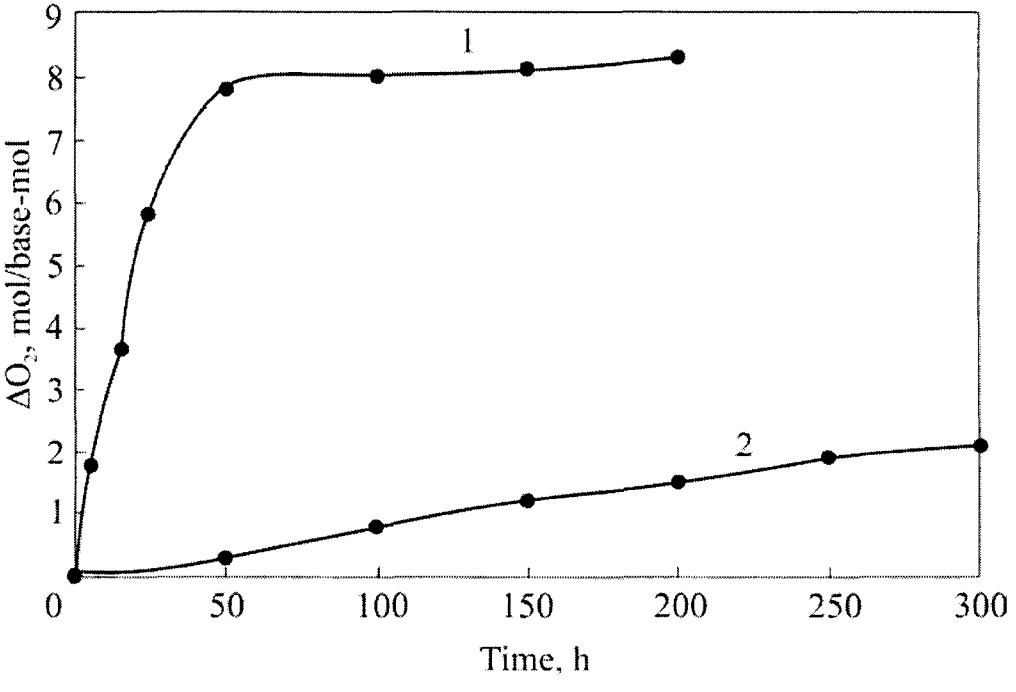

Figure 17. Kinetics of O_2 oxidation at thermal oxidation of PAI (1) and PM-1 (2) in air at 250°C

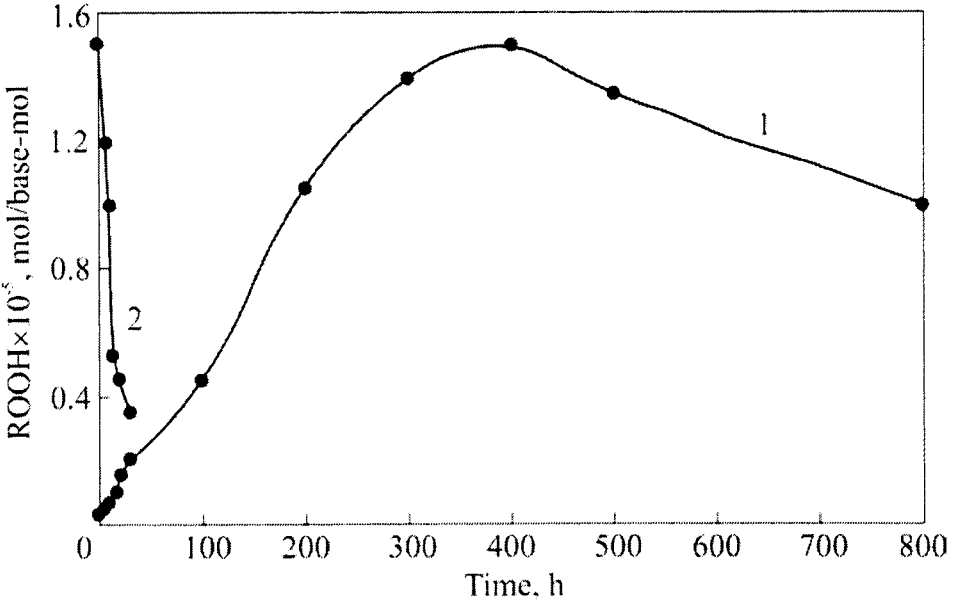

Figure 18. Kinetics of ROOH hydroperoxide accumulation (1) and decay (2) at PAI thermal oxidation at 200°C in air

As known in kinetics of liquid-phase reactions, oxidation of purely aromatic substances is induced by hydrocarbon additives as the source of peroxy radicals [8].

Predominant oxidation and degradation of fatty chains during thermal-induced aging noticeably exhausts the C and H element concentration in PAI (refer to Figure 14). As shown in experiments, 500 hour thermal oxidation at 200°C decreases C and H contents from 69.0 and 7.5 to 65.0 and 6.0%, respectively, with corresponded increase of oxygen concentration. Hydrogen is reliably detected during 800 hours of thermal oxidation. Hydrogen release kinetics correlates with the gel formation kinetics (Figure 19).

Thermal aging causes formation and accumulation of hydroperoxides (the iodimetric technique) in PAI (Figure 16). The kinetics of hydroperoxide ROOH accumulation is extreme. Accumulated ROOH concentrations (~1.5×10^{2} mmol/base-mol) are negligibly small (by five orders of magnitude lower) than absorbed amounts of O_2. Nevertheless, these negligible amounts are reliably detected during initial 800 hours of thermal oxidation. Meanwhile, ROOH is not

practically accumulated in methylene chains of PE, which oxidizes at extremely high rate of 2×10 mol/kg·s [10] at 200°C.

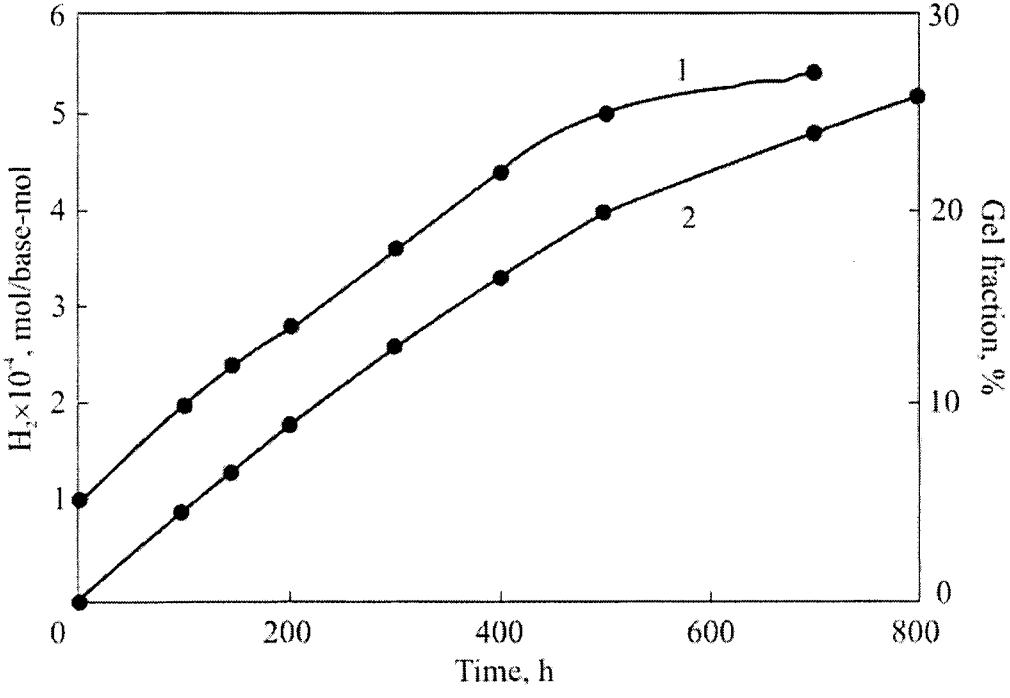

Figure 19. Kinetics of gel-fraction accumulation (1) and H_2 release (2) at PAI thermal oxidation at 200°C

In this case, high-temperature branching is assumed to happen via degradation of peroxy radicals. As known from the literature [152], ROOH is accumulated in PA-66 at 180°C. Similar to PAI, current kinetics of ROOH accumulation is extremely shaped, where maximal concentration $[ROOH_{max}] \approx 1.5 \times 10^{-2}$ mmol/base-mol is already reached 45 min after initiation of heating. In aliphatic PA, oxidized at 200°C, no hydroperoxides were detected. The absorption rate of O_2 at 200°C decreases in the sequence as follows: PE >> PA-66 > PAI (10^4, 0.1 and 0.01 mol/base-mol·h, respectively), whereas ROOH stability increases with the opposite order. Both sequences (directly and oppositely, respectively) correlate with the molecular mobility of polymers. At 200 °C, PE represents a melt, and PA-66 and rigid-chain PAI are solid. This comparison is valuable from positions of detecting the effect of the phase state

and macromolecule mobility on kinetics of the process proceeding in similar chemical structures in methylene backbones. Moreover, it is also important from positions of hydroperoxide exclusion from the process of high-temperature oxidation of polymers. Though thermal oxidation of PAI forms hydroperoxides, this classical direction of the oxidation process is apparently secondary due to the following reasons. Assume that the process is developed by the classical scheme with respect to additional, elementary reactions, suggested for hydrocarbon polymer thermal oxidation [10, 110]. Therefore, following from the balance equation for hydroperoxide in autooxidation reaction:

$$\frac{d[\mathrm{ROOH}]}{d\tau} = \alpha \cdot W(\mathrm{O}_2) - K_p[\mathrm{ROOH}]^n,$$

where α is hydroperoxide output per absorbed O_2; K_p is ROOH decay constant; n is the reaction order of ROOH degradation. At the extreme point, where $\frac{d[\mathrm{ROOH}]}{d\tau} = 0$:

$$\alpha = \frac{K_p[\mathrm{ROOH}]_{\max}}{W(\mathrm{O}_2)_{\max}}.$$

At 200°C, ROOH degradation (Figure 18) obeys the law of kinetic order one (n = 1) with $K_p = 1.7\times10^{-2}$ min^{-1}. E.g. at 200°C PAI autooxidation constant equals ~10^{-2}, which is much below values characterizing autooxidation of polyolefins in the solid phase [10]. Autooxidation of PAI at temperatures low for this polymer mostly develops by another way, but not via hydroperoxides, possibly by previously suggested mechanism of high-temperature oxidation [10, Chapter 3]. Definite similarity of cases follows from analysis of α for initiated, low-temperature oxidation and autooxidation of polyolefins [10]: α regularly decreases from 0.7 – 1.0 to 0.04 – 0.6 with oxidation temperature increase from 45 – 90 to 130 - 135°C.

The solid-phase oxidation of PAI at operation temperatures or intensified thermal aging (200 - 250°C) proceeds slowly, without releasing any heavy products. However, long exposures (about 1 year) induce formation of light-yellow pyromellite diimide crystals on the surface of molded PAI samples (Figure 20). Other heavy products of degradation, released at thermal oxidation

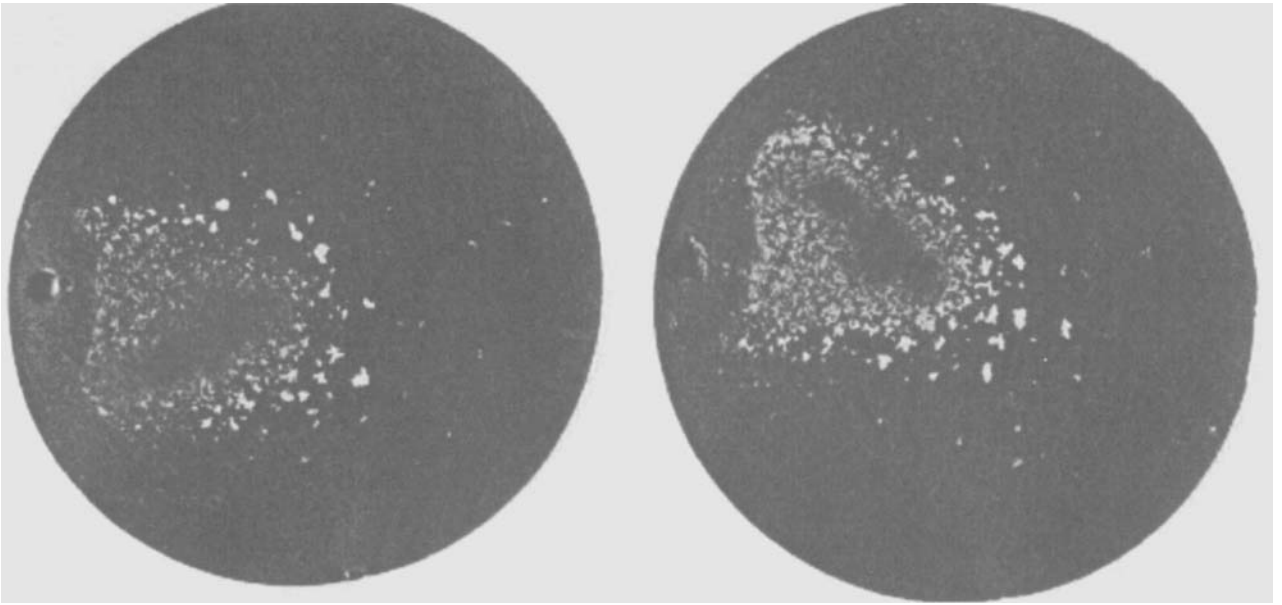

Figure 20. Aged polyalkanimide samples. Light crystals on the sample surface represent pyromellite diimide

of PAI in melt, are not identified here, though in this case random macrochain breaks occur, too, which is confirmed by permanent decrease of sol-fraction viscosity (refer to Figure 10). However, molecular mass of oligomers is so high that they do not practically diffuse into the solid phase and release from the surface, but remain in the polymer.

At statistical development of thermal oxidation along the macromolecule, formation of pyromellite diimide (attack 1 and 2) and other macrochain fractures, for example, methylpyromellitimide (attack 1 and 3), are of the same probability. Volatility of the latter is similar to that of diimide, i.e. formation of this product would be clearly observed.

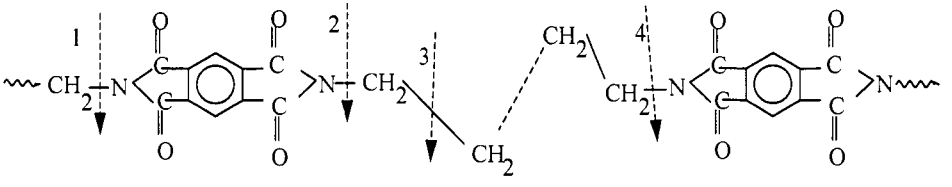

Similar explanation may be given to the alternative of attack 1 – 4 with release of undecane pyromellitimide. However, pyromellite diimide is the unique heavy product of PAI solid-phase oxidation. To put it differently, polymellit diimide formation testifies that, besides the mechanism of random O_2 attacks along the macrochain, the mechanism of α-CH_2-group oxidation activation in neighboring methylene chains, separated by pyromellitimide fragments, does exist or even dominates at relatively low temperatures.

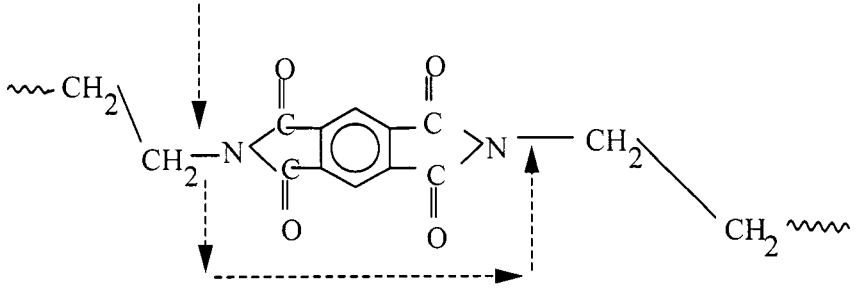

Quantum-chemical calculation of dimethylpyromellitimide model (refer to Figure 5) shows that σ-bonds of methylene groups are affected by π-systems of pyromellitimide fragment. Occurrence of new π-electron as a result of α-C-H-bond break at O_2 attack will affect the π-system of pyromellitimide fragment

and, further on, on σ-bonds of α-CH_2-groups in neighboring methylene chain, probably making them weaker or activating this group in any different way. A hypothetical mechanism of oxidation activation in PAI is somehow similar to the known allyl activation of PVC dehydrochlorination, when the structure defect, mainly π-system in the double bond or ketoallyl group, forms instability of neighboring Cl atom or entire elementary unit. In this labile fragment degradation is induced by Cl detachment. Hence, π-system develops originating the polyene sequence, which activates the following vinylchloride units [13]:

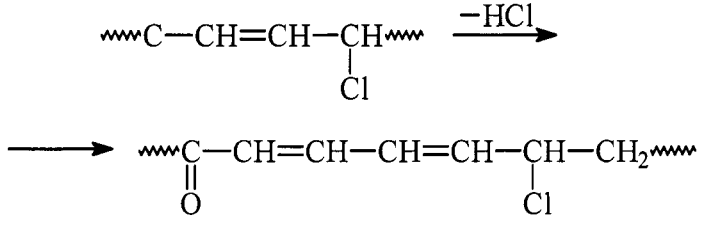

In the literature, another mechanism of oxidation center transfer is known, aimed at the immediate environment, but not statistically anywhere. At solid-phase oxidation of polyolefins, besides hydroperoxide groups, statistically disposed along macrochains, regular ROOH blocks are observed and frequently dominate [152]:

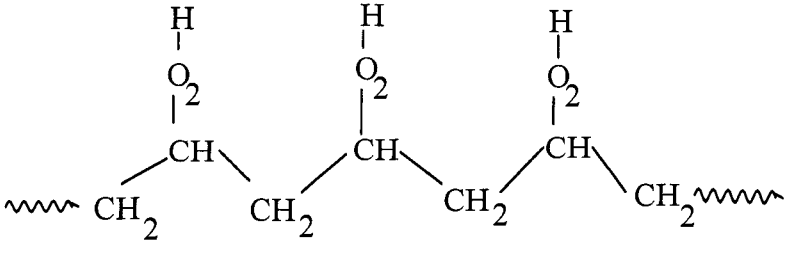

Formation of blocks is associated with kinetic disadvantage of intermolecular chain transfer

$$RO_2 + ROOH + R$$

and, vice versa, advantage of peroxy-radical isomerization via a six-term transition complex - the so-called "chemical relay":

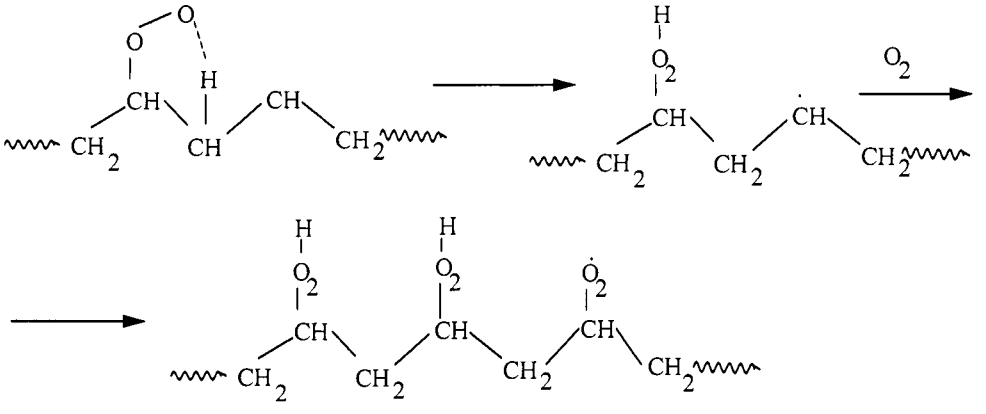

Obviously, such transfer of free valence in PAI is impossible due to geometrical hindrances:

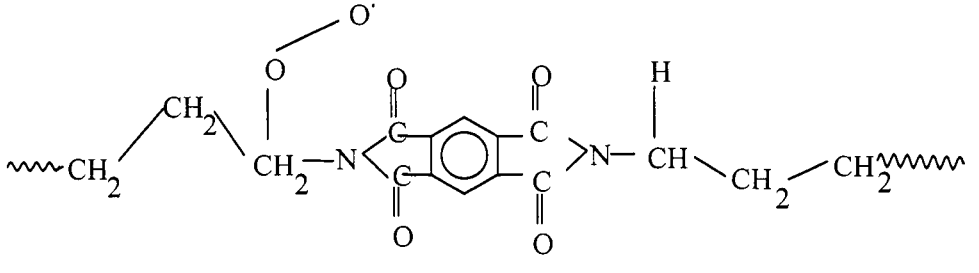

Most probably, RO_2 isomerization along self methylene chain would be expected. However, this does not create conditions for pyromellite diimide synthesis. Apparently, the hypothesis of α-CH_2-group electron activation by π-system of pyromellitimide fragment, linking them, has no alternatives.

Let us consider the probability of pyromellite diimide formation compared with longer macrochain fractures in neighboring methylene chains. Occurrence of the latter would be expected as a result of O_2 attack at all α-CH_2-groups. In the initial state, before the first O_2 attack, all α-CH_2-groups are basically equivalent, i.e. strengths of C-H-bonds in them are equal. Further on,

dealing with the experimental fact of exclusive pyromellite diimide synthesis at low temperatures (below 250°C), the authors suggest that any O_2 attack and middle macroradical formation

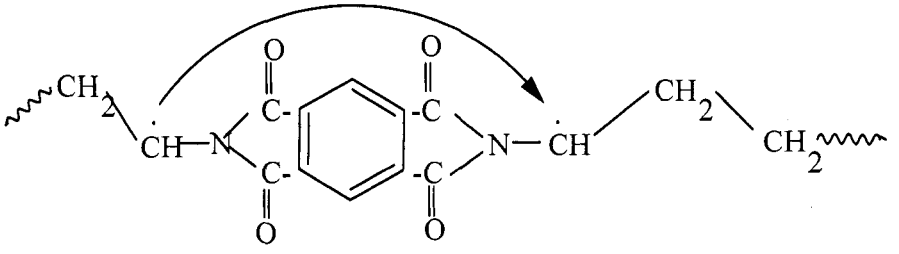

result in transiting excitation from π-system in peromellitic fragment to the electron system of neighboring α-CH_2-group due to occurrence of a free valence. As a result of additional α-C-H-bond weakening, oxidation is mostly realized at that place. Therefore, bonds break, and pyromellitimide "preparation" deteriorates.

The fact of bond weakening in radicals compared with their saturated analogues is known [78]. The known from the literature maximal weakening of C-H-bond, equal 21 kJ/mol, may be accepted [78]. The decrease of C-H-bond strength in α-CH_2-group, neighbor to previously attacked one, by 21 kJ/mol means that at 200 - 250°C the probability of new attack at this place is 100 – 120 times higher, than in other, not neighboring α-CH_2-groups. This means that precipitation obtained at PAI thermal oxidation would possess 1% or slightly less amount of other oligomers, for example, dodecamethylene dipyromellitimide. However, the practice shows that heavy products, formed at PAI aging up to 9,000 hours, give nothing except for yellowy crystals of pyromellite diimide.

Remind that pyromellite diimide is the unique heavy product of low-temperature oxidation of classical polyimide PM-1, or Kapton [32]. Moreover, the product of similar structure compared with the primary macromolecule – 2,2'-(1,4-phenylene)-bis-(3-phenylpyrazine) (PPP), is synthesized at aging of polyphenylquinoxaline [154]. Terephthalic acid amid was also detected at thermal oxidation of polyphthalimides [254].

Formation of PDI, TPC amide and PPP indicates a specific feature of thermal oxidation of poyheteroarylenes, which has not been discussed before in the literature. Mechanical description of their formation, i.e. oxidation or

"burning off" of one of pyromellitic (or phthalamide) fragment boundary first and subsequently induced destruction of another boundary may not explain the absence of competition from the side of analogous, but larger fractures even in the presence of a noticeable difference in C-H-bond strengths in induced and rest α-CH_2-groups. Two explanations may be given:

1. Induced weakening of C-H-bond is much higher – 41 kJ/mol, for example. In this case, the probability of PDI formation is by three orders of magnitude higher, than for other diimides. However, so abrupt strength loss by one bond in the α-CH_2-group, induced by a free valence formation at the periphery of conjugated fragment, must be accompanied by simultaneous strength loss of other bonds in this group (for example, C-C-bonds with β-CH_2-group). Taking into account lower strength of C-C-bonds compared with C-H-bonds, an additional strength loss would lead to preferable thermal breaks of α-C-C-bonds and noticeable content of methylpyromellitimide in degradation products. However, this was not observed even at high temperatures.
2. The second hypothesis is corresponded to the idea about molecular complexes of O_2 with substrates, which is not practically used in thermal oxidative degradation of polymers. The existence of O_2 molecular complexes with many individual organic compounds was proven (particularly, using NMR-spectra) in works by Buchachenko *et al.* [86]. As suggested before [154], oxidation of hydrocarbons is initiated by molecular complex formation with O_2. Formation of O_2 molecular complex with pyromellitic fragment and its consecutive decaying with oxidation initiation simultaneously on two methylene chains principally solves the problem of synchronization required for exclusive pyromellite diimide detachment, but not any other products of this type.

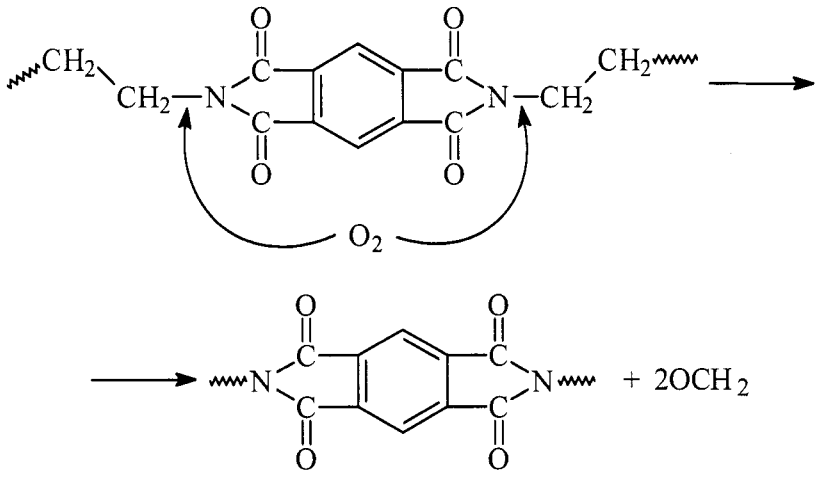

There are no direct proofs of such complex formation with PAI, as well as with other polyheteroarylenes. By analogy with [154], the authors studied a possibility of O_2 molecular complex formation with model PAI compound – didodecyl pyromellite diimide. To remove humidity and probably sorbed O_2, the model was preliminarily heated up at 120°C in vacuum during 1 hour and then dissolved in chloroform. The blend was degasified with argon first in a flask and then in a cuvette. UV-spectra of the model were measured compared with control cuvette, filled with chloroform, which was treated similar to the solution. After measuring the spectrum of argon-degasified sample, cuvettes were blowdown with pure O_2, and spectra were measured again. After O_2 blowdown spectra of the model display increased intensity that may be associated with O_2 absorption (direct influence) by didodecyl pyromellitimide (Figure 21).

Another experiment was performed on PAI. As heated in air, PAI intensively absorbs O_2, specifically during melting, when molecular motions are defrost. This is accompanied by an intense exothermal DTA effect. One may suggest that intensive absorption of O_2 in the melting range is associated with direct interaction between O_2 and imide fragments proceeding by the above-mentioned scheme. However, such interaction may also proceed at room temperature, possibly not only with oxygen, but, for example, with I_2, though oxidizing power of the latter is much lower. Thermograms for PAI, vacuumed at 200°C during 1 hour to remove humidity and sorbed O_2 and then exposed in

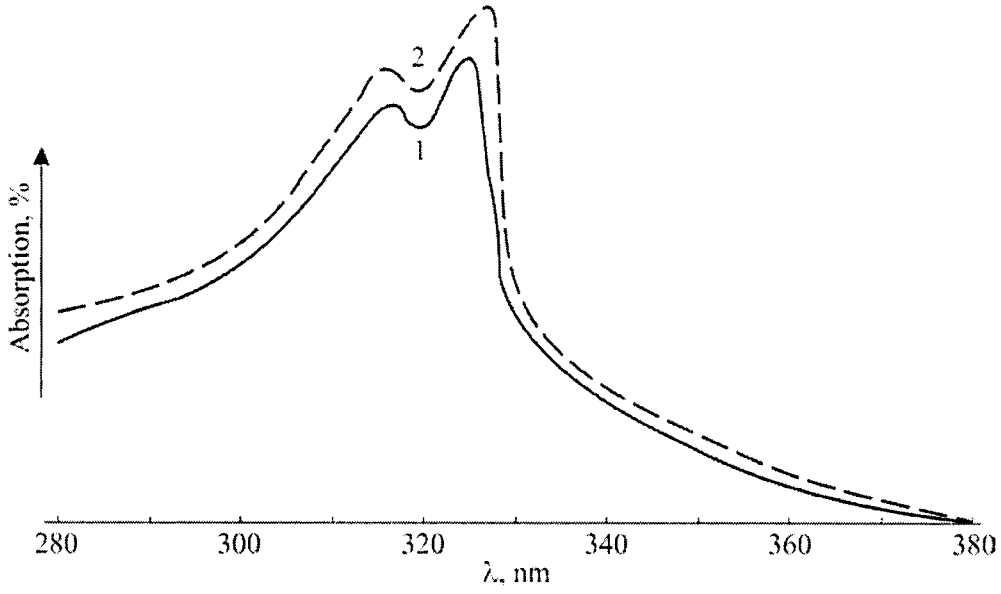

Figure 21. UV-spectra of model PAI compound – didodecyl pyromellite diimide, before (1) and after (2) blowdown by pure O_2

I_2 vapors during 1 and 24 hours, were measured in air and compared (Figure 22). It was observed that the intensity of exothermal peak decreases symbate with time of exposure in I_2 vapors. Seemingly, at room temperature O_2 (currently, I_2) really forms a complex with PAI fragments located on the surface. Molecular mobility increases with temperature, and zones previously located "deep inside" become capable of complex formation. Unfortunately, there is no I_2 in the system anymore, but free access of O_2 is provided, and it occupies free places and, thus, forms complexes. Some already mentioned features of PAI thermal oxidation and, the more so, its resistance to thermal oxidation, discussed below, may be explained only from these positions.

Let us consider another example – thermal oxidation and thermal stabilization of aliphatic polyamides, which by phenomenology are close to PAI. Thermal oxidation of PA, described in the literature [26], is identical to the classical scheme of hydrocarbon oxidation. Hence, these schemes do not explain some facts, for example, a significant increase of PA thermal stability at N-alkyl substitution. Moreover, high antioxidant activity of Cu^{2+}/I^- system may not be explained in the framework of hydroperoxide mechanism, though it exceeds all classical antioxidants in efficiency.

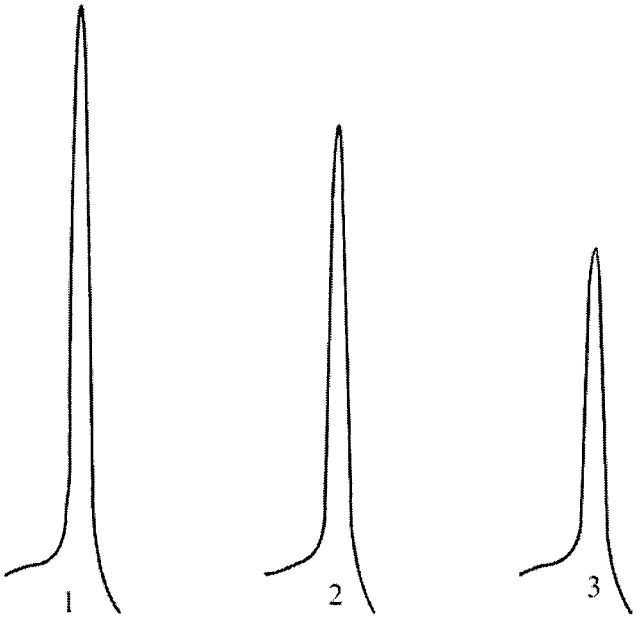

Figure 22. PAI thermograms before (1) and after processing by I_2 during 1 (2) and 24 hours (3)

Deactivation of peroxy-radicals or hydroperoxides by π-system is not confirmed because of specific action of the system in PA only and, at most, the absence of stabilizing effect in polyolefins which are exclusively subject to radical-chain oxidation reactions. Besides Cu, other transition metals are also effective in PA. Moreover, the sequence of their antioxidant activity coincides with the Poling sequence of electronegativity [155]. The latter, in turn, correlates with the ability to complex formation or stability of unitypical complexes. The idea of molecular complexes suggests an alternative to the act of thermal oxidation initiation and a possibility of inhibition. The idea that molecular complexes of organic substances with O_2 participate in oxidation occurred, when they were detected by Evans [154]. Complex formation with hydrocarbon is reversible reaction due to thermal instability, and it has no consequences for the substrate. Therefore, this reaction is not considered in schemes of thermal oxidation of polymers, though properties of the complex (for instance, with heterogroups) may be absolutely different, and the ways of transformation may destroy the polymer. Anyway, addition of the radical-chain scheme with this act allows explanation of thermal oxidation features of PAI

and other polymers containing secondary and tertiary amino groups (for example, hydrogen release at thermal oxidation).

The idea of O_2 molecular complex with π-system of heteroaromatic fragment does not exhaust all possibilities of explaining anomalies in thermal behavior of PAI and analogous polymers. Basing on the studies of thermal behavior of some highly heat-resistant nitrogen-containing, organic polymers, the authors [35] suggested transfer of macromolecules possessing developed conjugation system into electronically excited state as the initiation act for the radical-chain oxidation process. Here oxygen plays the role of suppressor – activator of intercombinatorial transitions, i.e. similar to O_2 role in photo processes. Experimental data indirectly prove participation of electronically excited states in the degradation process. Recently, quantum-chemical analysis of thermal behavior of phthalimide cycle as the polyimide model was performed [157]. The energetic possibility of purely thermal transferring the model to the triplet state already at 500°C is shown. From this state radical decays and H-transfers are initiated, which lead to crosslinking of models and destruction of imide cycle with carbon oxides and water release. Excitation levels in conjugated macromolecules are much lower than in low-molecular models. This is confirmed by quantum-chemical calculations of models and polyheteroarylene oligomers [158], and by disposition of the long-wave boundary in UV-spectra. Therefore, macromolecules may be transited into electronically excited state at temperatures lower than indicated by the authors [157]. The absence of O_2 increases the probability of intercombinatorial transition into reactive triple state.

In the present context we may not choose between two mentioned alternatives of pyromellitic fragment activation in PAI or polyimides. Here of importance is another thing: degradation behavior of PAI and other polyheteroarylenes displays a mechanism, conditionally called the "quick response", which leads to local development of degradation with specific product output. Such "quick response" may be performed only in the system of molecular orbitals of polymellitic fragment which, affected by O_2 and temperature, initiates or promotes initiation of radical-chain oxidation, yet developed in fatty chain of PAI. At low temperatures, pyromellitic fragment acts like somewhat a magnifying glass which focuses sunlight rays to a point and ignites the sample. However, as temperature increases to the processing level, degradation is also initiated in this rigid fragment of the macrochain.

Injection of additives is the common method for studying the mechanism of chemical reactions. Phenol antioxidants inhibit oxidation in

reactions with peroxy-radicals PO_2 and at 250°C, in concentration of $10^{-3} - 10^{-2}$ mol/kg slows down O_2 absorption in PAI (Figure 23). Kinetics of O_2 absorption by PAI is characterized by the absence of induction period. Therefore, critical concentration of antioxidant may not be determined. The concentration dependence of antioxidant efficiency, determined from the ratio of initial rate constants of O_2 absorption by unstabilized and stabilized PAI is optimal at concentration of 0.008 mol/kg. Though antioxidant effects induced by phenol injection are low (probably, due to high temperature [10] and the absence of optimal composition at the current stage), the fact of slowing down by low additions confirms once again the contribution of radical-chain oxidation to thermal oxidative degradation of PAI.

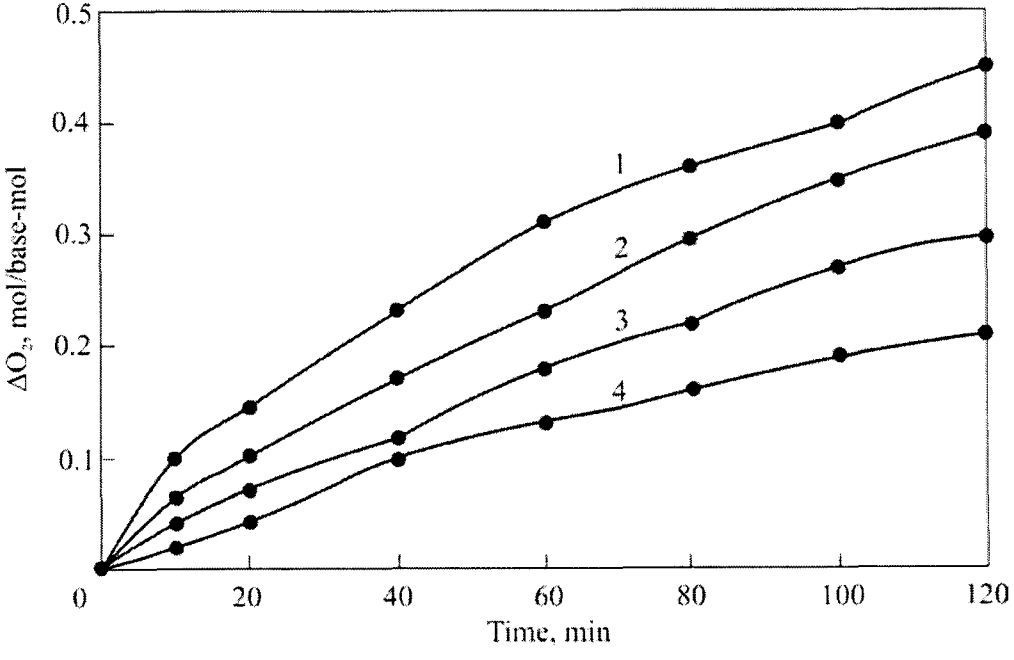

Figure 23. Kinetic curves of O_2 absorption at thermal oxidation of PAI: initial (1), added by 1 wt.% *Irganox 1010* (2), 2 wt.% *BT-5* (3), a mixture of 0.05 wt.% $CuSO_4$ and 2 wt.% *BT-5* (3).
$T = 250$°C, $P_{O_2} = 266.6$ kPa

As shown above, some features of PAI thermal oxidation do not fit traditional schemes. The suggestion about existence of molecular complexes

with O_2 or other nontrivial initiation acts leads to analogy of PAI with aliphatic PA or classical polyimides, thermal oxidation of which is hindered by addition of Cu^{2+}/I^- complexes [26] and organophosphorous compounds, respectively. For example, anilidophosphoric acid diphenyl ether (compound BT-5) is the most effective in polyimides [35]. Injection of the mentioned additives to PAI at 250°C slows down O_2 absorption more intensively (Figure 23) than phenol antioxidants. The effectiveness of additives is also observed at higher temperatures (Figure 24), at which phenols are absolutely ineffective.

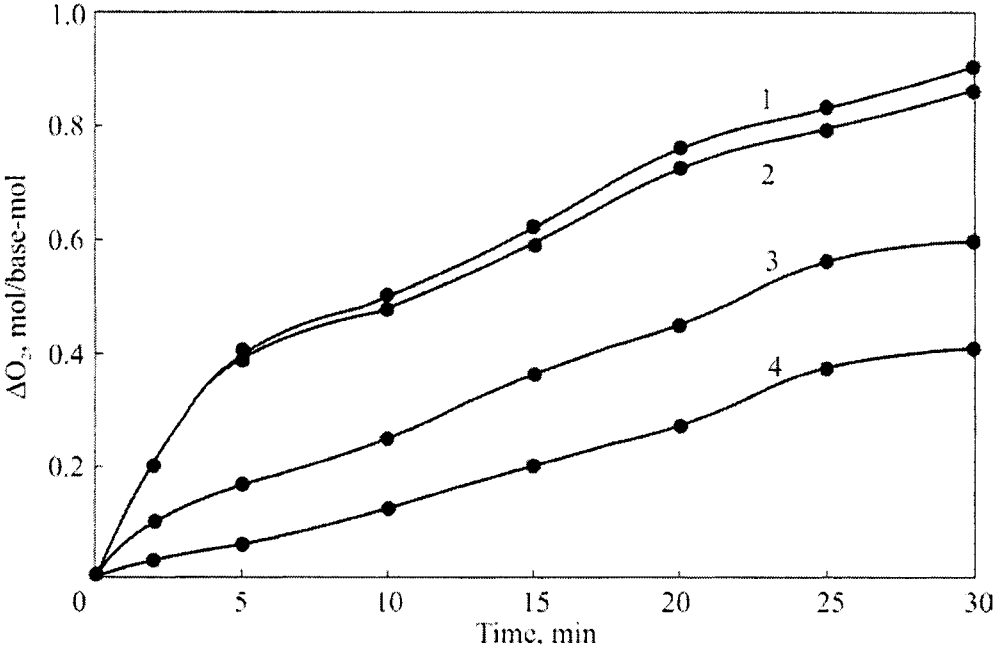

Figure 24. Kinetic curves of O_2 absorption at thermal oxidation of PAI: initial (1), added by 1 wt.% *Irganox 1010* (2), 2 wt.% *BT-5* (3), a mixture of 0.05 wt.% $CuSO_4$ and 2 wt.% *BT-5* (3).
$T = 320°C$, $P_{O_2} = 266.6$ kPa

The dependence of Cu^{2+}/I^- addition efficiency on concentration has a peak (Figure 25), analogous to the case of aliphatic PA. Even extremely low concentrations of Cu^{2+} are highly effective in PAI. On the contrary, injection of this system to PE destabilizes methylene chain at any temperatures (Figure 26). Though methylene chain in PAI is quite long, the test with the additive and

comparison with PE definitely indicate importance of a heterofragment in the oxidation process.

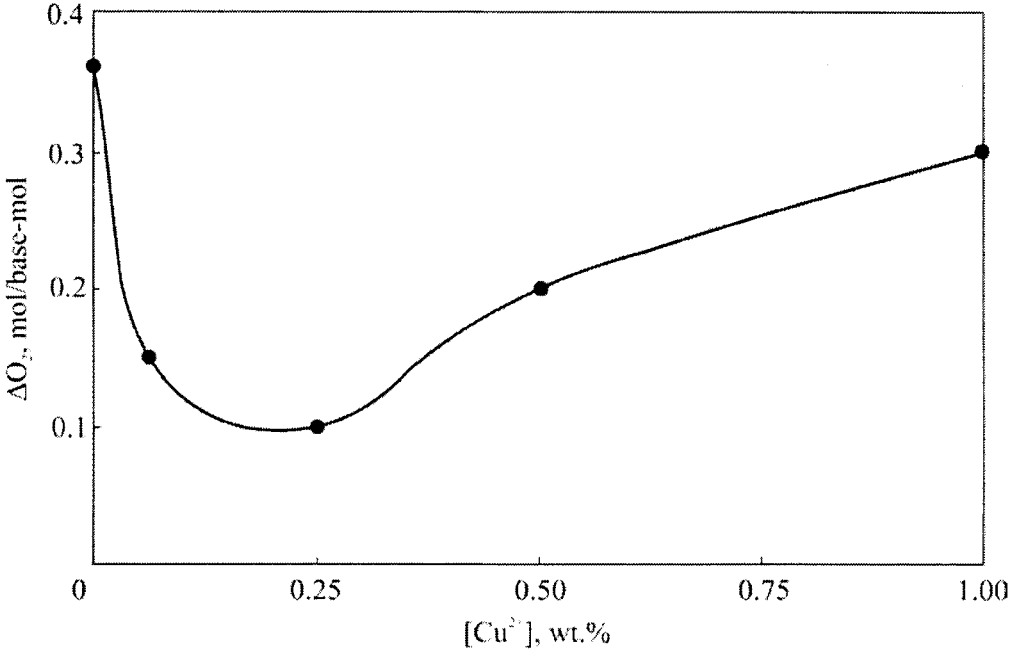

Figure 25. Dependence of PAI thermal stability (by O_2 absorption at 250°C during 1 hour) on Cu^{2+}/I^- concentration

Finally, PAI in its structure has quite long flexible methylene chain, oxygen attackable as any hydrocarbon chain, specially at heating, and a rigid pyromellitic fragment possessing high resistance to oxidation. As compared with other polymers having methylene chains in their structure, PAI are much more stable. This results not from chemical reasons, but from the action of kinetic factors, determined by physical structure of polymeric body, which remains solid up to high temperatures. Physical structure rigidity and limitation of molecular motions in the polymer are determined by pyromellitic fragment. To put it differently, these structures stimulate physical protection mechanisms for an aliphatic chain. On the other hand, from pure chemical positions, if physical limitations are eliminated, pyromellitic fragment increases reactivity of border methylene groups, more active in the reaction with O_2 rather than "internal" groups of methylene chain. Oxidation, hindered in the solid phase,

bursts out in the polymer melt affecting the whole aliphatic chain and partly, to a lesser extent, an aromatic fragment.

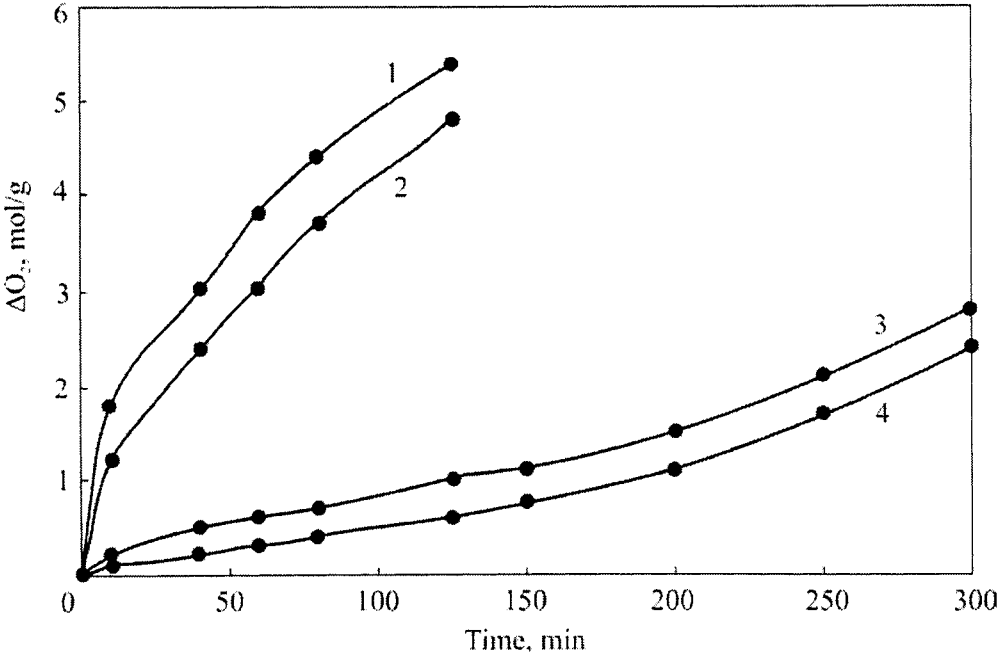

Figure 26. Kinetic curves of O_2 absorption by PE: initial (1, 2) and added by 0.05 wt.% $CuSO_4$ (3, 4) at $T = 320$ and 200°C, respectively. P_{O_2} = 399.9 kPa

Some specific features of PAI thermal oxidation are clearly displayed at low temperatures at the background of typical radical-chain hydroperoxide oxidation of hydrocarbon chain and, to the authors' point of view, indicate chemical functionality of pyromellitic fragment in the degradation process. Antioxidant action of classical antioxidants of the phenol type is much lower than that of copper ion and phosphate, seemingly untypical antioxidants. Oxidation leads to pyromellitic fragment emission from macromolecule in the form of pyromellite diimide or to crosslinking with H_2 release, which is fully absent at degradation of methylene chains in hydrocarbon polymers. One may suggest that pyromellitic and phthalamide fragments participate in the degradation process, besides, not only by activation of α-bonds in neighboring flexible chain, but possibly materially. Though direct proofs are absent yet, the

authors suppose that, besides classical initiation, for example, of the following type:

$$RH + O_2 = R + HO_2,$$

where PH is methylene chain, thermal oxidation is initiated by an act with participation of an aromatic fragment. It may be formation of a molecular complex from one or several molecules of O_2 with π-system of the fragment or thermal transfer of the fragment to the triplet state with the help of O_2. The following initiation reactions are of importance.

1. Classical direction

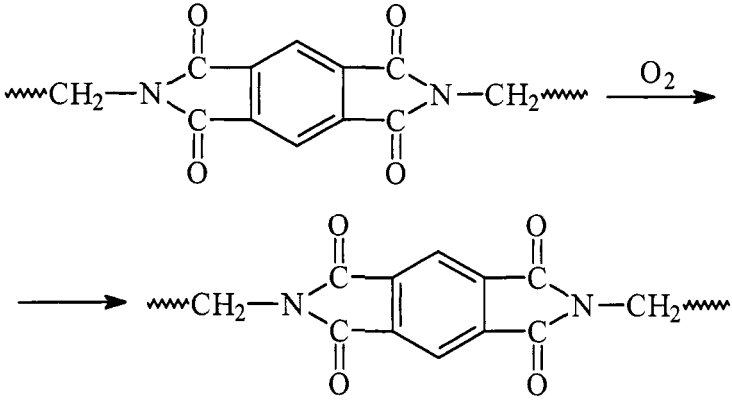

2. Formation and decay of molecular complex with O_2

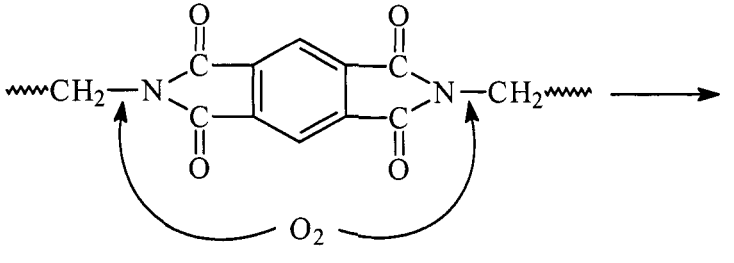

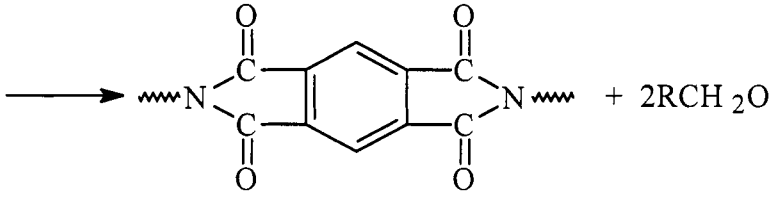

3. Transfer to electronically excited state

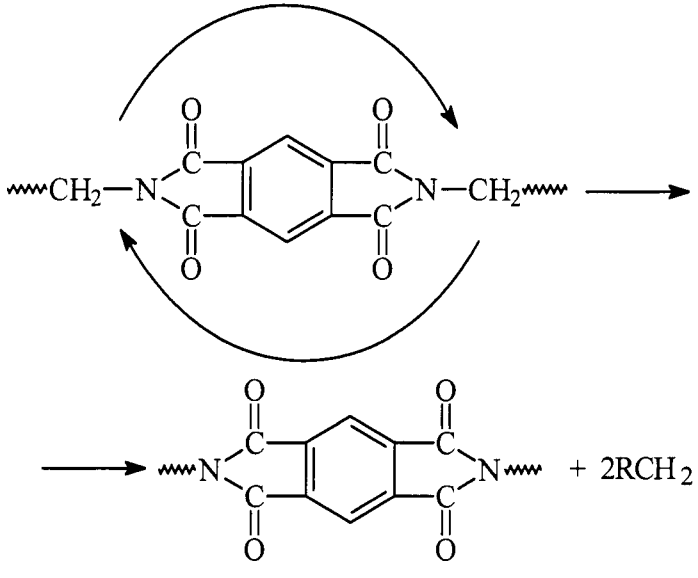

Further stages of the process fit traditional radical-chain scheme with the full selection of appropriate degradation products.

Chapter 2. Degradation of aliphatic-aromatic polyamides

This Chapter shows investigation results on two aliphatic-aromatic polyamides [254]:

Polyphthalamide 1 (PPA-1)

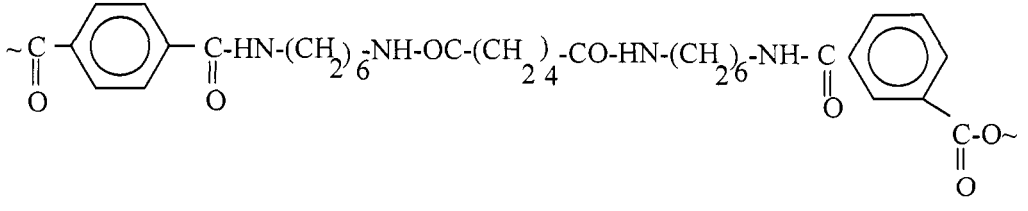

based on terephthalic (TPA), isophthalic (IPA) and adipic (AA) acids, and hexamethylene diamine. In accordance with ^{13}C and ^{1}H NMR data, the component ratio is the following (Table 4).

Table 4

Method	Concentration, molar parts			
	Hexamethylene diamine	AA	IPA	TPA
^{1}H	0.51	0.05	0.15	0.29
^{13}C	0.49	0.05	0.15	0.31

International analogue *Amodel* (Amoco).

Polyphthalamide 2 (PPA-2) based on terephthalic acid (TPA), 2-methyl-pentamethylene diamine (PMA) and hexamethylene diamine:

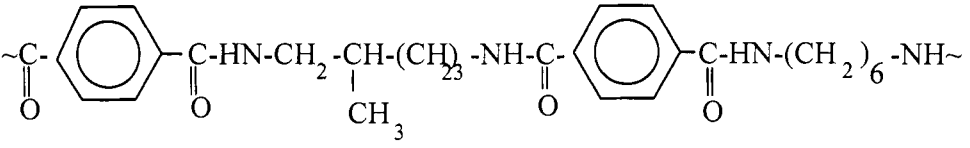

According to ^{13}C and ^{1}H NMR data, the ratio of components is the following (Table 5).

Table 5

Method	Concentration, molar parts		
	Hexamethylene diamine	PMA	TPA
^{1}H	0.25	0.25	0.5
^{13}C	0.25	0.25	0.5

International analogue HTN (DuPont).

HIGH-TEMPERATURE DEGRADATION

According to dynamic TGA data (Figure 27), mass losses of PPA-1 and PPA-2 in air and in argon are observed at temperatures above 330°C. Degradation in air proceeds in two stages:

- in the temperature range of 330 - 450°C mass losses reach 75%;
- at 450 - 475°C a bending is observed on TGA curve, and in the range of 475 - 575°C polymer degrades completely.

Degradation in argon flow proceeds in one stage, in the temperature range of 300 - 500°C. In this case, about 10% coke residue is formed. It should be noted that PPA-1, having a fragment of isophthalic acid in its structure, is characterized by slightly lower thermal stability. This correlates well with the observations [255 - 260] made by the authors who were the first investigating aromatic polyamides derived from various diamines and phthalic acids using TGA technique. It is shown that thermal stability depends upon location of carboxyl and amino groups in benzene ring and increases in the following sequence: ortho-ortho (200°C), ortho-meta, ortho-para, meta-meta, para-para

(530°C) compounds. This is explained by higher molecular mobility of isophthalic derivatives at the melting point, which is proved by data of thermomechanics and NMR [261 – 263].

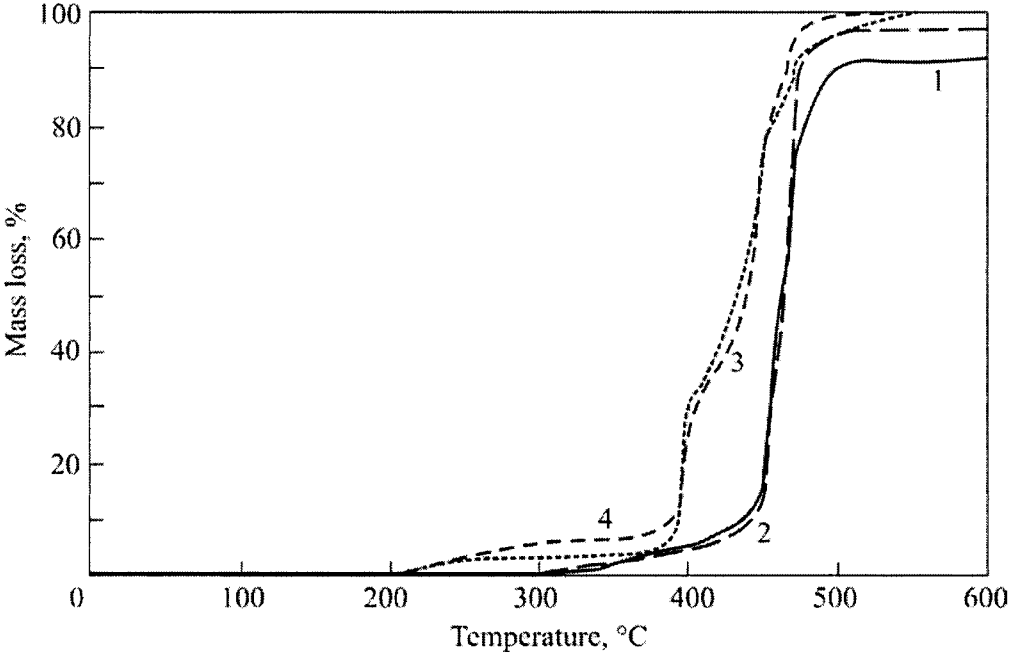

Figure 27. Dynamic TGA at 10°/min rate in argon flow (1, 2) and in air (3, 4) for PPA-1 (1, 3) and PPA-2 (2, 4)

At the initial stages, when mass losses are below 20%, thermal and thermal oxidative degradation of PPA-1 and PPA-2 obey order one kinetic law. Activation energies of PPA degradation in air and argon flow equals, respectively: for PPA-1 E_{air} = (126 ± 10.0) kJ/mol, E_{argon} = (184 ± 10.0) kJ/mol; for PPA-2 E_{air} = (118 ± 10.0) kJ/mol, E_{argon} = (165 ± 10.0) kJ/mol.

DTA curves (Figure 28) describe all stages of PPA-1 and PPA-2 degradation. The two-stage degradation in air is accompanied by exothermal and endothermic effects, whereas in argon it displays a wide endothermic peak which is the melting peak observed in the temperature range of 300 - 340°C. The absence of the melting peak for PPA in air (by analogy to PAI degradation [163, 164]) may be easily explained by intensification of thermal oxidation in softened or melted sample. Exothermal heat effects of oxygen absorption and

degradation overlap low endothermic melting peak. Closeness of melting (processing) temperatures and temperatures of degradation reactions makes processing of heat resistant polymers much more difficult. PPA-1 and PPA-2 are representatives of this class of polymers.

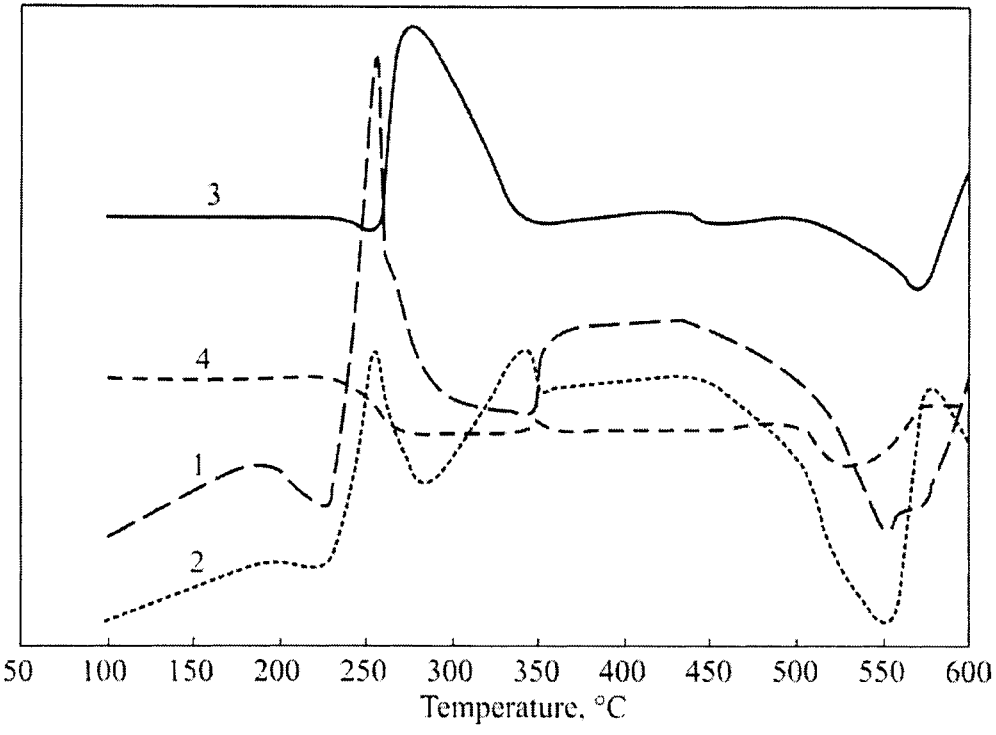

Figure 28. Dynamic DTA of PPA-1 (1, 3) and PPA-2 (2, 4) in argon flow (1, 2) and in air (3, 4)

Figures 29 and 30 show isothermal TGA data for air and argon flow at 300 - 340°C. The processing time interval with no respect to material presence in stagnation zones is low and, totally, does not exceed 15 – 20 min. In this case, mass losses of studied polymers do not exceed 1.0 - 2.0%. However, degradation is detected even visually, by yellowing of samples. Figure 31 shows dynamics of yellowness index (YI) increase during thermal processing of PPA-1 and PPA-2 in air and argon flow. Obviously, yellowing of polymers in the presence of oxygen is more intensive. For example, during 15 min of thermal oxidation in melt at 345°C $YI_{PPA\text{-}1}$ increases from 12.0 to 40.0 and $YI_{PPA\text{-}2}$ from

10.0 to 44.0. *MFI* is also sensitive to thermal load. The increase of thermal processing time leads to noticeable MFI decrease, especially in initial 20 min. For example, for PPA-1 $PTR_{10\ min}$ = 34.0 g/10 min, $PTR_{20\ min}$ = 6.0 g/10 min, and thermal stability coefficient (TSC) equals:

$$TSC = \frac{MFI_{10\,min}}{MFI_{20\,min}} = 5.7.$$

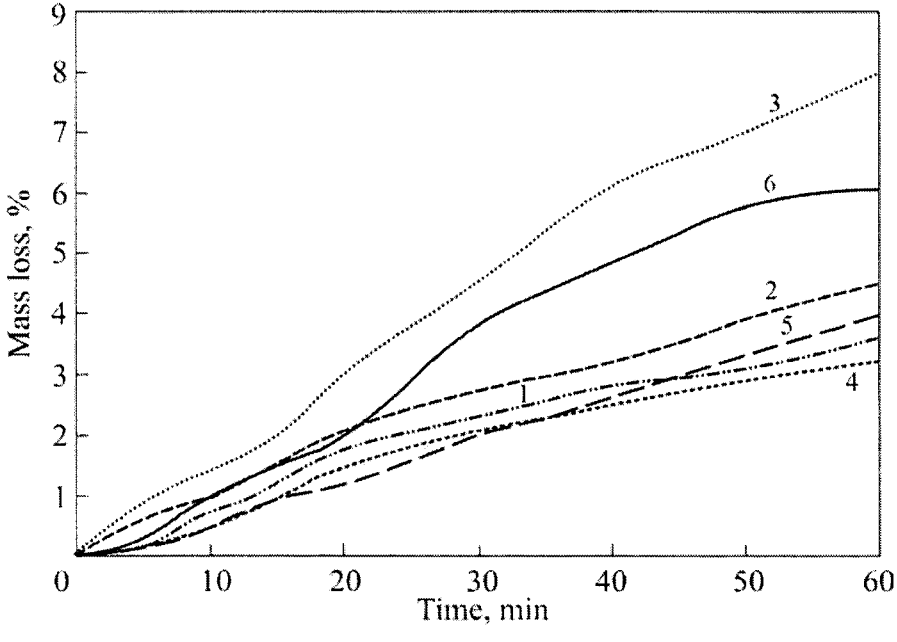

Figure 29. Isothermal TGA data in air for PPA-1 (1 – 3) and PPA- 2 (4 – 6) at T = 300°C (1, 4), 325°C (2, 5) and 340°C (3, 6)

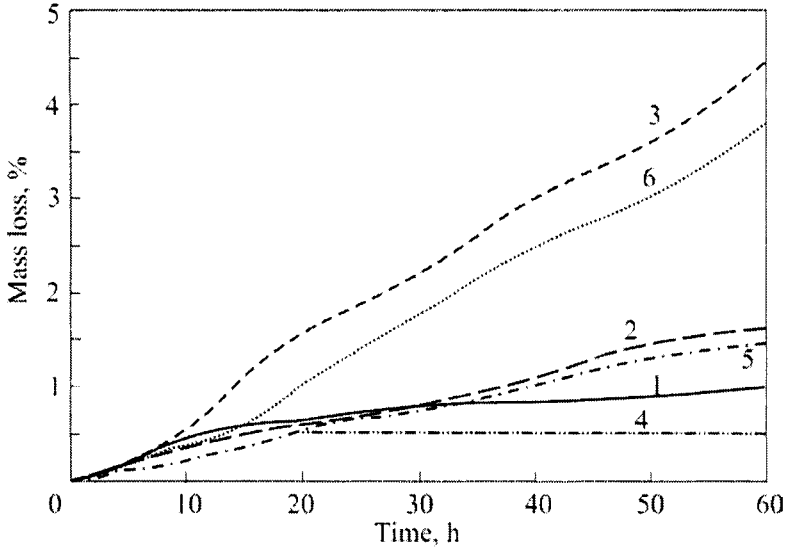

Figure 30. Isothermal TGA data in argon flow for PPA-1 (1 – 3) and PPA- 2 (4 – 6) at $T = 300°C$ (1, 4), 325°C (2, 5) and 340°C (3, 6)

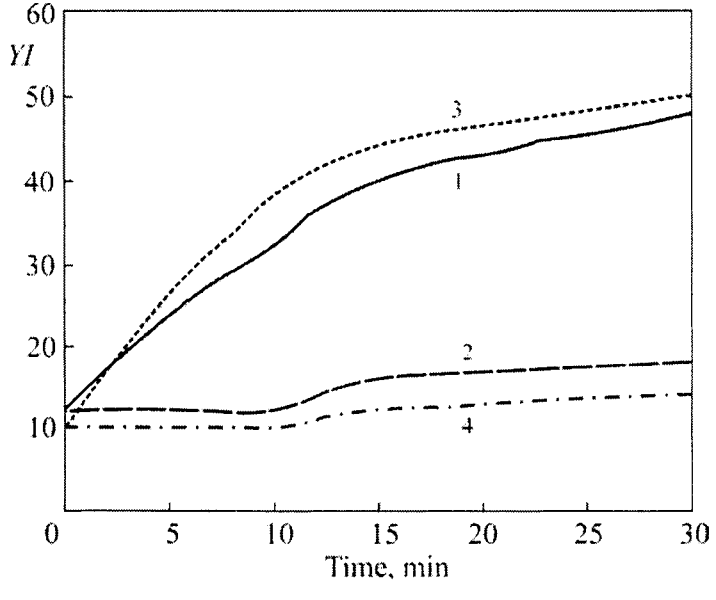

Figure 31. YI variation for PPA-1 (1, 2) and PPA-2 (3, 4) at thermal processing in air (1, 3) and argon flow (2, 4) at 340°C

Figure 32 shows data on the melt index changes for PPA-1 at melt exposure. The experiment simulates stages of obtaining basic polymer (temperature-time impact on polymer material):

1st extrusion (compounding after synthesis) ~ 5 min;
2nd extrusion (preparation of composite materials) ~ 5 min;
article press molding - the material is located in a machine cylinder ~ 10 - 15 min.

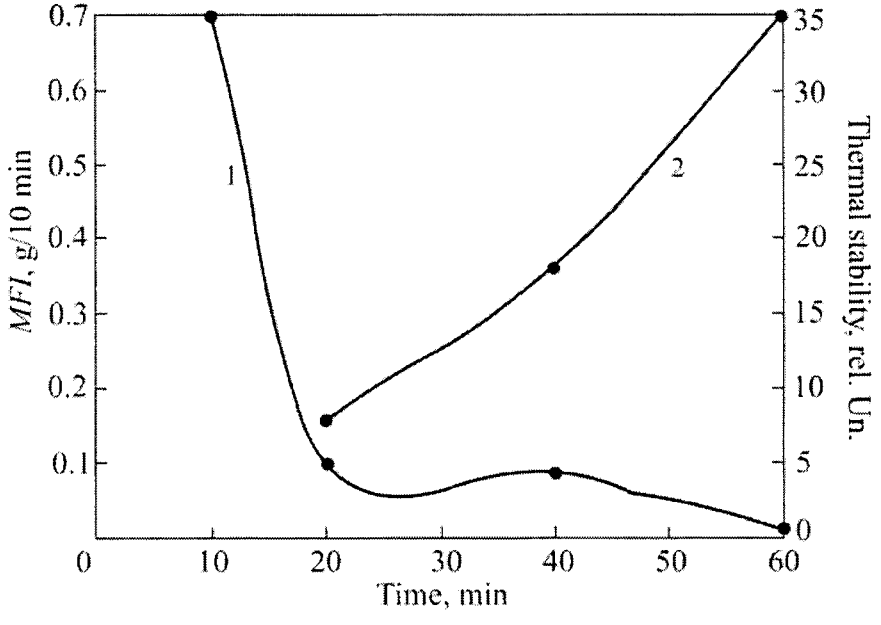

Figure 32. MFI (1) and TSC (2) variations for PPA-1 during thermal processing in IIRT device (350°C, 10 kg load)

Thus, high-temperature impact with no respect to material presence in stagnation zones lasts ~ 15 – 20 min. Investigation results (TGA data, YI) indicate PPA thermal stability decrease during the processing.

Essentially, similar to PI, aliphatic-aromatic polyamides represent complex objects for studying degradation transformations due to their limited solubility. For example, at room temperature PA derived from aromatic dianhydrides and aliphatic diamines dissolve only in concentrated sulfuric and trifluoroacetic acids [266]. Therefore, current data on molecular-mass

characteristics were obtained owing to good progress in development of high-temperature liquid chromatography, its GPC version, in particular [267]. PPA molecular-mass characteristics were determined from polymers dissolved in *m*-cresol. The studies were performed by chromatography methods at 135°C. The mean molecular mass of PPA samples was estimated using light scattering technique (LALLS) in h-fluoroisopropanol solutions. Then molecular mass momentums (M_w, M_n, M_z) were recalculated with respect to obtained calibration coefficients. For example, values obtained for PPA-1 were the following (Table 6).

Table 6

PPA-1 molecular masses

Sample	M_w (LALLS)	Calibration by PS			Calculated values		
		M_w	M_n	M_z	M_w	M_n	M_z
No. 1	36,300	90,200	15,000	360,000	39,700	6,700	196,000
No. 2	22,500	53,000	11,000	230,000	21,600	4,500	75,000

Two PPA-1 samples were tested, twice different in molecular mass. Drying in vacuum at 80°C caused a significant decrease of $PTR_{10\ min}$. Humidity contained in PPA acts as a plasticizing agent. For example, PPA-1 with M_w = 39,700 and equilibrium humidity ≅ 5% possesses $PTR_{10\ min}$ = 100 g/10 min. Drying during 4 hours (humidity release mass loss ≅ 4%) reduces the melt index to $PTR_{10\ min}$ = 0.6 g/10 min. High $PTR_{10\ min}$ values of uncured PPA-1 are also caused by hydrolysis reactions proceeding at high processing temperatures and inducing polyamide degradation. This is confirmed by TGA data on thermal stability of humid and dried PPA. As known [165, 166], oxygen addition in processing equipment varies from 30 to 50 torr. It is delivered with polymer and released to additive injection zones, where it may cause some effect on the process.

Therefore, let us consider the level of oxygen effect of PPA degradation. Figure 33 shows kinetic curves of oxygen absorption by PPA-1 in the mentioned temperature range at initial oxygen pressure of 20 – 300 torr. As compared, total amounts of absorbed oxygen at 325 and 340°C during the processing time (15 min) equaled 5.0 and 10.0 mmol/monomeric unit, respectively. As oxygen content in the system increases to 50 and 100 torr, symbate increase of oxygen absorption, for example, to 18.0 and 35.0

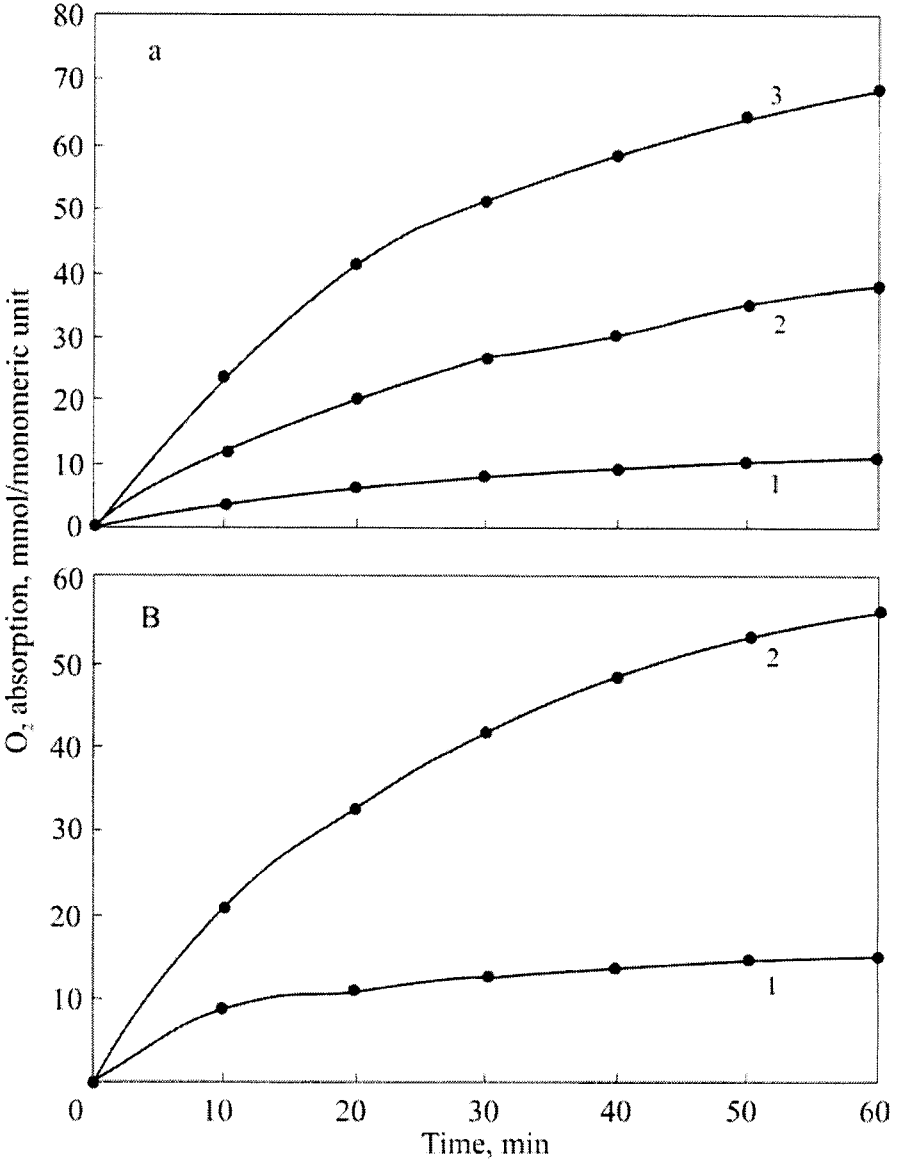

Figure 33. Kinetic curves of O_2 absorption by dried PPA-1 at 325°C (a) and 340°C (b) and oxygen pressure (mmHg): 1 – 20, 2 – 50, 3 – 100

mmol/monomeric unit at 325°C was observed. As the sample is humid, oxygen absorption also increases to 50.0 mmol/monomeric unit at 300°C and 100 torr oxygen pressure versus 12.0 mmol/monomeric unit in dried sample.

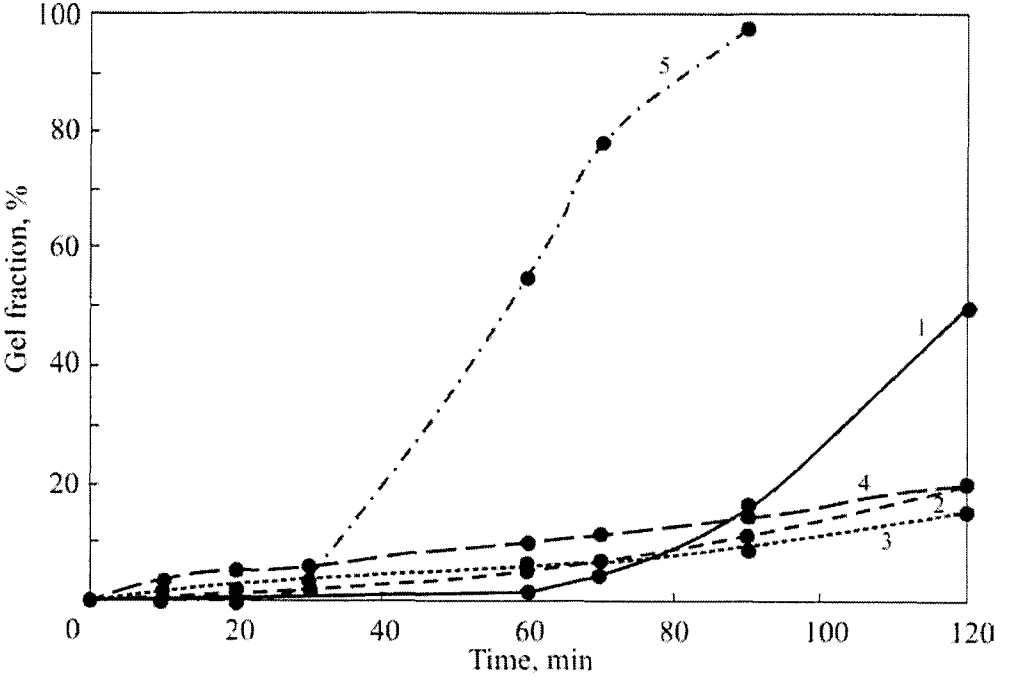

Figure 34. Kinetics of gel formation in PPA-1 (M_w = 39,700) at 300°C and oxygen pressure (mmHg): 1 – 20, 2 – 50, 3 – 100, 4 – 300, 5 – in vacuum

Thermal oxidation causes PPA yellowing. As PPA oxidizes, gel-fraction occurs and is accumulated. On the example of PPA-1, let us consider the effect of oxygen pressure on gel formation kinetics (Figures 34 and 35). It should be noted that kinetic curves of gel formation are of different type at different oxygen pressures. At 300°C and low pressure of 20 – 50 torr, kinetic curves display a short induction period up to 5 – 10 min long. Further thermal processing intensifies gel formation. At 100 - 300 torr oxygen pressure gel formation is initiated already after sample melting, displaying kinetics of the sigmoid type analogous to oxygen absorption kinetics (Figure 33). The gel formation is intensified with oxygen concentration increase, especially at

processing temperature increase, when PPA-1 possesses higher molecular mobility (lower viscous melt – $PTR_{10\ min}$ equals 10.0 and 25.8 g/10 min at 325 and 340°C, respectively). Tests performed in ampoules sealed in air also show that the gel-fraction concentration in PPA-1 increases with temperature (Figure 35).

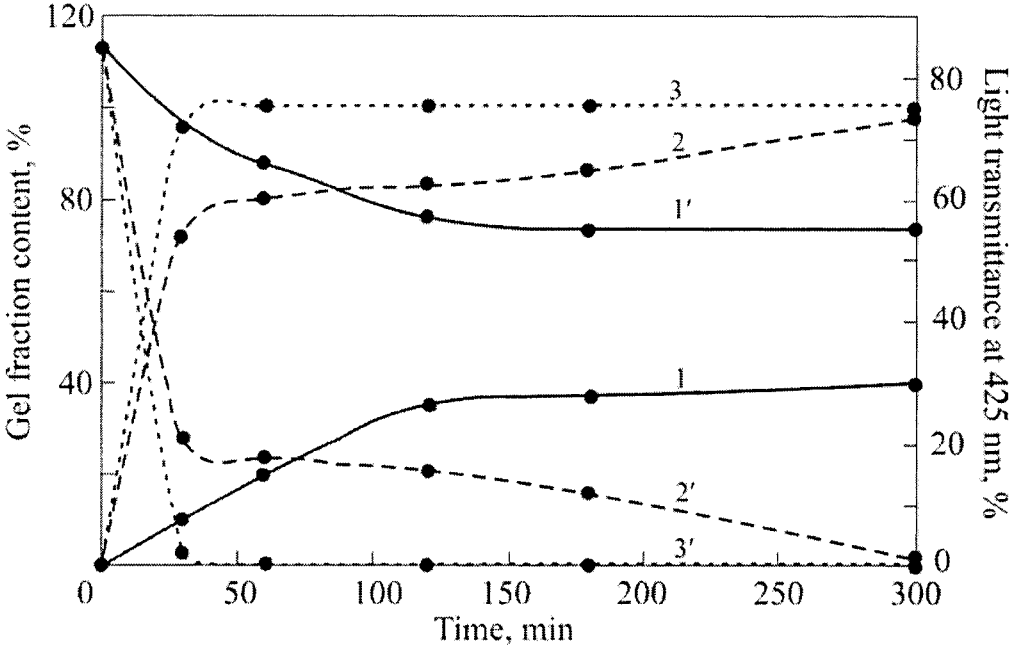

Figure 35. Gel formation kinetics (1 – 3) and light transmittance of sol fraction (1' – 3') for PPA-1 (M_w = 39,700) at 300 (1), 325 (2) and 340°C (3)

At 340°C oxygen pressure contribution is not so high, because oxygen penetration into melted polymer has no diffusion limits.

Figures 35 and 37 also show data on changes in light transmittance of the sol fraction in the visible spectrum (λ = 425 nm). As gel is accumulated, which is associated with branching and macrochain crosslinking, PPA become more yellow. PPA yellowing is induced by occurrence of new carbonyl groups, double bonds, etc. in their structure. Data in figures show that gel fraction concentration increase proceeds with a decrease of sol light transmittance. Data in Figure 34 are of special attention. Gel formation in vacuum has an induction

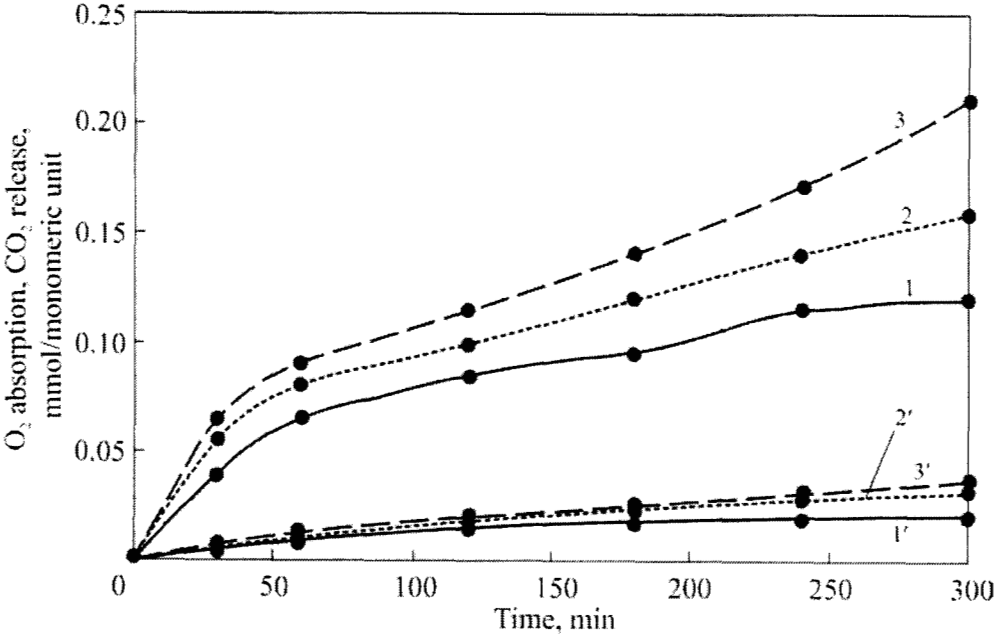

Figure 36. Oxygen absorption (1 – 3) and CO_2 release (1' – 3') kinetics at 300°C (1, 1'), 325°C (2, 2'), and 340°C (3, 3')

period 15 min long, and then the process proceeds with self-excited acceleration. Analogous situation is observed for sol fraction light transmittance change: during initial 15 min light transmittance decreases only by 10 units and then reduces abruptly, which makes the solution practically non-transparent during next 30 min. Figure 37 shows dependences of gel formation and light transmittance on the amount of absorbed oxygen. It clearly indicates the relationship between absorbed oxygen amount, gel fraction concentration and yellowing.

Studies of MMD changes during PPA-1 and PPA-2 processing were also performed. Data on PPA-1 with different molecular masses obtained by GPC technique show MMD changes during thermal processing up to the gel formation stage (Table 7).

Table 7

MMD variations for PPA at 325°C

Oxygen pressure	Time, min	Gel presence	MMD				
			M_w	M_n	M_z	$\frac{M_w}{M_n}$	$\frac{M_z}{M_w}$
PPA-1 (high-molecular)							
Before*	0	None	39,700	6,700	196,000	5.9	4.9
Vacuum	10	None	30,600	6,500	298,000	47.1	9.7
20 torr	10	None	29,500	9,900	360,000	29.8	12.2
	30	Pres.	24,800	8,500	320,000	29.2	12.9
100 torr	10	Pres.	74,800	6,700	603,000	11.2	8.1
	30	Pres.	10,300	5,700	190,000	18.1	18.4
PPA-1 (low-molecular)							
Before*	0	None	21,600	4,500	75,000	4.8	3.5
Vacuum	10	Pres.	67,000	4,000	30,000	16.7	4.5
20 torr	10	Pres.	130,000	6,200	45,000	21.0	3.4
PPA-2							
Before*	0	None	25,500	8,000	43,100	3.2	1.69
Vacuum	10	None	12,530	8,300	14,230	15.0	1.1
	30	Pres.	22,900	7,000	37,700	3.3	1.65
20 torr	10	None	25,000	8,400	42,000	2.9	1.68
100 torr	10	Pres.	18,000	6,500	34,000	2.8	1.9

* Before thermal processing.

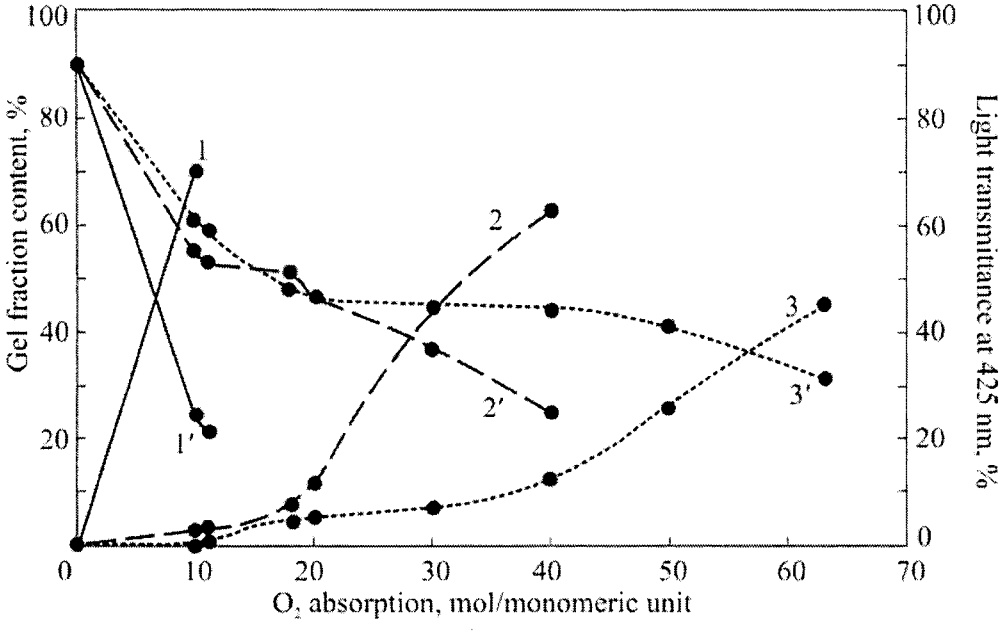

Figure 37. Dependencies of the gel formation (1 – 3) and light transmittance of sol fraction (1' – 3') for PPA-1 (M_w = 39,700) on the amount of absorbed oxygen at O_2 pressure (mmHg): 1 – 20, 2 – 50, 3 – 100. T = 325°C

Analysis of obtained data shows that at processing temperatures branching and crosslinking reactions actively proceed in PPA-1 and PPA-2. It should be noted that any thermal processing induces a significant increase of all moments of molecular masses and high-molecular shift in MMD chromatogram. A significant increase of moment M_z is observed at thermal processing in vacuum. Gel formation in PPA-1 with different molecular masses possesses different kinetics (Figure 38).

In a polymer with lower molecular mass gel fraction is accumulated at much lower rate: gel amount in two studied samples having M_w = 39,700 and 21,600, respectively, differs by an order of magnitude. However, the tendency to decrease of light transmittance with gel fraction concentration increase is the same. Less intensive gel formation in a polymer with lower molecular mass correlates with previous GPC data (Table 7). All MMD moments in PPA-1 with M_w = 21,600 change not so abruptly than in PPA with M_w = 39,700. Commonly,

thermal processing in melt causes crosslinking of the polymer matrix, but pure degradation reactions may not be exempt.

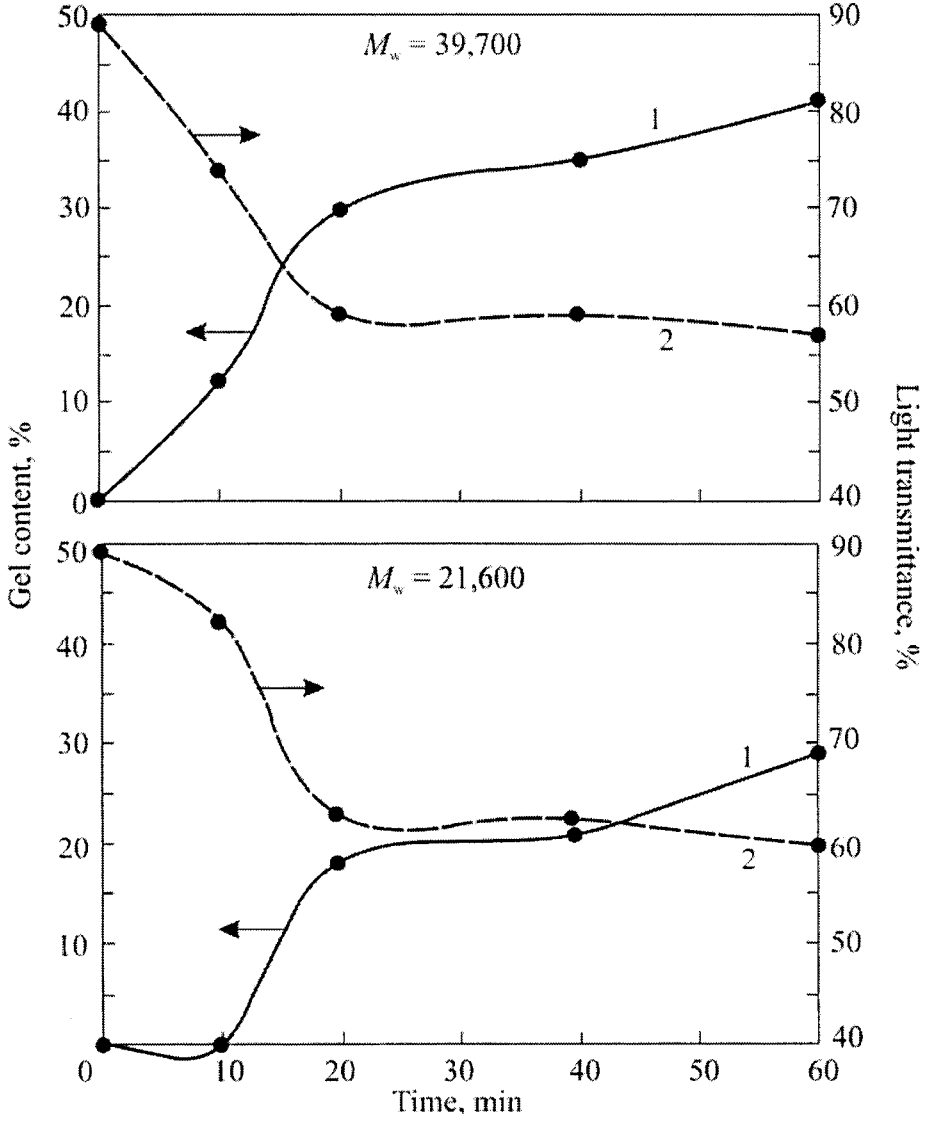

Figure 38. Gel formation kinetics (1) and changes of light transmittance (2) of PPA-1 (M_w = 39,700) at 325°C

It is believed that polymer aging depends on oxidation kinetics, whereas processing and quality of primary polymeric material depends on both pure thermal and thermal oxidative reactions. Since studies of pyrolytic transformations are suitable for understanding the mechanism of macromolecule reactivity, it seemed useful to study thermal degradation products simultaneously with thermal oxidative transformations of PPA.

At 300 - 340°C, degrading PPA-1 and PPA-2 release CO_2, H_2O, formaldehyde, ethylene, and lower alkanes (methane and ethane).

Figure 36 shows kinetic curves of oxygen absorption and CO_2 release at 300 - 340°C. Volatile product release increases with temperature. Activation energy of oxygen absorption and CO_2 and CO release equal: $E(O_2) = (52 \pm 15)$ kJ/mol, $E(CO_2) = (117 \pm 15)$ kJ/mol, and (139 ± 15) kJ/mol, respectively.

It is calculated that CO_2 released from the polymer removes about 20% of absorbed oxygen. Besides gas products which also include C_2H_6, C_2H_4, CH_4, CH_2O, and H_2O, degrading PPA release oily fractions of light yellow to dark brown colors, or even white crystals (TPA and TPA diamide). Structures of the products were identified with the help of NMR, IR-spectroscopy and mass-spectrometry techniques (see below). Oily fraction compositions were quantitatively determined using NMR technique. The ratio of aromatic (~$CH_2NHCOCH_2CH$~, $\delta_H = 3.2 - 3.3$ ppm) and aromatic (~$CH_2NHCOAr$~, $\delta_H = 3.4$ ppm) fragments, approximately equal 2/1, was estimated from the relation of integral intensities of corresponded structural fragments. Detected aliphatic structures represent derivatives of succinic and glutaric acid. Aromatic fragments represent derivatives of isophtalic and terephthalic acids (in PPA-1 degradation products) and TPA derivatives (in PPA-2 degradation products). The following structural fragments (with corresponded ^{13}C NMR signals) were detected:

R_1-OOC-Ar-COO-R_2 ($\delta_C = 169, 169$ ppm)
~Ar-N~ ($\delta_C = 118, 117$ ppm),
~ArOH ($\delta_C = 115$ ppm).

In the absence of air oxygen (at thermal degradation in vacuum), PPA degradation products displayed initial monomers, for example, adipic acid, hexamethylene diamine and their derivatives – for PPA-1. Moreover, mixtures of linear and cyclic aliphatic amines and linear oligomers with carboxylic and salt end groups ~CH_2COOH ($\delta_C = 180.5$ ppm), ~CH_2NH_2 ($\delta_H = 2.7$ ppm), ~$CH_2{}^+NH_3COO^-$ ($\delta_H = 3.2$ ppm), and oligomers with structural sequences in the

chain (~C(O)-$(CH_2)_4$-C(O)-NH-$(CH_2)_6$NH~, ~CH_2NH-C(O)-CH_2~) were detected. Main gas products detected were CO, CO_2, CH_4, C_2H_6.

In the absence of oxygen, none of aromatic oligomers and individual substances (TPA and TPA amide) were detected in the degradation products, whereas aliphatic and cycloaliphatic amines were observed.

The authors [264] have obtained data on thermal degradation of PA derived from aromatic, dicarboxylic acids and aliphatic diamines. With respect to the origin of dicarboxylic acid, the effective activation energy of thermal degradation equaled 42 – 117 kJ/mol. As electrons are shifted by the effect of benzene ring, primary act of thermal degradation proceeds by N-C-bond:

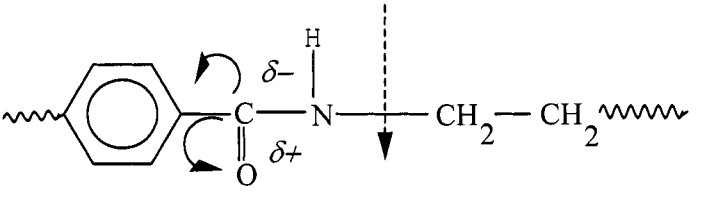

Radicals, occurring in this case:

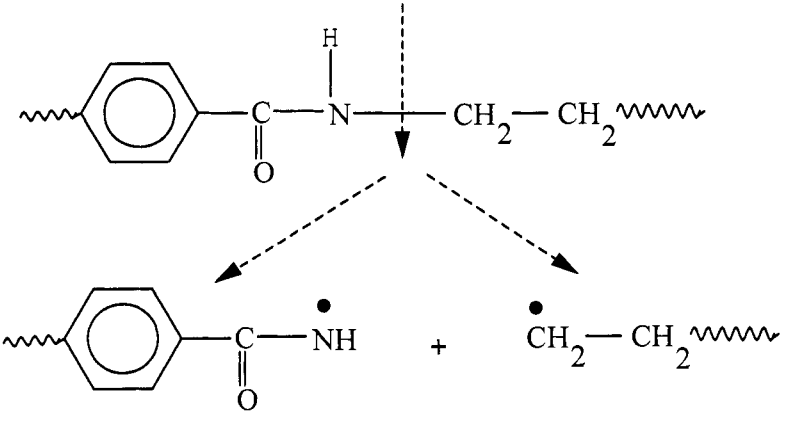

decompose and recombine by the following scheme:

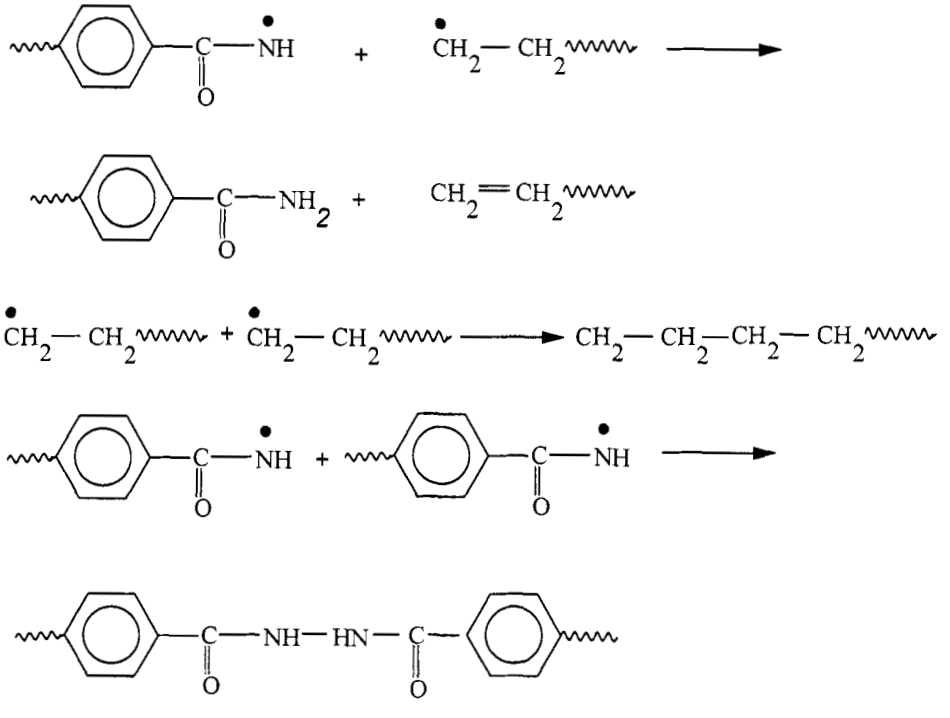

Finally, secondary reactions produce heat resistant secondary products:

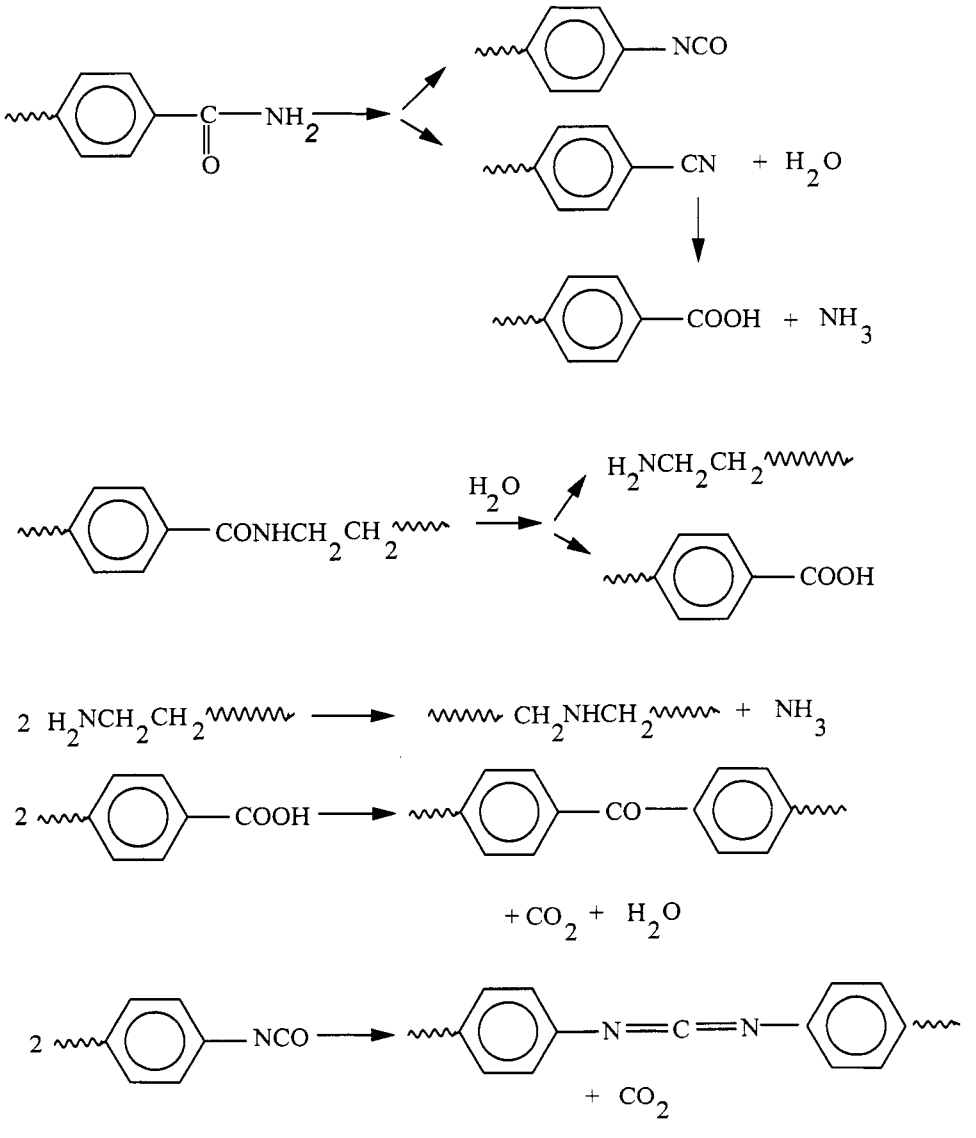

also observed in PPA-1 and PPA-2 degradation.

In the processing temperature range, a complex degradation process develops in PPA. Branching and crosslinking reactions proceed intensively on

the background of the radical-chain decomposition. IR-spectra of PPA, initial and oxidized in the mentioned temperature-time interval, are highly different. Table 8 shows relationships of characteristic absorption bands in IR-spectra of PPA.

Table 8

Relationships of frequencies in IR-spectra of PPA

Frequency, cm^{-1}	Structural element relationship
3,300	NH- (hydrogen bonds)
3,065	NH- (Fermi resonance)
2,920; 2,980	CH_2
1,630	Amide I CO
1,540	Amide II NH, CN, CO
1,500	CH-Ar
1,480	CH_2
1,410	CH_2
1,375	CH_2
1,280; 1,220; 1,200	Amide III + CH_2
1,040	CH_2
940	Amide IV
860	CH-Ar (TPA)
700	CH_2
820	CH-Ar (IPA)

A new absorption band at 1,720 cm^{-1} occurs in spectra of thermally oxidized PPA samples. Intensity of this band increases with oxidation development. Total background of IR-spectrum reduces simultaneously, which is usually associated with interchain crosslinking reactions. In the absence of oxygen, new absorption bands were not observed, however, total background of the spectrum significantly spreads. Table 9 shows analysis of the component composition of PPA-1 sample before and after thermal treatment in vacuum and in air at 340°C.

Table 9

The component composition of PPA-1 sample

Sample	Composition, wt.%					
	C	N	H	O	C/N	C/H
PPA-1	67.25	11.86	7.86	13.03	5.67	8.56
340°C, vacuum	66.73	11.15	7.83	14.29	5.98	8.52
340°C, air	67.46	11.26	7.62	13.66	5.99	8.85

Degradation in vacuum differs from degradation in oxygen.

Thermal oxidation under processing conditions is accompanied by MMD spreading and high-molecular shift of the curve. This process proceeds with respect to oxygen pressure in the system. Gel fraction was observed even at thermal oxidation in IIRT device channel. Figure 38 shows kinetic curves of gel fraction accumulation and PPA-1 yellowing on molecular mass. Intensive gel formation happens during initial 20 min ($G_{20\ min}$) of thermal oxidation. For example, polymer with M_w = 39,700 has $G_{20\ min}$ = 30%, and polymer with M_w = 21,600 has $G_{20\ min}$ = 19%. Light transmittance of solutions of these samples reduces from 48 – 49% for primary (untreated) ones to 9 and 21% after 20 min of thermal processing.

It should be noted that any thermal treatment, even drying at 80°C, causes molecular mass increase of PPA. The results obtained testify about degradation reactions proceeding in PPA, accompanied by molecular mass increase and crosslinking of macrochains.

THERMAL OXIDATION IN THE SOLID PHASE – AGING

Low-temperature impacts in air also cause degradation changes in PPA. Traditionally, these processes proceed at rates lower than at high temperature which is associated with lower molecular mobility in the solid phase and, consequently, hindered access for oxygen inside the matrix. The reactions mainly proceed on the sample surface or in very thin surface layer. Yellowing is the first sign of changes in chemical structure of the polymer. At 200°C, this occurs already on the first day. In the absence of oxygen at this temperature,

slight yellowing was observed only after 50 h exposure. Some observations must be considered in more detail:

- As noted, PPA mostly yellows by the surface. Cross-section of the PPA sample treated in vacuum or in air looks like as follows:

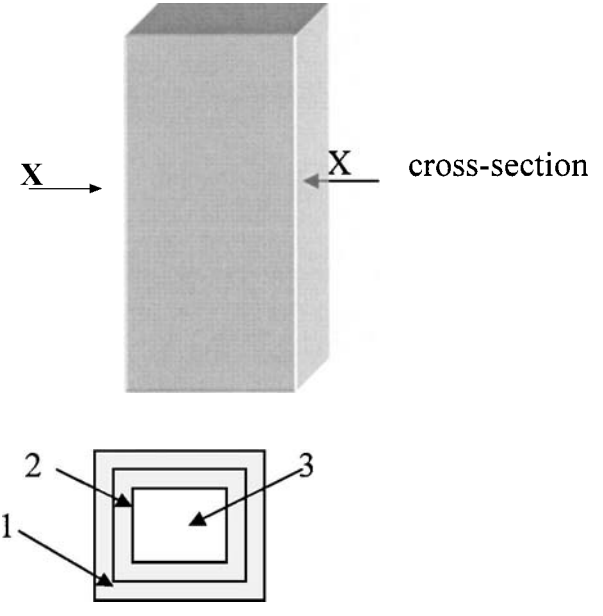

Table 10 shows notations in the Figure above.

Table 10

Layer colors after heat treatment*

Layer No. in the Figure	Vacuum	Air
1 – surface layer	Yellow	Brown
2 – transient layer	Light yellow	Yellow
3 – internal zone	Light yellow	Light yellow

* Maximal exposures: 300 h in air and 410 h in vacuum.

Table 11 shows GPC data on PPA heat treatment at 200°C.

Table 11

PPA MMD after heat treatment at 200°C

Time, h	MMD				
	M_w	M_n	M_z	M_w/M_n	M_z/M_w
In vacuum					
0	39,700	6,700	196,000	5.9	4.9
50	70,600	15,500	320,000	4.6	4.5
410	75,200	16,600	320,000	4.5	4.3
In air					
74	27,000	7,200	136,000	3.8	5.0
100 (gel)	23,300	7,300	108,000	3.2	4.6

These results were obtained at dissolution and corresponded analysis of the mean sample (cut piece of sample contained both external and internal layers). Obviously, this "gross" information is not enough for understanding degradation processes. Therefore, changes in molecular mass were studied separately for each oxidized layer. Layers were cut from the samples surface by a microtome. Table 12 shows MMD test results for PPA-2.

Table 12

Changes in PPA-2 MMD during solid-phase oxidation at 175°C

Time, h	MMD				
	M_w	M_n	M_z	M_w/M_n	M_z/M_w
Before aging	25,300	8,300	42,300	3.05	1.67
2 days					
External layer	29,200	6,300	54,800	4.63	1.88
Internal layer	25,500	8,350	43,000	3.10	1.68
12 days					
External layer	4,700	2,100	10,600	2.24	2.26
Internal layer	32,200	5,300	65,100	6.08	2.02

At early stages of thermal oxidation (initial two days) branching and crosslinking processes intensively proceed on the sample surface. In internal layers, where oxygen delivery is hindered, molecular mass does not change. At longer exposure the situation changes drastically: degradation processes accompanied by reduction of all moments of molecular masses dominate in the

external layer. Inside the sample, macrochains are crosslinked, and moments $\overline{M}_w$ and $\overline{M}_z$ increase.

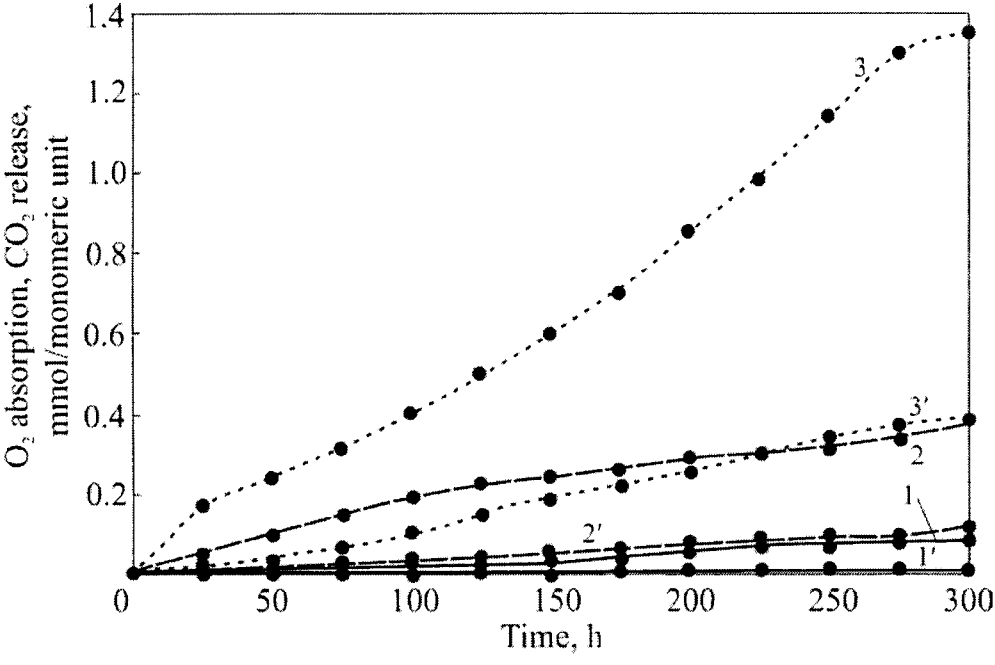

Figure 39. Kinetic curves of O_2 absorption (1 - 3) and CO_2 release (1' – 3') for PPA-1 at 150°C (1, 1') 175°C (2, 2'), 200°C (3, 3')

In air, primarily detected branching and crosslinking reactions, intensified by oxygen, compete with the degradation process. Figure 39 shows oxygen absorption and CO_2 release kinetics. Figure 40 shows Arrhenius temperature dependencies of initial rate constants for O_2 absorption and CO_2 release. Effective activation energies equal $E(O_2)$ = (24.0 ± 7.0) kJ/mol, $E(CO_2)$ = (28.0 ± 6.0) kJ/mol. Primarily, the solid-phase oxidation in PPA touches upon aliphatic regions of the structure. Besides CO_2, formaldehyde and hydrogen were detected in volatile products (refer to Chapter 1). As polymer oxidizes, oligomeric products and individual substances (in addition to low-molecular gases) are released and accumulated (TPA and amid-TPA), which precipitate on cold parts of the ampoule (for generalized composition of degradation products – see below).

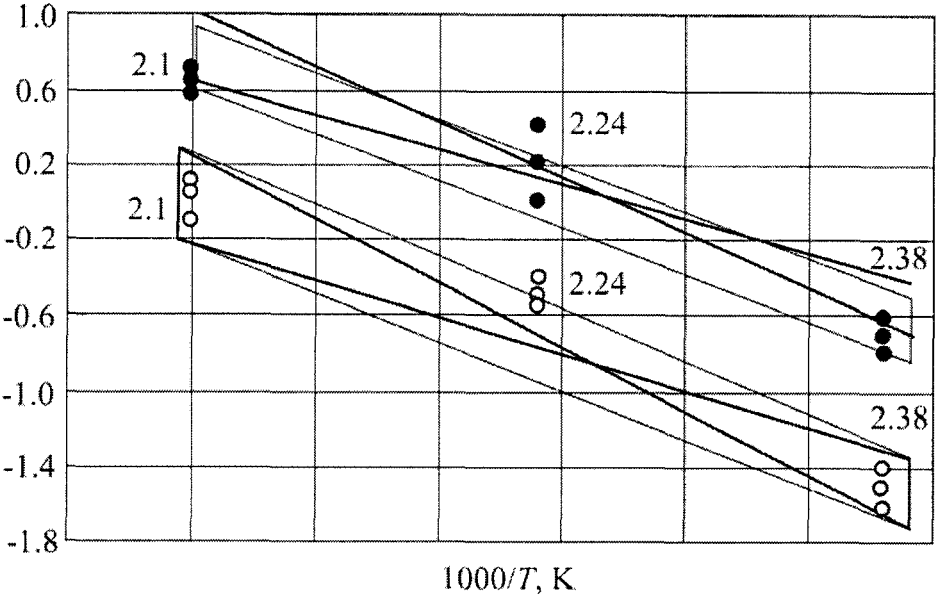

Figure 40. Arrhenius temperature dependencies of initial rate constants of O_2 absorption and CO_2 release for PPA-1 at 150, 175 and 200°C

In this case, solid-phase oxidation also increases the yellowing index increase, light transmittance of sol and gel fraction concentration (Figure 41). Figure 42 shows dependence of light transmittance on absorbed O_2 amount for PPA-1 sol fraction. Light transmittance decreases monotonously due to solution yellowing. As about 3 moles of O_2 per monomeric unit are absorbed, the solution becomes almost non-transparent, e.g. light transmittance approaches 0. The released CO_2 amount increases symbate linearly with absorbed O_2.

After 100 h of aging in air light yellow crystals occur and begin accumulating on the ampoule walls. The following structural fragments were identified by NMR technique: CH_3CO (δ_H = 1.9 ppm), aromatic protons from phthalic acids (8.3 and 7.6 ppm) and their derivatives with substituting groups in positions 1,3- and 1,4-, e.g. R-Ar-R, R-Ar-R' and R'-Ar-R", where R = COOH, R' = ~c(O)O$^-$M$^+$ or ~C(O)NH_2. Molar ratio of iso- and terephthalic structures in PPA-1 degradation products is ≈ 3.1. Besides the above-mentioned compounds, an oligomer with ~ArOH end groups was identified.

The composition of PPA-1 and PPA-2 solid-phase oxidation products

Gases: CO_2, CH_2O, H_2

Oligomers with structural sequences in the chain and end groups:

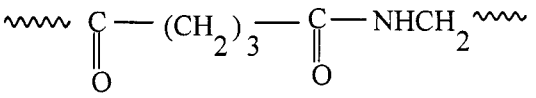

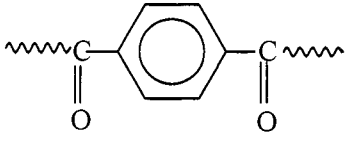

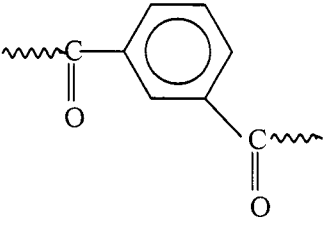

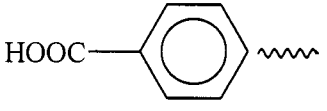

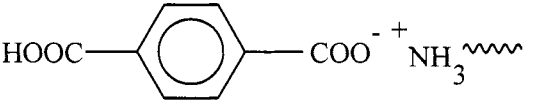

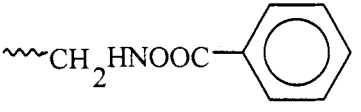

Individual substances (white crystals):

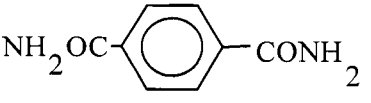

The presence or the absence of IPA fragments and branched amine is the main difference in the composition of PPA-1 and PPA-2 solid-phase oxidation products.

Similar to high-temperature oxidation, solid-phase aging gives a broad variety of products. Oxygen intensifies radical chain break reactions.

It is obvious that solid-phase oxidation of PPA includes not only degradation reactions associated with the change of chemical structure, but also purely physical aging processes which change morphology of samples. As mentioned above, PPA are crystallizing polymers. Figure 43 shows schematic curves for dynamic DTA in argon flow. They display the following heat effects: exothermal crystallization peak at 150°C, endothermic crystal melting peak at 320°C. Annealing in the temperature range of 130 - 150°C increases PPA crystallinity. Consequently, crystallization also happens during the solid-phase aging.

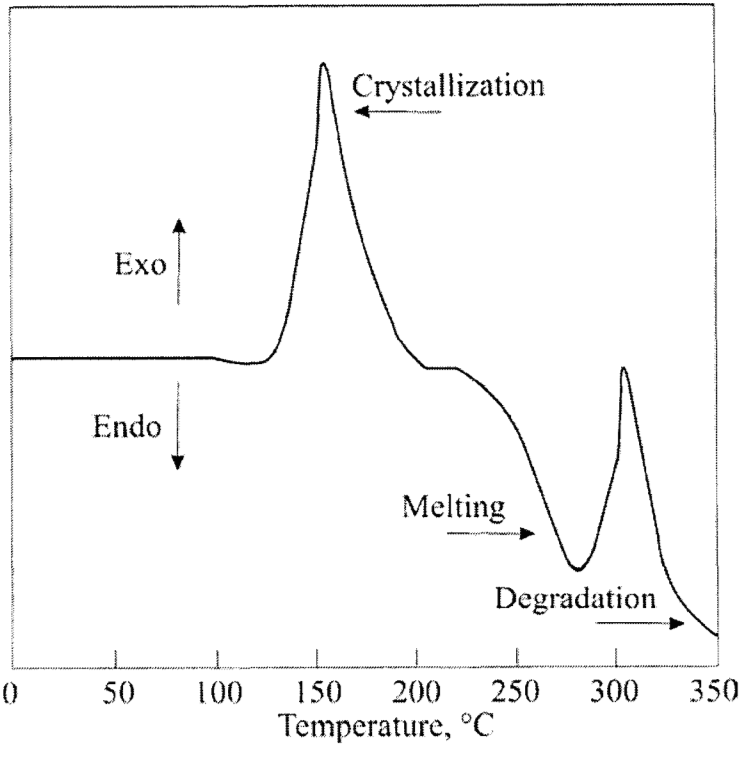

Figure 43. Dynamic DTA curve for PPA in argon flow

Let us consider this phenomenon in more detail on the example of PPA-2. Crystallization heat was calculated by DTA data on appropriate standard compounds. The results of calculations are shown in Table 13.

Table 13

PPA-2 crystallization heat

Sample	ΔH_{cryst}, cal/g
Powder	30
Granules	28
Molded sample	25.6
After aging at 175°C in air	
1 day	2.6
2 days	1.5
12 days	1.8
2 days in vacuum	1.7

As observed from the results obtained, crystallization processes in PPA do not end during thermal processing at article compounding and molding. Pre-crystallization still lasts in end products during operation. As the operation temperature increases, pre-crystallization processes are intensified. Air oxygen has no effect on crystallization processes. Sample annealing in vacuum induces analogous effects, and post-crystallization has a negative effect on properties of end products during operation and causes casting and crack formation.

Thermal behavior at processing temperature, composition of degradation products, kinetic curve shape, and polymer behavior in low-temperature solid-phase oxidation indicate the analogy with degradation mechanisms of previously studied aliphatic-aromatic polyimide PAI [166].

Chapter 3. Degradation of poly(phenylquinoxaline) (PPQ) and co-poly(imidophenylquinoxalines)

As oxidized at 200°C during 2000 h, PPQ absorb ~2.2 O_2 mol/base-mol and releases ~0.8 CO_2 mol/base-mol. Three stage are observed on kinetic curves of O_2 absorption by PPQ at 250°C (Figure 44):

- at the first stage, about 4 O_2 mol/base-mol are absorbed, and kinetics is order one;

$$\frac{dx}{dt} = K_1(x_0 - x), \tag{1}$$

where x_0 is the amount of oxygen, reacted by the reaction end (mol·base-mol); x is the amount of oxygen, reacted by time t (mol·base-mol); K_1 is the rate constant at the initial stage of oxidation, s^{-1};

- the second stage of thermal oxidation lasting 3000 h at constant O_2 absorption rate (kinetics order zero):

$$\frac{dx}{dt} = K_2, \tag{2}$$

where K_2 is the rate constant at the second oxidation stage (mol/base-mol·s^{-1});

- After 3000 h reaction is accelerated (exponential dependence):

$$x = A\exp(\gamma t), \tag{3}$$

where γ is self-exited acceleration factor (s^{-1}).

Equations (1) and (3) in semi-logarithmic coordinates and equation (2) in linear coordinates are presented by straight lines, tangents of which determine rate constants and reaction acceleration factor [83].

Table 14 shows values of K_1, K_2 and γ. Kinetics of O_2 absorption at 300°C is of analogous type (Figure 44). As might be expected, the process is accelerated with temperature increase (Table 14).

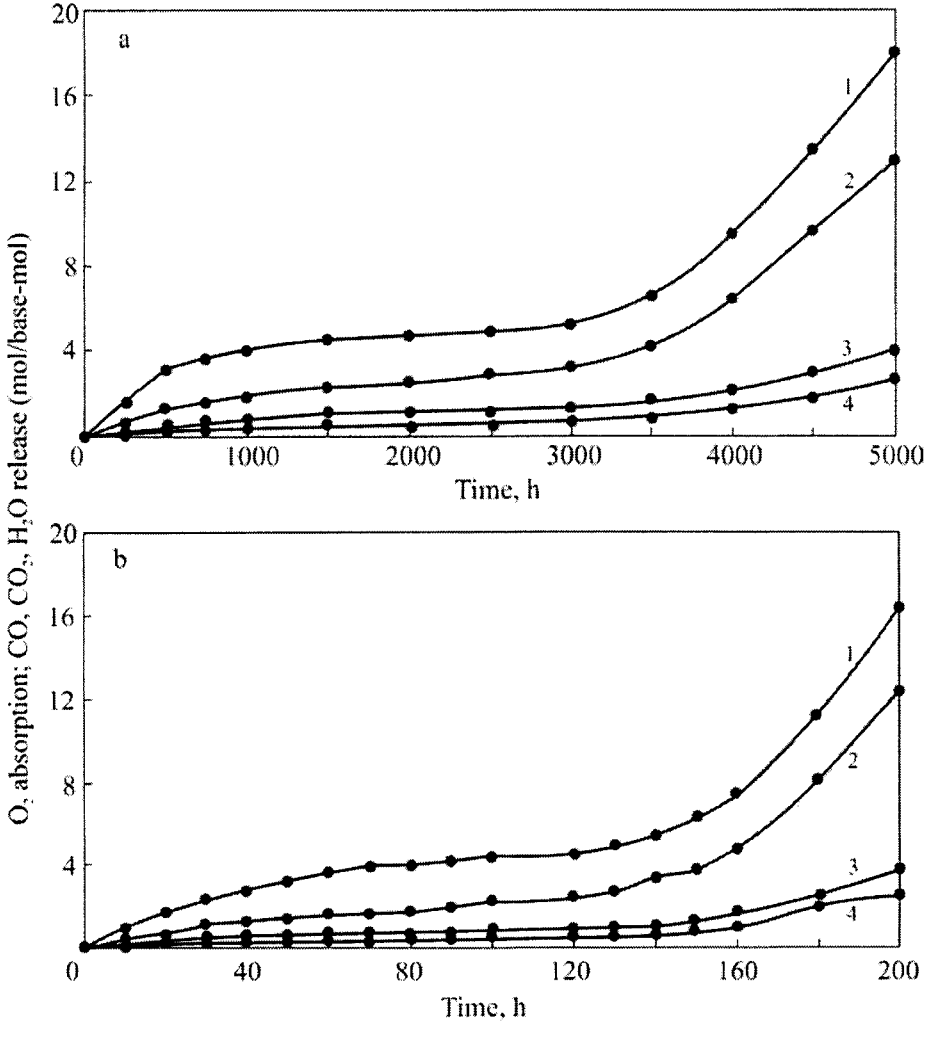

Figure 44. Kinetic curves of O_2 absorption (1) and CO_2 (2), CO (3) and H_2O (4) release at thermal oxidation of PPQ films. (a) T = 250°C, P_{O_2} = 26.7 kPa; (b) T = 300°C, P_{O_2} = 26.7 kPa

Table 14

PPQ thermal oxidation rate constants

T, °C	Parameter	O_2	CO_2	CO	H_2O
250	K_1, s^{-1}	$(6.3 \pm 0.12)\times10^{-7}$	$(3.7 \pm 0.27)\times10^{-7}$	$(2.9 \pm 0.033)\times10^{-7}$	$(2.4 \pm 0.017)\times10^{-7}$
	K_2, s^{-1}	$(1.2 \pm 0.034)\times10^{-7}$	$(1.1 \pm 0.011)\times10^{-7}$	$(1.0 \pm 0.045)\times10^{-7}$	$(3.6 \pm 0.011)\times10^{-7}$
	γ, s^{-1}	$(1.9 \pm 0.027)\times10^{-7}$	$(2.1 \pm 0.82)\times10^{-7}$	$(1.6 \pm 0.34)\times10^{-7}$	$(2.1 \pm 0.058)\times10^{-7}$
300	K_1, s^{-1}	$(7.2 \pm 0.11)\times10^{-6}$	$(4.3 \pm 0.059)\times10^{-6}$	$(3.3 \pm 0.052)\times10^{-6}$	$(2.9 \pm 0.039)\times10^{-6}$
	K_2, s^{-1}	$(8.6 \pm 1.5)\times10^{-6}$	$(7.2 \pm 0.13)\times10^{-6}$	$(2.9 \pm 0.057)\times10^{-6}$	$(3.7 \pm 0.057)\times10^{-6}$
	γ, s^{-1}	$(5.1 \pm 1.2)\times10^{-6}$	$(6.2 \pm 0.18)\times10^{-6}$	$(5.7 \pm 0.11)\times10^{-6}$	$(6.9 \pm 0.084)\times10^{-6}$

Kinetics of carbon oxides and water release, which are the main products of PPQ degradation, is analogous to O_2 absorption kinetics. At the first stage, rate constants of carbon oxides and water release are lower than K_1 of O_2 absorption.

Reduction of oxygen balance, absorbed by PPQ and released with thermal oxidation products, show that at the initial stage about 50% of oxygen remain in the polymer (Figure 45), i.e. it accumulates in PPQ in the form of oxygen-containing polymeric products. IR-spectra of oxidized PPQ films and model compounds display new bands at 1,640 – 1,670 cm^{-1}, corresponded to new oxygen-containing groups, apparently, of the quinoid type. PPQ film mass losses, detected at 300°C, exceed those, calculated by total yield of gaseous products and oxygen absorption that indicates formation of other volatile products. Condensed fractions, the so-called "cold ring", have a nitrogen-containing, aromatic compound with molecular mass 386, corresponded to 2,2'-(1,4-phenylene)-bis-(3-phenylpyrazine) (PPP), detected by mass-spectrometry method. By its origin, PPP is similar to PDI – thermal oxidation products of aliphatic-aromatic PA, PAI and pure aromatic PI (refer to Chapters 1 and 2).

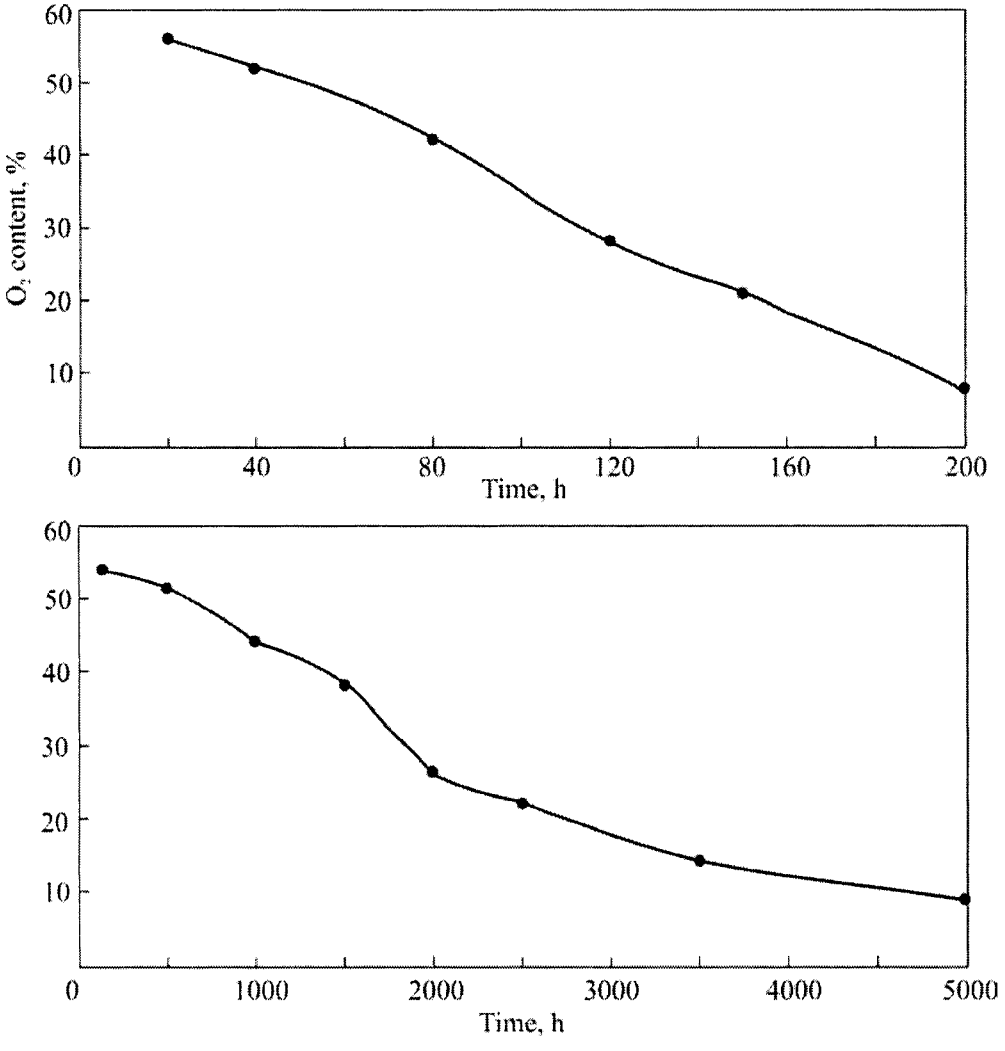

Figure 45. The amount of oxygen irreversibly absorbed by PPQ film during thermal oxidation at (a) 300°C and (b) 250°C

PPQ oxidation products, produced at 250 - 300°C, contain hydrogen. Its synthesis in this temperature range may be explained by crosslinking (Figure 46). PPQ heating at 250 - 300°C causes partial or full loss of solubility in chloroform. Calculation shows that about 4 crosslinks per macromolecule occur in the polymer during 20 h of thermal oxidation at 300°C. On the absence of

oxygen crosslinking is abruptly slowed down. PPQ affinity to crosslinking is confirmed in experiments with model PPQ compounds: besides carbon oxides and water, dimer with molecular mass 562 ($2M_{DPQ}$ – 2) and hydrogen are detected in products of diphenylquinoxaline oxidation during 100 h at 300°C. As DPQ is oxidized in vacuum, all other conditions being the same, neither dimer nor hydrogen was detected. As a consequence, oxygen is the compound that initiates formation of intermolecular crosslinks.

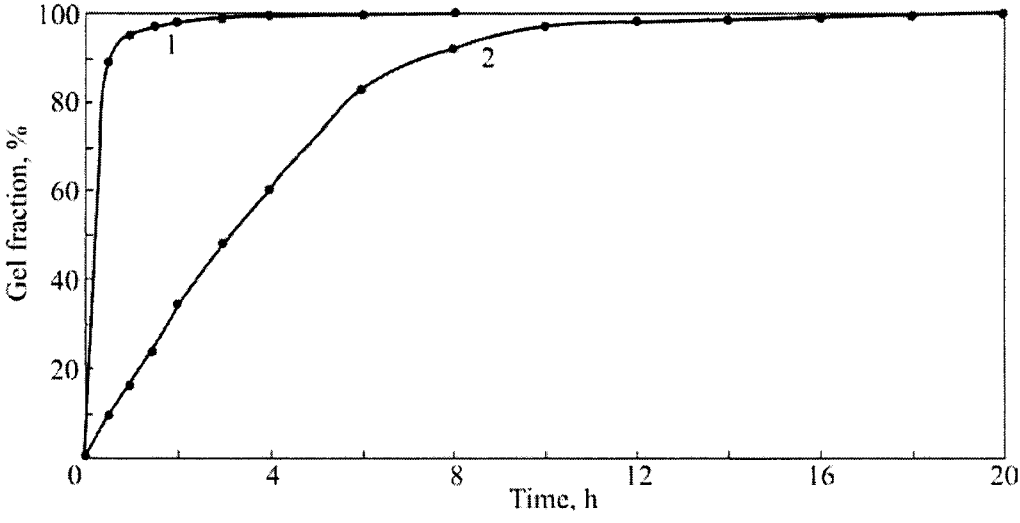

Figure 46. Kinetics of fatty-aromatic CPIPQ-11-3 gel fraction accumulation during thermal oxidation at 400°C (1) and 300°C (2); P_{O_2} = 26.7 kPa

Dynamic TGA data show that thermal stability of aromatic copolymers at dynamic heating in vacuum is independent of ether-aromatic unit content. For all studied CPIPQ-1 (see the structure in Table 15), temperature of 10% mass loss falls within the range of 570 - 580°C.

Table 15

Copolyimidophenylquinoxaline (CPIPQ) characteristics

CPIPQ-1				
Copolymer	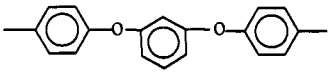 Group content in macrochain, wt.%	[η], dl/g (25°C, *m*-cresol)	Solubility	
			Chloroform	*m*-Cresol, tetrachloro-ethane
1-1	17.8	1.81	partly	soluble
1-2	13.3	1.15	partly	soluble
1-3	10.6	1.29	partly	soluble
1-4	8.8	0.97	soluble	soluble
1-5	5.2	0.77	soluble	soluble
1-6	2.6	1.10	soluble	soluble
1-7	1.3	0.88	soluble	soluble
CPIPQ-2				
Copolymer	-(CH_2)- Group content in macrochain, wt.%	[η], dl/g (25°C, *m*-cresol)	Solubility	
			Chloroform	*m*-Cresol, tetrachloro-ethane
2-1	12.3	2.32	partly	soluble
2-2	9.0	1.52	soluble	soluble
2-3	7.1	1.74	soluble	soluble
2-4	5.9	1.03	soluble	soluble
2-5	3.4	1.07	soluble	soluble
2-6	1.7	1.02	soluble	soluble
2-7	0.8	1.16	soluble	soluble

Thermal degradation of fatty-aromatic copolymers is initiated at lower temperatures. The increase of methylene group content induces reduction of CPIPQ-2 thermal stability (Table 15). For example, as $-CH_2$-group concentration increases from 0.8 (CPIPQ-2-7) to 12.3 wt.% (CPIPQ-2-1), temperature corresponded to 10% mass loss reduces from 520 to 450°C.

Ether-aromatic fragment replacement by aliphatic fragments deteriorates thermal stability of copolymers and changes the degradation type. TGA curves in Figure 47 show that CPIPQ-2 degradation proceeds in several stages, the clearer observed, the greater the number of methylene units in the chain is.

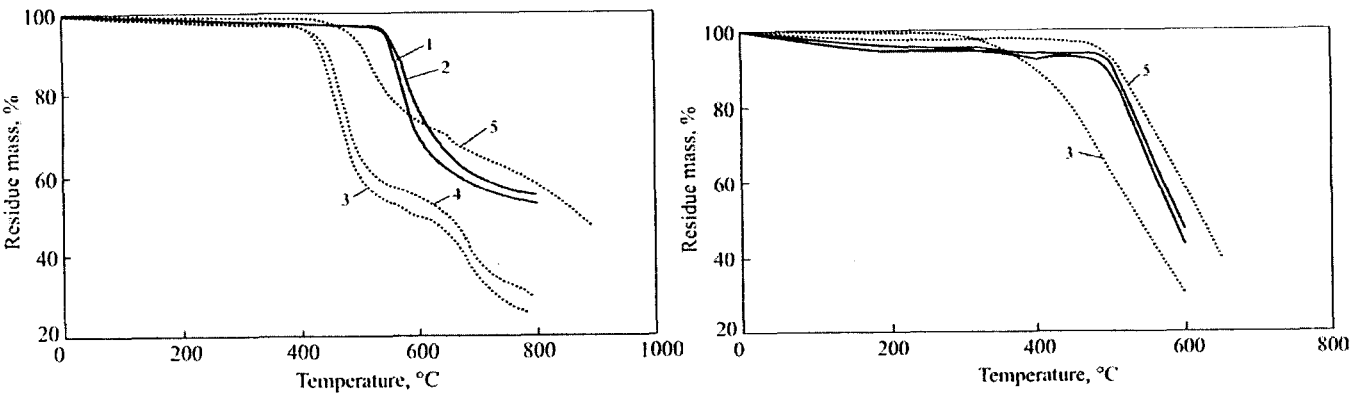

Figure 47. TGA curves for CPIPQ at the heating rate of 6°/min

(a) in inert medium:

CPIPQ with ether-aromatic fragments: 1 – CPIPQ-1-1; 2 – CPIPQ-1-7.

CPIPQ with aliphatic fragments: 3 – CPIPQ-11-1; 4 – CPIPQ-11-2; 5 – CPIPQ-11-7;

(b) in air:

CPIPQ with ether-aromatic fragments: 1 – CPIPQ-1-1; 2 – CPIPQ-1-7.

CPIPQ with aliphatic fragments: 3 – CPIPQ-11-1; 5 – CPIPQ-11-7.

Following intensive mass loss initiated at 420 - 500°C (for CPIPQ-2-1 and CPIPQ-2-7, respectively), the degradation rate decreases and then increases again above 650°C. The degradation rate decrease observed may be explained so that as methylene chains most subject to degradation are destroyed, the copolymer obtains more stable structure.

Oxygen sharply intensifies degradation: CPIPQ-1 degradation begins at 490 - 500°C. Dependence of oxidation resistance of aromatic copolymers on their structure was traced by isothermal TGA data, O_2 absorption and release of thermal oxidation main gas products – carbon oxides (Figure 48). CPIPQ-1 containing 1.3 – 5.2 wt.% ether-aromatic groups has the highest thermal stability.

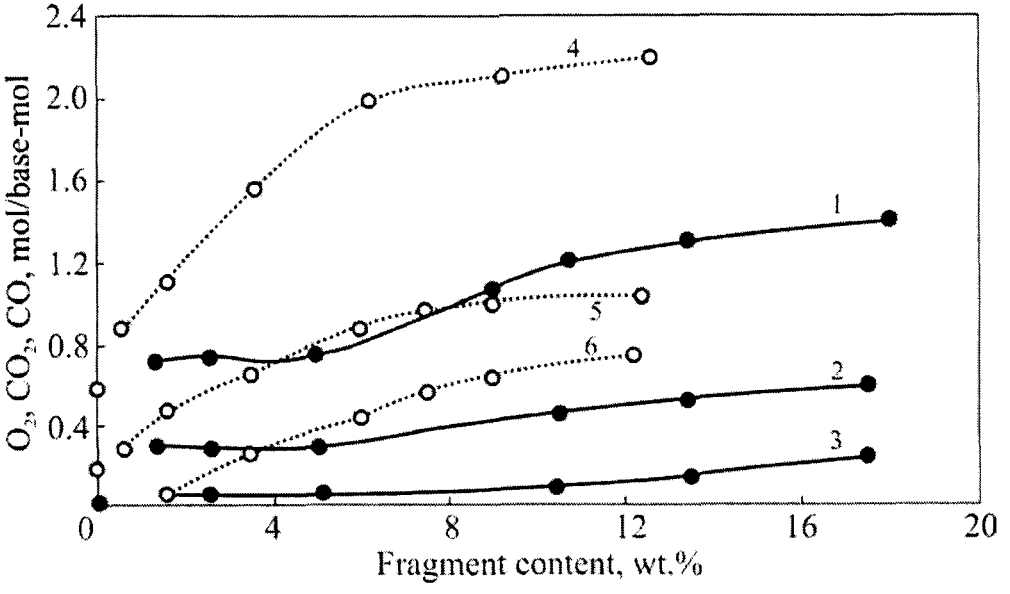

Figure 48. Dependence of O_2 absorption (1, 4), CO_2 (2, 5) and CO (3, 6) release at thermal oxidation on ether-aromatic (1 – 3) and aliphatic (4 – 6) fragments content in CPIPQ macrochain. $T = 300°C$, $t = 100$ h, $P_{O_2} = 26.7$ kPa

Fatty aromatic CPIPQ-2 resistance to thermal oxidation is defined by – CH_2-group concentration. For CPIPQ-2-7, temperature corresponded to 10%

mass loss equals 500°C which is similar to CPIPQ-1. For CPIPQ-2-1 with maximal concentration of methylene groups, this temperature equals 400°C.

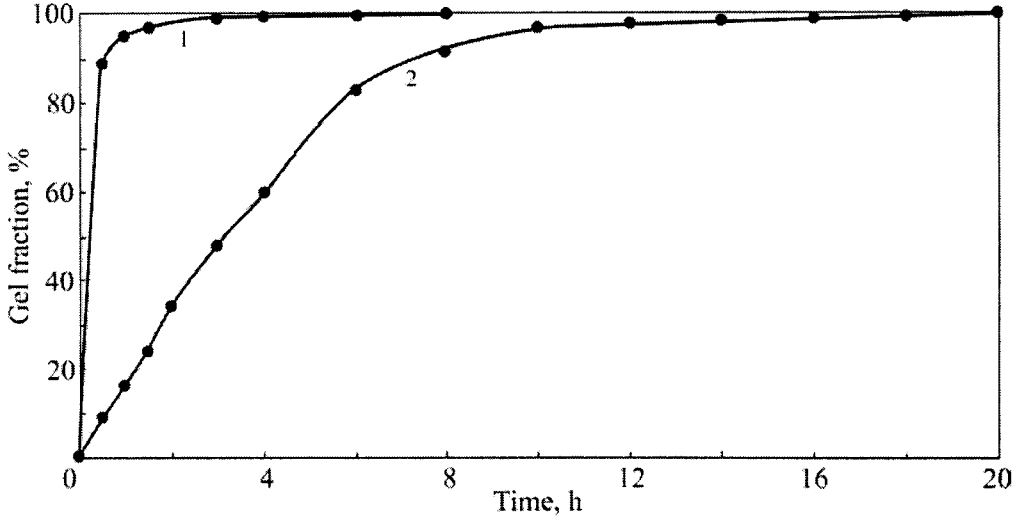

Figure 49. Kinetics of gel fraction accumulation in fatty aromatic CPIPQ-11-3 during thermal oxidation at 400°C (1) and 300°C (2); P_{O_2} = 26.7 kPa

The amount of absorbed oxygen increases with methylene group concentration in CPIPQ-2, and carbon oxides are formed simultaneously. The effective activation energy of O_2 absorption, calculated from kinetic curves of oxidation for CPIPQ-2-4, CPIPQ-2-6 and CPIPQ-2-7 equals 72, 106 and 116 kJ/mol, respectively.

Comparison of CPIPQ and homopolymers (PPQ) stability shows that copolymers containing 5.2 and 0.8 wt.% concentrations of ether-aromatic and aliphatic groups, respectively, are analogous to homopolymers. As content of mentioned groups increases, CPL thermal stability decreases compared with PPQ.

Comparison of mass loss and oxygen absorption kinetics for CPIPQ-2 with PI and PPQ indicates identical oxidation type: high rates at the initial stage, then an area with constant rate and accelerated degradation, clearly displayed at maximal test temperature. At the initial stage, the amount of oxygen, irreversibly bound by CPIPQ-2, equals 65% of absorbed oxygen, i.e. it is higher than for known thermoresistant polymers (PI, PPQ, PAI, etc.).

According to IR-spectroscopy data, as CPIPQ-2 oxidizes, absorption bands at 2,900 cm^{-1}, corresponded to CH_2-group oscillations, gradually disappear. Absorption bands corresponded to heteroaromatic structures (1700, 1670, 1740, 1300 and 1220 cm^{-1}) are preserved. Similar to PPQ homopolymers, CPIPQ oxidation is accompanied by crosslinking (Figure 49), hence, in the presence of aliphatic fragments in the structure crosslinking is accelerated. At 300°C during 20 h of heating, gel fraction concentration in CPIPQ-2 becomes twice higher that in PPQ.

To conclude current material, let us note general regularities of PPQ and CPPQ thermal oxidation. The first important similarity in degradation behavior is O_2 absorption at rather low temperatures (200°C). At temperatures (250°C or higher), when tracing of O_2 absorption kinetics in real time becomes possible, polymers demonstrate the same kinetic type of oxidation with no respect to temperature – the three-stage kinetics, sequentially described by order one and zero laws with further self-excited acceleration. The third kinetic stage of oxidation is of theoretical interest only, because deterioration of operation parameters of the materials is stopped already at the second stage.

Chapter 4. Degradation of polysulfones and polyesterimides

DEGRADATION IN MELT

Polysulfones

Thermal analysis at programmed temperature increase, starting from 390 - 420°C, displays the beginning of mass losses of the most well-known polysulfone (PSF) derived from dichlorodiphenilsulfone and bisphenol A. Intensive PSF degradation, initiated at 5°/min heating rate, is ended at 650°C forming no coke residues. A slight bending on TGA curve at 550°C and 50% mass loss indicates process proceeding seemingly in two stages. At the initial stage of the process, effective constants of mass losses in the presence and in the absence of oxygen (in pure argon flow) equal

$$K_{O_2} = 4.3 \times 10^7 \exp\left(-\frac{92 \pm 20}{RT}\right), \text{min}^{-1},$$

and

$$K_{Ar} = 2.4 \times 10^{13} \exp\left(-\frac{190 \pm 20}{RT}\right), \text{min}^{-1},$$

respectively. In this case, oxygen effect is displayed not by gross rates of initial PSF degradation which obeys the order one kinetic law, but exothermal DTA peak initiated at 400°C typical of thermal oxidation and the presence of 30 wt.% coke residue at purely thermal process.

Mass loss is a low-sensitive parameter of PSF degradation during processing. For example, at 320°C PSF mass is stable during 0.5 h. Only 4 h after the losses reach about 2 wt.%. Color and molecular-mass parameters of PSF are sensitive to high-temperature degradation. Let us limit current discussion of PSF high-temperature degradation by processing temperature interval and temperatures approaching it and observed in the processing because of some deviations from the procedure. Therefore, temperature range to be

considered is 280 - 350°C. Processing duration, including alerts, is about 1 h, mostly 10 - 30 min. Degradation changes in the mentioned exposures are noticeable, but kinetics of these changes is not clear enough. To clarify the mechanism of high-temperature degradation, the authors extended the observation period to 10 h, which allowed detection of the kinetic features of the process and basic chemical changes in the polymer.

Degradation changes in blocked PSF with the minimal concentration of additives are low in the mentioned temperature range without O_2. For example, as the sample is heated at 320°C in vacuum during 2 h, its light transmittance (λ = 425 nm, in solution) decreases from 98 to 95%. Index M_z, most sensitive to degradation, increases by 2 thousand, which is comparable with the measurement accuracy. Pure thermal transformation in PSF samples with non-optimal content of labile structures and additives are noticeable: heating at 320°C during 2 h may reduce light transmittance by 20 – 30 units and increase M_z by 10,000 – 20,000. Laboratory tests confirm analysis of samplings from real PSF production. Relatively short-term thermal impact (10 – 20 min at 300 - 320°C with respect to location in laminar flow) without air access reduces light transmittance by 5 – 7 units and increases M_z by 10,000. Let us accept that in the absence of oxygen PSF is stable in the processing temperature range.

Processing simulation on IIRT device at temperature below 300°C does not affect PSF. Though 1 h exposure at 300°C causes no effect on MFI, changes in molecular-mass parameters and coloring indicate PSF degradation (Figure 50). Kinetics of PSF coloring under thermal impact remain unchanged with temperature (order one law), effective activation energy equals (88 ± 15) kJ/mol in the temperature range of 280 - 350°C. Curves of molecular parameter changes are of more complicated shape. Thermal impact at 300°C increases all MMD moments, though this increase is low and does not affect MFI. At high temperatures powder-like sample tests indicate simultaneous increase of MFI and MMD moments. This is nontrivial rheological fact, because MFI is inversely related to molecular characteristics. Possible effects associated with powder melting and melt formation are not discussed in this monograph. Here we only note the initial tendency to molecular mass increase and not yet understandable MFI increase.

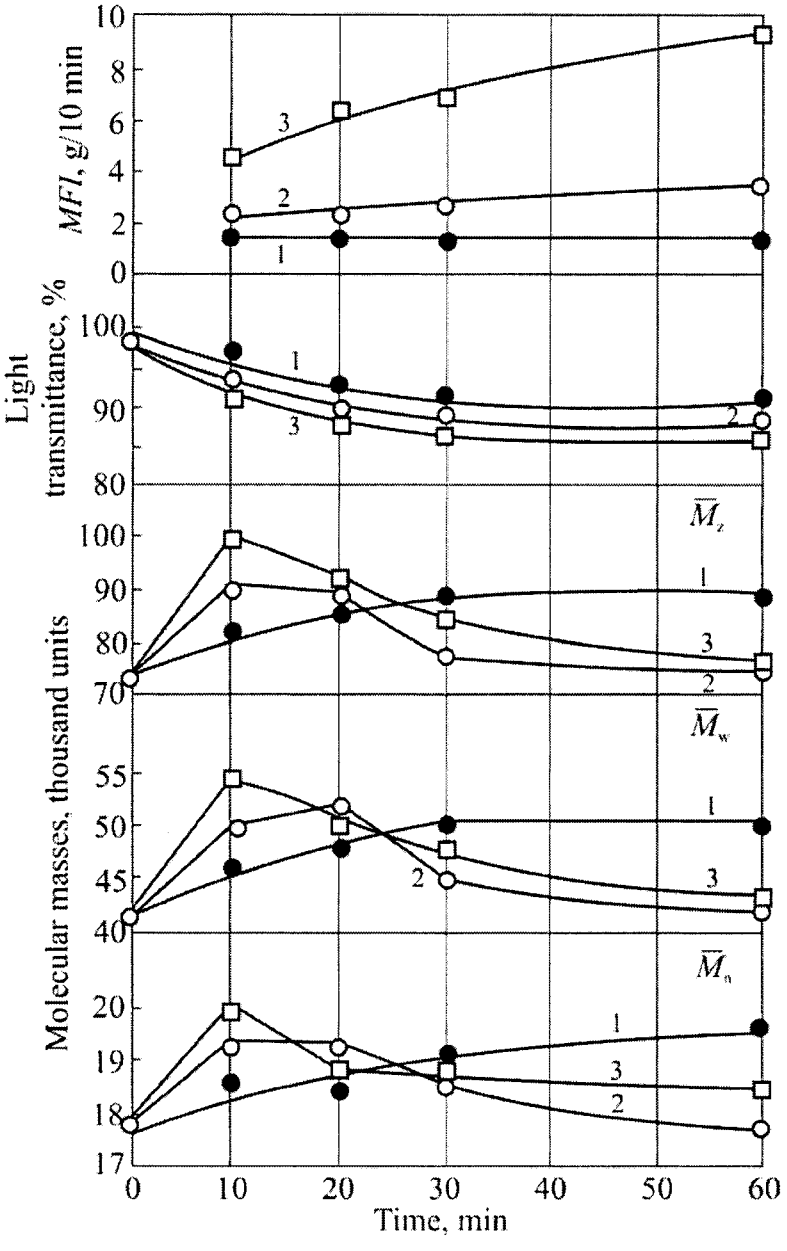

Figure 50. The effect of thermal processing on IIRT device (load 2.16 kg) on MFI, light transmittance, molecular-mass characteristics (M_z, M_w, M_n) of PSF at 300°C (1), 320°C (2) and 350°C (3)

Two reasons of these effects are possible: mechanical degradation caused by shift stresses in the channel and thermal oxidation by O_2 dissolved in the polymer. The first factor is altered in the experiment by varying the load, and the second is uncontrollable in tests on IIRT device.

Changes of PSF molecular characteristics and coloring were estimated by standard procedures of MFI determination with 2.16 and 21.6 kg loads in accordance with the following formula [176]:

$$\tau_n = \frac{Mgr}{2\pi R^2 (z + mr)},$$

where τ_n is the shear stress at IIRT channel wall; M is the load (in kg); g is acceleration of gravity; r is the capillary radius (in mm); R is the cylinder radius (in mm); m is a constant equal 2; z is the capillary length (in mm). In the present case, τ_n equals 1.3×10^5 dyn/cm^2. For comparison purposes a sample was estimated subject to analogous thermal impact (320°C, $\tau_n = 0$) at $P_{O_2} = 26.6$ kPa. Difference in light transmittance of these three samples equals 1 – 2 units. M_w and M_n values differ by 500 – 1,000 that falls within the experiment accuracy, and only M_z moment increases by 5,000 – 6,000 with the shear stress. Let us assess the shear stress for real processing equipment, for example, at the wall in single-screw extruder [176]:

$$\tau_n = \eta\gamma_w,$$

where η is PSF melt viscosity; γ_w is the melt shear rate at the wall; η is determined from MFI: for PSF $\eta = 5\times10^4\, G\rho/\mathrm{MFI}$ at the load $G = 2.16$ kgf and density $\rho = 1.24$ g/cm^2, and MFI of serial lots with the average 5 g/10 min *MFI*, $\eta = 2.7\times10^5$ dyn·s/cm^2. As $\gamma_w = 20$ s^{-1}, $\tau_n = 5.4\times10^6$ dyn/cm^2.

Thus, according to shear stresses determined, mechanical loads on PSF macromolecules at processing in the most rigid mode on IIRT device (maximal load is 21.6 kgf) are almost identical. Therefore, whenever in tests on IIRT device with τ_n changes by an order of magnitude mechanical degradation was low even on the background of spontaneously degrading sample ($\tau_n = 0$), further 3 – 5 time increase of τ_n at transition to processing equipment may hardly cause a sharp intensification of mechanical degradation. Actually, vacuum-extrusion (residual pressure equals 20 – 50 mmHg) of powder-like PSF increased just insignificantly the degradation effects detected in tests on IIRT device. Thus,

thermal effect in the presence of oxygen causes degradation changes in PSF. Mechanical impact applied in the form of loads corresponded to processing conditions specifically increases degradation. However, this effect is negligibly lower compared with the presence of oxygen, which increases M_w and M_n to 2,000 – 5,000, and M_z to 10,000 or higher. Mechanical loads do not affect coloring, which change is typical feature of high-temperature PSF degradation during processing.

The following fundamental fact should be noted: the main contribution to degradation changes in PSF under processing conditions and in processing temperature range is associated with the presence of oxygen in the system. The next stage of investigations will determine PSF and O_2 interaction features at high temperatures. Since mechanical loads under current conditions have an insignificant effect on the degradation process, and the atmosphere monitoring in processing equipment is difficult or impossible, high-temperature degradation of PSF in the presence of oxygen was studied on freely disposed sample.

As heated in melt, PSF quickly absorbs oxygen and releases CO_2 (Figure 51), water and formaldehyde that clearly indicates the oxidation type of interaction between PSF macromolecules and O_2. Kinetic curves of O_2 absorption are shaped identically at temperatures below 350°C and O_2 partial pressure corresponded to its concentration in air: the induction period is absent and two parts are clearly observed. The initial part is 2 – 3 h long and is characterized by high rates. The second part displays gradual decrease of the process rate with transition to linear process, traced up to 10 h exposure. The effective activation energy calculated from initial rates of O_2 absorption in the temperature range of 280 - 350°C equals (72 ± 12) kJ/mol. This E_a value for high-temperature oxidation is close to other arylaliphatic polymers - polyalkanimide (57 kJ/mol) and aliphatic-aromatic polyamides (52 - 54 kJ/mol), described in Chapters 1 and 2. Hence, this value drastically differs from $E_a \approx 0$ of PE high-temperature oxidation in the same temperature range [10, p. 103]. The second stage of PSF oxidation is almost independent of temperature - E_a = 11 kJ/mol, and by this parameter PSF oxidation in melt at deep stages is similar to PE behavior.

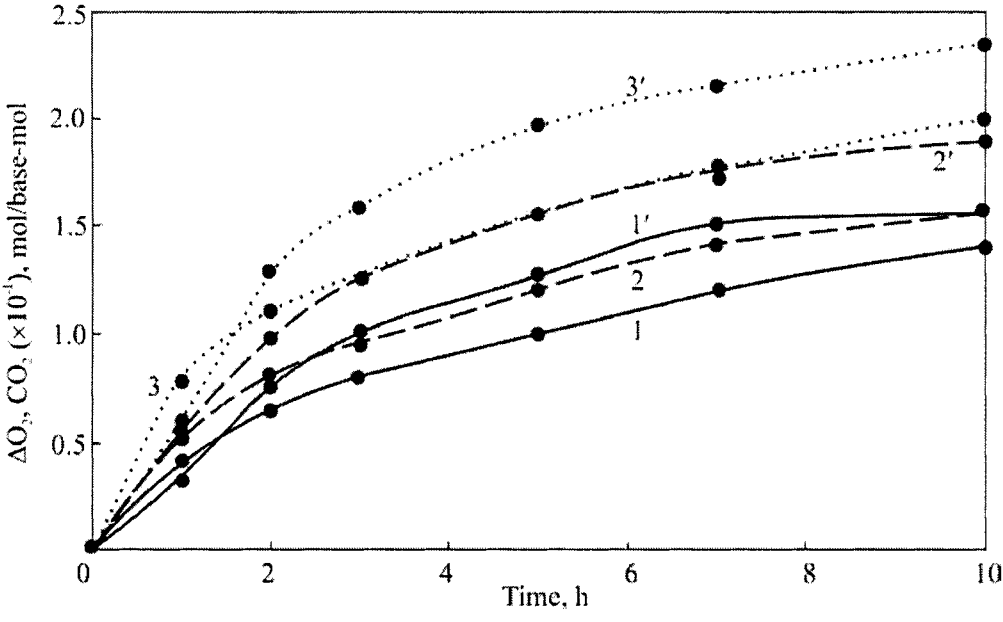

Figure 51. Kinetics of O_2 absorption (1 – 3) and CO_2 release (1' – 3') at PSF thermal oxidation in air at 300°C (1, 1'), 320°C (2, 2') and 350°C (3, 3')

Semi-logarithmic anamorphism of time dependences of the O_2 absorption rate at PSF heating in melt (Figure 52) with respect to O_2 pressure loss below 20% in a sealed ampoule due to O_2 expenditure displays a knee. This knee is associated with process transition from kinetic order one to kinetic order zero at the initial and developed stages with the boundary defined by absorption of 0.8 - 1.2 O_2 mol/base-mol. Similar phenomenon at thermal oxidation of arylaliphatic polybenzoxazole was interpreted [10, p. 104] as a two-stage consecutive oxidation of aliphatic and aromatic and heterocyclic fragments, i.e. quick expenditure of higher oxidizing aliphatic structures defines clearly expressed kinetics of the initial stage of the process.

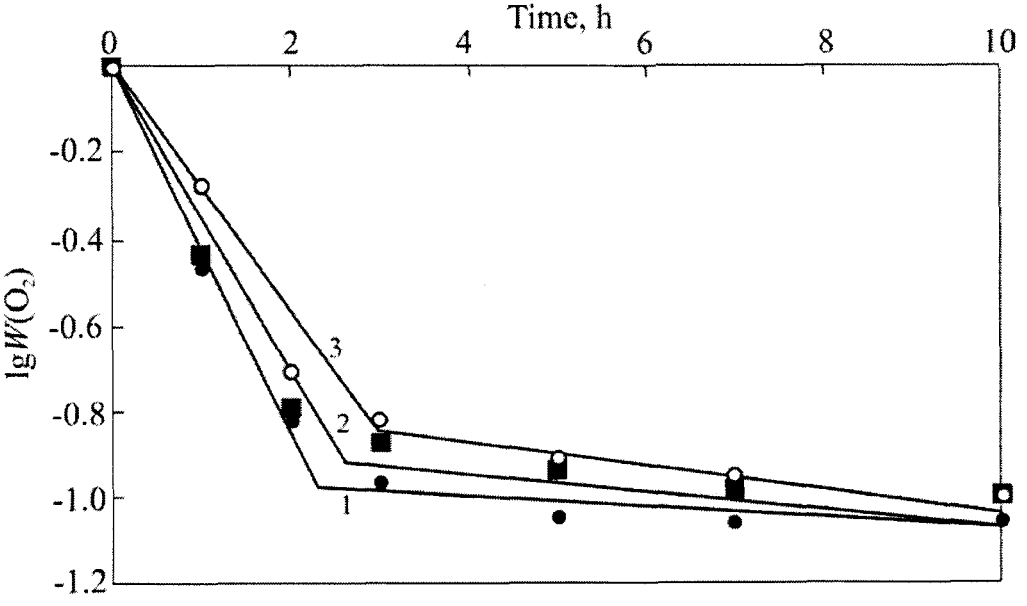

Figure 52. Time dependence anamorphism for PSF oxidation rate at 300°C (1), 320°C (2) and 350°C (3)

Kinetics changes with O_2 pressure (Figure 53). For processes proceeding under low pressure, sigmoid-shaped kinetic curves typical of P_{O_2} above 200 – 230 kPa (partial O_2 pressure in air) are transformed to S-shaped ones, and the induction period occurs not only in absorption kinetic, but also in gel accumulation. The dependence of initial O_2 absorption rates on the initial partial pressure of oxygen is approximately described by the following empirical equation:

$$V = P_{O_2}^{1/2}.$$

Such dependence may be caused by two reasons. The first is that the reaction proceeds in diffusion mode. This suggestion is rejected due to independence of specific O_2 absorption rates on PSF weighing (10 – 100 mg). As a consequence, kinetic dependence on P_{O_2} is inherent to the process mechanism.

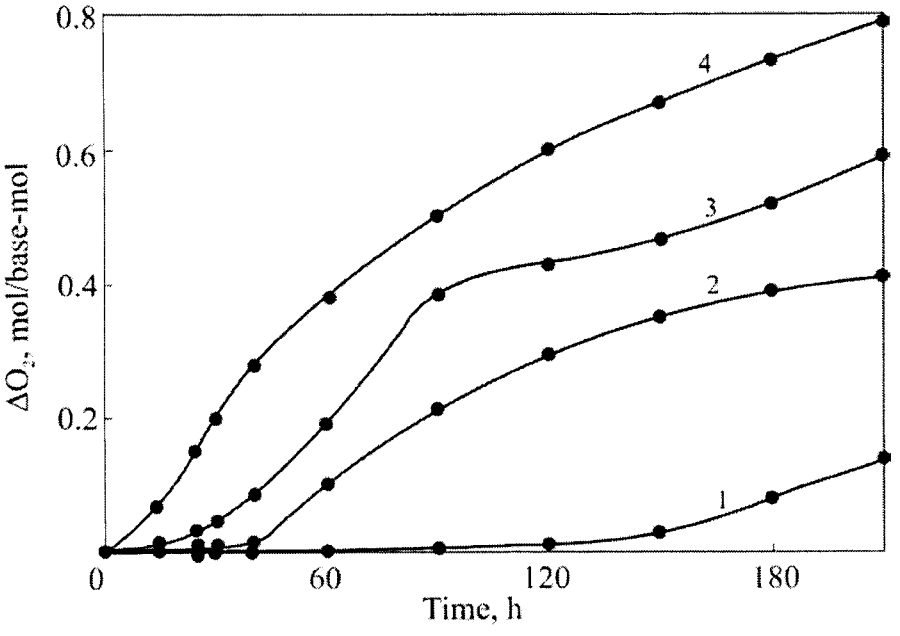

Figure 53. Kinetic curves of O_2 absorption by PSF at 320°C and O_2 pressure of 26.6 (1), 66.5 (2), 133.3 (3) and 399.9 kPa (4)

It is known that hydrocarbon liquid oxidation kinetics in the absence of diffusion hindrances is independent of P_{O_2} [8, p. 119]. Oxidation of carbochain polymers in solution is also independent of P_{O_2} [110, p. 132]. However, for low-temperature oxidation of solid polyolefins this dependence is associated with O_2 participation in oxidation initiation at hydroperoxide decay. It is suggested [110, p. 134] that the part of block hydroperoxides decaying faster that single hydroperoxides increases with P_{O_2}. Another contribution is associated with relatively low (compared with the liquid phase) rate of alkyl macroradical reaction with O_2 even in the kinetic zone. This leads to a competition between chain termination reactions which causes changes in the composition of hydroperoxides [110, p. 136].

Anyway, autooxidation rates at low temperatures are associated with hydroperoxides. Hydroperoxides were not detected at high-temperature PSF oxidation. This may be explained taking into account their thermal instability. Another idea about oxidation rate independence of P_{O_2} occurred during

studying high-temperature (270 - 360°C) PE oxidation [10, p. 101]. It is suggested that nearly linear dependence of V_{O_2} on P_{O_2} for PE at 300 - 360°C is associated with significant contribution of peroxy macroradical decomposition with formation of low-molecular mobile $OH^{\cdot}$ radical.

Besides the kinetics dependence on P_{O_2}, of special attention in PSF thermal oxidation is its self-excited accelerated type at P_{O_2} below 133.3 kPa. The time interval of autocatalysis at temperatures below 300°C is tens of minutes long (Figure 51). Therefore, autocatalysis may not be associated with branching products of low-temperature autooxidation, which are hydroperoxides, not accumulated at PSF high-temperature oxidation. As P_{O_2} changes, kinetic curves of O_2 absorption by PSF transform from S-shape to sigmoid. This phenomenon has no analogy in the literature (for example, σ-shape of PE oxidation kinetic curves at 240 - 300°C is also preserved at low P_{O_2} [177]). However, similar transformation was observed for oxidation kinetics ($H_2^+ + O_2$) at 485°C and various initial pressures [156, p. 106], i.e. in well-studied radical-chain, branched process. For high-temperature oxidation of polymers, it is suggested [10, p. 107] that self-excited accelerated type of reaction is associated with degenerated chain branching. Though the origin of intermediate branching products is not clear yet, by analogy with hydrocarbon oxidation in the gas phase the so-called "aldehyde branching" is suggested, but the existence of different, not yet defined alternatives also accepted.

Thus, comparison of PSF high-temperature oxidation phenomenology with examples from the literature indicates the signs of radical-chain, apparently branched process.

PSF thermal oxidation in melt causes quick gel formation and yellowing (Figure 54). Gel formation kinetics at high P_{O_2} at the initial stages obeys the order one law with the activation energy E_a = (49 ± 15) kJ/mol. Besides the proximity of kinetic parameters - $E_a(\Delta O_2)$ = 72 kJ/mol and symbate property of corresponded curves shown in Figures 5 and 6, possessing $\Delta G = 0.09\Delta O_2$, the interrelation of oxidation and gel formation is outlined by dependence of the latter on P_{O_2}: P_{O_2} decrease to 26.6 kPa causes occurrence of the induction period in gel-fraction accumulation kinetics. Analogous dependence is also observed for PSF yellowing (Figure 54).

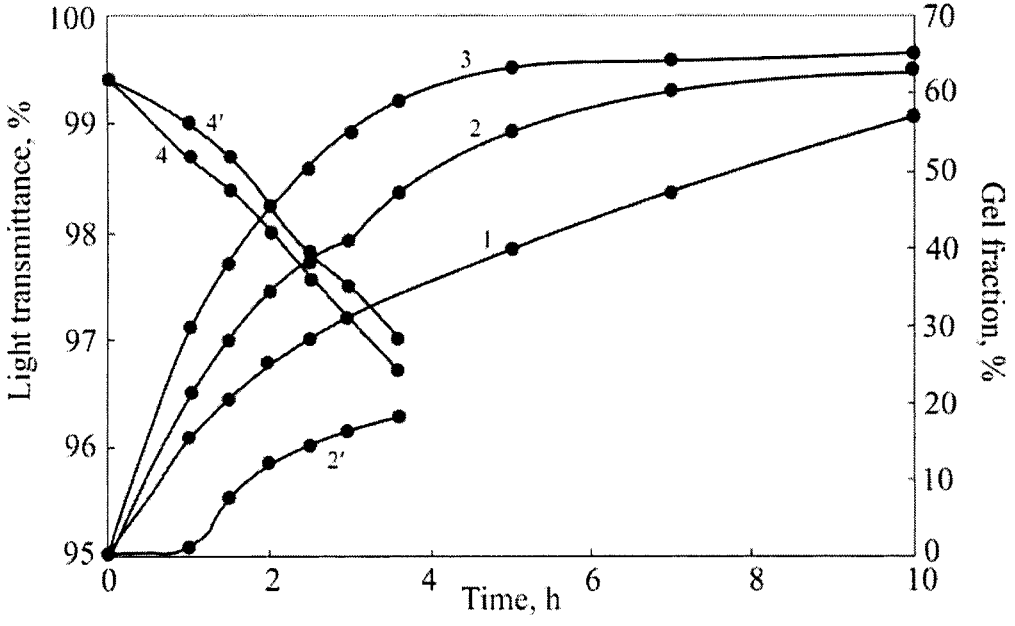

Figure 54. Kinetics of gel-fraction accumulation (1 – 3) and yellowing (4, 4') of PSF at 300°C (1), 320 °C (2, 2', 4, 4') and 350°C (3). Oxygen pressure: 212.8 (1 - 4) and 26.6 kPa (2', 4')

Gel formation and yellowing are the effective result of macromolecule size change and accumulation of functional groups in them. Before considering these processes separately, let us find a correlation between thermal processes in PSF at O_2 free access and standard tests in IIRT chamber, simulating polymer processing. As shown by this index (Figures 50 and 54), PSF degradation kinetics in IIRT chamber is adequate to thermal oxidation with free access of oxygen at partial pressure of 26.6 kPa. Under these conditions, gel formation points also approximately coincide. As contribution of PSF mechanical degradation is insignificant at shear stresses realized in IIRT, it is desirable to simulate processing by heating PSF up at P_{O_2} = 26.6 kPa.

As PSF is heated up at free access of oxygen with P_{O_2} = 26.6 kPa and exposure durations limited by the gel formation point (3 h), a constant shift of MMD curve towards greater masses and simultaneous broadening are observed (Figure 55). All MMD moments subsequently increase during PSF free thermal

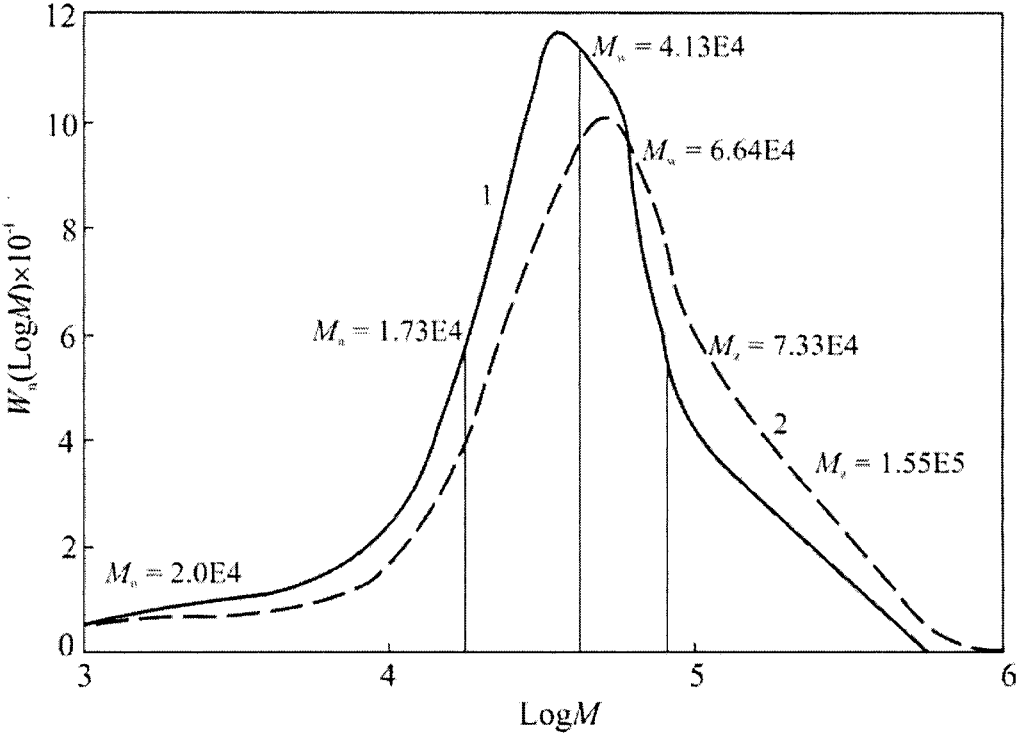

Figure 55. MMD for PSF before (1) and after (2) thermal oxidation during 1 h at 320°C

oxidation (Figure 8). Such curve shape nearly corresponds to the initial stage of MMD change only in PSF tests in IIRT cylinder (Figure 50), when some decrease of molecular masses is observed after initial rise, except for tests at 300°C, where all MMD moments increase. By kinetic curve shape (but not by absolute changes) PSF behavior in the cylinder is similar to free degradation in the absence of oxygen (Figure 50). For long stay in IIRT it may be simulated as follows. From positions of dissolved O_2 presence in the polymer, conditions in IIRT represent a superposition of controllable presence or absence of O_2. As polymer melts, it still contacts O_2 residues located in a gap between the nozzle and the piston free from polymer. No external air is delivered. The process develops as thermal oxidation with O_2 deficiency (i.e. like with P_{O_2} = 26.6 kPa) until all O_2 in the system is spent. When O_2 resource is exhausted, the process transits from thermal oxidation to pure thermal reaction, for which

kinetics of PSF molecular mass change is studied well. In case of thermolysis in vacuum at 380°C, degradation dominates over crosslinking. The first phase corresponds to real processing; in this phase melted PSF interacts with O_2 dissolved in it and O_2 gas residues, i.e. it oxidizes.

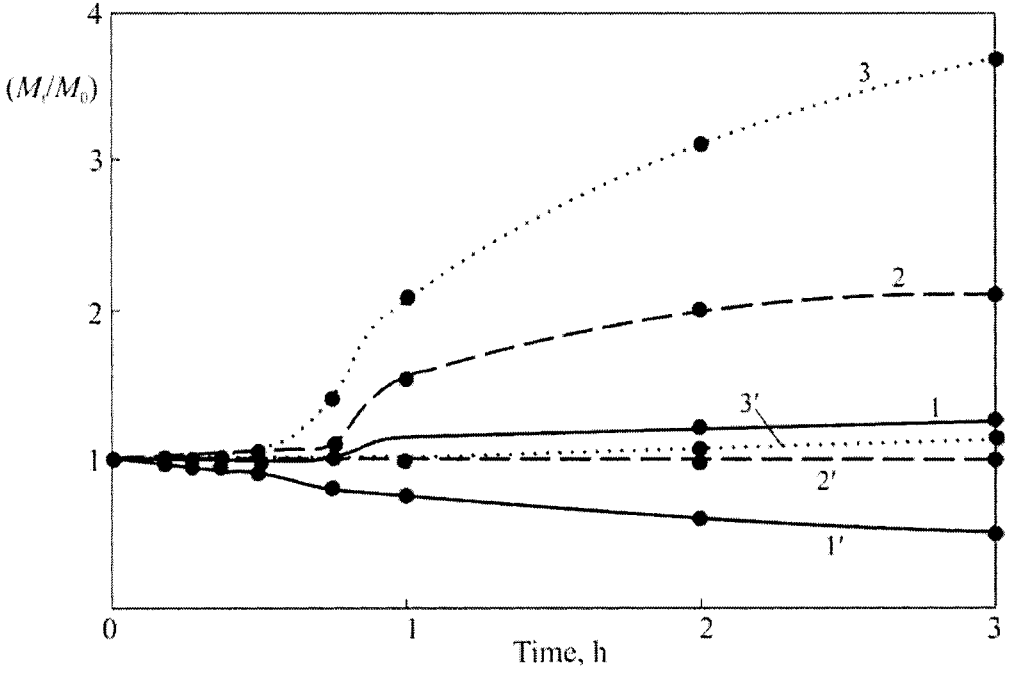

Figure 56. Relative change of PSF molecular mass during thermal oxidation at 320°C with P_{O_2} = 26.6 kPa (1 – 3) and in vacuum (1' – 3'); M_n (1, 1'), M_w (2, 2'), M_z (3, 3')

PSF molecular mass increases during thermal oxidation due to branching. A combination of viscosity gage and any other detector "on-line" gel chromatographer and the use of computer calculation in the framework of Zimm-Stockmayer theory made analysis of polymer branching much simpler. The method is designed to solve the reverse task – "adjustment" of experimental characteristic viscosity (viscosity gage) and its calculated value, obtained from MMD data from the neighboring "on-line" detector. To analyze the branching degree, one should know the so-called *g* factor, which is the relation of square radii of coils from analyzed and linear polymers. This factor is calculated by the

relation of characteristic viscosities of branched and linear polymers with equal molecular masses. The factor is determined by direct file comparison for linear and branched polymers. The information is presented as a function

$$g = f(M)$$

and the number of branchings per molecule, B_n, calculated from the Zimm-Stockmayer equation in the frame work of statistical model as follows:

$$g = \left[1 + \frac{B_n}{\sqrt{7}} + \frac{4B_n}{9}\right]^{0.5}$$

and branching frequency

$$\lambda(M) = P \cdot \frac{B_n}{M},$$

where P is the repeating unit of the molecule, for example, monomeric unit, and the average branching frequency:

$$\overline{\lambda} = \frac{\sum c_i \lambda_i}{\sum c_i}.$$

Data in Figure 57 illustrate the branching increase during PSF thermal oxidation, which initially is the linear polymer ($g = 1$). The g function indicates regular increase of the branching degree with molecular mass. The branching frequency averaged by MMD $\left(\overline{\lambda} = \frac{\sum c_i \lambda_i}{\sum c_i}\right)$ increase linearly first with exposure and, finally, reaches the border value (0.25 branchings per base-mole) near the gel formation point (Figure 59). Therefore, branching, as well as molecular mass increase, happens during the induction period of O_2 absorption (Figure 53). The average inter-crosspoint distance M_c equals 4,000 – 5,000. According to the long-chain model, this is also the length of side chains. Temperature increase speeds up the branching process in PSF due to thermal oxidative degradation. The gel formation point at 340°C shifts to 1.5 h; $\overline{\lambda}$

increase is accelerated, simultaneously, for example, this index for 1 h exposure equals 0.36.

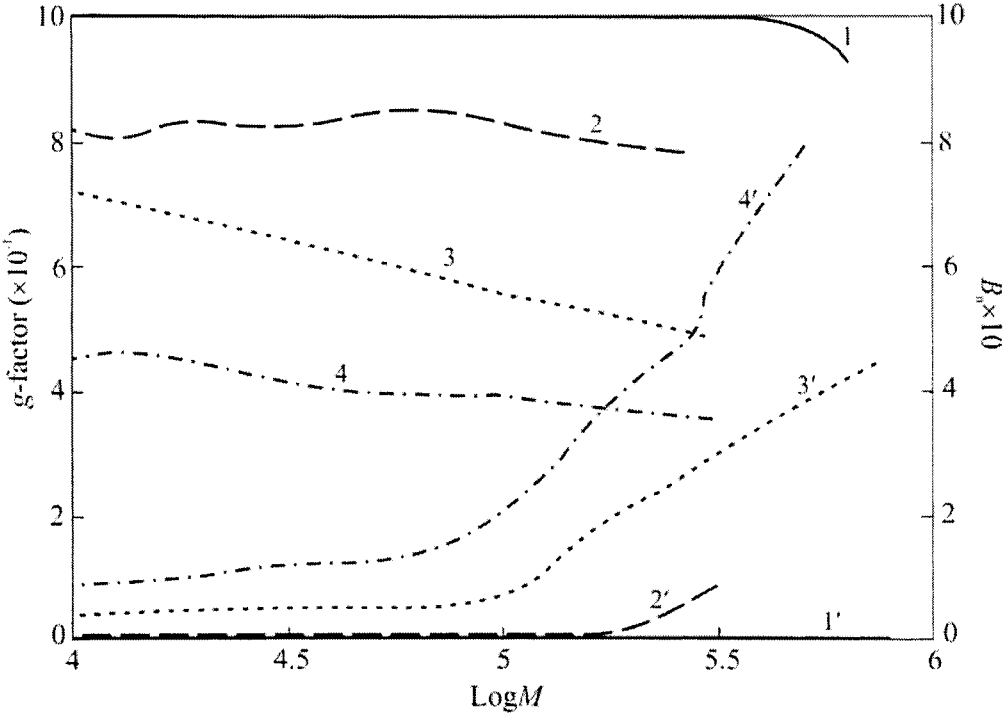

Figure 57. The effect of thermal oxidation (320°C, $P(O_2)$ = 26.6 kPa) on PSF branching indices: *g*-factor (1 – 4) and B_n^2 (1' – 4') at exposures of 0 (1, 1'), 0.5 (2, 2'), 1 (3, 3'), and 3 (4, 4') hours

The result of PSF thermal oxidation at $P(O_2)$ = 26.6 kPa correlates with the data on branching occurring in MFI determination. The *g* function run is also similar: deviation from 1 increases with molecular mass. Processing simulation (10 min, 320°C) performed with primarily linear polymer induces branching with $\overline{\lambda}$ = 0.008 – 0.015 per base-mole. Similar to the above-described indices (MMD moments, color), shear loads have a low effect on branching: 10-time increase of the load causes $\overline{\lambda}$ increase by 1.2 – 1.3 times only. Occurrence of branches is explained by MFI increase with PSF molecular mass due to exposure in IIRT device (Figure 50): viscosity of branched polymer

melt is usually much lower than for linear polymer of the same molecular mass [176].

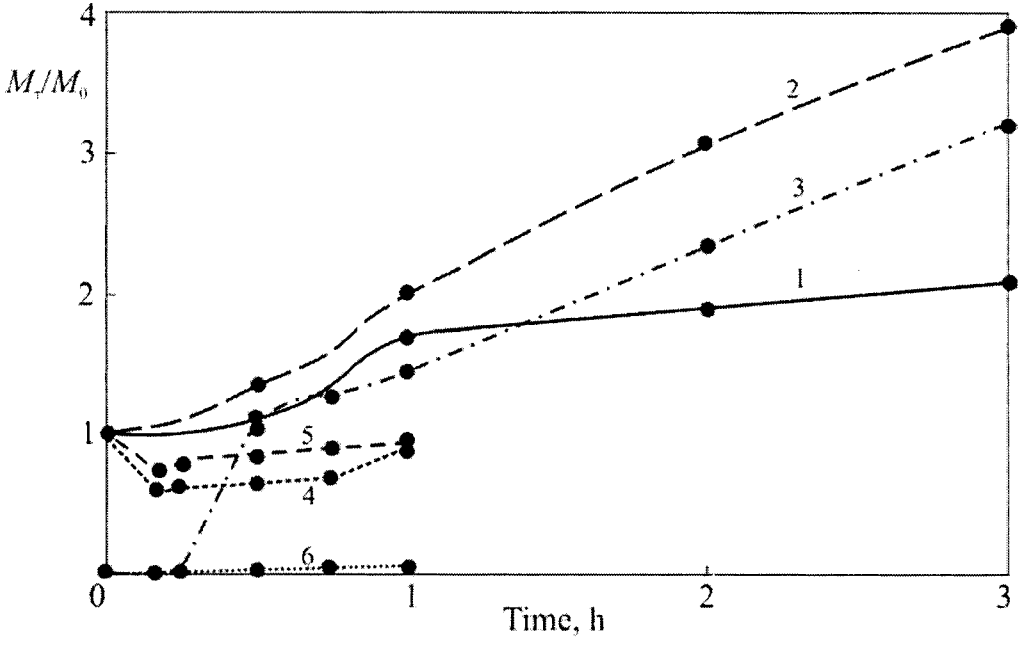

Figure 58. Changes of molecular masses (1, 2, 4, 5), rel. un., and λ (3, 6) during thermal oxidation (320°C, $P(O_2)$ = 26.6 kPa) of PSF (1 – 3) and PC (4 – 6): 1, 4 – M_w; 2, 5 - M_z; 4, 6 - λ.

Thus, one may conclude that PSF thermal oxidative degradation is of specific, structuring type. Contrary to pure thermolysis, in which degradation of macromolecules dominates over structuring even at 380°C [67], according to GPC data, high-temperature oxidation of PSF displays intensive molecular mass increase due to branching of macromolecules. In vacuum at 320°C, the gel formation point is not observed in PSF during 10 h at very low branching $\overline{\lambda}$ = 0.0055, whereas O_2 partial pressure equal 26.6 kPa is enough for observing gel formation already after 3 h. As a consequence, chain initial and propagation acts are different for high-temperature oxidation and thermolysis of PSF.

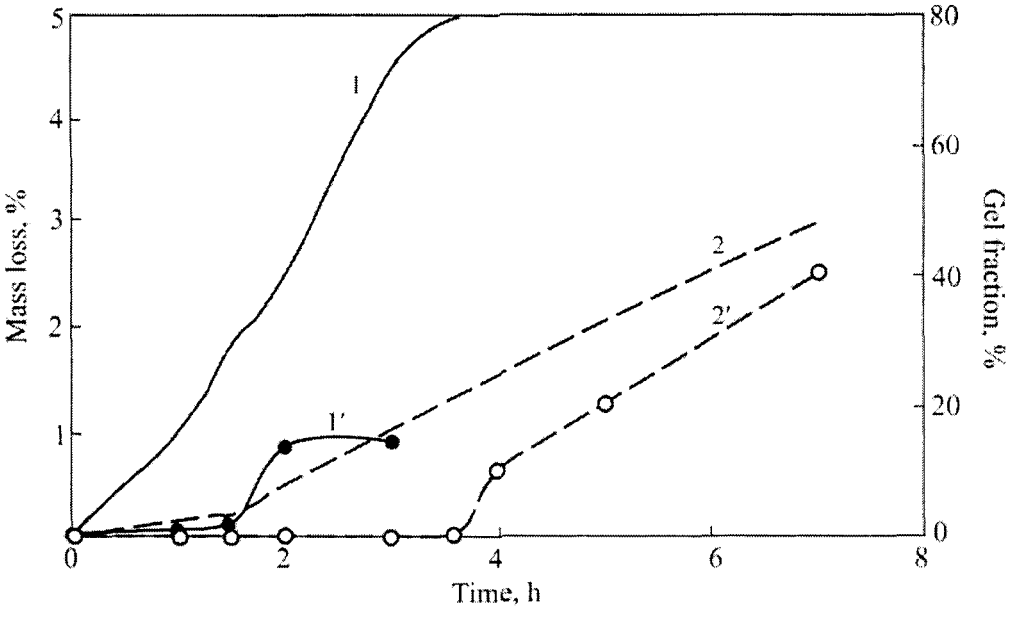

Figure 59. Mass loss (1, 2) and gel formation (1', 2') of aromatic polymers derived from bisphenol A: PC (1, 1') and PSF (2, 2'); 320°C in air

There are no experimental data in the literature about structure of the structuring center, but the authors have detected new signals of substituted aromatic C atoms with chemical shifts equal 146.59 and 147.53 ppm in ^{13}C NMR spectra of thermally oxidized PSF. In the initial PSF signals from 1,4-aromatic C atoms, which form an entire chain, locate at 136.15, 148.71, 153.54 and 162.74 ppm. It is shown [117] that chemical shifts of new signals from substituted C atoms are close to Ph-substituted aromatic C atoms. Additionally, substitution in aromatic rings during degradation may also be confirmed by occurrence of new signals (113.46, 116.09 and 116.98) in ^{13}C NMR spectrum. Compared with the initial PSF, these signals relate to unsubstituted aromatic C atoms shifted towards strong fields. Such shift occurs at C-H substitution by a strong electron-donor group. For the current system, the unique alternative is an oxygen-containing group, OAr~, for example. Signals from new substituted aromatic C atoms linked to O atom are masked by signals from analogous C atoms in the backbone with ether bond.

Though NMR data are not ideal as a confirmation, as they correlate with PSF structuring they indicate phenylation and/or oxyphenylation of PSF

aromatic structure at degradation, i.e. structuring centers are of the following composition:

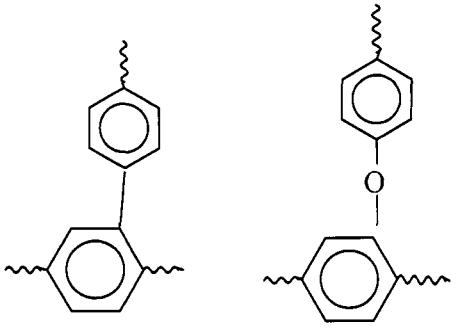

Besides the radical attack, structuring and crosslinking may be realized in reactions of active, valence-saturated structures. Mechanisms of this type are suggested for structuring polymers [26]. It is believed that at moderate temperatures, in the absence of aliphatic and aromatic structure dehydrogenation (below 350 - 400°C), structuring proceeds via interaction between active end groups and heteroelements, for example, in polyimides in reaction of end amino groups with imide groups. In PSF, end hydroxyl groups and, apparently, chlorophenyl groups are active. During thermal processing of PSF at standard processing temperatures in the absence of oxygen, re-polycondensation makes no significant contribution into changes of molecular-mass characteristics. Moreover, GPC data clearly indicate branching of macromolecules as the phase prior to gel formation. As end groups compete in hypothetical intermolecular reactions, hydroxyl end groups should be much more active than chlorophenyl ones. It should be noted that the result of this interaction (structuring and crosslinking) will depend on concentration of end groups, temperature and the absence of O_2 in the system. However, experimental data testify about clearly expressed dependence of the gel formation rate on O_2 pressure in the system and low dependence of crosslinking kinetics on end hydroxyl group content. For instance, crosslinking rates of PSF with hydroxyl group contents differing by an order of magnitude are comparable.

It should be concluded that structuring and crosslinking in PSF are performed as a result of macroradical attachment to aromatic rings in the macrochain. As suggested above, these rings are, most probably, end phenyl or

aroxyl ring. The first case represents benzene arylation [118], well-studied in physical organic chemistry. The second reaction is not practically investigated.

Now we approach the concept of substituting group polar effects in aromatic compound reaction kinetics, including homolytical substitution. This concept lies at the basis of quantitative theory of individual organic compound reactions [119]. Meanwhile, polar effects were almost neglected in the analysis of degradation behavior of aromatic polymers. To begin with there are end aromatic macroradicals. Macroradicals:

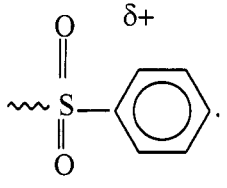

I $\sigma = 0.76$

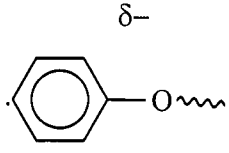

II $\sigma = -0.32$

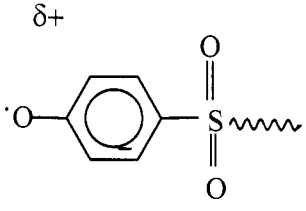

III

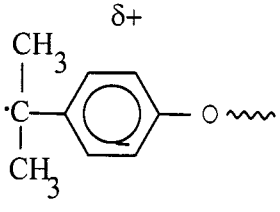

IY

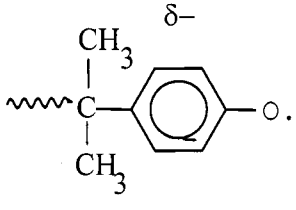

Y $\sigma = -0.197$

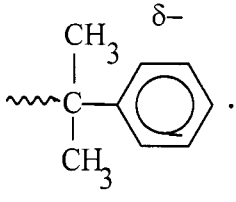

YI

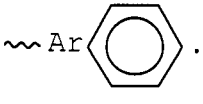

YII $\sigma = -0.01$

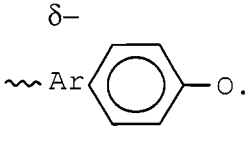

YIII

have bridge groups of different electronegativity in *para*-position at the free valence. They are strong electron-acceptor substituting group SO_2, relatively strong electron-donor ether group and weak electron-donor substituting group –

isopropylidene group having Hammett constants equal 0.76 – 0.32 and -0.197, respectively. Polar effect of the substituting group has a dual display:

- firstly, electron-acceptor substituting group delocalizes unpaired electron and kinetically stabilizes macroradical;
- secondly, depending on polar effect the radical becomes something like an ion-radical. As it was conditionally shown in structures of macroradicals I – VIII, the main atom with free valence obtains a charge of any sign.

Let us pass on to valence-saturated aromatic structures. In most cases, reactivity of monosubstituted benzenes, including homolytical reactions, obeys the Hammett equation [118]. Values of σ_n constants also allow estimation of the charge sign, formed by the substituting group at the main atom of benzene ring. So what are we to do with polymeric aromatic chain? It is obvious that there is no dislocation of electron density on aromatic rings in 1,4-arylene chain with bridge groups possessing equal electronegativity. It is a different matter, if the chain includes groups with different electronegativities as it takes place, for example, in polysulfones. As substitutes do not compete for electron, one may forecast for following charge distribution (or a tendency to distribution) for PES with strong electron acceptor SO_2 and electron donor ArO.

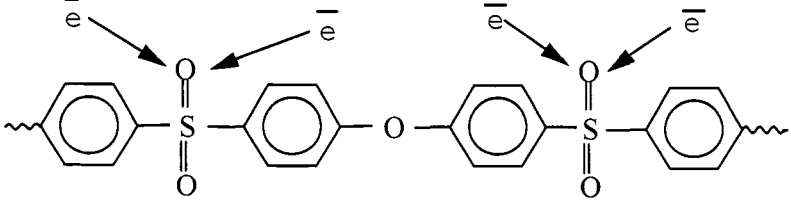

The case of PSF with three types of substitutes in the macromolecule seems to be more complex. It happens so that basing on table values of σ_n constants, we assume the possibility of electron density dislocation on aromatic rings, but are unable to assess it, because there are no proofs of additive approach reliability for disubstitution.

The ^{13}C NMR-spectroscopy theory forecasts almost linear dependence of chemical shift on electron density on C atom in π-systems [120, 121].

According to Popple, in the general case, chemical shift represents a totality of contributions:

$$\delta = \delta_g + \delta_n + \delta',$$

where δ_g is the contribution of diamagnetic electron current at observed atom; δ_n is paramagnetic contribution of electron orbitals possessing characteristic angular momentums; δ' is the contribution of all interatomic circular currents. Solution of the Carplus-Duss equation deduces the following expression for ^{13}C chemical shifts in aromatic systems compared with benzene:

$$\delta_{^{13}C} = \frac{1}{\Delta E\left(A_\pi \Delta Q_\pi + B_\sigma \Delta Q_\sigma - C_p \Delta p\right)},$$

where ΔQ_π and ΔQ_σ are relative π- and σ-charges on aromatic C atom, compared with benzene; Δp is the sum of mobile orders of bonds in relation to benzene; A_π, B_σ and C_p are constants (ppm) depending on atomic orbital compression at bond formation (the Coulson parameter); ΔE is the average excitation energy. It is shown [120] that only for alternate hydrocarbons σ-charge contribution is noticeable, whereas for benzene substitution

$$\delta_{^{13}C} = -K\Delta Q_\pi .$$

^{13}C nucleus shielding by π-electrons shifts the signal towards low fields.

The comparison of calculation data on electron densities performed by empirical, semi-empirical and *ab initio* MO-methods with chemical shifts of corresponded C atoms in NMR spectra of numerous aromatic hydrocarbons, cyclic compounds of purine, cumarin, etc. type indicated their good correlation [122 – 125] with linear dependence coefficient K, equal 160 – 200 ppm per electron (theoretical analysis gives 240 ppm). The sole exception are quaternary main C atoms only [123], to chemical shifts of which polarizability of atoms, π-bond orders, excitation energy and electron-nucleus distance contribute noticeably.

As a consequence, the fundamental dependence of chemical shift on π-electron density on carbon is reduced to direct or inverse linear dependencies of chemical shift on Poling electronegativity of substitutes, Hammett and Alfrey-Price constant values [126 – 128].

For aromatic hydrocarbons, most often representing a case of arylene disubstitution, of importance is that non-additive effects of two or more substitutes in the aromatic structure are either absent due to substitute interaction at electron levels or are low [125]. Therefore, it may be assumed for polymers that chemical shifts of secondary C atoms characterize π-electron densities on them.

^{13}C chemical shifts in benzene with equivalent aromatic carbon atoms equal 128.7 ppm. Minor variations in them in diphenyl are completely eliminated in 1,4-polyphenylene due to symmetrical, unitypical substitution (chemical shifts and ppm):

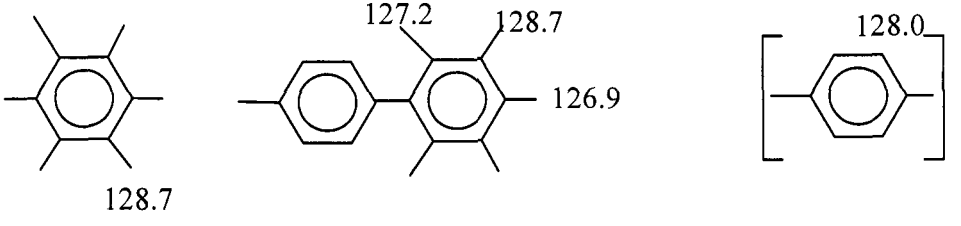

Similarly, variations in chemical shifts by ring disappear at transition from diphenyl ether to poly-(1,4-phenylene oxide):

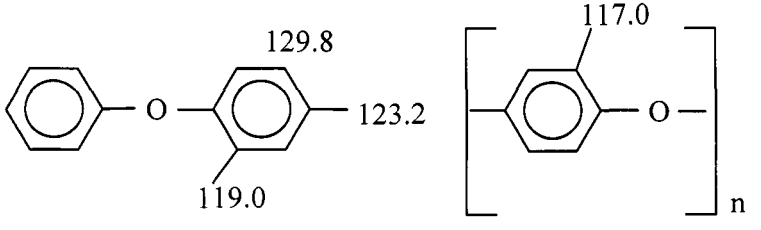

As we might expect, the diverse 1,4-substitution in polysulfones leads to significant variations in chemical shifts of secondary aromatic carbon atoms:

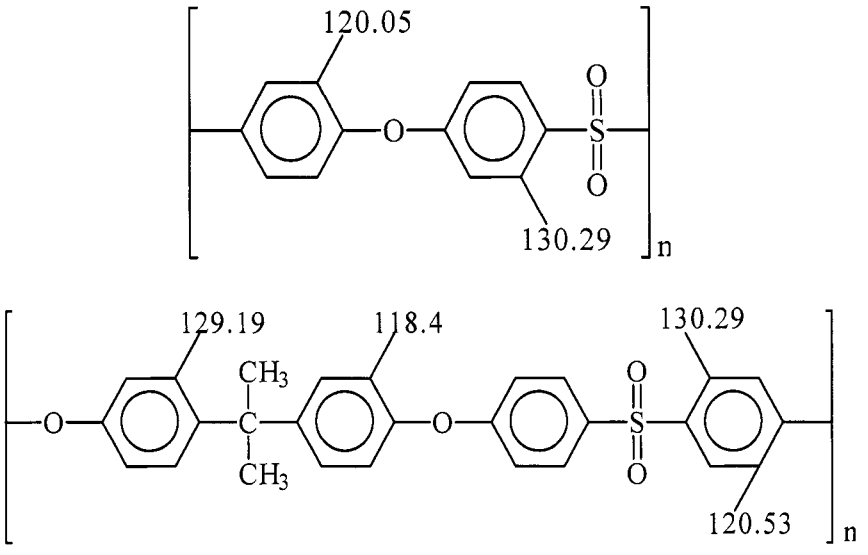

The variation of ring carbon atom chemical shifts indicates the alternation of π-electron density in the ring, which is associated with charge alternation [129]. If accepted average value of proportion coefficient equals 180 ppm per electron, the difference in chemical shifts of neighbor C atoms in the ring and PES, equal 10.24 ppm, gives difference in π-electron density up to 0.057 e.

Thus, polysulfones and their macroradicals have polar structures. This factor, on which the reactivity concept of organic chemistry is base, was not yet taken into account, though direct analogies are traced. Simamura [116] shows the dependence of substituted benzene homolytical arylation rate on the substitute type both in substrate and attacking aryl-radical. Compared with benzene, *para*-arylation rates are described well by the equation similar to Hammett one:

$$\lg \frac{K_n}{K} = p + \tau_n,$$

where p constant takes into account Hammett constants of substrate and radical; τ_n term, constant for every substituted benzene independently of attacking radical origin, is determined by the conjugation energy in intermediate aryl-hexadienyl radical. Similar equation describes kinetics of elementary chain

transfer reactions at polymerization as a result of radical addition to π-system of the monomer [114, Chapter 12]:

$$\lg K = \lg K_0 + \alpha\sigma + \beta,$$

where K_0 is the transfer rate constant via toluene – "nonpolar" component of the agent reactivity; σ is a parameter characterizing polar properties of substitutes in the radical; α and β characterize monomer or chain transferring unit properties. The polar effect was also observed in elementary reactions of radical inhibition by phenol antioxidants [80, 130]. It is believed that kinetically, the polar effect represents a decrease of the activation barrier due to positive Coulomb's interaction [114, p. 252]. Moreover, it is shown [116] that the summand in Simamura's equation correlates with the resonance energy of intermediate aryl-hexadienyl radical, and maximal stabilization is realized in systems with strong electron-acceptor substitute – five-fold different in resonance integral values may occur. However, as shown by MO-calculations for aromatic ions [129], the combination of substitutes with different electronegativity (donor-acceptor) is the most favorable for stabilization. Two electron-donor and electron-acceptor substitutes in *para*-positions destabilize aromatic ion due to occurrence of equal charges on neighbor C atoms in the ring.

Owing to alternation of π-electron density and stabilizing effect on aryl-hexadienyl structure of a pair of substituents (strong acceptor-donor), polysulfone structure promotes reactions between macromolecules and macroradicals, which cause structuring and crosslinking. Structuring that compensates polymer chain breaks may be considered as a stabilizing factor until, at least, this process affects technological and operation properties of polymeric material. Moreover, structuring by arylation or oxyarylation mechanism replaces active end macroradical by aryl-hexadienyl radical, stabilized by polar effects of the substitutes. Finally, aryl-hexadienyl radical decays, releasing H atom or a macromolecule fragment [65, 68, 73]:

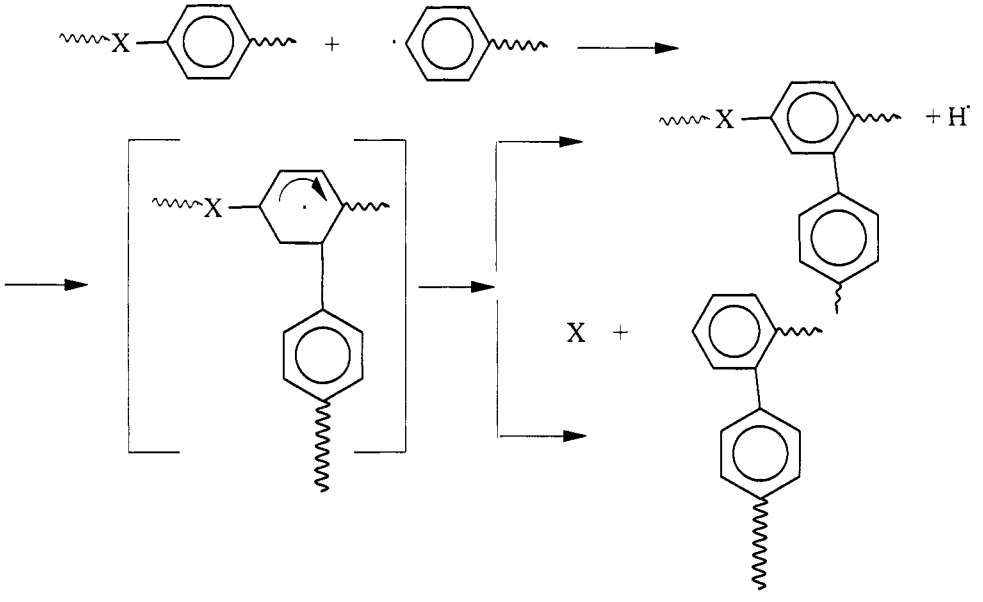

It seems that the situation recovered, and structuring in the arylation reaction has no stabilizing function. However, it should be taken into account that in the following act of chain transfer by macroradical the reaction will also form stable hexadienyl radical. The chain transfer by H atom with a macrochain break, dangerous for macromolecule integrity,

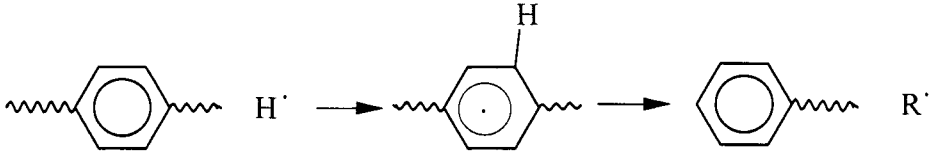

will also pass through formation of the intermediate hexadienyl radical [65].

Thus, from positions of stability, at aromatic polymer degradation of importance is how their structure promotes arylation displayed in polymer structuring of crosslinking. If the tendency is weak, macromolecules mostly degrade; in the opposite case, they are crosslinked.

^{13}C NMR spectra of aromatic polymers giving an insight into variations of electron density correlate with the tendency of polymers to structuring. Compared with benzene, polyester and polycarbonate displaying low variations

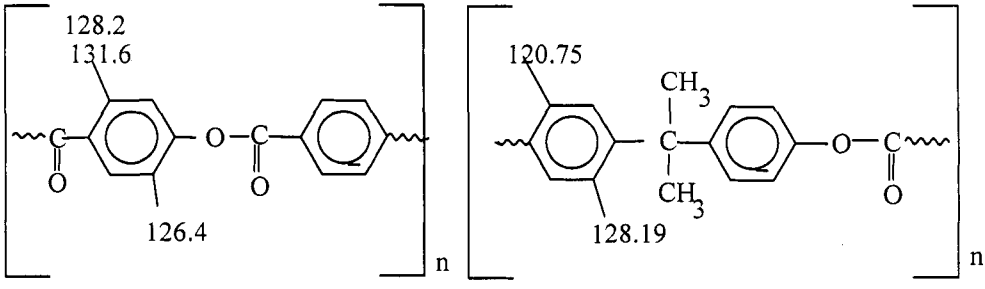

of ring C atom chemical shifts are less subject to structuring and are lower thermoresistant than the above mentioned polysulfones (Figure 59).

The assessment performed indicates relative weakness (380 kJ/mol) of CH_2-H-bond in diphenylisopropylidene structure. This bond break initiates the chain process. The following way of chain propagation:

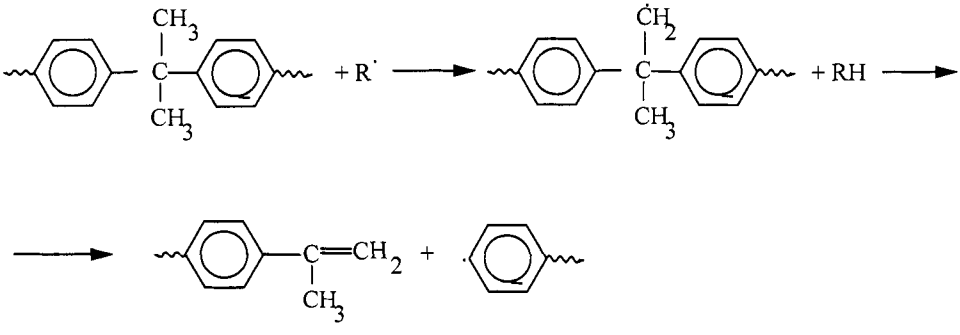

via β-decay leads to macrochain break and end phenyl macroradical formation. Similar pyrolytic transformation of bisphenol A residues in polyesters is suggested [178].

At rather low temperatures, oxidation initiation in the following reaction:

$$PH + O_2 = P{:}HO_2^{\bullet}$$

is kinetically more profitable than bond breaks in oxidizing molecule [1]. Anyway, this or alternative three-molecular reaction is considered as the most probable at hydrocarbon oxidation in the gas phase at temperatures above 400°C. The weakest C-H-bond in PSF structure is located in CH_3-group of isopropylidene bridge. It is as strong as 380 – 390 kJ/mol, which is by 70 – 80 kJ/mol lower than C_{arom}-H-bond strength.

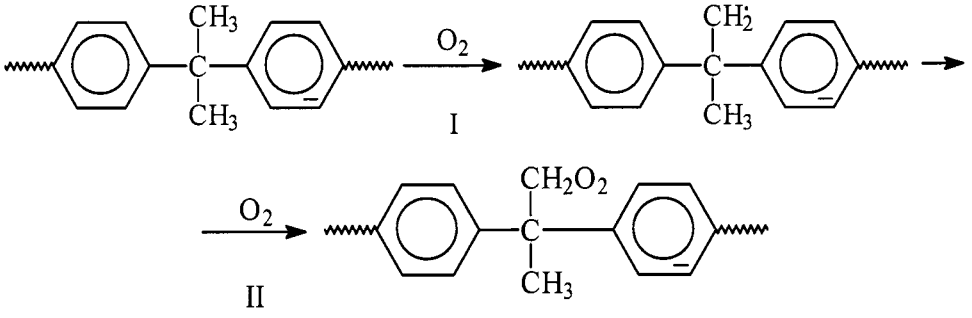

Such approach was already suggested [70] basing on intuitive idea about lower strength of aliphatic C-H-bonds compared with aromatic ones, as well as by analogy with the known oxidation schemes for hydrocarbons and aliphatic polymers. However, it should be noted that the reaction proceeds through the middle macroradical 1, identical to the same in PSF pyrolysis schemes. In pyrolysis, decay 1 induces macrochain degradation.

Contrary to thermolysis, no macrochain degradation was observed at thermal oxidation. Therefore, in the absence of oxygen the reaction "passes-by" thermal decay of the macrochain and propagates to formation of the middle peroxide macroradical 2. This is the conclusion important for degradation, because it argues with the common opinion on O_2 role at high temperatures as pyrolysis activator only.

If imagine that all events happen in isopropylidene bridge, the phenomenology of PSF degradation behavior may be hardly explained. Let us outline dissimilarity in degradation behavior of PSF and polycarbonate (PC) - another polyester derived from bisphenol A. In contrast with PSF, PC displays lower (by two orders of magnitude) tendency to branching (Figure 58). It would be very desirable to consider two stages on O_2 absorption kinetics (Figure 51) as separate stages of isopropylidene bridge and PSF aromatic structure oxidation. Unfortunately, to the authors' point of view, occurrence of branchings since the very beginning of thermal oxidation and rather long absence of branching in

pure thermolysis indicate participation of the whole PSF structure in thermal oxidation process.

Kinetic curves of O_2 absorption and CO_2 release (the main product of thermal oxidation) are symbate (Figure 51) and their effective activation energies are close: (72 ± 12) and (100 ± 15) kJ/mol, respectively. Only 10 mol% of absorbed oxygen is released with CO_2. Nearly the same amount is released with water. The part of CH_2O in the balance is also low: its yield is by an order of magnitude lower than CO_2 and H_2O. SO_2 (analysis sensitivity is 10^{-5} mol/base-mol), methane and other hydrocarbons, C_2 or higher aldehydes, ketones – thermal degradation products of isopropylidene group, and oxidation products of branched hydrocarbons [2] were not detected. The latter substances somehow simulate isopropylidene bridge, if neighboring aromatic rings in PSF are inactive. The main amount of absorbed oxygen remains in PSF, in polymeric oxidation products. Hydroperoxides were not detected in oxidized PSF.

IR-spectrum of PSF shows the following absorption bands of middle and high intensity (cm^{-1}) related to oscillations of the following groups: 3,099 – 3,038 ($\nu_{C_{ar}-H}$); 2,967 – 2,873 ($\nu_{C_{aliph}-H}$); 1,587 ($\nu_{ar\ C=C}$); doublet 1,505 and 1,589; 1,014, 835 (*para*-C_6H_4); 1,411 – 1,364 (δ_{-CH_3}); 1,247, 1,107 and 763 (SO_2); 1,081 and 1,014 (C-O-C). IR-spectrum analysis of PSF thermally oxidized (320°C, 20 h) shows occurrence of new absorption bands at 3,400, 1,900, 1,737, and 1,660 – 1,680 cm^{-1}, corresponded to (ν_{-OH}), absorption band harmonics which characterize substitutions of aromatic rings [138]: C_{aliph}=O and C_{arom}=O. The relation of bands at 1,737 and 1,660 – 1,680 cm^{-1} correlates with previously obtained data [94, 96]. Initial exposures corresponded to the beginning of O_2 absorption kinetic curve (Figure 51) are characterized by a low decrease of band intensity, associated with methyl group oscillations, with simultaneous increase of aliphatic and aromatic C=O bond bands, characterized by very high extinction coefficients, and band at 1,900 cm^{-1}.

Expenditure of methyl groups becomes obvious at exposures longer than 5 h, though after 15 - 20 h up to 60 - 80% of their initial amount remain in PSF. Even thermal oxidation (350°C, 100 h) cannot eliminate all aliphatic groups in PSF. Relative stability of CH_3-groups at processing temperatures (300 - 320°C) and times is indicated by ESR spectra, in which changes in intensities of both proton signals from end OCH_3 (3.76 ppm) and isopropylidene (1.67 ppm) methyl groups and aromatic protons (6.91 – 7.82 ppm) are not observed. Thus, in the case of PSF, a suitable mechanical model of high-temperature oxidation

of alkyl (alkylene) aromatic polymers [96, 148] with separate oxidation of aliphatic and then aromatic structures, based on the two-stage type of isothermal kinetics of O_2 absorption (Figure 51), is not proved experimentally. In degraded, intensively colored, insoluble polymer, which already absorbed 2 mol/base-mol of oxygen, a great part of methyl groups is preserved. Therefore, "evanescent" type of the first kinetic stage of PSF oxidation is not the consequence of CH_3-group exhaustion.

Besides occurrence of new bands, IR-spectra of oxidized PSFdisplay changes of intensive band ratio. These bands characterize backbone oscillation. Using the absorption band of aromatic C=C-groups (1,587 cm^{-1}) as the reference band, expenditure of *para*-phenylene structures (1,500 and 1,014 cm^{-1}) was observed since the very beginning of the process. This correlates with occurrence of the band at 1,900 cm^{-1}, which is associated with the type of aromatic substitution.

IR-spectroscopy data correlate with ^{13}C NMR results similar to the above-discussed situation. In oxidized PSF, OH-groups detected by IRS are interpreted [117] by ^{13}C NMR-spectra as C_{ar}-OH signal of 116.09 ppm, which is suggested to be of the end group.

According to NMR-spectrum catalogues, low signals with chemical shifts equal 26.97 (^{13}C) and 0.8 – 1.25 (^{1}H) ppm belong to methylene chain, which is absent in the initial PSF.

This observation may not be considered as an artifact, because there is a direct connection between intensity of mentioned signals and degradation temperature, and linear alkanes are identified among PSF pyrolysis products (450°C) [70]. The specific source of aliphatic products is isopropylidene group. It is apparent that at high temperatures this group isomerizes into a linear structure. There are no other ways of methylene chain formation. For example, suppositions about internal lubricant incrementing to PSF or vacuum grease from the device were discarded.

According to IRS data, besides expenditure of *para*-phenylene structures, thermal oxidation at temperatures up to 320°C causes less noticeable expenditure of sulfo-groups and ether bonds (bands at 1,247, 1,107 and 763, 1,081 and 1,014 cm^{-1}, respectively). However, temperature increase to 350°C or higher significantly intensifies degradation of the mentioned structures. Most likely, these degradation changes relate to deeper PSF transformation stages and may be neglected in the time-temperature range of its processing.

Thus, the initial stage of PSF high-temperature oxidation, which defines the quality loss by the material during processing (coloring and structuring),

represents O_2 absorption, CO_2 and CH_2O release, C=O-group accumulation in alkyl and aromatic components of macrochains, branchings and, finally, macromolecule crosslinking.

Polyesterimides

Heat resistance of polyesterimides (PEI), which differ by structures of diamine and dianhydride components, was studied using dynamic TGA/DTA (Figure 60). Table 16 shows PEI structures and data on mass losses at appropriate temperatures.

Aromatic PEI-2 is characterized by higher heat resistance rather than PEI-1, PEI-3 or PEI-6, which have aliphatic fragments in the composition. Injection of isopropylidene group to either diamine or dianhydride component equally decreases heat resistance of PEI. A significant decrease of heat resistance is observed in case of using diamines with dimethylamine substituting groups (PEI-4 and PEI-6).

In the absence of oxygen all PEI degrade in one stage, forming about 40% of coke residue. In air, aromatic PEI (PEI-2 and PEI-5) also degrade in one stage. Degradation of PEI with aliphatic fragments in the structure (PEI-1, PEI-3, PEI-4, PEI-6) is a two-stage process. At the first stage, mass losses are up to 10%. Then TG curve obtains a bending, and the second stage proceeds at lower rate up to full combustion of the coke residue. Degradation is accompanied by clear exothermal effects (see DTA curve). The first exothermal peak is present on the DTA curve for PEI with aliphatic fragments and is absent on the curve for pure aromatic PEI. Such difference is explained by degradation (oxidation) of aliphatic structures. The same regularity is observed for high-temperature (350°C) oxidation in pure oxygen: pure aromatic PEI possess the highest heat resistant, whereas PEI with dimethylamine substituting groups display the lowest heat resistance (Figure 61).

Table 16

Thermal stability of PEI of various chemical structures

Diamine structure	Dianhydride structure	Thermal stability by temperature (°C) at corresponding mass loss				
		T_1	T_5	T_{10}	T_{20}	T_{50}
1	2	3	4	5	6	7
PEI-1						
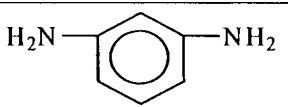	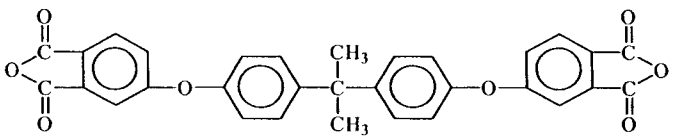	424	508	526	542	602
PEI-2						
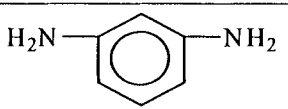	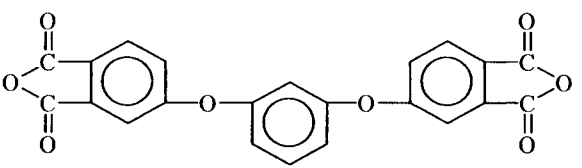	423	512	555	570	623

1	2	3	4	5	6	7
PEI-3	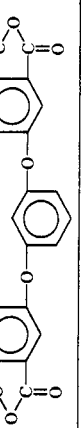	420	499	525	550	610
PEI-4	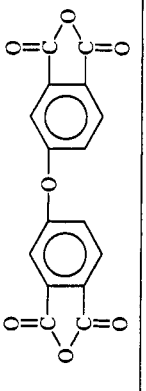	258	300	346	414	475
PEI-5	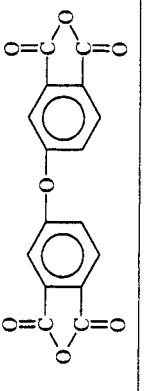	401	452	484	512	539
PEI-6	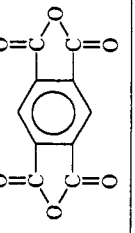	254	288	324	439	492

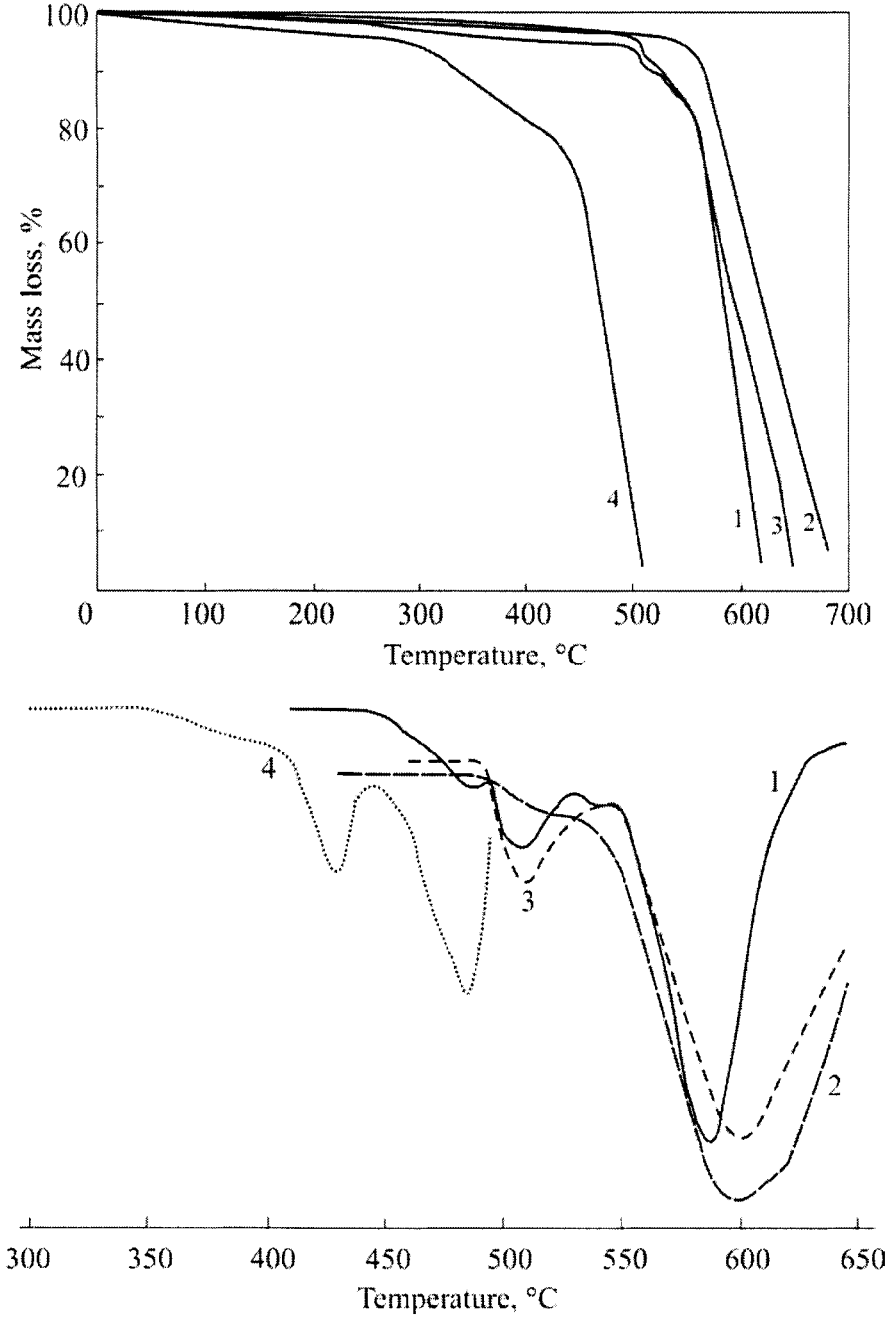

Figure 60. TGA/DTA data on polyesterimides of different structure

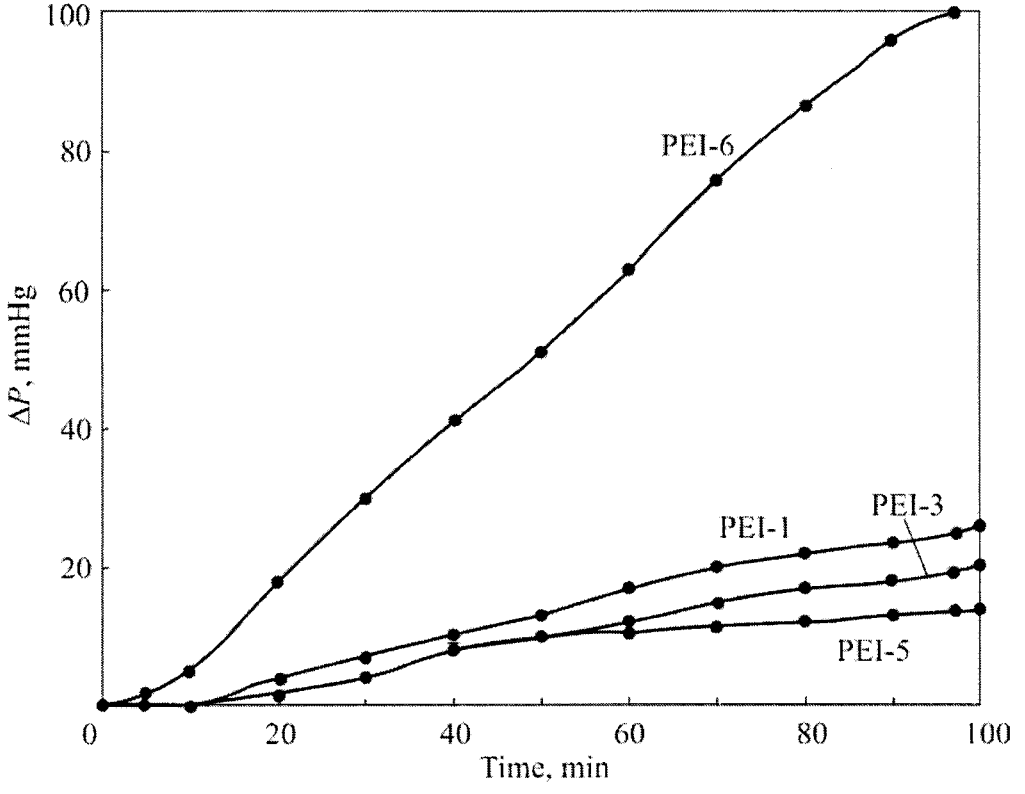

Figure 61. Oxygen absorption kinetics at thermal oxidation of PEI: T = 350°C, $P(O_2)$ = 300 mmHg

Thermal transformations in the processing temperature-time interval were studied on the example of polyesterimide derived from anhydride A and *m*-phenylene diamine, which was introduced into industry (trademark of international analogue is *Ultem 1000*, General Electric Plastics):

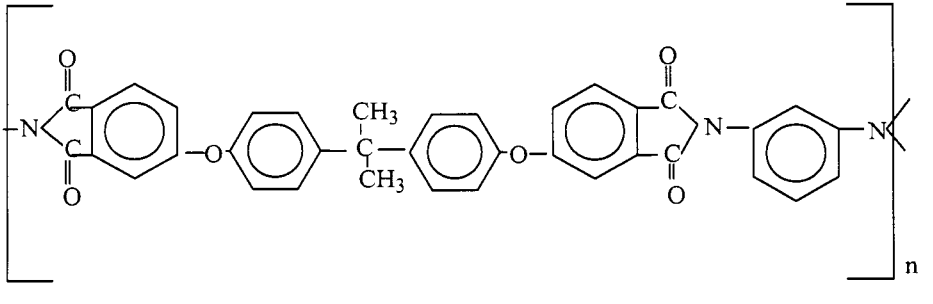

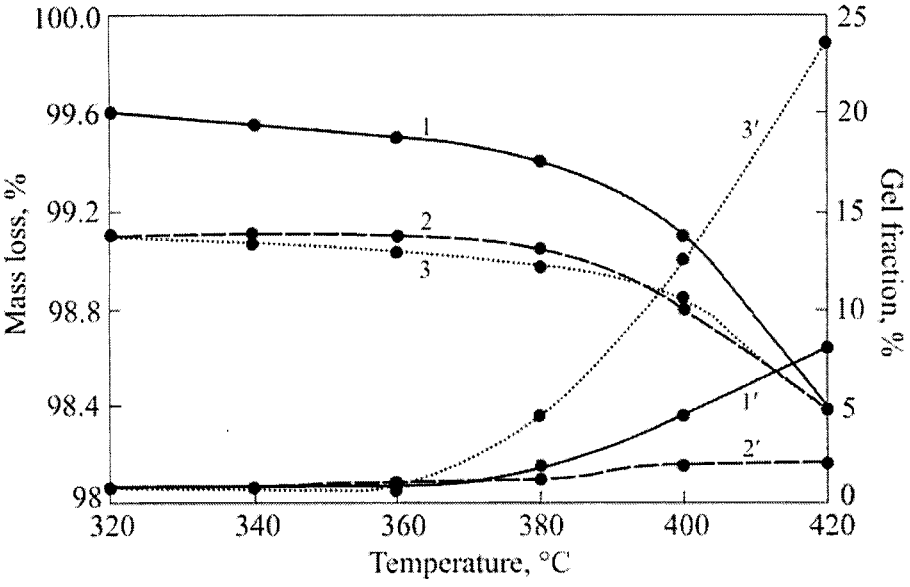

Figure 62. Mass loss (1 – 3) and dependence of gel-fraction content on temperature (1' – 3') of PEI heating in argon (1, 1'), vacuum (2, 2') and under air pressure of 50 mmHg (3, 3'). Time of heating is 30 min

PEI heating in the temperature range of 320 – 360°C during 30 min (Figures 62 – 66) causes no significant changes in heat resistance. The mass loss equals 0.4% in argon and 0.8% in vacuum. As shown by GCA and MS data, the main gas products in the mentioned temperature-time interval are water and carbon oxides (Figure 66). Water may be the delocalization product, which is also testified by the presence of *m*-phenylene diamine additive $\left(\frac{m}{z}=108\right)$. Methanol, formaldehyde and hydrogen traces were also detected.

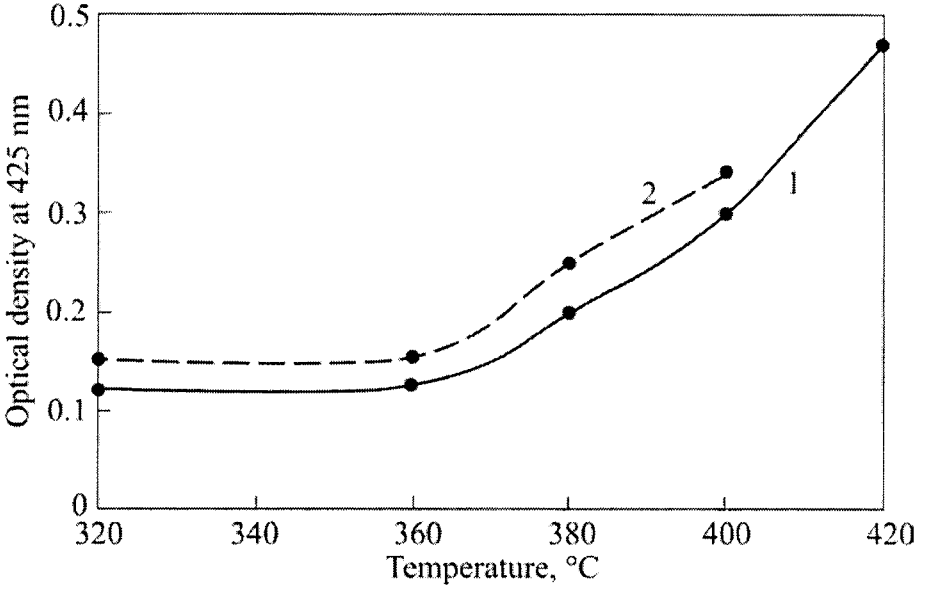

Figure 63. Temperature dependence of optical density for PEI in vacuum (1) and under air pressure of 15 mmHg (2). Heating time is 30 min

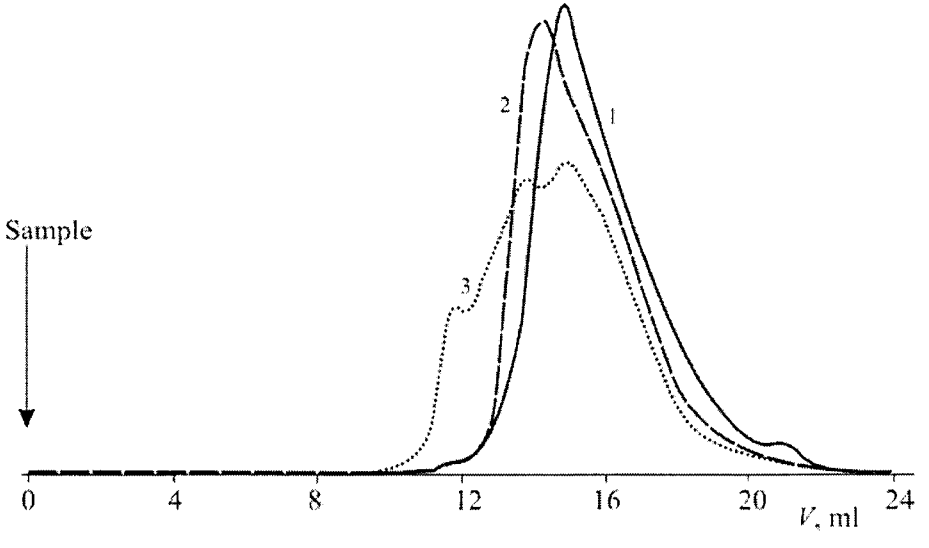

Figure 64. Chromatograms of polyesterimide samples: 1 – initial PEI; 2 - 360°C; 3 - 420°C. Heating in argon flow during 30 min

Insoluble fraction content (0.9%) does not change during thermal processing below 360°C (Figure 62). Therefore, some increase of optical density at $\lambda = 425$ nm (Figure 63) and molecular mass (M_w, M_z) was observed at almost constant polydispersion coefficient (Figures 64 and 65). The increase of MM moments also testifies about proceeding of pre-polycondensation. Changes in molecular-mass characteristics during PEI thermal processing in argon flow are shown in Table 17.

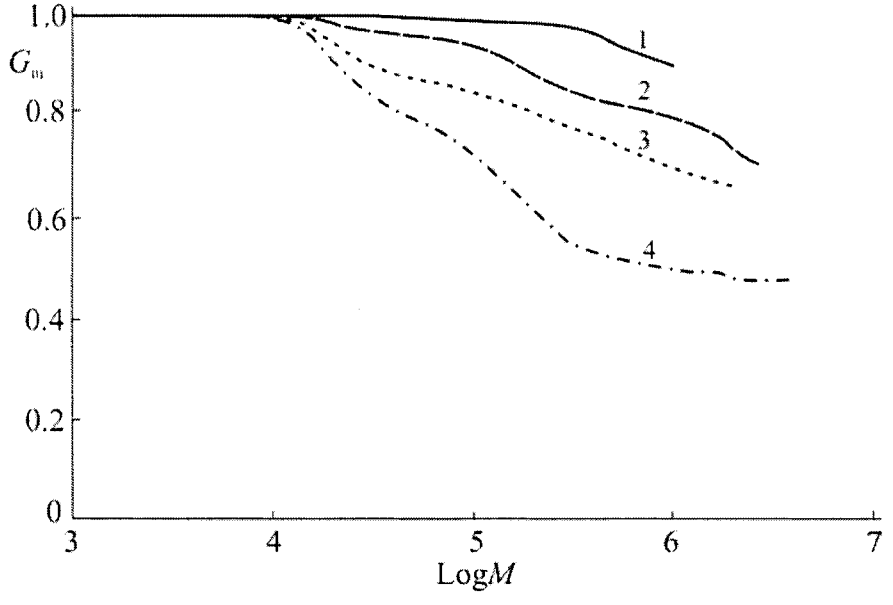

Figure 65. PEI *g*-factor: 1 - 360°C; 2 - 380°C; 3 - 400°C; 4 - 420°C; heating in argon flow during 30 min

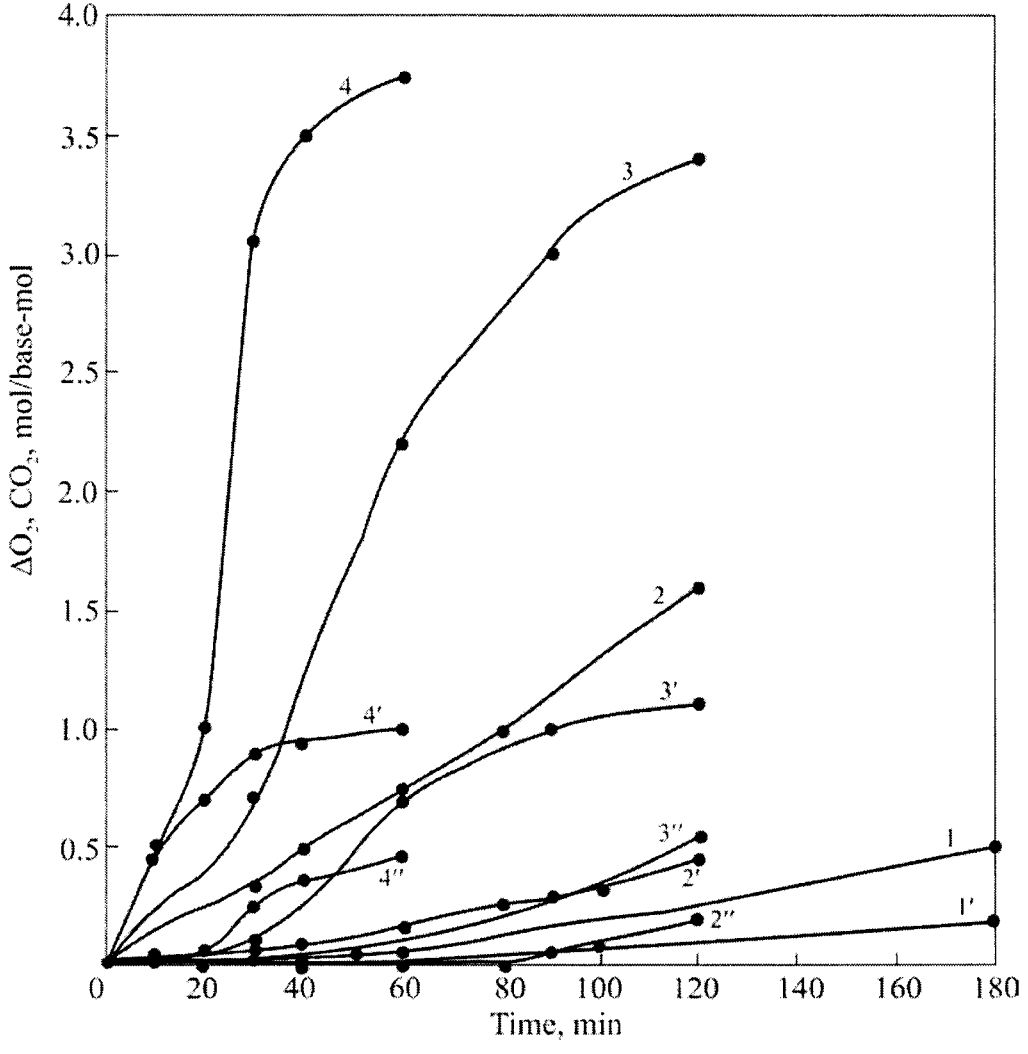

Figure 66. Kinetics of oxygen absorption (1 – 4), and CO_2 (1' – 4') and CO (2" – 4") release during PEI thermal oxidation in air at 300°C (1, 1'), 330°C (2, 2', 2"), 350°C (3, 3', 3"), 380°C (4, 4', 4")

Table 17

Changes in molecular mass characteristics of PAI during thermal processing in argon flow during 30 min

Temperature, °C	MMD				
	M_w	M_n	M_z	M_w/M_n	M_z/M_w
Before thermal processing	30,800	13,900	55,800	2.22	1.81
320	44,200	18,600	83,800	2.38	1.9
340	46,000	19,100	86,300	2.41	1.87
360	47,800	19,500	91,500	2.45	1.91
380	57,300	20,300	130,200	2.83	2.27
400	81,800	22,300	232,000	3.66	2.83
420	97,300	17,400	427,200	5.6	4.39

The shape of chromatographic curve is changed already at 360°C (Figure 64). Here, unimodality disturbance is observed; temperature increase at thermal processing leads to MMD shift to high-molecular zone and significant change of the chromatogram shape. Similar events, observed at polysulfomnes degradation, are usually associated with formation of branched structures. In this case, values of molecular masses, determined by GPC technique, may occur underestimated. Therefore, the two-detector (on-line viscosity and spectrophotometry gages) GPC technique was used. Table 18 shows results of this analysis.

Table 18

Changes in PAI molecular-mass characteristics at thermal processing (30 min, in argon flow). The two-detector technique

Temperature, °C	MMD			M_w/M_n	M_z/M_w	*g*-factor
	M_w	M_n	M_z			
360	49,100	20,100	90,100	2.45	1.84	0.99
380	73,800	24,300	180,100	3.03	2.44	0.9
400	102,300	22,900	336,200	4.45	3.29	0.86
420	126,100	17,100	536,000	7.16	4.25	0.79

Significant differences in MMD assessment by two methods were detected starting from 380°C or higher. The *g*-factor, which characterizes the

branching degree of the polymer, also significantly changes above 380°C (Figure 65).

In the presence of oxygen PEI heat resistance is decreased already at 320 – 360°C (Figures 61 and 67). Even at the lowest air pressure (15 – 50 mmHg), more than twice increase of optical density was observed. As oxygen content in the system increases, the polymer becomes more yellow (Figure 67). Table 19 shows results of MMD assessment. Thermal processing increases all moments of molecular masses. In the presence of air oxygen PEI polydispersity was also determined, due to MMD broadening.

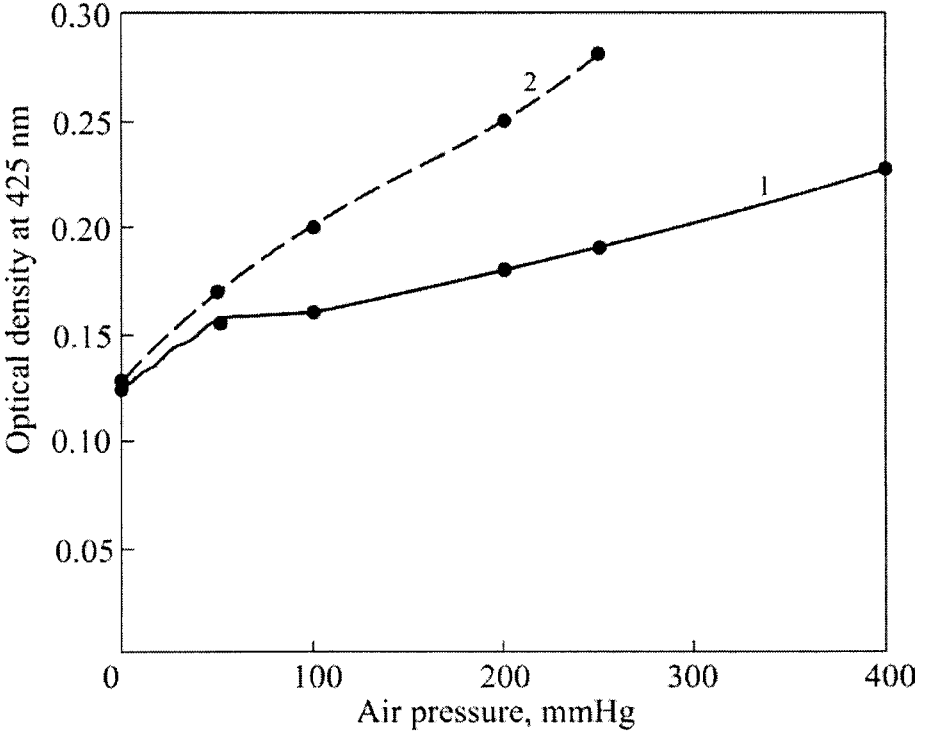

Figure 67. Dependence of PEI optical density on the air pressure. Heating time is 30 min at: 1 - 320°C; 2 - 360°C

Table 19

Changes in PEI molecular-mass characteristics during thermal processing (320°C, 30 min)

Conditions	MMD			M_w/M_n	M_z/M_w
	M_w	M_n	M_z		
Before thermal treatment	30,800	13,900	55,800	2.22	1.81
In vacuum	46,800	21,000	86,000	2.23	1.84
50 mmHg	39,800	17,000	75,000	2.35	1.87
Atmospheric pressure	38,800	15,700	81,100	2.48	2.09

Table 20

Changes of PEI molecular-mass characteristics during thermal processing (30 min, 420°C)

Medium	MMD					
	M_w	M_n	M_z	M_w/M_n	M_z/M_w	*g*-factor
Vacuum	75,800	20,000	276,000	3.79	3.64	0.9
Argon, 650 mmHg	60,100	17,700	201,000	3.4	3.34	0.95
Air, 50 mmHg	83,300	13,500	563,000	6.17	6.76	0.88

As follows from mass loss data, a noticeable decrease of PEI heat resistance is observed in the temperature range of 380 - 420°C (Figure 62). The gel fraction content and optical density of sol fraction increase simultaneously (Figure 63). After heat treatment (30 min, in vacuum), optical density of PEI sol-fraction is increased by 4.5 times compared with the initial value. All MMD moments are significantly increased in the temperature range of 380 - 420°C. The M_w value, determined by low-angle light scattering for PEI samples heated in argon at 380 and 420°C equaled 68,500 and 138,400, respectively. These data exceed M_w values calculated from GPC analysis (refer to Table 17). The comparison of M_w values determined by light scattering and two-gage GPC methods are similar, which is proved by the presence of branching in PEI. The branching degree depends upon the processing medium (refer to Table 20 for GPC data on *g*-factor).

The results obtained show that the presence of air oxygen in the system significantly intensifies PEI structuring. Degradation reactions proceed simultaneously, which is proved by M_n moment decrease and polydispersion increase (Figure 64, Tables 17, 19, 20).

The composition of thermal (in vacuum) and thermal oxidation (in air) PEI degradation products was studied using chromato-mass-spectrometry and NMR analysis in the mentioned temperature-time interval.

Analysis of thermal degradation identified: phenol and its derivatives (2-, 4-methylphenol, 2,1- and 4,1-methylethylphenol), benzene, toluene, of benzofuran and diphenyl derivatives, acetic and benzoic acids, phenyl acetate, diethyl 1,2-benzyldicarbonate, phenyl-*p*-isopropylphenyl ester, dibutyl ester of 1,2-benzyldicarboxylic acid, and phthalic anhydride.

This complex mixture of compounds possesses products of monomers and polymer synthesis (toluene, phthalic anhydride, acetic acid, etc.). Products formed in heterolytical reactions (phenol, at Ar-O-Ar bond decay) and thermal decay (phenol derivatives at bisphenol A degradation by isopropylidene bridge), The central carbon atom bond sensitivity in bisphenol A was NMR confirmed. The fragment ~Ph-C(CH_3)CH_2 was also observed by NMR spectra of degradation products.

Table 21 shows assessment of gas product amount, released from PEI at thermal oxidation.

Table 21

The composition of gas products of PEi thermal degradation

T, °C	Exposure, h	Absorbed O_2 amount, mmol/base-mol	Released product amount, mmol/base-mol		
			CO_2	CH_2O	CH_2OH
300	0.5	0	10	0.07	0.07
340	0.5	90	20	0.09	0.10
380	0.5	180	36	0.16	0.30
420	0.5	330	93	0.34	1.00
200	1,600	30	5.25	-	-

Besides gas products, similar to conditions under vacuum, a sufficient amount of various heavy products is formed in the presence of oxygen. The composition of these products was identified by NMR and CMS methods.

The composition of PEI thermal oxidative degradation:

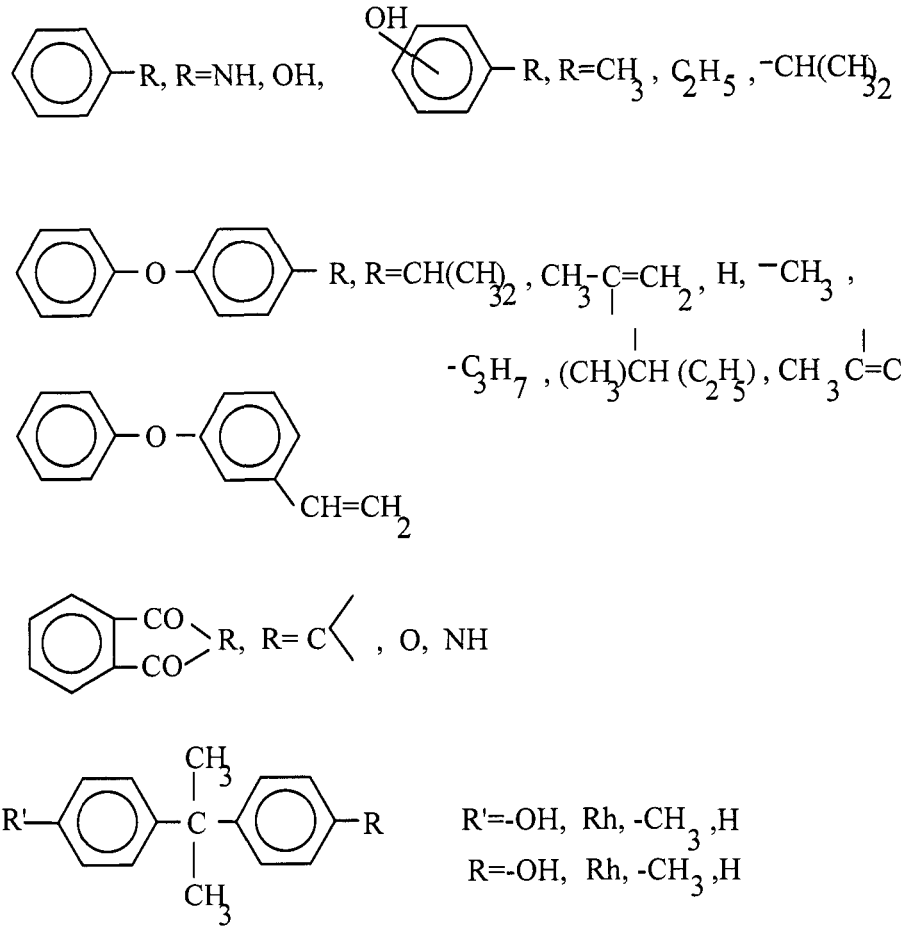

Phenol, bisphenol A and their derivatives are detected both in thermal and thermal oxidative degradation.

Changes occurring in PEI at high-temperature oxidation were estimated by IRS data. Heating up to 400°C did not cause significant changes in IR-spectrum. At stability of phthalimide cycles (1775, 1718 and 1358 cm^{-1}), reduction of absorption band intensity was observed in the spectrum of the sample heated up to 420°C or higher at 2900 – 3000 cm^{-1} ($\nu_{C_{aliph}-H}$), 1400 – 1300 cm^{-1} (δ_{CH_3}) and 848 cm^{-1} (*para*-C_6H_4).

The initial stage of PEI high-temperature oxidation, which defines the quality loss of the material during processing, is characterized by coloring. In this case, oxygen is absorbed, gas and heavier products are released, carbonyl groups are accumulated in the structure, and branched structures are formed in the polymer.

The structural fragment, bisphenol A - general for PEI and PSF – and almost equal composition of thermal oxidation products (in relation to polymer structure) allows simultaneous discussion of thermal oxidation mechanism of these two polymers.

On the mechanism of PSF and PEI thermal oxidation

The following factors clearly indicate contacts of aromatic rings with oxygen since the very beginning of the oxidation process: high O_2 absorption rate and low expenditure of CH_3-groups, the shape of kinetic dependence for the ratio of absorption band intensities at 1600 and 1737 cm^{-1}, which characterize oscillations of aromatic and aliphatic carbonyl groups, and the extreme type of accumulation of carbonyls in the aromatic component with the maximum at 6 – 8 h exposure (320°C). If it is different, quicker expenditure of methyl groups will be observed rather than observed in the experiment. The initiation of aromatic ring oxidation by isomerism of peroxy radical via non-conjugated 7-term complex with degradation by the type below:

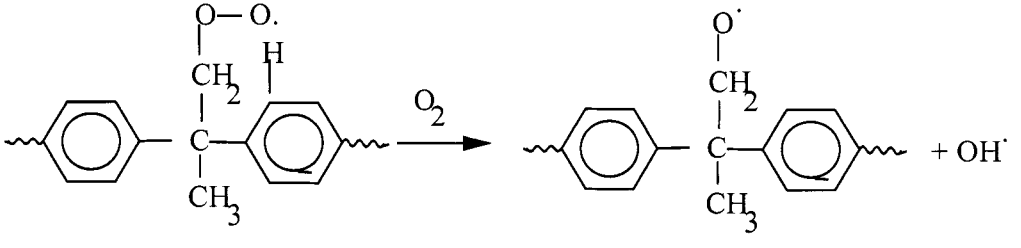

forms formaldehyde shell (side alcoxyl radical) and initiates oxidation of the neighboring aromatic ring. Nevertheless, it "links" the oxidation process to the zone around isopropylidene group. Compared with other radicals in the viscous medium, "light" and mobile HO-radical plays a significant role in the mechanism of high-temperature oxidation of polymers [10, p. 110] and at chain propagation attacks the most mobile C-H-bond, e.g. the side methyl group is

attacked again. Any analysis based on traditional schemes of radical-chain oxidation, even with respect to "high-temperature modifications" [10, p. 111], leads to oxidation dominance, which means CH_3-group expenditure. The latter fact is not confirmed by any data, both experimental and literary [179].

Two more circumstances should also be taken into account. Firstly, the preferable oxidation of side methyl groups, which leads to detachment of side C-atom in the form of CO, CO_2 or CH_2O, may not shift the oxygen balance abruptly towards its retention (about 90%) in the polymer (Figure 51). Moreover, the fundamental argument [148, 180] for the benefit of primary oxidation of aliphatic fragments – the two-stage kinetics (Figure 52) – is argued by the observation of kinetics type of fully aromatic PES, PI and PEI (Figures 51 and 68). To put it differently, both oxidation initiated by aliphatic structures and direct oxidation of aromatic rings should be taken into account.

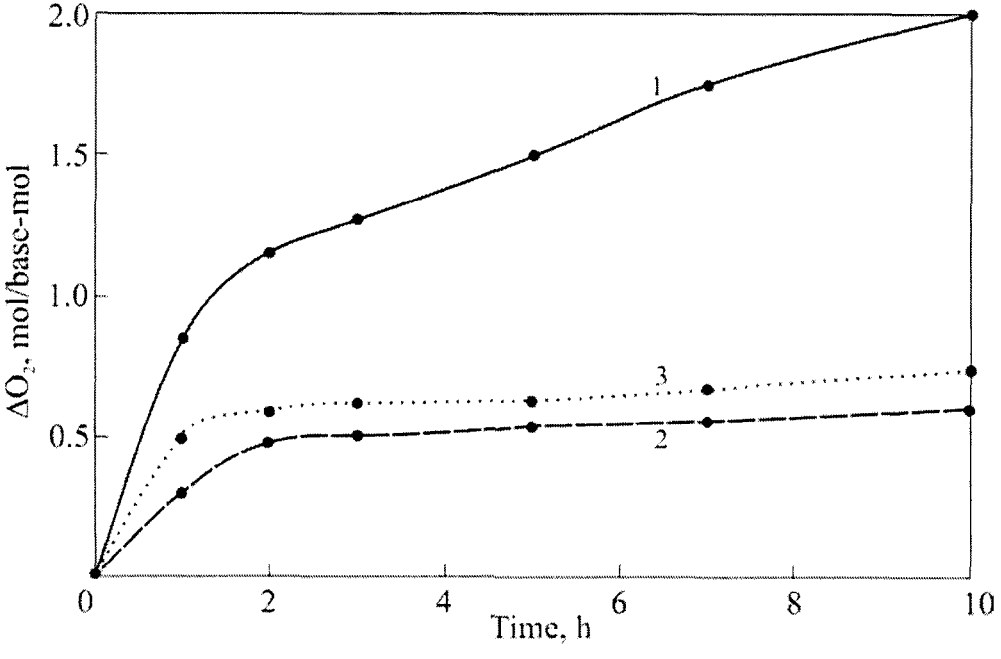

Figure 68. Oxygen absorption kinetics by PSF (1), PES (2) and PES-B (3) at 350°C in air

Among aromatic substances, only benzene oxidation is studied in detail. As suggested [181], oxidation proceeds by the chain mechanism, forming phenol as the primary product by the following reaction:

$$C_6H_5O_2^{\bullet} + C_6H_5 \rightarrow C_6H_5OH + C_6H_5O.$$

Self-excitation acceleration of the oxidation kinetics was the argument for the benefit of oxidation chain branching due to side (not mentioned) products. Since investigations were performed above 450°C, i.e. in the pyrolysis range, the following reaction was considered as the oxidation initiator:

$$C_6H_6 \xrightarrow{-H} C_6H_5 \xrightarrow{O_2} C_6H_5O_2.$$

For the current case, of importance is the concept of radical-chain oxidation mechanism of benzene ring, though the above-mentioned initiation [181] is unreal in the temperature range of 300 - 350°C.

Photo oxidation of aromatic and heterocyclic compounds is developed via endoperoxides [87, 92, 103]. Though there are no proofs of endoperoxide formation at high-temperature oxidation of aromatic polymers, this idea has already been applied to schemes of thermal oxidative degradation of organic, heat-resistant polymers [28]. Pure thermal transition of these polymers to electronically excited state at 300 - 400°C is quite real [32]. Structure-less UV-spectrum of PSF with the maximum at $\lambda = 275$ nm corresponded to n-π junction (for PEI, the maximum in UV-spectrum is located at $\lambda = 284$ nm) has the long-wave boundary at 450 nm. The long-wave boundary of real industrial PSF and PEI samples may reach 600 nm. Thus, the minimal energy of electron-excited states in PSF and PEI do not exceed 200 – 300 kJ/mol. Though direct determinations of this energy from emission electron spectra are much below the approximate assessments by absorption spectra, the part of electron-excited structures at 350°C must be negligibly small:

$$\exp\left(\frac{E_{\text{excite}}}{RT}\right) \sim 10^{-19} \div 10^{-17}.$$

The reaction of electron-excited (e.g. triplet) aromatic molecule with oxygen (usually also triplet, $\sum \bar{g}$) simulated by the following expression:

$$P^{\bullet} + O_2 \xrightarrow{K_1} PO_2^{\bullet}$$

using maximal reliable values of the rate constant (K_1) and recalculating table values for 600 K, and O_2 concentration in polymers is taken equal to its maximal value in the gas phase. Even under these favorable conditions and assumptions the calculated rate is by many orders of magnitude lower than the observed rate of O_2 absorption.

In the discussion of the mechanism of aromatic polymers, the reaction of O_2 addition to double bond with peroxy radical formation was not taken into account:

$$CH_2{=}CHP + O_2 \rightarrow {}^{\bullet}OOCH_2CHP.$$

In the classical kinetics, this reaction is considered as one in the sequence for initiation of the oxidation chain, for example, of vinyl group in styrene [8]. Even at room temperature, benzene ring forms a molecular complex with O_2 [182]. As shown [182], these are charge transfer complexes (CTC), in which O_2 is the acceptor of electrons, accepting them to free $\pi g^2 p$ orbital. Despite the fact that oxygen CTC are weak, because oxygen affinity to electron is 0.15 eV, they should be considered as contact pairs at the beginning of chemical interaction, for example, peroxide formation [184].

Therefore, the increased resistance of aromatic polymers with SO_2-groups to thermal oxidation is quantitatively described. This dependence was traced via unitypical aromatic polymers with different types of bridge structures [185]. SO_2-groups are strong acceptors and compete with molecular O_2 for aromatic π-electrons. In PEI this function is performed by the imide cycle.

A rough estimation of O_2 absorption rate in reaction of addition to aromatic ring using the chain initiation rate constant in styrene

$$K = 3.6\times10^{10}\exp\left(-\frac{125{,}000}{RT}\right) \text{ [110, p. 125]}$$

and O_2 solubility values (10^{-3} mol/kg at 266.6 kPa), approximated by data on dissolution heats and O_2 solubility in polymers of PSF and PEI structure at 300°C [10, pp. 20 – 23] on their processing conditions, give the value close to experimental by the order of magnitude. This fact may also be considered as an

additional confirmation of direct O_2 interaction with aromatic rings in PSF and PEI during high-temperature oxidation.

Thus, besides the above-described isopropylidene pathway, high-temperature oxidation of PSF and PEI is, apparently, realized in aromatic structure reactions, which may be present by the following scheme:

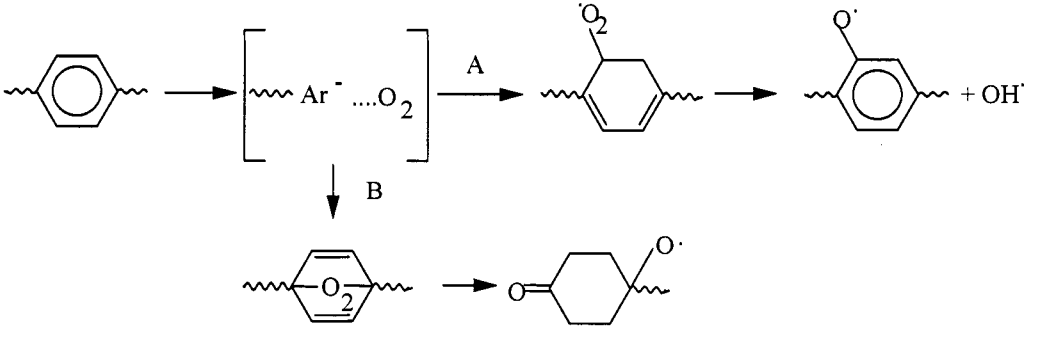

Intermediate CTC transformations by pathways A and B develop oxidation in the aromatic ring. Conjugation increase induces oxidation chain transfer and branching.

This scheme might be added by chain transfer reactions with phenol group formation and macroradical transformations with aromatic ring decay and oxidation of their residues to CO_2. Of higher importance are the following schemes of intermediate radical decay proceeding with macrochain breaks and occurrence of end macroradicals. At first sight, such conclusion argues the experimental increase of PSF and PEI molecular masses as a result of high-temperature oxidation. However, the phase of macromolecule branching prior to crosslinking may not be explained without accepting the injection of end groups to the model. Intermediate recombination of intermediate macroradicals does not introduce a kinetic element to the branching process, but induces the immediate crosslinking. As compared, degradation changes in PSF and PEI in the presence and in the absence of oxygen indicates a relation between branching and oxidation processes. As a consequence, end macroradicals occurring in pure thermolysis and oxidation, which has a weak tendency to branching, are different in their origin. In accordance with backbone bond strength at thermolysis of PSF and PEI, the occurrence of end macroradicals is very probable. Unpaired electron of the phenyl radical is not delocalized. Polar effects of *para*-substitution are transferred to phenyl radical, which is the σ-radical, due to weak induction mechanism. Therefore, the activity of *para*-

substituted phenyl radicals in reactions of homolytical arylation of substrates weakly depends upon donor-acceptor properties of the *para*-substitute [116]. Phenyl radical is active in hydrogen detachment reactions, but in arylation reactions this radical is weakly supported by polar effects.

Phenoxyl radical is the conjugated system [186]. This system also includes a *para*-substitute. Compared with phenyl radical, phenoxyl radical is also less active at H atom detachment, but its reactions with aromatic systems must be promoted by polar effects.

The above-mentioned decays of intermediate macroradicals and endoperoxides occurring at PSF and PEI oxidation (by both alkyl and aromatic groups) may cause just occurrence of the end, phenyl macroradical, for example, at the mentioned decay by the B path. In order not to pass to the thermolysis phenomenology, one should accept the addition of O_2 and phenoperoxide macroradical, the internal and intermolecular decay of which by the reaction:

$$PhOO^{\bullet} + PhOH \rightarrow PhOH + PhO^{\bullet} \text{ [181]}$$

leads to the sought active center – the phenoxyl end macroradical, the existence of which may explain phenomenology of PSF and PEI high-temperature oxidation.

Therefore, high-temperature oxidation of PSF and/or PEI transforms their initially linear macromolecules transform to a macroformation, which partly loses the initial chemical structure, but obtains new elements. These elements distort the structure of conjugation blocks, which induces coloring of the polymer.

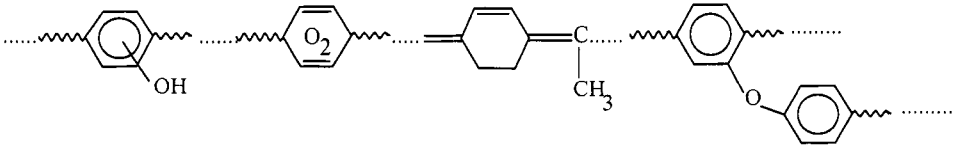

It the degradation process is thermodynamically preferable, the irreversible effect, currently, the quality loss, may not happen, the degradation kinetics is affected by inhibitors – thermostabilizers.

SOLID-PHASE OXIDATION

Polysulfone

PSF ages even at room temperature. During storage (3 years, the average data on production lots) strength at break decreases by 4 - 10%, and relative elongation changes from 30 – 70% to 10%. Kinetics of strength property change are shown in Figure 69. Of special attention is sharp change in properties during initial 2 – 10 days of aging followed by monotonous reduction at a low rate, traced up to 1 year. Of similar character is yellowing kinetics, characterized by initial abrupt decrease of light transmittance by 2 – 4 units and further low yellowing at exposures of hundred hours.

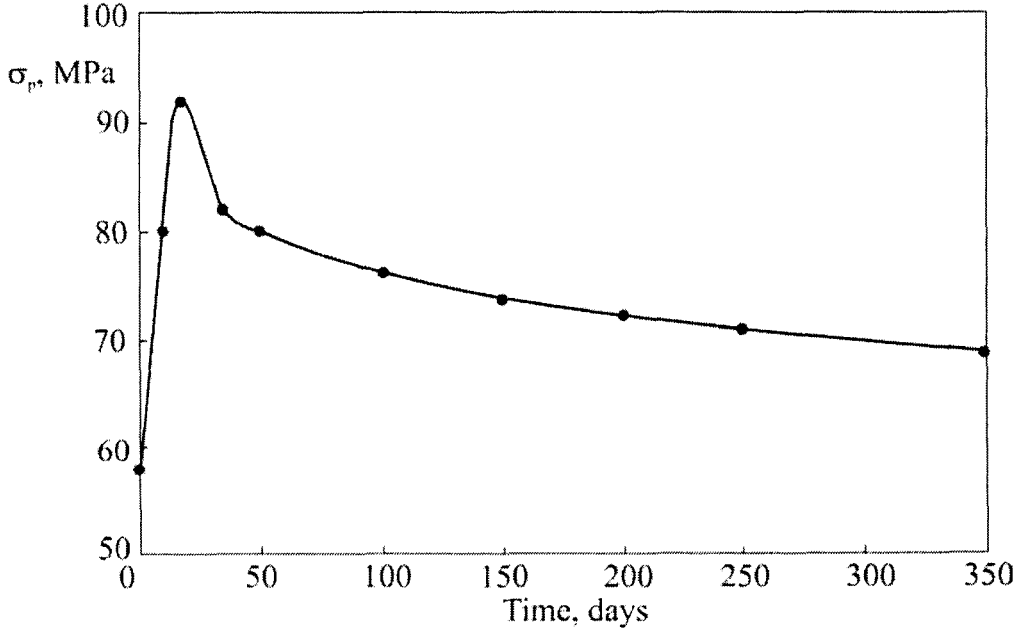

Figure 69. The change of PSF strength at break caused by aging in air at 160°C

The aging kinetics correlates with kinetics of low-temperature PSF degradation, which was performed at higher-temperatures because of technical difficulties (analytical method sensitivity), but anyway within PSF heat

resistance range (below glass transition temperature). PSF absorbs O_2 and releases CO_2 and H_2O. All MMD moments decrease simultaneously (M_w, for example; Figure 70).

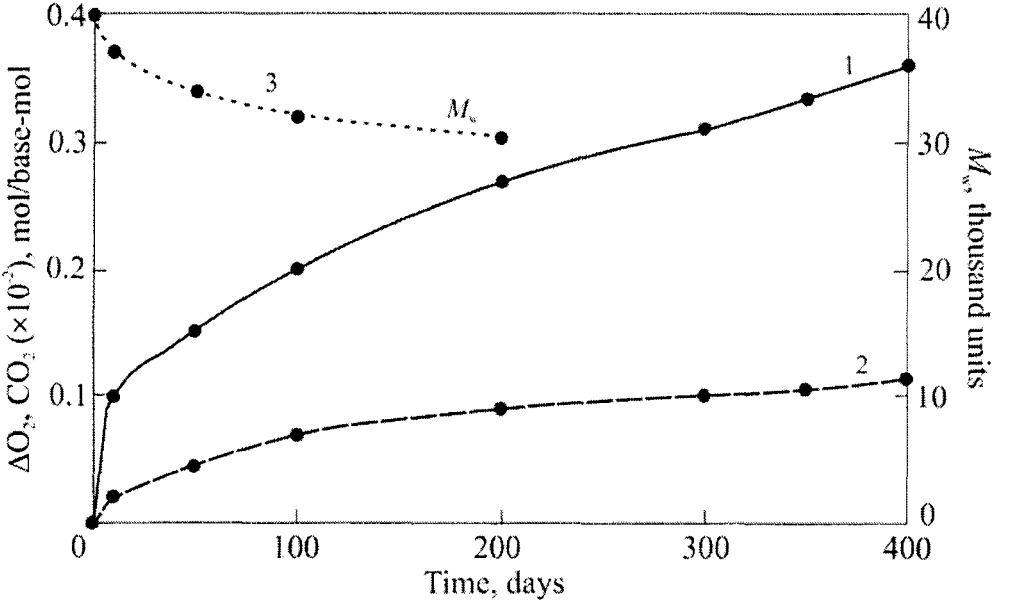

Figure 70. Kinetics of O_2 absorption (1), CO_2 release (2) and M_w change (3) at solid-phase aging of PSF in air at 180°C

As judged by the amount of absorbed O_2, the oxidation degradation does not develop at PSF aging even after thousand hours of exposure in a furnace. Compared with high-temperature oxidation which accompanies the processing, the oxidation rate during operation is by 2 – 2.5 orders of magnitude lower. Occurrence of carbonyl groups (weak band at 1740 cm^{-1}) is detected by IR-spectra. The expected hydroperoxides are not identified by the iodometric method, possibly, due to low concentration.

Noticeable changes of PSF physicomechanical properties induced by thermal aging do not correspond to negligibly low level of the oxidation damage of macromolecules. Analysis of industrial lots of PSF shows that M_w differences of 5,000 - 8,000 do not affect the level of physicomechanical properties. Therefore, an insignificant decrease of M_w caused by oxidation may be hardly related to macroscopic proofs of PSF aging, observed already on the day 2 – 5.

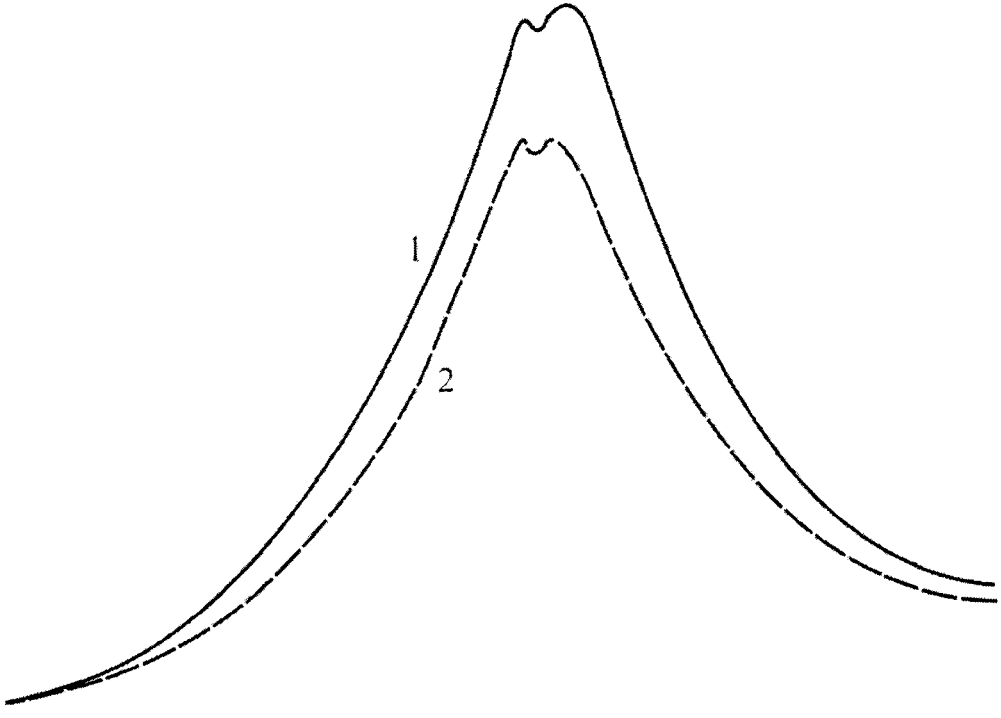

Figure 71. X-ray pattern of PSF: initial (1) and aged during 2 days at 150°C (2)

PSF is the amorphous polymer, which is shaped as the amorphous halo on the X-ray pattern (Figure 71). Two days of aging at 150°C is the limit, corresponded to sharp change of macroscopic and molecular PSF properties (Figures 70 and 71). It is enough for getting noticeable changes in X-ray patterns: the decrease of reflex intensity testifies about structure disordering during thermal processing. According to electron microscopy data, permolecular structure possesses overall uniform scheme of globular structures with quite high density of domains sized 1,000 Å (Figure 72). Two days of thermal aging cause a significant change of permolecular structure: we obtain spongy, loose structure of globules at the same size of granules instead of the initial, dense packing (Figure 72). Further aging does not practically change the system disordering.

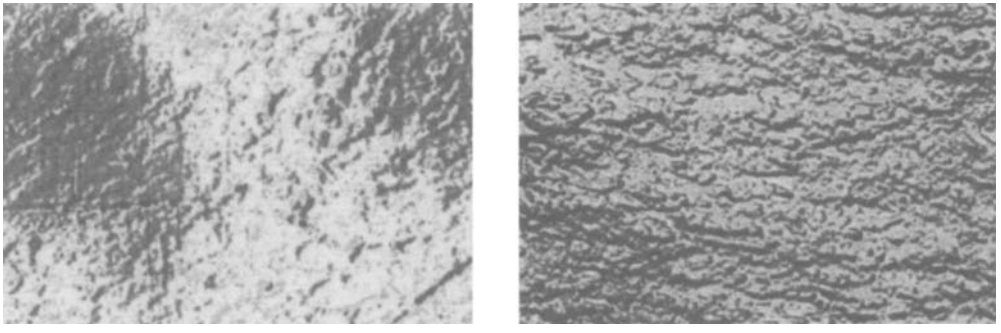

a b

Figure 72. Microphotographs (×15,000) of PSF: initial (a) and after 2 days of aging at 150°C

Thus, physical degradation of PSF during thermal aging is obvious. This type of degradation is typical of amorphous polymers, for example, polycarbonate exposed at temperatures below T_g [187]. As shown by non-comparable level of physical and chemical PSF structures already at the initial stage of thermal aging, physical degradation is responsible for changes in macroscopic PSF properties. Destruction of dense permolecular structure leads to activation of oxidation processes in PSF, which have many analogies in oxidation of other solid polymers [110, p. 11 - 57].

Solid, low-temperature oxidation of PSF at temperatures below T_g is a secondary degradation process. It does not cause any interpretation difficulties due to broad data in the literature on this point [10]. Generally, side methyl groups are oxidized, and reactions with aromatic rings are decelerated. This is clear from the absence of branchings in macromolecules typical of high-temperature degradation. The specific feature of PSF solid oxidation is extremely short kinetic chains (in the best case of thermal stabilization classical inhibitors become ineffective - phenol antioxidants, for example, *Irganox 1010*). This is explained by isolation of methyl groups in PSF by aromatic structures and, consequently, hindrance of the chain transfer. Therefore, PSF protection from aging, e.g. expansion of PSF lifetime as the operation material must be aimed at stabilization of solid PSF morphology.

Polyesterimide

Thermal oxidation is displayed at PEI thermal aging. As heated during 1,600 hours at 200°C, PEI absorbs about 30 mmol/base-mol of oxygen. Simultaneously, 5.25 mmol/base-mol CO_2 and 0.32 mmol/base-mol H_2 are released.

Aging is accompanied by higher yellowing of PEI and the change of molecular-mass characteristics (Table 22).

Table 22

Changes in MMD parameters at PEI aging

PEI	Molecular mass moments			Polydispersity		g	$\lambda \times 10^2$	Light transmittance at 425 nm
	M_w	M_n	M_z	M_w/M_n	M_z/M_w			
Before aging	38,400	16,800	75,100	2.28	1.95	-	-	77
200°C, 1600 h	47,600	16,500	78,800	2.88	1.65	0.71	6.8	63

Hydrogen release and, as a consequence, increase of the branching degree are the factors distinguishing PEI and PSF degradation at low temperature and displaying the analogy with PAI, PPA and PPQ degradation, described in Chapters 1 – 3.

Chapter 5. Degradation of aromatic co-polyesters derived from n-oxybenzoic, tere- and isophthalic acids, and dioxydiphenyl

Special attention to these polymers is defined by their specific feature, which is orientation in the melt, mostly associated with the intense development in computer technologies. Owing to this property such polymers are devoted to the "family" of liquid-crystal polymers. The liquid-crystal properties are also observed for PAI with uneven number of CH_2-groups [42]. It should be noted that polyalkanimide (PA-12), discussed in Chapter 1, also displays liquid-crystal properties under definite processing modes.

Liquid-crystal aromatic copolyesters (LCP) were studied. They were derived from dioxydiphenyl diacetate, acetoxybenzoic, iso- and terephthalic acids (IPA and TPA, respectively): 100/0, 75/25, 50/50, 25/75, 0/100.

$n = 50, m = 25, f = 25$

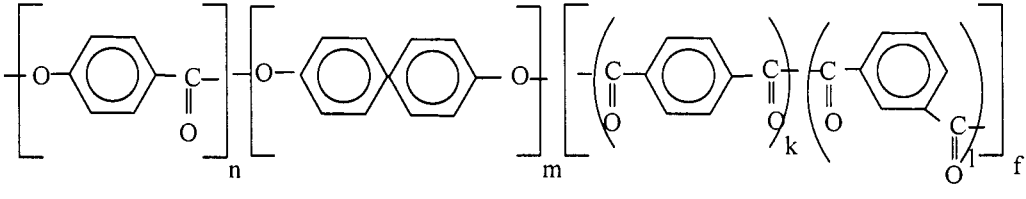

International analogue – *Xydar* (Amoco).

Thermal stability of LCP with different TPA/IPA ratio was studied by dynamic TGA/DTA techniques. Table 23 shows DTA/TGA data obtained in argon flow. Data obtained in air are shown in Figure 73.

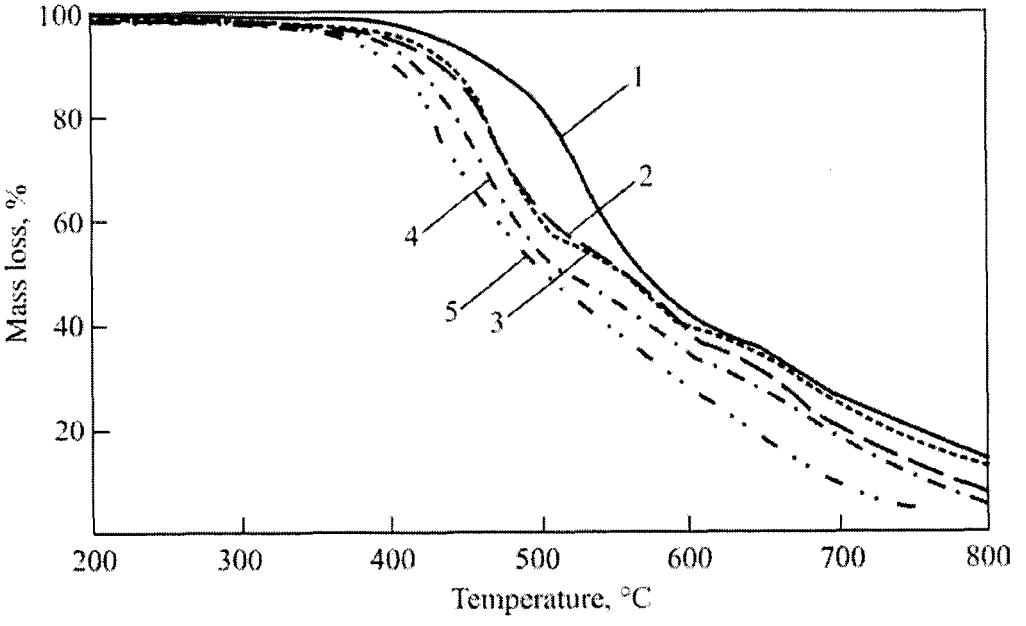

Figure 73. TGA data obtained at the heating rate of 5°/min in air for liquid-crystal polymers (LCP): KI-0 (1), KI-25 (2), KI-50 (3), KI-75 (4), and KI-100 (5)

Table 23

LCP sample characteristics

Sample	TPA/IPA ratio, mol%	TGA/DTA data in argon flow (with heating rate 10°/min)	
		Melting range, °C	Degradation initiation temperature, °C
KI-0	100/0	410 - 415	490
KI-25	75/25	360 - 365	480
KI-50	50/50	340 - 350	472
KI-75	25/75	300 - 315	455
KI-100	0/100	315 - 325	450

Without air oxygen LCP degrade in one stage, forming significant amount of coke residue (up to 40wt.% at 700°C). Two endothermic heat effects were observed on DTA curves: a low one in the melting range and quite intense

one in the polymer degradation zone. Calculation of the heat effect gave ΔH = 1 – 2.5 kJ/mol. As decided from the studies of 4-hydroxybenzoic and 2,6-hydroxynaphthoic acid copolymer by DSC method [256], the heat effect of about 1 kJ/mol relates not to real melting, but to changes in the order strength at transition from crystal to mesophase. Apparently, due to superimposition of heat effects which accompany degradation, and transition to the isotropic melt, nobody succeeded in detecting temperature transition associated with LCP changing the isotropic degree.

Thermal stability of LCP in air is significantly (by 25 - 30°C) lower than in argon. According to dynamic TGA data in air (Figure 73), mass losses of studied LCP are observed in the temperature range of 350 - 800°C. The degradation proceeds in two stages: the first stage at 350 - 550°C is accompanied by mass losses up to 40 wt.%; the second stage is slower and proceeds in the temperature range of 550 - 800°C up to full degradation of the polymer. The coke content at 750 - 800°C equals 1 – 3 wt.%. As shown by DTA data, LCP degradation stages are accompanied by exothermal heat effects. As tested in the air, a low endothermic heat effect is absent in the melting range, apparently, due to overlapping by exothermal effects of degradation reactions. LCP rating in the sequence with thermal stability decrease is the following: KI-0 > KI-25 ≥ KI-50 > KI-75 > KI-100.

The increase in IPA content shifts the melting range towards lower temperatures and reduces LCP thermal stability. The study of LCP phase transitions by X-ray analysis in the temperature range of 20 - 400°C indicates similar changes in all LCP. Annealing at 300°C causes an insignificant increase of the main crystalline reflex. As an example, Figure 74 shows the difractogram for powder-like and mold samples of KI-75 LCP. No phase transitions (reflex occurrence and elimination) were detected in the studied temperature range in LCP. This may prove the DTA results and suggestions about closeness of degradation temperatures and transitions to mesophase [256]. The ability of studied materials to transit to the so-called "liquid-crystal state" characterizes their behavior at processing temperatures. At softening temperature (as regards to the structure, this range falls within 300 - 400°C) a jump-like viscosity decrease is observed in all polymers. Hence, extremely strong fibers are formed from the melt. This effect is explained [251] by cooperative orientation of large macromolecule axes along the flow direction (viscosity anisotropy), which is realized only in LCP.

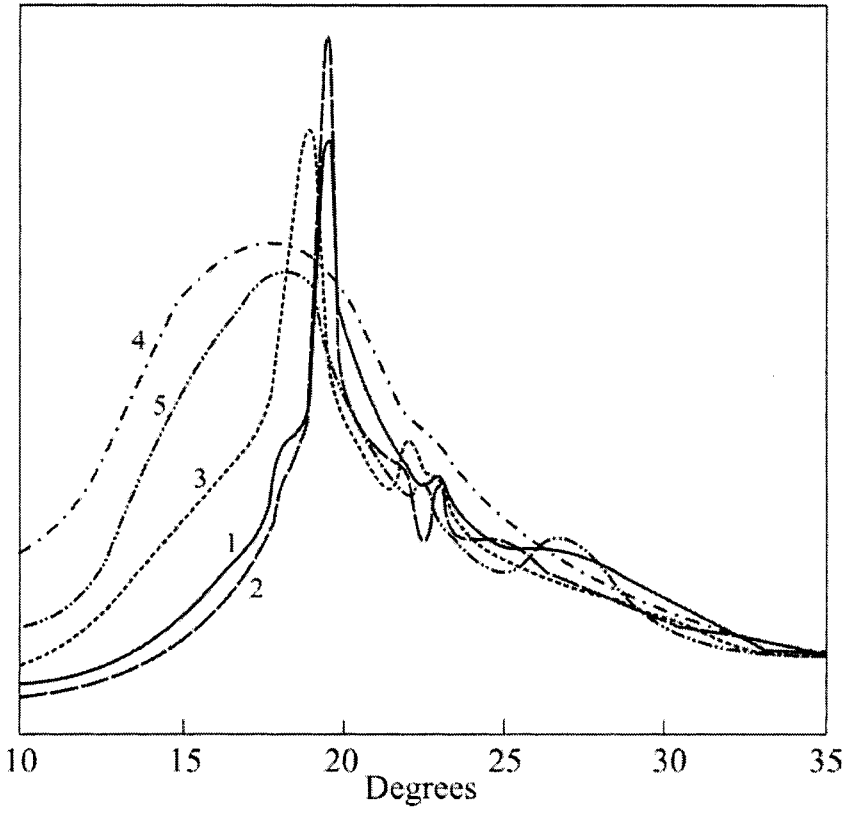

Figure 74. Diffraction patterns for LCP-2 powder at heating
1 – powder-like sample (20°C)
2 - powder-like sample (300°C)
3 - powder-like sample (350°C)
4 - powder-like sample (400°C)
5 – mold sample

Thermal stability of polymers depends upon several factors: structure, molecular-mass parameters, content of macrochain defects, labile end groups (currently, hydroxyl ones), low-molecular organic (non-reacted, residual monomers) or inorganic (increments of metal ions from the raw material and equipment) additives in the macromolecules.

The composition of inorganic additives in monomers and LCP were studied by plasma-emission spectroscopy technique. The example of KI-75 LCP, studied by TGA, shows the effect of some metal increments on thermal

stability. The additive content was increased by injection of inorganic salts of appropriate metal into the polymer. Table 24 shows comparative data on Cu, Fe, Ni, Ca, and Al content and temperatures of degradation initiation by TGA.

Table 24

The effect of metal increments on the thermal oxidative stability of KI-75 LCP

Metal	Content, wt.%	Degradation initiation temperature (T_d) by TGA in air, 10°/min heating rate
Fe	1.3×10^{-3}	320
	1.3×10^{-2}	300
Al	1.4×10^{-3}	320
	1.4×10^{-2}	320
Ca	4×10^{-3}	320
	4×10^{-2}	320
Ni	1.0×10^{-3}	320
	2.0×10^{-2}	325
Cu	1.3×10^{-5}	320
	2.0×10^{-3}	330

The results obtained show different effect of metal increments on LCP thermal oxidative stability. In the studied range of concentrations, aluminum and metals of the alkaline sequence (Ca, Na, K, etc.) do not practically affect the thermal stability. Iron causes the negative effect, whereas Cu and Ni, vice versa, increase thermal stability of LCP. It should be noted that injected concentrations are quite corresponded to usual content of metal increments in industrial samples of engineering, bulk polymers, such as polycarbonate, aliphatic polyamides, polystyrene, etc.

The composition and content of organic additives to LCP were studied by the mass-spectrophotometry technique. Phenol and sioxydiphenyl (94 and 186 m/e, respectively) were identified. They represent the hydrolysis products of the initial monomer of dioxydiphenyl diacetate and heavy fragments of the following structure:

m/e=214

m/e=306

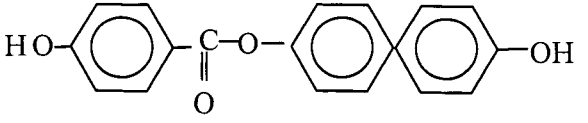

Total amount of organic additives in different samples has not exceeded $(1.0 - 2.0)\times10^{-2}$ wt.%, which does not practically affect thermal stability of the polymers.

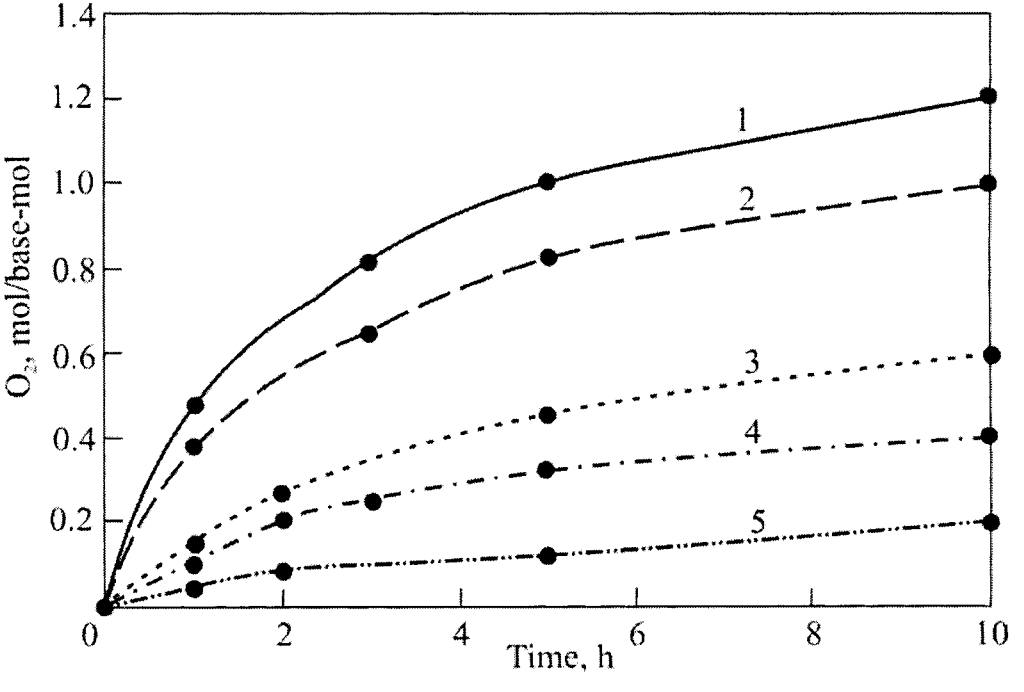

Figure 75. Kinetics of O_2 absorption by LCP KI-100 (1), KI-75(2), KI-50 (3), KI-25 (4), and KI-0 (5)

As shown by kinetics of oxygen absorption at 350°C (the processing temperature), thermal stability of LCP is reduced with increase of IPA content (Figure 75). This result confirms the TGA data. The kinetics of O_2 absorption is the two-stage process with absorption of 1 mole of O_2 per monomeric unit at the first, quick stage (2 – 3 h), and 0.2 mol/base-mol during following 7 – 8 h of thermal oxidation. Analogous dependencies are displayed by CO_2 release (Figure 76) - the main gas product of the studied LCP degradation product. Shown below are heavy, highly boiling LCP degradation products, identified by NMR and MS techniques [245 – 248].

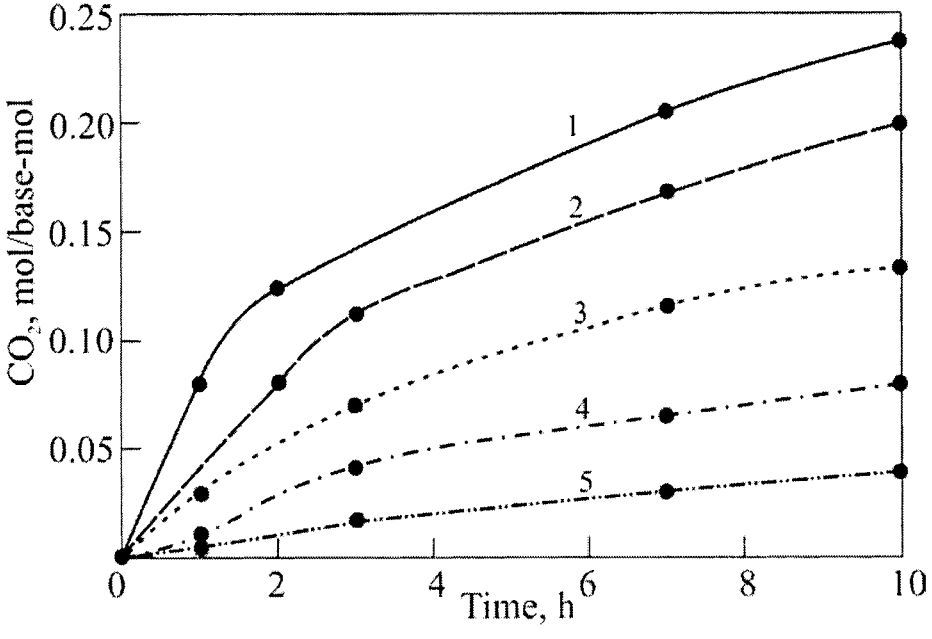

Figure 76. Kinetics of CO_2 release during LCP thermal oxidation (350°C, in air): KI-100 (1), KI-75 (2), KI-50 (3), KI-25 (4), and KI-0 (5)

Heavy products of LCP degradation

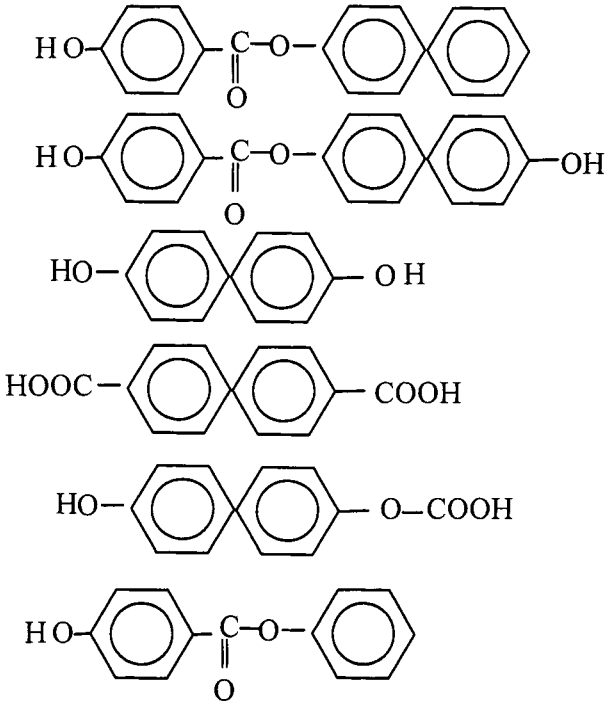

As observed from the composition, heavy products of LCP degradation, precipitated on cold zones of the ampoule, represent a mixture of the initial monomer (dioxyphenyl diacetate), products of its hydrolysis (dioxydiphenyl – DODP - for example), and products of DODP and *p*-OBA interaction. It should be noted that the composition of the above-mentioned products is identical for all studied LCP and slightly differs just by the ratio of components.

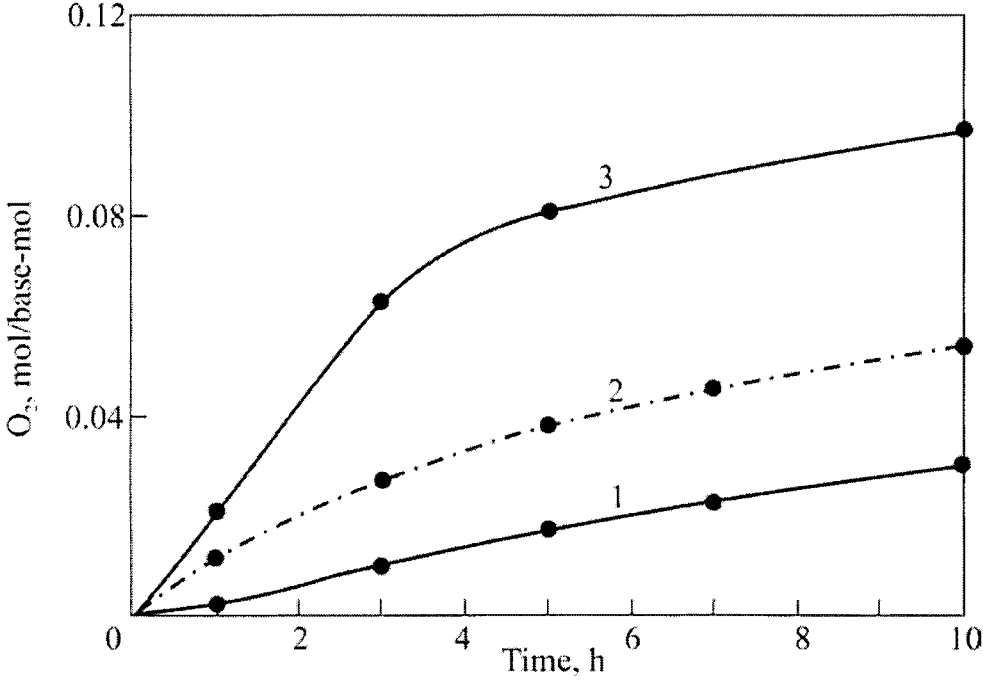

Figure 77. Oxygen absorption kinetics for KI-75 at 300 (1), 320 (2) and 350°C (3) in air

Degradation transformations were studied on the example of KI-75 LCP in the processing range. As shown (Figures 77 – 78), at the melting point or during melting (300 and 320°C) the oxidation rate is much lower than at 350°C, when according to the X-ray diffraction analysis the whole polymer transits to isotropic melt. Besides the main gas product (CO_2), hydrogen (at early oxidation stages at 0.5 – 1 h exposure) and water (at 4 h exposure) were also detected. As observed from dynamics of the elemental composition change, hydrogen content decreases and carbon content increases in KI-75 during its thermal oxidation, e.g. a graphite-like structure is formed. This process proceeds intensively at 350°C. IR-spectroscopy data [138, 249, 250] show that initial changes happen in the absorption range of ester aromatic fragments: absorption band intensity at $\nu_{C=O}$ = 1740 cm^{-1}, ν_{C-O} = 1270 и 1160 cm^{-1}, $\nu_{C=C}$ = 1600 and 1500 cm^{-1}, $\delta_{C=C}$ = 720 cm^{-1} is reduced. At maximal exposure (thermal oxidation at 350°C during 10 h) only ether absorption bands at ν_{C-O-C} = 1080 cm^{-1} and

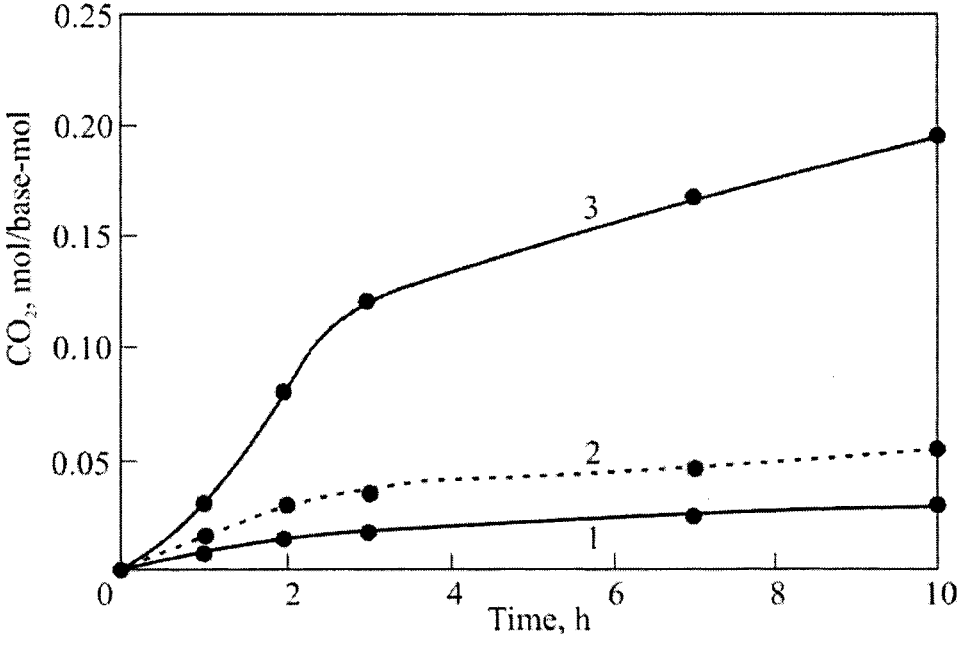

Figure 78. Carbon dioxide release kinetics at KI-75 thermal oxidation at 300 (1), 320 (2) and 350°C (3) in air

aromatic structure bands are preserved. The spectral background significantly decreases, which is caused by formation of intermolecular crosslinks. At 350°C a great amount of oligomers is formed. They precipitate in the ampoule near the reaction zone at temperature ≈ 150°C. The structure and ratio of oligomers with appropriate end groups, identified by ^{13}C NMR technique in the oligomer degradation products, are shown below:

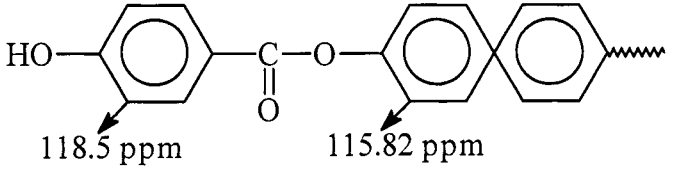

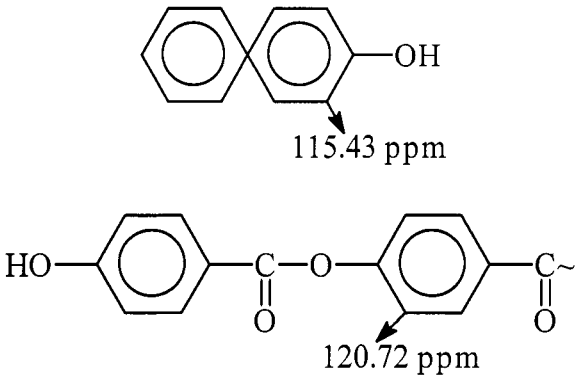

The amount of oligomers was estimated by the ratio of reflex squares with appropriate chemical shifts: 118.5 and 115.82 ppm (*product a*); 115.43 ppm (*product b*), and 120.72 ppm (*product c*). According to these data *product a* gave 15 mol%, *product b* – 31 mol%, and *product c* – 10 – 12 mol%.

The observation of *p*-oxybenzoic acid in thermal oxidation products of neighboring units allows a suggestion about simultaneous proceeding of copolycondensation and homopolycondensation of *p*-acetoxybenzoic acid. Free *p*-oxybenzoic acid output is 3 – 4 times higher than in the bound state in the form of end groups of oligomers. Apparently, free *p*-oxybenzoic acid is formed in thermal reactions at degradation of labile bonds in structural *p*-oxybenzoic blocks.

Analysis of kinetics and LCP degradation products in the processing temperature range allowed detection of some general features, observed in degradation behavior of heat resistant polyheteroarylenes [252]: structure graphitization, H_2 release, thermal oxidation stability increase at transition metal injection, etc. The idea of their stabilization is based on the following suggestions about degradation mechanisms:

- classical radical-chain thermal oxidation mechanism;
- formation of a molecular complex with oxygen;
- molecule transition to electronically excited state.

Injection of additives is the common method for investigating the mechanism of chemical reactions. It was found that of high effectiveness is the mixture stabilization by the triple system of copper compound, phenol antioxidant and phosphite in polyalkanimide, polyphthalamide and other heat-

resistant polymers. The idea of such mixture is based on the action mechanism of such additives:

- phenol antioxidant inhibits thermal oxidation by interacting with peroxy radicals $ROO^{\bullet}$;
- phosphite, secondary antioxidant, destroys hydroperoxides;
- Cu^{2+}-containing compound acts differently, for example, forms complexes during inhibition of peroxy radical or macrochain defects.

Table 25 shows comparative data on thermal oxidative stability for non-stabilized and stabilized KI-75 LCP.

Table 25

Thermal oxidation of KI-75 LCP in air at 350°C during 30 min

Stabilization compounding	Oxygen absorption, mol/monomeric unit	CO_2 release, mol/monomeric unit
Nonstabilized	0.22	0.033
0.005% $CuSO_4$ + 0.3% *Irgafos 126* + 0.1% *Irganox 1010*	0.08	0.019

The results obtained show that stabilizer injection causes a significant (over two times) deceleration of thermal oxidation in LCP. Of interest is the effect of additives on polymer morphology, determined during studying stabilized and non-stabilized samples (before and after thermal oxidation in air) by the X-ray diffraction analysis. It is found that crystalline reflex is preserved in stabilized polymers, whereas it disappears in non-stabilized samples. The stabilization effect on the physical structure of polymers was not studied well with respect to chemistry of degradation processes. Only complex consideration of the problem (chemistry + change of physical permolecular structure) may cause the increase of thermal stability of prepared product and extension of the material lifetime in articles".

Chapter 6. Fundamental regularities of thermal oxidation of heat-resistant heterochain polymers

The above Chapters considered phenomenological features of degradation process developing in PSF and PEI, PAI and PPA in the presence of oxygen at processing temperature (300 - 400°C) and solid-phase oxidation (150 - 250°C). These processes define loss of operation properties by polymers and materials derived from them. Before passing to description of attempts to decelerate degradation processes, let us generalize the above-mentioned experimental material and present the mechanism of thermal oxidation of the studied polymers.

The primary important similarity in the degradation behavior of all studied TP is their absorption of oxygen already at relatively low temperatures (150°C). At temperatures, when oxygen absorption kinetics (200°C or higher) becomes possible to trace, polymers display identical kinetic type of oxidation with no respect to the test temperature (refer to Figures 12, 17, 33, 36, 39, 44, 45, 51, 53, 61, 66, 68, 70, 75, 76, 77, 78), the process proceeds in two stages, subsequently obeying order one and zero laws. The existing data from literature [32] show that kinetics of the solid-phase oxidation includes one more stage, associated with self-exited acceleration of the process. Such complex kinetic type of oxidation was not previously observed.

Of special interest is the initial stage of aging, during which oxygen absorption and CO_2 release follow the order one kinetic law. At this very stage physicomechanical characteristics of heat-resistant polymers decrease significantly. Quick development and completion of this stage nudges possible anomalies in the structure of polymers or additives. If the first stage of aging of PEI and PSF, PAI and PPA, LCP etc. is the artifact, and it may be removed by some technical steps, Kinetics of the process leads to quite widespread type of thermal oxidation, when primarily, slowly developing thermal oxidation with the induction period transits to the self-excited acceleration mode. This indicates the radical-chain branched oxidation process. As discussed in Chapter 4, the induction period of oxidation may be observed at PSF thermal oxidation in the system with oxygen deficiency. However, correspondence of the first oxidation

stage to inadequacy of the polymer structure is impossible, because it argues the experimental data. Let us discuss these contradictions in more detail.

In the first stage, up to 10% of carbon is removed with carbon oxides. Relation of this percent to the content of anomalous structures in the polymer indicates that different structure degree is too high, much higher than the sensitivity of spectral methods. Meanwhile, preliminary analyses of studied TP showed their correspondence to postulated formulae, i.e. PSF corresponds to bisphenol A-derived polysulfone structure, PAI corresponds to fatty-aromatic polyimide derived from PDA and dodecamethylene diamine, etc.

Further on, we will discuss in detail the effect of organic and inorganic additives on thermal stability of TP, which will show their negative impact on thermal transformation rate. Anyway, this effect is drastically lower than displays of the first TP aging stage.

Moreover, differences in kinetics of different stages of aging are not accompanied by the change in composition of products released at every stage. No typical products of thermal transformations of solvents, used in syntheses of corresponded polymers, possess oligomers, which release should be expected under acceptance of regular structure deterioration by anomalous, thermally labile groups. Meanwhile, at high-temperature thermal oxidation a broad selection of heavy oligomeric products: all homologues in PAI and a selection of structure fragments in PSF, PEI, PPA, LCP, etc.

According to [230], defect zones are the first which degrade and initiate degradation of the main polymer structure. The most practical statement is that the first stage of TP aging is associated with the features of their chemical structure. This kinetic type of oxidation is displayed by PI, PPQ and co-polyimidophenyl quinoxalines [32]. The second similarity in TP degradation behavior is formation of the similar type of the degradation product (with respect to structure of the elementary unit). More precisely, it is PDI in PAI and PI:

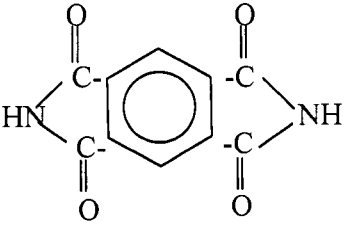

and it is TPA amide for PPA

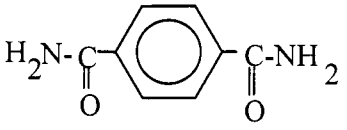

It is also PPP for PPQ

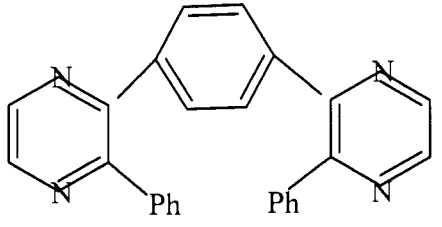

Formation of these products as a result of thermal oxidation of appropriate polymers was not previously known in the literature, but gave new information on understanding of the TP aging mechanism. To separate such fragments, one should make an "impact" and "tear out" these structures from the macromolecule. The relation of PDI and CO_2 outputs (in moles) at PI thermal oxidation (300°C) is close to 1/24, and for PAI (200°C) – 1/10, i.e. diamine components must be oxidized completely to CO_2.

If the primary oxygen attack is random, as oxidation develops a definite tendency to activation is observed.

The random O_2 attack on the next amine residue would cause formation of several oligomeric structures with appropriate end groups. However, besides the mentioned fragments, no other oligomeric products were detected in the "cold ring" or at PPA and PAI aging directly on the surface of mold samples. Thus, TPA amid formation in PPA, PDI in PAI and PI, PPP in PPQ and CPIPQ, and the absence of such oligomeric compounds among these products testifies that oxidation of a single amine residue activates oxidation of the nearest amine residues, remaining the oxidizing component unchanged and releasing it under the same conditions, in the form of individual compound (PDI, PPP, TPA-amide).

Invulnerability of the oxidation component to O_2 attack and, under these conditions, stability of the imide cycle, preserved even in degradation products, eliminates the thermohydrolytic mechanism, discussed in the literature.

Thus, during TP aging oxidation is aimed at amine residues of macromolecules; oxygen is added to these structures and oxidizes them: PDI,

PPP and amide-TPA are exclusive products of thermal oxidation. Therefore, the role of oxygen may not be reduced to oxidation of thermal degradation products.

According to the data obtained [231], the absence of nitrogen-containing products and nitrogen content (%) increase in oxidized residue are typical of PI oxidation. This was explained [232, 233] by easiness of nitrogen introduction into combination reactions; therefore, it remains in the polymer residue until deep degradation stages. It has been found [32] that PDI release at PI oxidation in the solid phase under relatively "soft" conditions", when the film transformation degree is below 5%.

Intermolecular crosslinking is general for all TP which leads to full loss of polymer solubility in the solvents, where they dissolved before thermal oxidation. In the absence of oxygen crosslinking at the solid-phase oxidation, i.e. at relatively low temperatures, either proceeds or proceeds at much lower rate. During high-temperature oxidation oxygen also activates crosslinking and branching processes. Apparently, this is one more proof for the activating effect of oxygen at some place of macromolecule and then along the backbone. This is the only way to explain formation of products (TPA amide, PDI, PPP) in appropriate polymers. In this case, common hypothesis about molecular complex formation between a macromolecule and oxygen, described in previous Chapters, is actual.

Hydrogen release was also associated with the crosslinking process. Hydrogen is the main product of purely thermal degradation of PI and other TIP above 500°C. In the presence of oxygen, H_2 release at high temperature is abruptly decreased. Hydrogen is not released at oxidation of aliphatic hydrocarbon polymers, below 300°C, i.e. in the well-studied process reliably described by the radical-chain scheme. Hydrogen was identified among thermal oxidation products, such TP, as PEI, PAI, PI and PPQ under soft conditions, and O_2 initiates its formation. Apparently, O_2 interaction with the aromatic structure activates C-H-bond break, which then enter intermolecular interaction.

Analysis of external manifestations of PI, PPQ, PAI, PPA, PEI, PSF, etc. thermal aging induces a conclusion about general regularities:

- kinetic features of the oxidation process are similar;
- with respect to structure of the elementary unit, the selection of thermal oxidation products is also similar;
- tendencies to branching and crosslinking of macrochains are the same.

Thus, thermal oxidation mechanisms of studied polymers are similar. Differences in thermal behavior are of the quantitative type.

Let us dwell on consideration of thermal oxidation at high processing temperature.

Let us start with O_2 molecule. The strength of O-O bond in this molecule is 493 kJ/mol. TP degradation form products containing a half of O_2 molecule: CO, H_2O, quinones, i.e. O_2 molecules dissociate during oxidation. In the theory of oxidation processes, including combustion theory, oxygen dissociation is possible due to energy reasons only via peroxide or peroxy radical formation. Scientists from Institute of Chemical Physics, Russian Academy of Sciences discovered the effect of isotropic enrichment by oxygen in hydrocarbon and hydrocarbon polymer oxidation [234, 235]. The theory explains this phenomenon by spin effects at the second degree recombination of peroxy radicals and macroradicals. To some extent, the phenomenon may be considered as an indirect proof of peroxide radical participation in thermal oxidation.

Another reaction may compete with usual oxidation initiation in rigid structures:

$$RH + O_2 = R^{\bullet} + HO_2^{\bullet}$$

which requires energy consumption equal the bond strength ($E_{R\text{-}H}$ = 196 kJ/mol, for aromatic about 251 – 263 kJ/mol). Figure 79 shows the fluorescence spectrum for PI film at light excitation, λ = 320 nm. The long-wave boundary of the spectrum characterizes energy required for electron transfer from external, occupied orbital to lower, loosening orbital. For PI film, the long-wave boundary of fluorescence falls at 520 – 530 nm, corresponded to energy of 217 – 226 kJ/mol. Thus, macromolecule transition to the active state via electron excited one is by 40 kJ/mol more energetically profitable than by usual (for aliphatic polymers) reaction between P-H-bond and molecular oxygen. Electron excitation contributions were discussed in works by Belyakov *et al.*, and light flashes were observed at thermal oxidation [236].

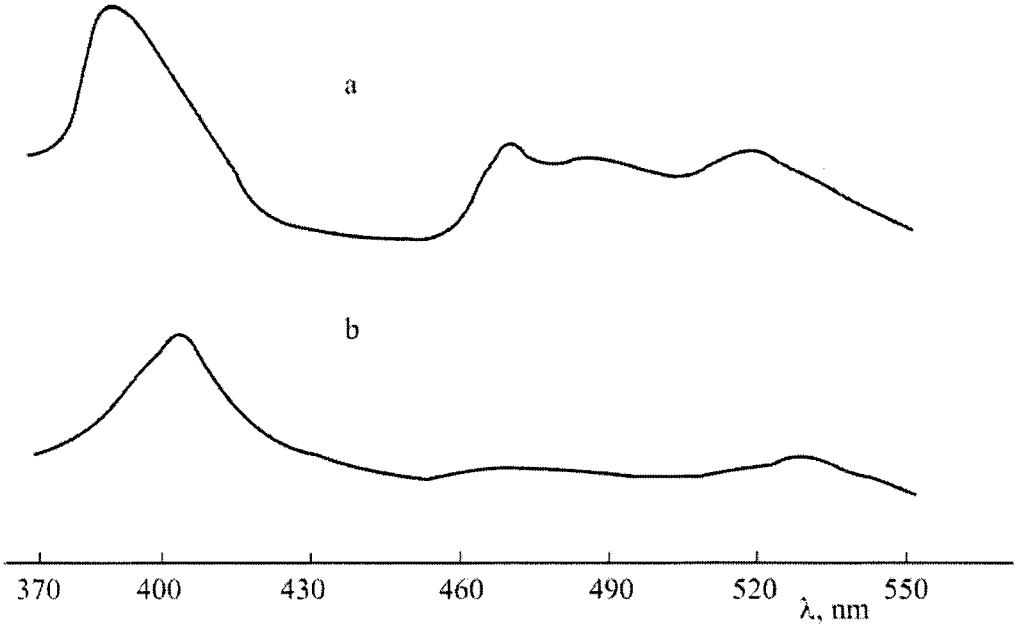

Figure 79. Fluorescence spectrum of PI films (a) without increments and (b) with 2 wt.% *BT-5*

Oxygen is added as biradical to the aromatic system in the triplet state. The internal peroxide or endoperoxide is formed. The possibility to initiate this act was assessed using quantum-chemical calculations, and reactivity of imide, quinoxaline and phthalamide structure were compared [32, 265].

Quantum-chemical calculation techniques were found efficient for studying reactivity of organic compounds in various reactions [158, 237, 238]. Molecular diagrams for many models of heat resistant polymers were calculated [158]. Quantum parameters of the system are low dependent on doubling or tripling of the molecule which imitates the elementary unit. Therefore these parameters may also be related to the macromolecule. A correlation between energy of higher occupied molecular orbital (E_{HOMO}) in the system and its thermal oxidation stability was found. The authors used the Waters idea in which oxidation as the electron migration process is considered [239].

We based upon a suggestion on endoperoxide formation in thermal oxidation of heat resistant polymers. The possibility of cyclic peroxide formation is also shown [241 – 243]. Moreover, endoperoxide transformation to quinoid structures may also be imagined. Occurrence of these structures during

PI, PEI, PSF etc. oxidation were proved experimentally. As forming on aromatic ring, endoperoxides change the primary π-system of the compound which corresponds to localization of two π-electrons of the ring. The appropriate change in π-electron energy may be considered as the localization energy (α_π) [237]. The value of α_π was selected as the measure of endoperoxide formation probability. The higher α_π (its absolute value) is, the lower is the gain of O_2 and the higher is polymer resistance to oxidation.

Molecules of model compounds under consideration, PI and PPQ [32], contain 28 atoms each. Calculation of so large molecules requires taking a tremendous number of integrals. The reactivity study of a single multi-atom molecule using non-empirical calculation of the electron structure demands many hours of computer time. Usually, these tasks are solved using semi-empirical methods, in which some groups of electrons are neglected. In this case, some integrals of electron energy become zero or are reduced to different integrals; some Hamiltonian terms are neglected or expressed through some empirical parameters.

In the current case, the Parizer-Parr-Pople (PPP method) semi-empiric, quantum-chemical method was used [240]. This method considers only π-electrons in the calculation. It allows quick obtaining of reliable π-electron energy values, required for α_π determination. Besides α_π, both molecular orbital energies (E_{HOMO} values are shown in Table 26), changes on atoms and bond orders (Figure 80) are calculated. The standard series of parameters selected for reactivity calculation is used [244]. The values of α_π were determined as the difference between π-electron energies of the initial compound (E_π^0) and endoperoxide (E_π). The value of E_π represents a sum of π-electron energies of endoperoxide fragments and energies of two π-electrons excluded from the conjugation system due to O_2 addition.

The bond length between phenyl cycles equals 1.5 Å. It is suggested that all compounds have flat structure. The variation of geometrical parameters indicated independence of calculation results on bond length changes below 0.05 Å and valence angles in the range of ±5°. Therefore, average bond lengths and average valence angles were used in the calculation (Figure 81).

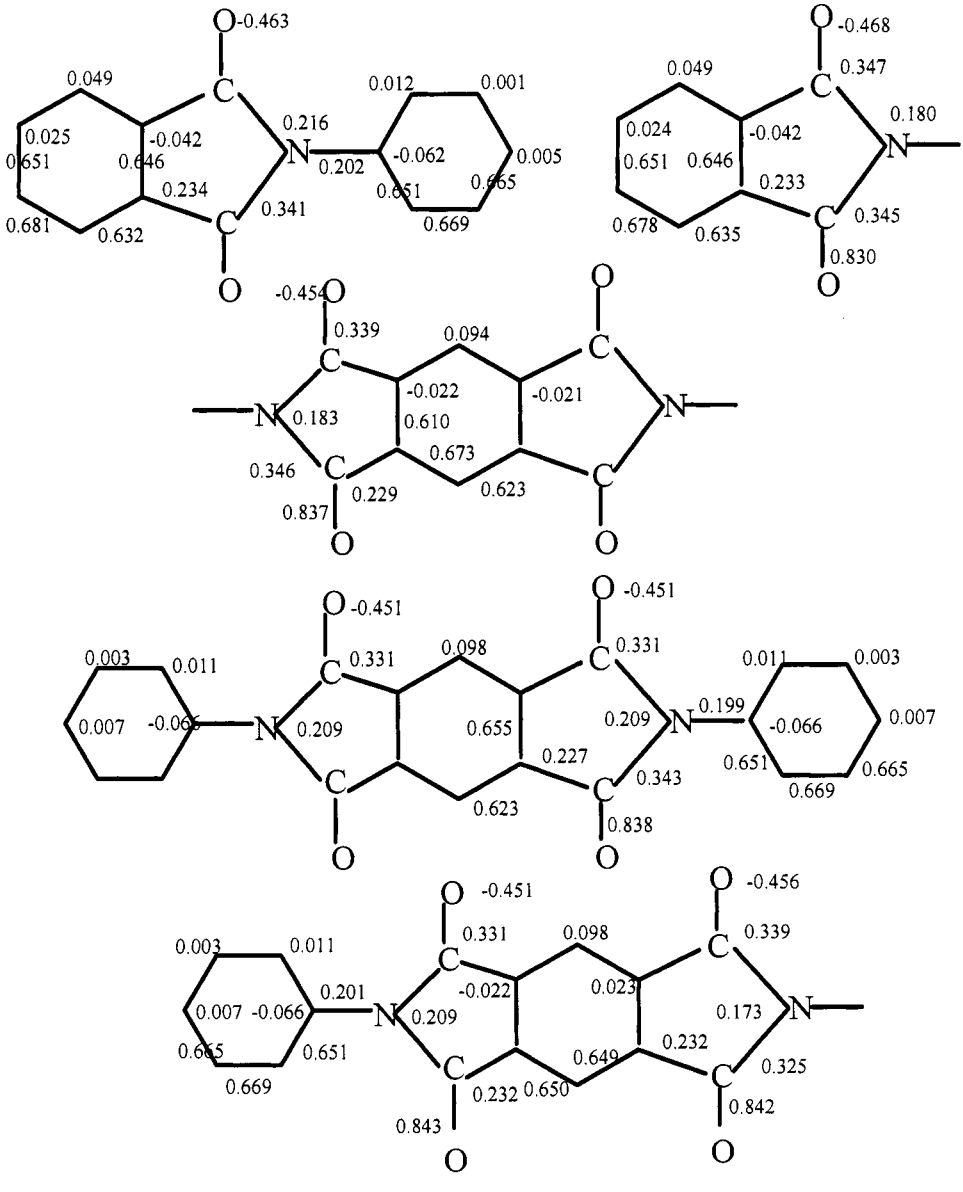

Figure 80. Charges on atoms and bond degrees in model compounds of polyimides

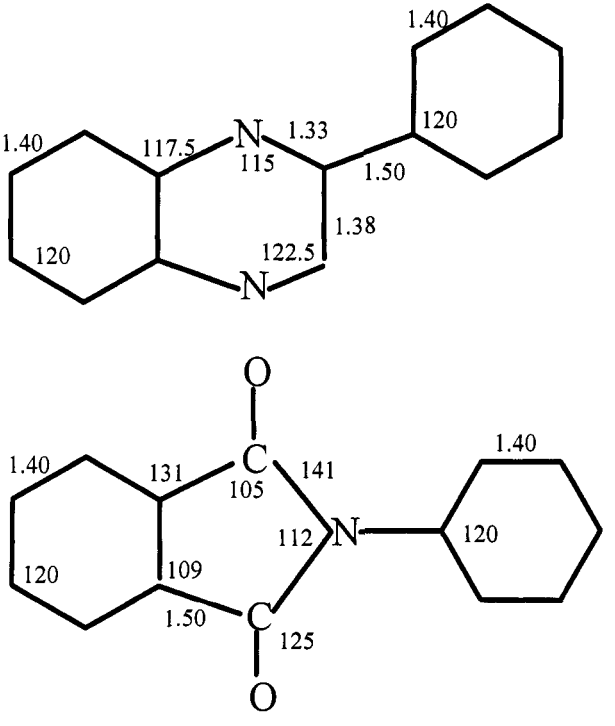

Figure 81. Bond lengths and valence angles in 2-phenylquinoxaline (1) and N-phenylphthalimide (2)

To compare resistance to oxidation of different macrochain fragments in polymers, α_π values were calculated for endoperoxide formation on aromatic rings of acid and amine components of PI model compounds and ketone and amine fragments of PPQ and PPA model compounds. Table 27 shows that for all compounds α_π values are lower for the amine component that testifies about its higher attackable by oxygen compared with ketone and acid components. These results correlate with already discussed experimental data on PI and PPQ thermal oxidation [32].

The value of may be suggested as a criterion of both polymers and macromolecule fragments heat resistance.

Table 26

Higher occupied molecular orbital energy and π-electron localization energy in model compounds

Structure	E_{HOMO}, eV	α_π, eV	
		Amine component	Acid component
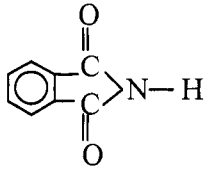	-12.04	-	6.95
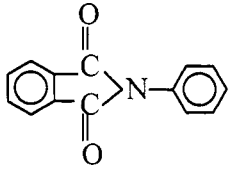	-10.99	6.33	6.96
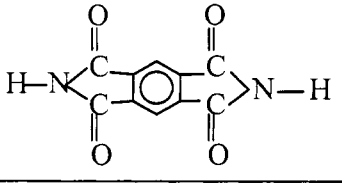	-12.68	-	7.48
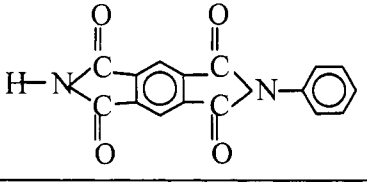	-11.20	6.18	7.33
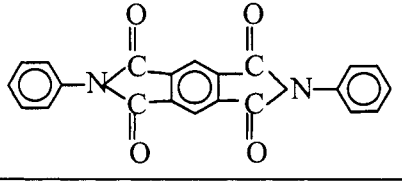	-11.16	6.32	7.34
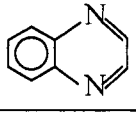	-10.71	5.75	-

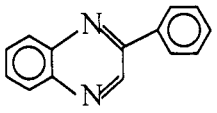	-10.47	5.76	6.42
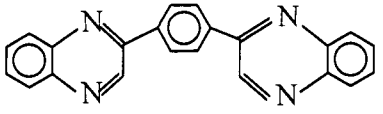	-10.31	5.76	6.68

Table 27

The amount of absorbed oxygen and release carbon oxides as a result of PI and PPQ model compound oxidation (T = 300°C, t = 100 h, $P(O_2)$ = 26.7 kPa)

Compound	Absorbed oxygen, mol/base-mol	Oxidation products, mol/base-mol	
		CO_2	CO
N-phenylphthalimide	0.034	0.02	0.002
N,N'-diphenylpyromellitimide	0.045	0.03	0.003
6,6'-oxy-bis-(2,3-diphenylquinoxaline)	1.71	0.91	0.09
2,2'-(1,4-phenylene)-bis-(3-phenylquinoxaline)	0.28	0.16	0.014
2,3'-diphenylquinoxaline	0.27	0.19	0.021

As previously shown by Kosobutsky [158], there is the opposite dependence of polyheteroarylene thermal stability in the presence of oxygen and their E_{HOMO}. The correlation is also confirmed by calculation results obtained by the authors of the current monograph (Table 26) [32] and assessment of PI and PPQ models of thermal stability. However, the use of α_π both indicates the formal substance disposition in the thermal stability sequence among other substances and binds thermal stability with particular elementary act which is O_2 linking with endoperoxide formation.

In the quantum-chemical study the probability of molecule ionization at TP decomposition, for example, by proton detachment, was also taken into account. In the frames of semi-empirical FNDO/2 method (Full Neglecting of Differential Overlapping) the energy of H^+ detachment (Table 28) was calculated by the difference between total electron energy of the molecule and energy of its negative ion (H^+ detachment). These observations do not correlate

in any way with the experimental data on thermal stability. This, apparently, removes the problem of ionic state participation in the degradation process.

Table 28

The energy of H^+ detachment from aromatic rings in model compounds

Structure	Energy of H^+ detachment, eV	
	ΔE_1	ΔE_2
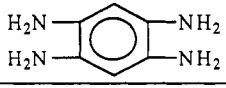	25.773	-
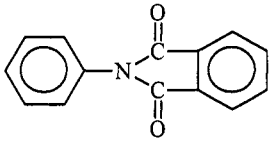	25.836	24.805
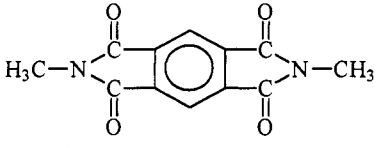	-	24.391
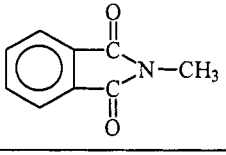	-	24.969
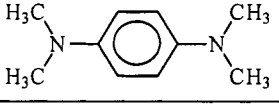	25.447	-
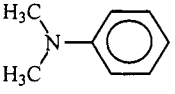	25.564	-
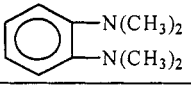	25.698	-

Quantum-chemical calculations based on the endoperoxide model confirm experimental conclusions:

- oxidation is developed in the amine component of imide and quinoxaline structure;

- oxygen addition causes changes in electron densities on structure skeleton atoms e.g. activation or conjugation;
- electron effects conform to higher reactivity of the imide (or amide) or quinoxaline structure in oxidation processes. Thus, there is no direct proof (positive analysis) of endoperoxide formation in PI, PPQ, PSF, PEI and PPA, but positive calculation prerequisite and indirect experiments proofs are observed.

Endoperoxide decomposition causes occurrence of oxygen-containing structures in the phenylene structure. Deeper oxidation causes the ring break, CO_2 and CO release, where carbon from the aromatic ring "combusts" (e.g. oxidizes).

It is suggested that the acts of endoperoxide electron excitation, formation and dissociation form the initial oxidation stage. As degradation proceeds, paramagnetic properties of PI, PSF, PAI, etc. increase. This may be associated with accumulation of hexadienyl oxidized structures, radicals and biradicals in the macrostructure, and increase of the system conjugation degree. The excitation level is reduced, and the system becomes self-catalytic. This is the third stage of the process, described for PI and PPQ [32]. For oxygen absorption and gas product release, γ values are almost the same. This indicates that oxygen absorption and structure degradation elementary acts become maximum close in time. Apparently, the stage of endoperoxide formation disappears, whereas O_2 is added to numerous elementary centers in the conjugated structure and C atom is immediately detached from already linear residue of the aromatic structure. This stage of the aging process is of just theoretical interest, because the loss of operation properties of the material is ended at the second thermal oxidation stage. At this stage, for the gross, one aromatic ring in the elementary unit decomposes (as deduced from carbon oxide yield).

Concerning the above experimental material (refer to Chapters 1 – 5), Schemes of PI, PAI, PPQ, PEI and PSF thermal oxidation schemes may be shown as follows:

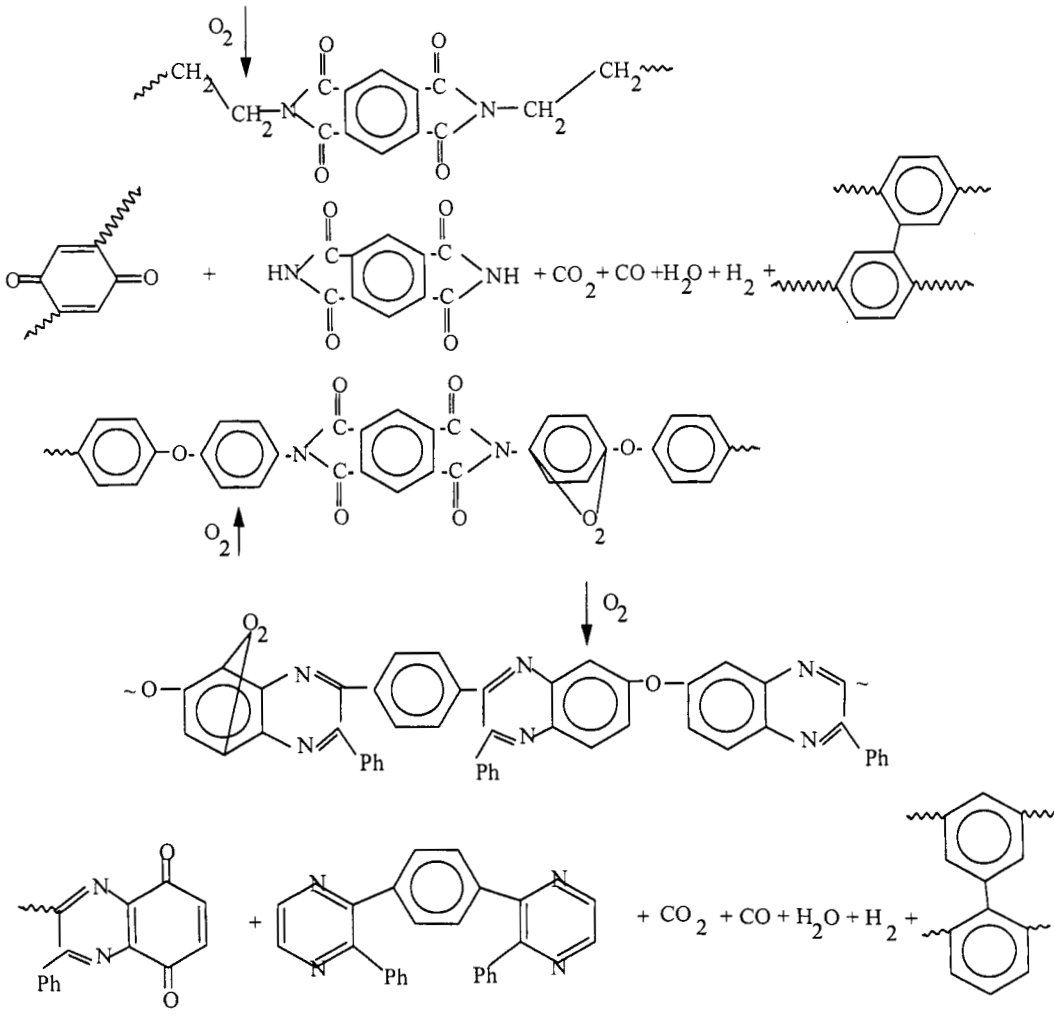
O2
CH2
CH2
N
C
O
CH2
CH2
N
CH2
HN
NH
+ CO2 + CO + H2O + H2 +
O2
O2
O2
N
Ph
Ph
Ph
+ CO2 + CO + H2O + H2 +

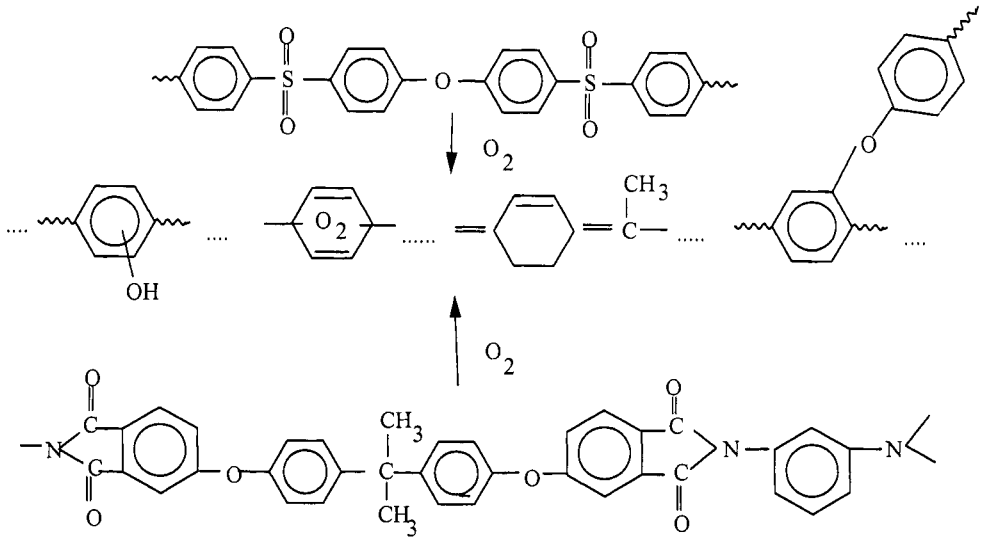

The problem is: what is the way of TP thermal stabilization in the context of their degradation?

The classical inhibition of oxidation processes is based on kinetic chain break and deactivation of branching, intermediate products. In the case of TP, chain type of the process is not obvious. The chain break in chemical increments suggests the inertness of residual inhibitor radical. These radicals are active above 200°C. Therefore, classical antioxidants are ineffective at high temperatures.

It is accepted that TP must be thermally stabilized towards the structure transition into electron-excited state (quenching these states), prevention of CTC formation (interaction or complex formation between O_2 and amine residues in macromolecules for PI, PPQ, PEI, etc.) to reduce their reactivity, for example, down to acid or ketone residues and, finally, free radical deactivation.

Chapter 7. Practical stabilization of heat resistant polymers

Previous Chapters discuss the features of thermal and thermal oxidation transformations in highly heat resistant polymers. Polymers selected for the experiment were had "ideal" structure which contained no increments. Many experiments were performed on "model" samples, which were compounds with lower molecular mass, or oligomers. Such searching approach is required for understanding the degradation mechanism. However, under real conditions, there is no opportunity to obtain a polymer of either "ideal" structure or the above-mentioned purity. Therefore, to solve the applied tasks, the most important of which is stabilization, the investigators must base upon studies of degradation mechanisms, developed on appropriate models, and take into account "negative" contributions characterizing real polymeric structures. These are all reasons why this Chapter thoroughly discusses the effect of structure defects, end groups, MMD, organic and inorganic additives on thermal stability of polymers.

LABILE STRUCTURES AND ADDITIVES

Polysulfones

To make the regularities not only characteristics of the studied sample, but the regularities of a class of substances, one should understand how strong are effects of labile groups in the polymer structure, processing and other additives on the degradation process. To put it differently, selection of the polymer sample is of the principal meaning.

Similar to other compounds, polymer may be "real" or "ideal" product. In the first case, structure and composition of the polymer, usually produced by an industrial or semi-industrial way, represents a compromise of production costs and competitive ability of the product by its quality. Most frequently, "ideal" or similar product is obtained in laboratory *in vitro*, using pure monomers and optimal technique. The latter should provide the absence of labile structures. However, quantity of "ideal" samples is limited, so it is not

enough for performing pilot studies of aging and stabilization, in which the effect of these factors on macroscopic properties of polymers are considered. Therefore, a standard must be selected among industrial PSF. It should approach the "ideal" polysulfone in purity and the presence of labile structures. We mean not full absence of the mentioned defect, but their minimal content that causes no significant effect on thermal behavior.

Data from the literature [98] and industrial laboratory tests [99 – 101] indicate specific danger from the side of hydroxyl end groups in the PSF molecule for thermal oxidation stability.

Let us make an assessment, how high is the effect of end OH-group on thermal oxidation stability of rather long macromolecule, for example, the one containing 30 – 50 units, each containing two side methyl groups the fragments of isopropylidene bridge from bisphenol A residues) tender to oxidation at high temperatures. The model is the following. Oxygen molecule attacks the macromolecule according to common autooxidation initiation mechanism [1, 8 – 10]:

$$RH + O \rightarrow R + HO_2.$$

Aromatic rings are eliminated from the consideration. Since experimental data [96] show relative stability of the aromatic structure, as compared with aliphatic one, even at thermal oxidation of alkyl-aromatic polymers, at the initial stage aromatic rings are not involved in the process. Thermal oxidation by chlorophenylene end groups (end Cl-groups) may not be initiated by this reaction. Initiation by dehydrochlorination is also improbable due to high strengths of C_{arom}-Cl and C_{arom}-H bonds - 400 and 450 kJ/mol, respectively [78].

The activation energy, E_a, of the above-mentioned elementary act of initiation is approximately equal to its heat [1], because

$$Q = E_a^{-1} + E_a^1,$$

where E_a^1 and E_a^{-1} correspond to direct and reverse radical recombination, respectively. According to [1], they approach zero. Generally speaking, one of the features of the solid-phase oxidation is high E_a value of macroradical recombination. For instance, E_a of the second degree recombination of peroxy radicals reaches 50 – 100 kJ/mol [110, pp. 64, 69]. However, it is also known

that PO recombination mechanism is superimposed with migration of free valences. Intensification of molecular movements due to plasticization or transition to amorphous systems causes an abrupt decrease of E_a to 10 – 20 kJ/mol [110, p. 64]. These values are typical of transfers in liquids [8, p. 81]. In the present case, oxidation proceeds in the polymer melt, i.e. molecular movements are unfrozen. Moreover, macroradical recombination with a small HO_2 radical but not recombination of two peroxy macroradicals [9, p. 85] is considered. Therefore, the assumption that

$$E_a^{-1} \sim Q$$

seems to be true, i.e.

$$E_a \sim Q.$$

Similar approach was used in other investigations [110, p. 126].

Initiation is endothermic reaction. The heat of it equals the difference between breaking and forming bond strengths. This means that

$$Q = D_{R\text{-}H} \cdot 221 \text{ kJ/mol [110, p. 125].}$$

As shown [78], CH_2-H bond strength in linear alkanes equals 400 – 410 kJ/mol. The same bond strength in $C_6H_5CH_3$ is decreased to 356 kJ/mol (nearly by 50 kJ/mol) [78] due to delocalization energy in benzene radical. Methylene group in isopropylidene bridge of PSF is located in β-position in relation to aromatic rings. The π-system impact is weakly transferred by σ-bond chain and attenuates on β- and γ-atoms [114]. This is illustrated well by the change of chemical shifts of methyl protons in ESR spectra of alkylbenzenes, from toluene to *n*-decanebenzene: 2.32, 1.25, 0.89, and then the same (0.89) ppm. The latter result is similar to chemical shift of methyl protons in hexane, which is 0.99 ppm [170].

As another example we may accept the rate constant of H atom detachment from methyl group in toluene by phenyl radical. It is by an order of magnitude higher than for tert-butylbenzene [172]. Therefore, let us assume that delocalization energy of alkyl radical with free valence on β-C atom is 4 times lower than for benzene radical. Moreover, additional bond strength decrease by 4 – 8 kJ/mol in alkyl chain branchings [78] should also be taken into account.

Finally, the strength of CH_2-H bond in the PSF isopropylidene bridge may equal 380 – 390 kJ/mol.

The bond O-H is phenol is as strong as 351.5 kJ/mol [76], whereas *D*(O-H) strength in 2,6-di-tert butylphenols is about 320 – 340 kJ/mol [172]. The strength of O-H-bond in unshielded and shielded para-substituted phenols is defined by electron effects of substitutes. This is shown up by the empirical *D*(O-H) dependence on the Hammett constant: for example, for shielded phenols *D*(O-H) = 343.5 – 23. As accepted for the end hydroxyl group in PSF, $\sigma_{para} = 0.197$ [83]. Then applying the mentioned dependence, we get:

$$D(\text{O-H}) = 351.5 + 23\times(-0.197) = 347 \text{ kJ/mol}.$$

Since we consider competing, unitypical reactions of the same macromolecule, pre-exponential terms of the rate constants may be equal. As a consequence, the competition between elementary initiation acts at the end hydroxyl groups or side CH_3-groups is ruled by the relation of activation energies of competing reactions, which according to

$$E_a = Q \text{ and } Q = D(\text{P-H}) - 221$$

equal 126 and 159 – 169 kJ/mol, respectively.

As already shown empirically [99], end hydroxyl groups negatively affect the quality of PSF. Therefore, an excess chlorine-containing monomer is used in the synthesis. This allows a decrease of end OH-group amount in PSF to 0.02 – 0.15% at the mean molecular mass of 8,000 – 15,000. Let us estimate the ratio of side CH_3- and end OH-group concentrations under the most "unfavorable" conditions for OH-groups: M_n = 15,000 and OH-group concentration 0.02 wt.%. It may be simply calculated that

$$\frac{[CH_3]}{[OH]} \sim 400.$$

At 350°C the ratio of competing initiation act rates equals:

$$\frac{v_{CH_3}}{v_{OH}} = \frac{K_0^{CH_3}[CH_3]}{K_0^{OH}[OH]} = \frac{\exp\left(E_a^{OH} - E_a^{CH_3}\right)}{RT} \cdot \frac{[CH_3]}{[OH]} = 0.1 \div 0.7.$$

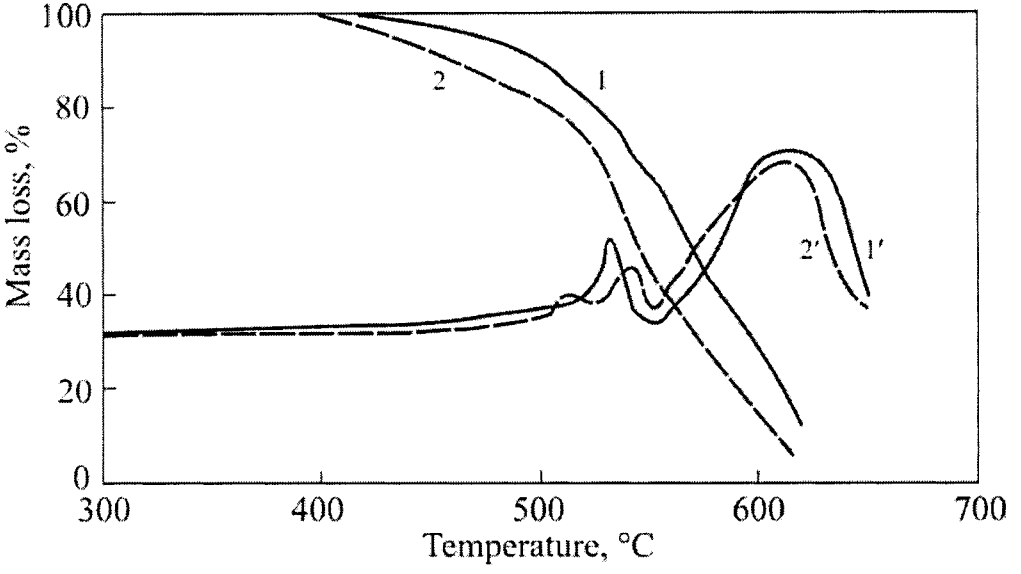

Figure 82. TGA (1, 2) and DTA (1', 2') curves for blocked (1, 1') and unblocked (2, 2') PSF in air, the heating rate of 6°/min

Therefore, the calculation performed with assumptions of maximum favorable conditions for the main CH_3-group main structure in initiation of high-temperature oxidation of PSF already indicates much higher activity of end hydroxyl groups in initiation of PSF thermal oxidation. Hydroxyl end groups are labile elements of the PSF structure. Therefore, they should be blocked, for example, by treating PSF with methyl chloride which substitutes OH-groups by OCH_3-groups. Other monofunctional agents ($PhCH_2Cl$, C_2H_5I, alkylarylchlorosylanes) are also used for blocking PSF. Unfortunately, blocking may not fully deactivate OH-groups. In marketable PSF their concentration reduced by an order of magnitude, but still remains at a level of 0.005 - 0.007 wt.%. Nevertheless, according to TGA the degradation initiation temperature of blocked PSF in air is by 20 - 25°C higher than for unblocked one (Figure 82). The run of two-stage TGA curves of the above-mentioned samples is similar. Effective activation energies of degradation (dynamic TGA data) equal 90 and (96 ± 20) kJ/mol. DTA curves are of similar type, except for the area corresponded to the initial degradation stage. For blocked and unblocked PSF, the one-stage degradation type in the absence of O_2 with the degradation start at

300 - 400°C, coke residue formation up to 30 wt.% at 700°C with equal E_a = (192 ± 20) kJ/mol is also similar, whereas in this case blocked PSF is higher heat resistant, though not so high as in thermal oxidation.

As improving the quality of Russian marketable PSF, thermal behavior of blocked and unblocked PSF was compared by analysis of both TGA data and other, higher informative degradation signs, for example, changes in molecular mass characteristics. In all cases, it was observed that at similar type of degradation, thermal oxidation damage kinetics effective kinetic constants of unblocked PSF samples degradation are greater (at similar values of effective activation energies). It is desirable to suggest that PSF thermal oxidation mechanism is independent of the end group origin. Labile hydroxyl end groups define higher degradation initiation rate, and the main process is then developed in the macrochain according to the same scheme. Similar situation is observed for PVC dehydrochlorination, when chain process initiation is defined by the type and content of allyl, ketoallyl and other labile end groups [13]. The change of the degradation mechanism proceeding via depolymerization with respect to the end group origin [174] is known for polyacetals only. PSF is not the depolymerizing polymer. Therefore, preservation of thermal oxidative degradation mechanism in samples with end groups of different heat resistance is quite clear. Though the above calculation indicates 0.02 wt.% content of labile hydroxyl groups as the boundary of the initiation mechanism change (equality of initiation rates at end OH- and side CH_3-groups), one should take into account the approximate type of calculations , i.e. interlocking of hydroxyl groups up to their content of 0.005 – 0.007 wt.%, apparently, provides for preferable initiation of random thermal oxidation. As a matter of principle, substitution of OH-groups by CH_3O-groups is not unambiguous because of reduced C-H-bond strength in methoxy group as a result end $ArOCH_2$-radical delocalization. This radical is formed after the bond break at thermal oxidation initiation. However, any empirical assessments do not conform to experimentally determined independence of thermal oxidation of PSF with end OCH_3-groups on molecular mass of the polymer in the range M_w = 17,000 – 70,000 [94], i.e. thermal oxidation of interlocked PSF is initiated statistically on side CH_3-groups.

Instability of hydroxyl end groups is typical of all polysulfone types. Polysulfone thermal stability regularly decreases with OH-group content increase in samples with similar molecular masses. For instance, the initial degradation temperatures for PES derived from 4,4'-dioxydiphenyl with reduced viscosity equal 0.65 at hydroxyl end group content of 0.018 and 0.9 wt.% equal 425 and 330, respectively. Another example is shown by copolymer

polysulfone (PSB-230 trademark, derived from bisphenol A and a mixture of 4,4'-dichlorophenylsulfone and bis-(4-chlorophenylsulfonyl)bisulfone), in which end OH-group content decrease from 0.24 – 0.28 to 0.15 wt.% at close values of reduced viscosity (0.4 – 0.5) three times reduces the gross degradation rate at 400°C. Similar to PSF, the effective activation energy of mass loss in PES at dynamic heating is low-dependent on the concentration of hydroxyl end groups. The determining factor for this parameter is the presence of the absence of isopropylidene e.g. aliphatic group in the aromatic structure of polysulfones. Polysulfones derived from bisphenol A (PSF and PSB-230) degrade both in the absence and in the presence of O_2 with E_a equal 90 - 100 and 190 – 205 ± 20 kJ/mol, respectively.

Degradation of fully aromatic PES under the same conditions is characterized by higher E_a values: by 20 and 40 kJ/mol, respectively.

Experiments with injection of additives [175] show that inorganic and organic increments cause some negative effect on PSF thermal stability. The analysis of various PSF samples performed by chemical techniques, GLC, ion chromatography, atom-absorption and emission spectroscopy indicated the presence of various admixtures in PSF (Table 29). Admixtures of bisphenol A (DPP), 4,4'-dichlorodiphenylsulfone (DCDPS), dimethylsulfoxide (DMSO) and chlorobenzene (CB) represent residues of monomers and reaction mixtures in PSF polycondensation and extraction technology. Oxychlorodiphenylsulfone (OCDPS) and, apparently, dioxydiphenylsulfone (DODPS) traces represent DCDPS hydrolysis products at the polycondensation stage as a result of deviations from stoichiometric relation between alkaline and DPP and at water presence in the reaction mixture [175]. Anions Cl^- and SO_4^{2-} form secondary products of both DCDPS hydrolysis and decomposition. Among inorganic additives, Na^+ and K^+ additives only may be associated with participation of alkaline agents during PSF production. The rest metals (cations) occur in the polymer from raw materials and the equipment.

With respect to end OH-groups and additive content, PSF thermal stability represents a multifactor reflex surface with direct and interrelated contributions of every admixture. Analysis of data from Table 29 shows that the sample No. 1 possessing optimal thermal oxidative stability is similar to other PSF samples by concentration of organic admixtures (metals and anions). A significant difference (an order of magnitude or higher) is observed for hydroxyl end group content (blocked and unblocked samples) and organic admixtures, as well. From positions of quality, the maximum permissible content of

Table 29

PSF sample characteristics

Sample	Organic admixture content, wt.%					Metal admixture content, cations (10^{-5}) wt.%						
	DPP	DHDPS	OHDPS	DMSO	CB	Na	K	Ca	Cr	Ni	Zn	Mn
1	$<10^{-3}$	$<10^{-3}$	$<10^{-3}$	0.005	0.017	260	5	57	$<10^{-1}$	3	4	2
2	0.08	0.063	0.15	0.06	0.012	900	4	50	2	4	2	2
3	0.06	0.049	0.06	$<10^{-3}$	0.01	600	100	10	$<10^{-1}$	$<10^{-1}$	1	2
4	0.05	0.03	0.02	0.009	0.1	400	10	80	4	4	3	15
5	0.05	0.058	0.03	0.008	0.01	-	-	-	-	-	5	2.4
6	$<10^{-3}$	$<10^{-3}$	$<10^{-3}$	0.003	$<10^{-3}$	240	4	50	$<10^{-1}$	-	3	2

Sample	Metal cations (10^{-5}) wt.%				Anions (10^{-3}), wt.%		End OH-groups, wt.%	MMD (10^{3})			Thermal stability		
	Mg	Fe	Cu	Ba	Cl^-	SO^{2-}_4		M_w	M_n	M_z	O_2 absorp. *	Light transmit. **	MFI ratio ***
1	6	8	6	0.5	2.2	3.1	0.006	38.3	14.7	60.8	0.35	89	1.0
2	7	8	$<10^{-1}$	$<10^{-1}$	440	2.7	0.096	38.5	12.6	80.4	1.1	27.1	0.88
3	100	8	$<10^{-1}$	14	180	1.7	0.087	36.8	15.1	64.9	0.85	38	0.9
4	100	10	$<10^{-1}$	1	5.6	3.1	0.063	40.7	16.2	69.1	0.45	78	0.98
5	7	40	24	0.23	35	3.0	0.067	39.2	13.8	68.1	0.42	80	1.0
6	6	7	$<10^{-1}$	$<10^{-1}$	2.1	2.0	0.0061	41.0	17.0	73.1	0.32	92	0.99

Notes: * O_2 absorption (1 h, at 350°C), mol/base-mol;

** Light transmittance at 425 nm, %;

*** $MFI_{10\ min}/MFI_{20\ min}$ at 320°C.

admixtures, determined in experiments with polymer filling and further regression analysis [175], equals: DPP – 0.005 wt.%, OCDPS – 0.1 wt. %, DCDPS – 3 wt.%, NaCl – 0.005 wt.%, CB is practically inert. Experiments with DMSO additives show that concentration MFI and extrudate light transmittance dependence (320°C) is characterized by a plateau up to DMSO content of 0.05 wt.%.

Further increase of DMSO content leads to MFI increase and yellowing. Degradation changes become catastrophic at DMSO content above 0.5 wt.%. As DPP content is that mentioned in Table 29, concentration of its active hydroxyl groups is, approximately, two orders of magnitude lower than at macromolecule ends. Extension of the above reactivity assessment at oxidation initiation on end OH- and side CH_3-groups in PSF macromolecule leads to the border concentration of end hydroxyl groups defined by the equality of rates on the mentioned structural elements: 0.002 – 0.01 wt.%. Tests show full identity in thermal behavior of interlocked PSF samples (No. 1 and 6) with equal content of additives (Table 29). They differ by concentration of hydroxyl end groups only: 0.006 - 0.009 wt.%. These samples possess the elemental composition (C – 73.7%; H – 5.4%; S – 7.5%; O – 13.4%) approaching theoretical one (C – 73.3%; H – 4.98%; S – 7.34%; O - 14.48%, respectively). ^{1}H and ^{13}C NMR-spectroscopy data fully confirm the main polymer structure. These samples also display the highest thermal stability.

Polyesterimide

Polyesterimide (applied to marketable products) is produced by dianhydride A and *m*-phenylene diamine nucleophilic substitution with further thermal cyclization. The first stage of the synthesis is obtaining polyesteramido acids (PEAA), performed in methylene chloride mixed with water, and the second stage is performed in melt.

To increase thermal stability, macromolecular structure of PEI is controlled in two ways: end group interlocking by phthalic anhydride (PA) and varying cyclization conditions.

Comparison data on PEI with different admixture content, MMD, end groups and, correspondingly, thermal stability are shown in Table 30. All studied samples displayed actual 100% cyclization degree (IR-spectroscopy data). Introduction of phthalic anhydride (PA) as the interlocking agent to PEI synthesis causes a decrease of carboxylic end group content, and the polymer

Table 30

PEI sample characteristics

Sample	Elemental composition, %			Metal additives (10^{-3}), wt.%								MMD (10^{-3})			
	C	N	H	Co	Ni	Ca	Fe	Mg	Na	K	Cr	M_w	M_n	M_z	M_w/M_n
1.	74.78	4.58	4.11	2.5	1.3	1.3	12	8.7	5.0	1.5	0.3	43.1	18.8	86.2	2.28
2.	75.27	4.46	4.27	0.57	0.38	26	4.4	2.0	5.2	1.4	6.4	48.3	20.1	97.9	2.03
3.				0.54	0.5	12	40	3.0	5.0	1.2	6.0	42.6	18.2	85.4	2.0
4.												46.3	20.9	81.6	1.76
5.												52.6	20.3	111.5	2.59
6.												88.8	22.2	225.5	4.0
7.												28.3	13.4	59.8	2.1
8.												107	30.5	256.0	3.51

Sample	End groups, %		Thermal stability		Gel fraction **	Anion content ***
	COOH	NH_2	Mass loss at 500°C during 30 min in air, %	Optical density*		
1.	0.2	0.07	25.5	-	-	-
2.	0.15	0.03	17.0	0.17	0	2.0
3.	-	-	27.0	-	-	2.5
4.	0.1	0.06	12.0	0.14	0	3.0
5.	0.24	0.07	-	-	-	-
6.	0.36	0.2	22.0	0.32	42	-
7.			39.0	0.37	41	-
8.	0.35	0.32	44.0	0.45	49	500

Note: * Optical density at 425 nm, after thermal processing at 320°C during 20 min in air;

** Gel fraction after thermal processing at 320°C during 20 min in air, %;

*** Anion content (Cl^-), $\times 10^{-3}$ wt.%.

obtains narrower MMD (the polydispersion index decreases). Decreasing optical density, mass losses and insoluble fraction content in the polymer after thermal processing testify about thermal stability increase in interlocked PEI. Another way of thermal stability increase is polymer synthesis with equimolar ratio of monomers (PEI 4, Table 30).

Thermal stability of PEI is significantly deteriorated by the use of unpurified monomers. PEI obtained using unpurified dianhydride A possesses poorer molecular-mass characteristics even if all production conditions are maintained (PEI 7, Table 30). Mass-spectrometry analysis of dianhydride A allowed detection of three admixtures: bisphenol A, nitrophthalic anhydride (initial monomers for dianhydride A synthesis), and phthalic anhydride. Moreover, PEI thermal stability may be definitely reduced by solvent traces (PEI 8): increased Cl^- ion content at insufficient washing off of methylene chloride. As known, inorganic admixtures (metal ions) may occur in the polymer both from raw materials (monomers and solvents) and directly from the equipment. In case of iron increments, PEI thermal stability is decreased by its 10-fold exceeding of the permissible level only (PEI 3 compared to PEI 2).

Thus, analysis of data shown in Table 30 allows the following conclusions about PEI thermal stability. The ways of thermal stability increase must include the following stages: purification from organic and inorganic admixtures, end group interlocking and stabilization.

Problems of stabilization will be discussed in detail in the following section.

Polyphthalamides

To understand reasons for thermal stability change, a complex study of pilot PPA-1 and PPA-2 series was performed. The studies were performed in several directions:

1. The study of humidity effect on PPA thermal stability.
2. the Study of molecular-mass characteristic effect.
3. The study of low-molecular organic admixture effect (residues of non-reacted monomers).
4. The study of inorganic admixture effect (metals occurring in the polymer with raw materials and from the equipment).

The results are generalized in Table 31.

Table 31

PPA sample characteristics

Sample	Elemental composition			Metal additives (10^{-2}), wt.%							MMD×10^3				Thermal stability	
	C	N	H	Cu	Ni	Ca	Fe	Al	Na	K	M_w	M_n	M_z	M_w/M_n	Mass loss*	*MFI* ratio**
PPA-1 (theor.)	67.85	11.48	7.56													
1.	66.54	12.23	13.33	0.013	0.01	4.0	13	1.4	22	230	39.7	6.7	196	5.9	390	8/0
2.	67.25	11.86	13.03	200	2/0	40	1.2	14	2000	220	21.6	4.5	75	4.8	350	16/0
PPA-2 (theor.)	68.29	11.38	7.32													
3.	67.25	12.42	7.42	13	10	4	1.3	1.4	30	640	25.5	8.0	43.1	3.2	380	6/0
4.	68.02	11.94	7.46	200	200	40	13	14	480	600	25.0	8.4	42.0	2.9	350	10/0

Note: * Temperature of 10% mass loss according to dynamic TGA (5°/min rate) in air, %

** $MFI_{10\ min}/MFI_{20\ min}$ at 310°C.

Table 32 shows data on humidity effect on thermal stability of the material.

Table 32

PPA mass losses during 15 min at 300, 325 and 345°C

Sample	Mass loss(wt.%) during 15 min at temperature					
	300°C		325°C		345°C	
	Ar	Air	Ar	Air	Ar	Air
PPA-1 with 0.005% residual humidity	0.8	1.8	0.9	2.0	1.0	2.2
PPA-1 with 2.5% humidity	2.1	3.0	2.2	3.5	2.6	5.2
PPA-2 with 0.005% residual humidity	0.98	1.2	1.15	1.45	1.2	1.90
PPA-2 with 2.5% humidity	2.97	3.03	3.0	3.5	3.15	5.82

The data show effect of, at least, two factors on the degradation behavior of PPA: sorptive humidity and air oxygen additives. Obviously, humidity may be easily removed by drying. The oxidation effect was discussed in detail in Chapter 2.

Changes in molecular-mass characteristics of PPA-1 and PPA-2 during material processing were studied. The MMD change during thermal processing to the gel formation stage was described before.

Analysis of the data obtained indicates actively proceeding branchiong and crosslinking reactions at PPA-1 and PPA-2 processing temperatures. Note that any thermal treatment leads to a significant increase of all molecular mass moments and MMD chromatogram shift to the high-molecular zone. In polymer with low molecular mass, gel-fraction is accumulated at much lower rate – the gel amount in two studied samples (with M_w = 39,700 and 21,600, respectively) differ by an order of magnitude. However, their tendency to decrease light transmittance with increase of gel-fraction content is the same. The change of

all MMD moments in PPA-1 (M_w = 21,600) proceeds at lower rate than in PPA-2 (M_w = 39,700). Though thermal processing induction of the polymeric matrix crosslinking is obvious, proceeding of purely degradation processes may not be eliminated.

The composition and content of organic admixtures in PPA-1 and PPA-2 were studied with the help of thermal mass-spectrometry analysis by heating PPA-1 and PPA-2 samples placed directly to ionization chamber ("at direct injection" method of analysis). Easily volatile products with molecular ions, *m/z* = 77, 92, 127, released from the samples below 100°C, were identified according to MS database:

m/z = 77 ÷ 78 – benzene;
m/z = 91 ÷ 92 – phenol;
m/z = 127 – cyclic aliphatic amine of $(CH_2)_5$-CH-NH-CH_2-CH_3 type.

As heated above 100°C, heavier products are released from the samples:

m/z=259-260

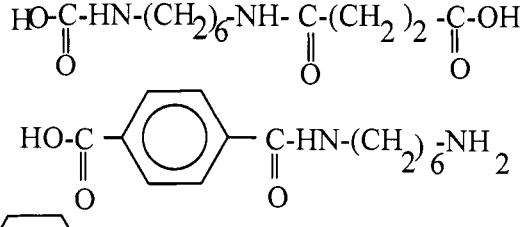

mz=343-360

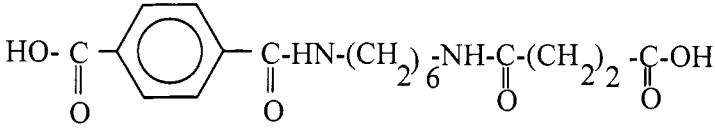

Detected compounds represent low-molecular fragments of PPA-1 and PPA-2 structure. Of importance is that these oligomers possess both carboxylic and amine and carboxylic end groups.

The experimental results reliably demonstrate imperfection of PPA-1 and PPA-2 chemical structures. According to elemental analysis, empirical and experimental data on H/C/N/O contents are significantly different.

Compared with the empirical value, increased nitrogen content in the element composition of PPA testifies about amine end group dominance over carboxylic ones. The effect of end (amine or carboxylic) groups on thermal stability of polyamides and polyimides was studied in detail [13, 166, 167]. In case of amine end groups dominance all studied polymers displayed a decrease

of thermal stability and viscosity increase of the melt, and approach of processing and degradation initiation temperatures. In the present case, analogous effect of amine end group concentration on PPA thermal stability is also observed. The content of amine end groups was assessed using nonaqueous pH titration technique. Four PPA-1 samples with equal MMD were tested. The content of end amino groups varied from 0.166 to 0.198 wt.%, which is quite significant.

The atomic emission spectroscopy method was used in the study of inorganic admixture composition in PPA-1 and PPA-2, usually occurring from the equipment. The effect of metal increments on thermal stability was assessed by isothermal TGA, MFI and melt thermal stability data.

Besides serial samples, model PPA species were studied, to which additional increments of inorganic salts of corresponded metal were injected. The data are generalized in Table 31. The studies show different effects of metal increments on thermal oxidation stability of PPA. Alkaline metals (Ca, Na, K) and Al do not actually affect thermal stability in the studied range, whereas Fe causes an adverse effect, And Cu and Ni in concentrations below 10^{-2} – 10^{-1} wt.% significantly increase thermal stability of PPA. The analogous situation was already observed for aliphatic polyamides.

Summing up the performed studies, one may conclude about imperfection of PPA-1 and PPA-2 chemical structures and about insufficient purity of the polymers. This causes an adverse effect on thermal stability of the polymers at processing and, consequently, on operation properties of the articles.

Poly(alkane imide)

Dynamic heating of PAI in pure argon flow and in air causes the mass loss (for samples, preliminarily heated up in vacuum at 120°C for the purpose of removing solvent traces and drying) at 400 and 320°C, respectively (Figure 83). At the initial stage, thermal and thermal oxidative degradation of PAI (mass losses are below 20%) fit kinetic order one law with the rate constants equal, respectively:

$$K_{Ar} = 3.9\times10^{15}\exp\left(-\frac{232\pm20}{RT}\right);$$

$$K_{O_2} = 1.8\times10^{14}\exp\left(-\frac{202 \pm 20}{RT}\right).$$

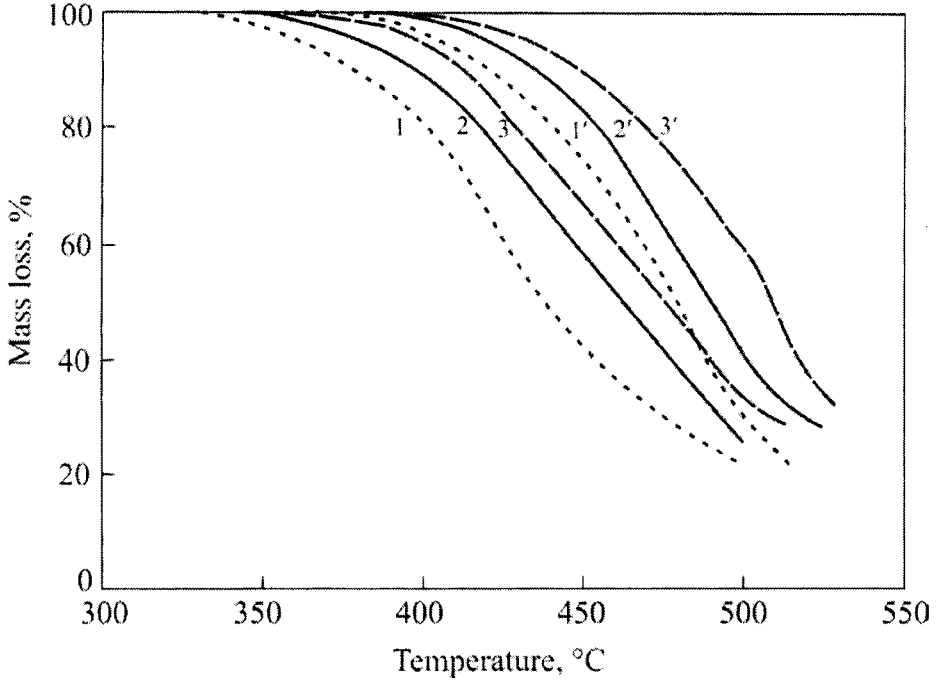

Figure 83. TGA of powder-like (1, 1'), granular (2, 2') and molded (article) (3, 3') PAI samples at the heating rate 5°/min in air (1 – 3) and argon flow (1' – 3')

Though corresponded recalculation shows absence of mass losses in PAI under processing conditions (temperature and treatment duration), degradation is observed even visually by polymer yellowing: resulting the two-stage processing (powder – granules – article) the yellowing index of PAI is increased from 24.9 to 42.3 (measured on three-coordination colorimeter Pulsar) Melt Flow Index (MFI) is also sensitive to thermal load. It gradually increases at two stages of PAI processing (granules, mold sample) from 0.6 to 2.5 g/10 min. TGA data (Figure 86) indicate a decrease of PAI thermal stability at transition from granules to the article.

Table 33

PAI sample characteristics

Sample	Composition			Metal additives (10^{-2}), wt.%					MMD (10^{-3})			
	C	N	H	Ca	Fe	Mg	Na	K	M_w	M_n	M_z	M_w/M_n
1.	71	7.36	6.9	1.6	0.67	2.4	0.8	0.33	105	31	201	3.4
2.	73	7.6	7.2	1.6	3.6	2.6	0.9	0.29	126	36	241	3.5
3	73	7.4	7.3	0.76	0.14	1.2	0.35	0.24	87	25	167	3.5
4.	71.9	7.5	7.1	1.0	0.39	1.5	0.18	0.18	158	26	409	6.1
5.	69.0	7.1	7.5	0.51	0.06	0.8	0.8	0.24	120	50	150	2.4

Sample	η_{spec}	Gel fraction, wt.%	Thermal stability			
			Mass loss *	Mass loss **	O_2 absorption ***	*MFI* ratio ****
1.	0.98	5.0	3.5	0.7	0.48	1.11/1.12 = 0.99
2.	1.42	10.0	6.0	1.1	0.62	0.04/crosslinked
3	1.13	6.0	6.0	1.3	0.5	5.63/5.85 = 0.96
4.	1.31	5.5	5.0	1.0	0.5	1.93/1.65 = 1.17
5.	0.92	5.1	3.0	0.5	0.45	1.62/1.43 = 1.13

Note: * Mass loss according to dynamic TGA (5°/min rate) at 350°C, %;

** Mass loss according to TGA during 1 h at 320°C, %;

*** Oxygen absorption during 60 min at 250°C, mol/base-mol;

**** $MFI_{10\ min}/MFI_{20\ min}$ at 310°C.

To understand the reasons effecting thermal stability of PAI, a complex study of serial lots were performed. Metal increments, elemental composition and molecular-mass characteristics were analyzed.

The results on several most demonstrative samples are shown in Table 33.

Current studies indicated significant difference in elemental composition of PAI. Compared with calculated values, increased nitrogen concentration testifies about amine end group predominance over carboxylic groups. In turn, this reduces thermal stability of the melt, increases melt viscosity and causes approach of processing and degradation initiation temperatures [55]. All samples displayed very high content of metal admixtures. For example, they contained Mg. Fe and Ca by two orders of magnitude higher than PSF. A dramatic scatter of molecular-mass characteristics in studied serial lot should also be mentioned: M_w range equals 70,000, and M_z – 150,000. There were samples observed, possessing up to 10 wt.% gel in the primary state (before thermal processing).

The interrelation between defect structures, admixtures and thermal stability is illustrated well on the example of sample No. 2, in which 10 wt.% gel-fraction was detected. The calculated nitrogen content in the composition was exceeded, and high amounts of Mg and, specifically, Fe were observed. These drawbacks affect thermal stability. At short-term heating in IIRT channel the polymer is crosslinked: $MFI_{10\ min}$ = 0.04 g/10 min. Further exposure causes "complete crosslinking", and the material may not be processed. According to isothermal, dynamic TGA results in air and oxygen absorption data, this sample also displays low thermal oxidative stability.

The experimental data are convincing that chemical structure of studied PAI lots is imperfect and polymer purity is poor. This makes processing more complicated and adversely affect the quality of marketable products, including material behavior during operation.

STABILIZATION

Polysulfones

As is obvious, this problem is primarily associated with PSF high-temperature oxidation. The initial prerequisite to screening of admixtures was the experience obtained by the authors [26, 35] on thermal stabilization of polycarbonates by phosphite increments. This experience was transferred to polysulfones at the early stage of their development [188]. The idea of polysulfone stabilization using phosphorus-containing additives (PCA) is also present in international patents [189, 190]. Besides PCA, all types of classical antioxidants and substances, considered in the literature as high-temperature stabilizers for polymers (boron compounds, metal salts and complexes, organoelemental compounds) were used in the screening [33]. The empirical experience on antioxidant stabilization [31] concerning the efficiency of extremely unexpected substances, the structure of which is often different from the notions of antioxidants, was also used.

The important part of screening is selection of an optimal method for admixture tests. It should be highly informative and require minimal experimental costs for tests a mass of compositions. Since degradation damages in PSF under processing conditions are caused by oxidation, O_2 absorption kinetics is the most informative for screening. However, these experiments are rather complicated and require long-time performance which eliminates the full-scale application of the method to test of about a hundred of admixtures with varying concentrations. The assessment of thermal stability of PSF laboratory samples and production lots (both Russian and foreign) showed almost linear dependence of oxygen amount absorbed by the polymer (mol O_2) and light transmittance change (abs.%) on $\left(\frac{M_z}{M_w}\right)$ ratio: at 320°C, $\Delta[O_2] \sim 0.005\Delta T$; $\Delta[O_2] = 0.012\left(\frac{M_z}{M_w}\right)$. Therefore, these two parameters which are determined technically quickly (the first permanently, and the second and TGA by case) were used for screening.

Among the abundance of tested classes of substances, PCA is the only additive reliably protecting PSF from oxidation in concentrations below 0.3

wt.%. As expected, by analogy with polycarbonate and other heterochain polymers processed at temperatures about 300°C, classical primary antioxidants (hindered phenols and aromatic amines) are at most neutral (amines catastrophically color PSF), which proved existence of the effective inhibition temperature limit (120 - 125°C) [110, p. 218]. It is stipulated by activity of phenoxyl radicals in reactions with hydroperoxides. Commonly, all so-called "non-chain inhibitors" intensify PSF degradation, though a combination of transition metal and phosphorus atoms in the same molecule, for example, $(PhP(O)O)_2Cr$, is quite effective. An abrupt shortening of the list of potential stabilizers allowed, using all methods of degradation behavior assessment, detection of organic phosphates as the most effective additives among PCA. At high temperatures, alkylphosphites and non-substituted in *ortho*-position arylphosphites are extremely sensitive to humidity and foam the polymer up when hydrolyzing. Only in laboratory, at intimate drying of PSF, injection of additives in a "dry" atmosphere with immediate processing of the composition gives a stable effect. Similar situation is known for polycarbonate stabilization [35]. Only since 1980's the so-called "sterically hindered" or low-hydrolyzing arylphosphites (SHP), discovered at that time, may be used for real thermal stabilization of PSF at processing temperatures. By analogy with hindered phenols, these newly discovered compounds contained volumetric tert-butyl groups in *ortho*-position at the ester bond. Among this class of phosphates, cyclic hindered phosphates, including ones derived from pentaerythritol, are the most effective. They are known under trademarks: *Ultranox 626* (Borg Warner), *Irgafos 126* (Ciba) and dibenzospiroarylphosphite *Stafor 11* (NIIKhIMPolymer). The optimal concentration of additives to PSF is 0.1 – 0.8 wt.% (1.5 - 5 mmol/kg). Such a broad range of concentrations is caused by the individuality of approaching stabilization of particular PSF samples. Similar to the scale of degradation transformations, the stabilization effect possesses the inverse dependence on PSF sample purity. The higher concentration of additives and labile structures in the polymer is, the more noticeable the stabilization effect is. Unfortunately, "impure" sample may not reach the quality of pure PSF even by means of stabilization. The mentioned compounds in concentrations 0.1 – 0.3 wt.% slow down high-temperature degradation of samples with the minimal impurity degree, 1.5-2-fold decrease O_2 absorption (Figure 84) and CO_2 release rates. Degradation changes observed by IR-spectra occur much slower (C=O-group occurrence and accumulation is observed by 1660 and 1737 cm^{-1} bands).

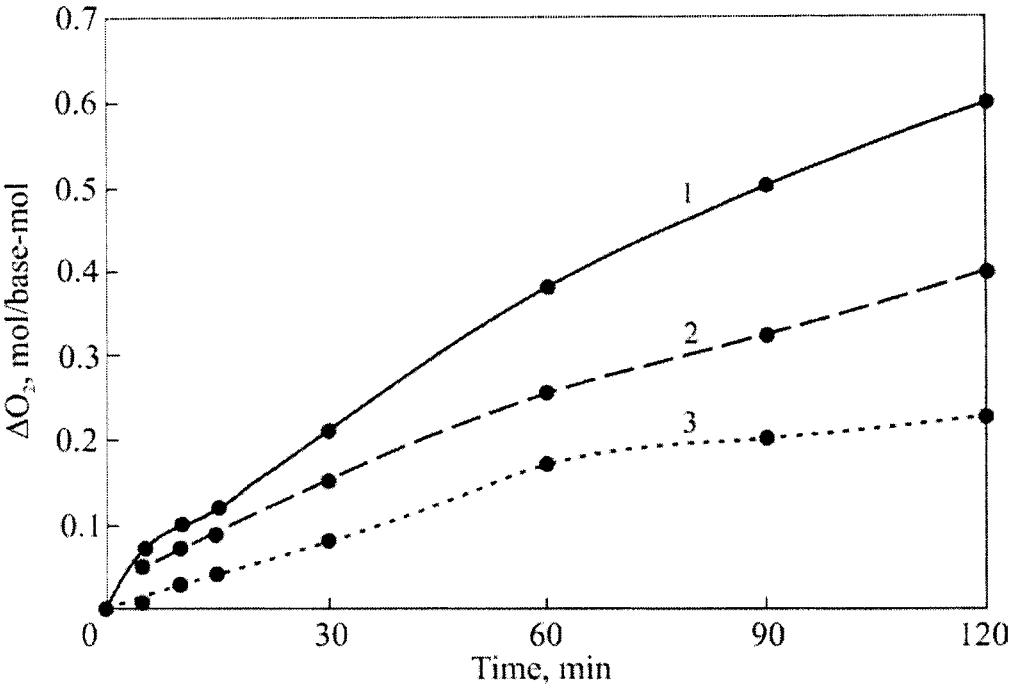

Figure 84. Oxygen absorption kinetics (T = 320°C; $P(O_2)$ = 399.9 kPa) for PSF: (1) initial, stabilized by (2) 0.3% *Ultranox 626* and (3) *Stafor 11*

In tests simulating processing conditions, SHP injections promote MFI increase, increase thermal stability index, decrease coloring degree, and prevent M_z increase induced by degradation branching and crosslinking of macromolecules (Figure 85). SHP stabilizing effect on branching was determined by direct GLC analysis. At solid-phase aging (180°C) of films during 75 days no changes in G-factor of stabilized (0.3 wt.% AO-118) sample (G = 1), whereas in nonstabilized PSF G-factor decreases to 0.8 by the aggregate stabilizing effect (O_2 absorption kinetics, coloring, *MFI* thermal stability and MMD moment changes were studied). For PSF processing, cyclic SHP are optimal stabilizing additives, pentaerythritol diphosphites, above all. SHP with open chain, for example, tris-(2,4-di-*tert*-butylphenyl)phosphite, are much less effective.

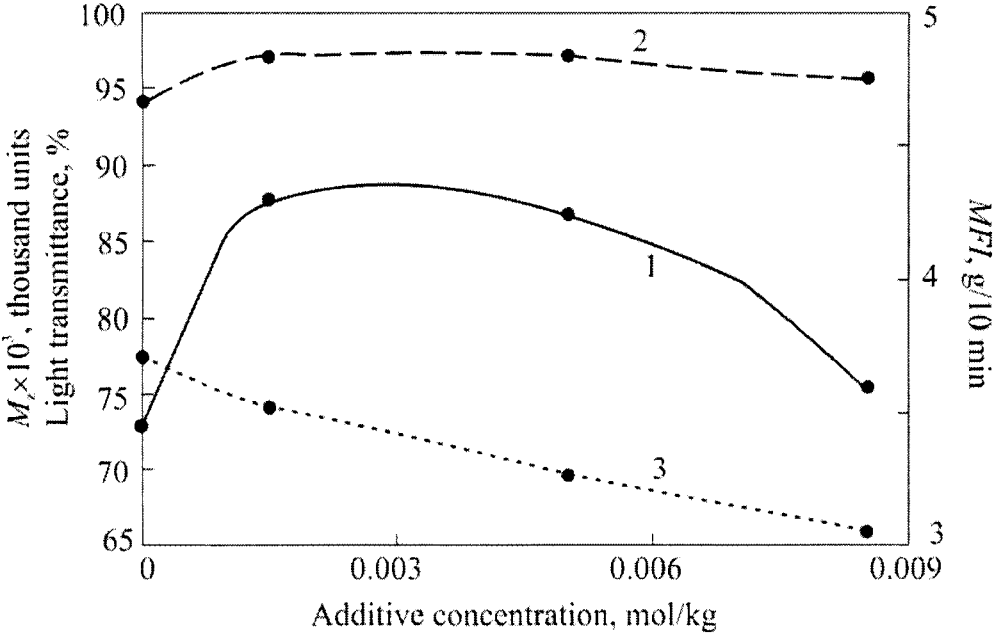

Figure 85. Concentration dependence of SHP effect (*Ultranox 626*) in PSF tests on IIRT device (T = 320°C; 2.16 kg load): MFI (1), light transmittance (2), and M_z (3)

Note also positive effect of SHP additives at PSF aging. According to scanning electron microscopy data (Figure 86), injections decrease domain size from 1,000 to 500Å and significantly increase their disposition density (compare with Figure 72). Contrary to nonstabilized PSF (Figure 86), thermal processing of stabilized PSF at exposure critical for operation properties (2 days) does not destroy the permolecular structure, but even promotes its further improvement: the domain size is reduced to 300 - 400Å, homogeneity and packing density increase. Obviously, chemical stabilization at processing also affects physical aging of PSF.

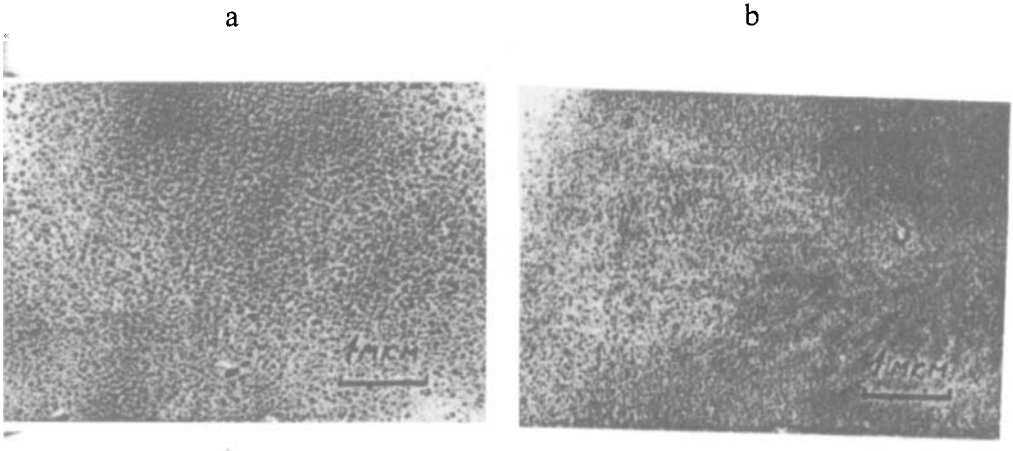

Figure 86. Microphotoes (× 15,000) of initial (a) and thermosabilized PSF, after 2 days of aging at 150°C (b)

One more circumstance should be mentioned. PSF thermal processing in vacuum, at temperature above 300°C causes degradation changes, insufficient as compared with thermal oxidation effect, but also noticeable. Similar to thermal oxidation, degradation change degree depends on the additive content in PSF. SHP increments slightly slow down thermal transformations in PSF. Unfortunately, this effect is much lower than similar effect of the same increments in thermal oxidation process. For example, after tests in vacuum at 350°C injections increase PSF light transmittance by 3 – 5 units. In the presence of oxygen, under the same conditions, the effect reaches 20 units or more. As a consequence, the contribution of direct deactivation of additives via complex formation is, apparently, not the decisive one, and the main role of SHP is activity of high-temperature antioxidants.

Thus, high-temperature antioxidant stabilization of PSF by SHP (and possibly other phosphorus-containing compounds) injections is realized via inhibition of the radical-chain oxidation process and deactivation of additives activating these reactions. However, unexpected stabilizing effects, for example, a noticeable color stabilizing effect of negligibly small injection of copper sulfate or patent data on efficiency of tin-organic compounds in PSF [222] indicates the possibility of additional contributions and other stabilization mechanisms, for example, deactivation of electron-excited compounds or interlocking of a charge transfer complex with O_2 (refer to Chapters 1 – 6 for

detail). High-temperature oxidation and stabilization of aromatic heterochain polymers are complex processes which differ from the known low-temperature oxidation and inhibition of hydrocarbon polymers.

To some extent, these processes are closer to combustion, and stabilizing activity in them is obtained by substances which, at first glance, are not antioxidants, but, most likely, fire retardants. To discover new mechanisms of high-temperature stabilization, more comprehensive studies of behavior of these substances are required, for example, metal compounds in degrading polymer. In this case, the additive screening is aimed at searching for effective stabilizers to be used in PSF processing. The highest efficiency and raw material availability are the factors that defined our selection of SHP for industrial tests and selection of additive injection techniques.

Development of thermal stabilizers for construction PSF trademarks was required for increasing quality of Russian-produced materials, namely, their physicomechanical and heat-physical properties, optical characteristics and thermal stability.

The efficiency of stabilizers conforms to laboratory test data and their concentration in marketable product. According to laboratory assessments, the efficiency of tris-nonylphenylphosphite (a moderate stabilizer), was found low due to high volatility: only 30% of injected phosphorus remained in granules.

Table 34

Polysulfone pilot lot properties

Sample	*MFI**	*MFI***	ε, %	Tensile strength, MPa	Heat resistance		Light transmittance (426 nm), %
					Vick	Deform.	
PSF without additives	2.6	0.86	14.4	68.0	175	153	45.8
PSF + *AO118*	2.9	1.08	54.0	72.0	180	164	54.0
PSF + *Ultranox 626*	2.9	0.96	64.0	74.0	184	168	64.0
PSF + *Stafor11*	3.2	0.98	44.0	76.0	180	162	52.0

The stabilizing effect is manifested in melt viscosity decrease and increase of melt thermal stability, physicomechanical characteristics, heat resistance and light transmittance. Comparison results of stabilized and nonstabilized PSF quality within the same lot are shown in Table 34.

The above results indicate that injection of thermostabilizing additives improves quality of PSF.

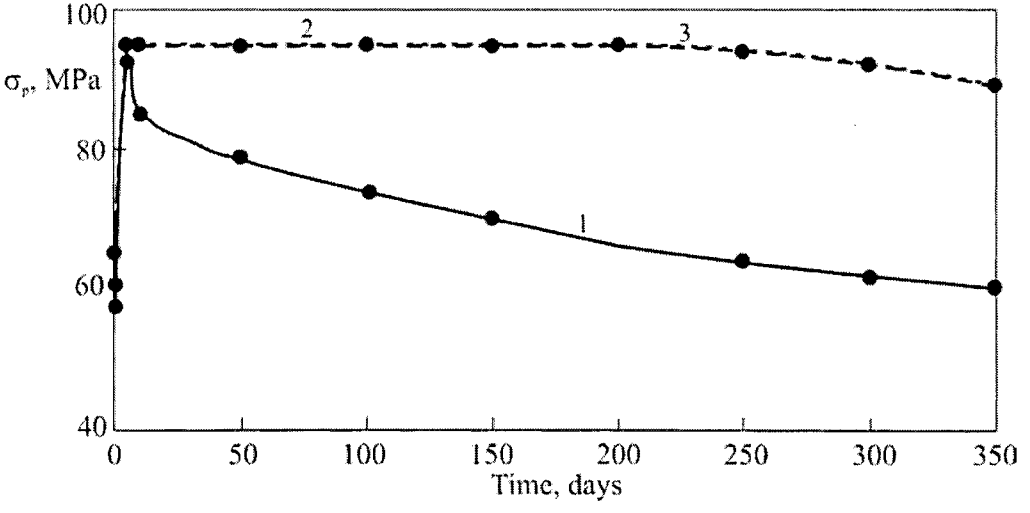

Figure 87. Tensile strength change for PSF: nonstabilized (1) and stabilized by additives *Stafor* (2) and *Ultranox 626* (3). Thermal aging in air, T = 160°C

The behavior of test stabilized and nonstabilized PSF lot was studied during aging at (160 ± 5)°C up to 1 year. Figure 87 shows dynamics of the tensile strength change in stabilized PSF during aging. In initial two days, resulting purely physical changes in permolecular PSF structure, the material becomes much stronger, by 35 – 40% above the initial value. However, already on the fifth day, the strength of nonstabilized PSF decreases by 10%. A year after this index decreases to the value of the primary PSF.

In initial two days, stabilized PSF behaves itself similar to nonstabilized PSF. However, further aging does not cause so quick decrease of strength characteristics: an insignificant strength decrease is observed after 250 days only, and reaches 10% after 1 year of aging.

Table 35

Polyesterimide stabilization

Stabilizing compounding	Light transmittance, % *	Mass loss ratio **	Melt viscosity ***		MMC for PEI ****				
			242 c^{-1} (10^4)	2912c^{-1} (10^3)	M_w	M_n	M_z	M_w/M_n	M_z/M_w
-1-	-2-	-3-	-4-	-5-	-6-	-7-	-8-	-9-	-10-
PEI without additives	48	-	1.3	3.2	46.9	18.2	94.0	2.58	2.0
0.05% *Irganox1076*	49	1.2	1.3	3.2	46.9	18.2	-	-	-
0.1-0.5% *Irgafos 126*	54-33	3.5-2.2	1.6-1.9	2.9	42.2	17.3	84.7	2.44	2.0
0.1-1.0% *Irgafos 168*	53-48	1.0-1.5	1.2-1.6	2.8	41.4	18.0	76.2	-	-
0.5% *Irgafos 126*/0.05% *Irganox 1076*	54	2.2	1.4	-	-	-	-	-	-
0.5% BT5	44	1.5	1.1	2	40.3	17.6	74.3		
0.1-5.0% TNPP	51-22	1.0-0.5	0.11-0.85	3.2	46.9	18.4	82.0	-	-
0.1-1.0% benzoin	58-49	0.6-0.5	0.1-0.77	2.8-2.0	43.2-35.3	17.7-14.6	86.3-70.8	2.44-2.42	2.0

-1-	-2-	-3-	-4-	-5-	-6-	-7-	-8-	-9-	-10-
0.05% MKS21	44	0.9	1.0	3.0	43.2	17.9	78.0	-	-
0.05% $CuSO_4$	45	1.1	1.1	3.0	44.1	18.2	72.0	-	-
0.1% KI	60	-	1.0	-	-	-	-	-	-
0.1-0.5% $NaHPO_4$	62	0.8-0.7		2.8	41.1-40.9	17.2-17.1	80.2-79.8	2.4-2.38	1.95
1.0% $Na_5P_3O_{10}$	58	0.7		3.2	46.5	18.9	92.9	2.46	2.0
0.5%TiO_2	-	1.2		2.9	40.3	17.0	78.4	2.37	1.95

Note: * Light transmittance (in %) at 425 nm, after thermal processing in rheoviscosimeter at 340°C and 242 s^{-1} shear rate during 30 min;

** The ratio of mass losses for PEI (initial to stabilized) after thermal processing in rheoviscosimeter at 340°C and 242 s^{-1} shear rate (TGA data at 450°C during 60 min in air);

*** Effective melt viscosity (pz) during 30 min at shear rates mentioned;

**** Molecular mass characteristics (10^3) of PEI after thermal treatment in rheoviscosimeter at 340°C during 30 min at the shear rate of 2912 s^{-1}.

Tests of thermal stabilizers under production conditions indicated efficiency of PSF stabilization by additives. They improve processing and initial properties of PSF, and increase operation time of polysulfone materials.

Polyesterimides

To increase PEI thermal stability during production (unloading from the device and extrusion), a broad list of additives was screened, including compounds from different chemical classes (phenols, phosphates, alternating valence metal compounds, etc.). According to mass losses obtained, the highest and the most stable antioxidant effect is displayed by phosphites (Table 35), though metal salts are quite stable, too. Moreover, among phosphates, hindered aromatic cyclic phosphates of *Irgafos 126* should be outline. Their injection increases light transmittance of PEI by 10 – 15%, decreases mass losses by 20 – 50%, and significantly increases stability of the melt viscosity. Note also that SHP are the most effective antioxidants for PEI, too.

Aliphatic-aromatic polyamides and glass-filled composite materials derived from them

There is a wide material in the literature on stabilization of aliphatic PA [4, 10, 13, 14, 16, 18]. However, at present, there are no data on optimization of the stabilizing system for aliphatic-aromatic PA. Therefore, until now PPA were stabilized as aliphatic PA, using the traditional Cu^{2+}/I^- system.

Basing on the data obtained for the degradation mechanism, it should be taken into account at stabilizer selection that injected additives must inhibit degradation reactions during processing and operation.

As a consequence, the additives must:

- fully suppress or significantly decelerate initiation reactions of PPA high-temperature degradation which, as already suggested, develop untraditionally, via formation of "molecular complexes with oxygen" or "electron-excited states";
- inhibit radical-chain process of solid material degradation in the operation temperature range.

Moreover, obtaining of the required quality of polymeric material necessitates:

- maximum possible elimination of hydrolytic reactions at all stages of polymer "life";
- inhibition or maximum possible suppression of post-crystallization processes.

Various compounds were injected to PPA both individually and as complex mixtures, and their effects on the following indices were studied: oxygen absorption, *MFI* and melt thermal stability, gel-fraction content and sol-fraction color change.

Table 36

The effect of stabilizers on O_2 absorption, CO_2 release (180°C) and mass losses (330°C) at PPA-1 thermal oxidation in air

Composite	O_2 absorption, mol/monomeric unit	CO_2 release, mol/monomeric unit	Mass losses, %
PPA-1 without additives	0.21	0.029	5.4
PPA-1 - *Irganox 1098* (0.5%)	None		3.8
PPA-1 – Cu/I (0.2%)	0.16	0.09	3.5
PPA-1 - *Irganox 1098* (0.08%)/*Irgafos 168* (0.08%)/*HALS 944* (0.2%)	0.07	0.014	4.2
PPA-1 - *Irgafos168* (0.08%)/$CuSO_4$ (0.2%)	0.20	0.024	4.1
PPA-1 - $CuSO_4$ (0.2%)/*Irgafos 168* (0.08%)/*HALS 944* (0.2%)	0.10	0.01	3.6
ПФА-1 - Zn acetate (0.2 %)/ *Irganox1098/ Irgafos 168* (0.16%)	0.16	0.02	4.3

Phenol antioxidants, thioesters, thiophosphates, ester fluorides, sterically hindered amines (HALS), carbodiimides, alternate valence metal complexes and salts, phosphates, phosphites, etc. were studied. Copper and Nickel salts are the most effective compounds. Injection of these compounds increases *MFI* at quite

high stability of the melt viscosity, the strand is strong and elastic, O_2 absorption and gel formation are suppressed, and the polymer becomes lighter colored. The known Cu^{2+}/I^- mixtures are also highly effective for MFI increase and oxygen absorption suppression. However, they do not practically improve thermal stability of the melt. A mixture *Irganox B1171* (Ciba, aminophenol *Irganox 1098* with phosphite *Irgafos 168*) is lower effective compared with transition metal compounds (Cu and Ni). Table 36 shows effects of stabilizers on the amount of absorbed oxygen and released CO_2, and PPA mass losses at thermal oxidation (180°C) in air.

The decrease of oxygen absorption and CO_2 release (the main thermal oxidation product) was observed at *Irganox 1098/Irgafos 168* or $CuSO_4$/*Irgafos 168/HALS 944* mixture injection.

Analysis of the results obtained show that PPA may not be processed and material with required operation parameters obtained without injection of any stabilizer.

Therefore, further investigations were targeted at comparison assessment of PPA inhibited oxidation in the operation temperature range of 150 - 200°C.

Thermal oxidation solid degradation (at the operation temperature) mostly proceeds on the surface and is limited by the oxygen access deep in the polymer matrix. As aged, PPA becomes yellow. The lower yellowing degree is observed for application of *HALS Chimassorb 944/Irganox B1171* and *Irganox B1171*/Zn acetate mixtures.

Stabilization of glass-filled composite materials derived from PPA

Compounding of the most effective glass-filled (glass fiber content 30 and 35%) thermostabilized PPA composites are the following:

Compounding 1: PPA-2 + 35% glass fiber + Cu acetate/KI (0.4%) + talcum (0.35%);

Compounding 2: PPA-2 + 35% glass fiber + Zn acetate (0.1%) + *Irgafos 168* (0.2%) + talcum (0.35%);

Compounding 3: PPA-2 + 35% glass fiber + Zn acetate (0.1%) + *Irgafos 168* (0.2%) + *HALS 944* (0.3%) + talcum (0.35%);

Compounding 4: PPA-2 + 35% glass fiber + *Irganox 1098* (0.2%) + *HALS 944* (0.3%) + talcum (0.35%);

Compounding 5: PPA-2 + 35% glass fiber + *Irganox 1098* (0.2%) + *Irgafos 168* (0.2%) + talcum (0.35%);

Compounding 6: PPA-1 + 30% glass fiber + $CuSO_4$ (0.1%) + *Irganox 1098* (0.1%) + *Irgafos 126* (0.1%) + talcum (0.35%);

Compounding 7: PPA-1 + 30% glass fiber + Na hypophosphite (0.2%) + *HALS 944* (0.3%) + talcum (0.35%).

As described in Chapter 2, the solid-phase oxidation is developed from the surface with oxygen penetration inside the sample. Table 37 shows assessments of oxidized layer thickness at application of various stabilization systems.

Table 37

The change in oxidized layer during aging at 175°C of glass-filled stabilized PPA-1 and PPA-2 samples

Composite/time (h)	Layer thickness (mm) and appearance		Total oxidation layer
	Surface layer	Intermediate layer	
1. Cu^{2+}/I^- (0.4%):			
120	0.15, strong	-	0.15
288	0.15, strong	-	0.15
500	0.13, friable	0.14, friable	0.27
2. Zn acetate (0.1%) + *Irgafos 168* (0.2%)			
120	0.05, strong	0.1, strong	0.15
288	0.07, strong	0.1, friable	0.17
500	0.1, friable	0.1, friable	0.2
3. Zn acetate (0.1%) + *Irgafos 168* (0.2%) + *HALS 944* (0.3%)	0,04, strong	0.06, strong	0.1
120	0,13, strong	-	0.13
288	0,13, friable	-	0.13
500			
4. *Irganox 1098* (0.2%) + *HALS 944* (0.3%)			
120	0.13, friable	-	0.13
288	0.18, friable	-	0.18
500	0.18, friable	-	0.18

5. *Irganox 1098* (0.2%) + *HALS 944* + *Irgafos 168* (0.2%)			
120	0.13, friable	-	0.13
288	0.18, friable	-	0.18
500	0.05, friable	0.15, friable	0.20
6. $CuSO_4$ (0.1%) + *Irgafos 126* (0.1%) + *Irganox 1098* (0/1%)			
120	0.15, strong	-	0.15
288	0.18, strong	-	0.18
500	0.05, friable	0.15, strong	0.20
7. Na hypophosphite (0.2%) + *HALS 944* (0.3%)			
120	0.14, strong	-	0.14
288	0.18, strong	-	0.18
500	0.05, friable	0.15, strong	0.20

The results obtained show that stabilizers affect both formation of the initial polymer material morphology and its change during aging. It should be noted that at thermal oxidation of compoundings stabilized by metal compounds, specifically by copper compounds, a rigid film is formed on the sample surface (samples become dark quickly), which loosens with exposure. As phenol antioxidants (SHP or HALS) are used, this rigid film is not formed, and the sample color becomes darker (from light yellow to brown and, finally, black) much slower.

It is known [3 – 7, 13, 166, 167] that yellowing is associated with formation of conjugated structures, carbonyl groups, and quinoid-type structures in the polymer. The MIIR method was used in the study of the sample surface structure. New absorption bands at 1700 cm^{-1} (C=O group oscillations) and 1400 cm^{-1} occur in spectra already 100 h after the aging beginning. After 3,000 h more bands at 2750 – 2500 and 1950 cm^{-1} (H-substitutions of aromatic nuclei) occur in the spectrum. Table 38 shows calculation results for optical density relation of newly occurring absorption bands to the absorption band of CH_2-group oscillations at 2960 cm^{-1}.

Table 38

The relation of optical densities in IR-spectra

Compounding	Exposure, h					
	D_{1720}/D_{2960}			D_{1400}/D_{2960}		
	100	1000	3000	100	1000	3000
175°C						
#1. Cu/I 0.4%	-	-	0.49	-	-	0.54
#2. Zn acetate (0.1%) + *Irgafos 168* (0.2%)	0.29	0.77	0.7	0.53	0.97	1.09
#3 *Irganox 1098* (0.2%) + *Irgafos 168* (0.2%) + *HALS 944* (0.3%)	0.34	0.99	1.54	0.67	1.03	1.00
#4 *Irganox 1098* (0.2%) + *HALS 944* (0.3%)	0.43	0.78	159	0.76	0.8	1.21
#5 Na hypophosphite (0.2%) + *HALS 944* (0.3%)	-	1.03	1.74	-	0.87	1.09
200°C						
#1	0.3	0.66		0.5	0.66	-
#2	0.3	0.69		0.68	1.24	-
#3	0.37	1.3		0.53	1.24	-
#4	0.48	0.69		0.7	0.74	-
#5	0.35	1.03		0.51	0.9	-

Of importance is the observation of changes in the structure of surface layers in different compoundings. In case of compounding 1 and 6 aging, already at initial stages a rigid film was formed on the sample surface, which loosens with exposure to aging. Compounding 1 and 6 composites becomes yellow quicker: at 150°C coloring approaches the "absolute black body" after 2000 h exposure, at 175°C – after 1000 h, and at 200°C – already by 500^{th} hour of aging. In other compoundings, coloring becomes darker at lower rate, and the surface layer becomes friable. The results obtained show the highest efficiency for complexes with transition metal compounds, specifically Cu, in the composition. Possible mechanisms of transition metal compounds were discussed before [166, 175] and will be discussed in more detail here a bit later.

In the above-shown experiment with PPA, apparently, the ability of copper to complex formation is displayed. Macrochain crosslinking results in formation of a dense structure preventing oxygen access inside the polymeric matrix. In other compoundings containing no transition metal compounds, crosslinking reactions were not observed on the sample surface: oxygen gradually, layer by layer, destroys the polymeric matrix that makes the sample friable by the surface. MMD of the layers were studied by the GPC technique. For compoundings containing no copper compounds, it is shown that if degradation processes mostly proceed in the surface layer, accompanied by gradual, though insignificant molecular mass decrease, then macrochain branching processes dominate in the intermediate layer. Compoundings 4 and 6 contain only traditional additives: aminophenol, phosphite and polymeric *HALS*. Phenol antioxidant reacts with free radicals, and prosphite destroys hydroperoxides. *HALS* was injected in order to "extinguish" electron-excited molecules.

The structure of three compoundings of glass-filled PPA-2 differing by stabilization systems, were studied by the mercury porosimetry technique. Physicomechanical properties of the materials prior to aging are shown in Table 39.

According to Hg porosimetry data, more dense structure is formed in the compounding with Na hypophosphite. It possesses surface pores of $2.917 \cdot 10^2$ Å. In compoundings with Cu/I and Na hypophosphite + *HALS 944* larger surface pores were detected: $(5.698 - 6.267) \cdot 10^2$ Å. The compoundings also differ by the pore shape, which is indicated by the amount of Hg remained in the composition after pressure relief. It is believed that if Hg flows off the sample completely, the pores are of "proper", cylindrical shape, whereas if some

Table 39

Physicomechanical characteristics of stabilized glass-filled PPA-2

Stabilization compounding: As a nucleating agent, 0.5% low-dispersion talcum powder was injected, the filler is 35% glass fiber	Tensile strength, MPa	Relative elongation, %	Statistical treatment data		
			Max/min strength values	Standard deviation	Variation coefficient
Cu/I stabilizer	207.0	4.5	193.3/211.9	6.87	1.2
Na-hypophosphite	177.4	3.7	163.0/193.8	10.37	2.0
Na-hypophosphite, *HALS 944*	192.8	3.8	174.5/206.7	11.2	2.0

Table 40

Color change, mass loss and oxidized layer thickness at aging of glass-filled, stabilized PPA-2 compoundings

Compounding	*YI* before aging	1000 h			2000 h		
		YI	Δm,%	*h*, μm	*YI*	Δm,%	*h*, μm
Cu/I stabilizer	5.752	90.28	0.217	40	-511*	0.242	45
Na-hypophosphite	1.105	11.25	0.177	30	48.58	0.817	32
Na-hypophosphite *Chimassorb 944*	7.199	9.90	0.112	15	13.63	0.501	20

* This *YI* value is determined for absolutely black body.

amount of Hg remains in the sample, it has pores of "improper" shape, for example, a bottle-like one [253]. In this case, it is assumed that Hg is pressed to a thing "bottle neck", and at pressure relief it poured out incompletely through a narrow mouth. The most proper pore shape was detected for the compounding with Na hypophosphite, where residual Hg pressure equaled 3.5% versus 6.29 and 15.02% in compoundings with Cu/I and Na hypophosphite/*HALS 944*, respectively. In the heat aging during 2000 h at 175°C, the following parameters were detected: mass loss of the samples (Δm), yellowing index (*YI*) change, total thickness of oxidized layer (h) (Table 40), changes in physicomechanical properties and structure density (Table 41).

Sample density changes differently during aging.

In the compounding with Cu/I, kinetic dependencies of maximal pore volume and square on aging time are almost linear: maximal volume and square of pores decreases with exposure increase (Figure 88). In the compounding with Na-hypophosphite, these curves are of the extreme type (Figure 88), e.g. loosening of surface layers is observed at the initial stages of aging, and then some increase of the structure density. Note also that at 2000 h exposure samples are already somewhat friable, and layers are quite loose. In the compounding with Na-hypophosphite and *HALS 994*, the dependence of pore maximal volume has a maximum at practically linear increase of maximal porosity (Figure 88). Hence, a change of pore shape is also observed: in compoundings with Cu/I and a mixture of Na-hypophosphite and *HALS 944* pores become almost cylindrical with the exposure increase, which is testified by almost complete Hg drain. Vice versa, in the compounding with Na-hypophosphite pores are deformed, and the amount of Hg remaining in the samples after 1000 and 2000 h of aging equals 16.49 and 21.18%, respectively. Of importance is that current observations display the effect of the stabilizer type, its chemical structure and, as a consequence, the action mechanism on the physical structure formation of the composite. E.g. we observe a relation between chemical reactions and morphology of polymeric composites. The change of composite morphology is directly related to the change of physicomechanical properties (Tables 41 and 42). This problem has not yet been comprehensively discussed in the literature and remains practically uncovered still.

Table 41

Tensile strength change during aging of glass-reinforced, stabilized PPA-2 compoundings

Compounding	1000 h			2000 h		
	Tensile strength, MPa	Relative elongation, %	Strength preservation, % of initial	Tensile strength, MPa	Relative elongation, %	Strength preservation, % of initial
Cu/I stabilizer	172.5	3.5	83.3	170.1	3.1	82.17
Na-hypophosphite	136.5	3.0	76.9	121.3	2.5	68.38
Na-hypophosphite/ *Chimassorb 944*	156.0	3.3	80.9	125.6	2.4	65.15

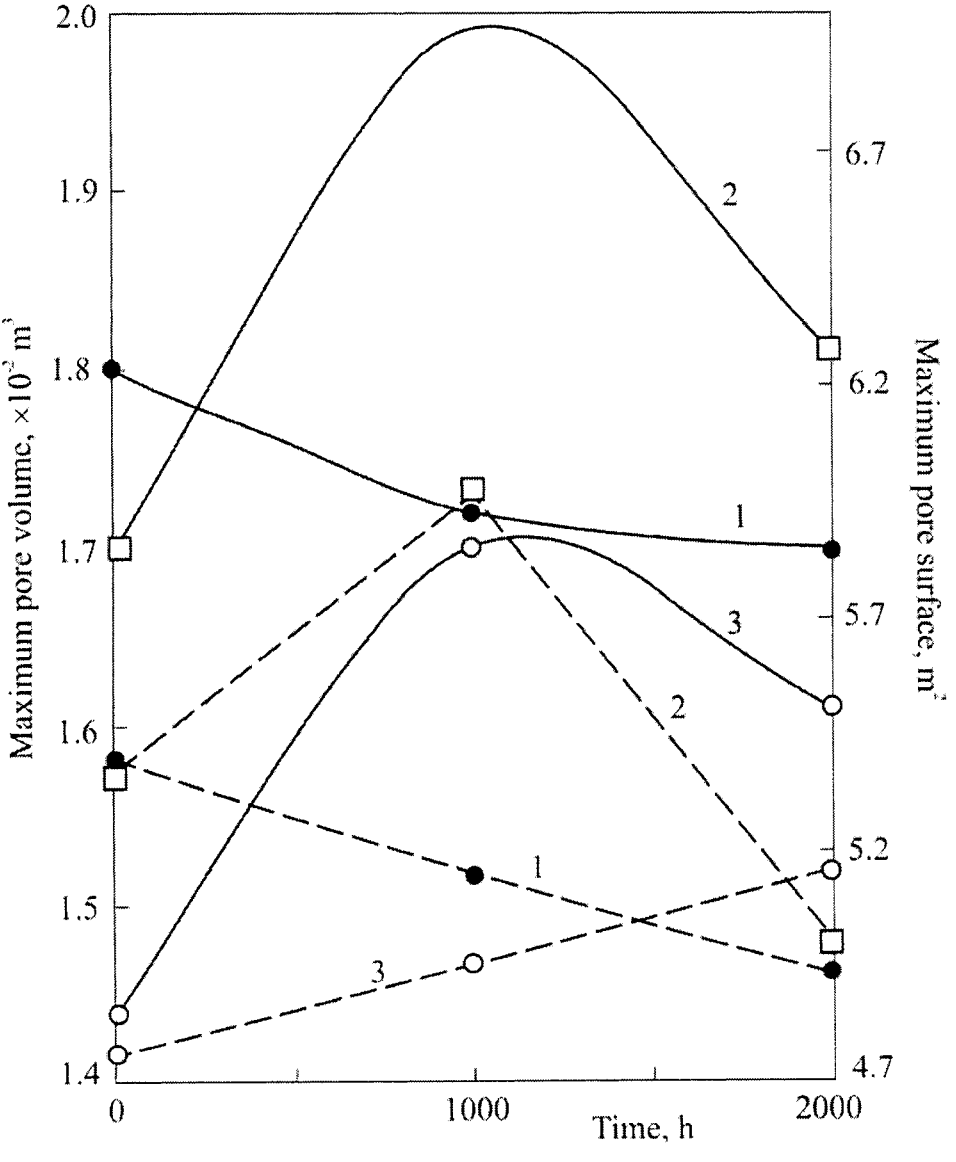

Figure 88. Kinetic curves of pore maximal volume (1 - 3) and maximal surface (1' – 3') change for PPA samples, stabilized by Cu/I (1, 1'), Na-hypophosphite (2, 2') and Na-hypophosphite/*Chimassorb 944* (3, 3') during aging at 175°C

Table 42

The change of physicomechanical properties of glass-reinforced PPA-2 (after 5000 h of aging)

Temperature/ compounding	Tensile stress, MPa	Preserved strength, % of initial	Elongation, %	Preserved elongation, % of initial	Bending strength, MPa	Preserved strength, % of initial	Blow viscosity, kJ/m^2	Preserved blow viscosity, % of initial
Prior to aging								
#1 Cu/I 0.4%	**207**	-	**2.85**	-	**278**	-	**57.4**	-
#2 Zn acetate 0.1%+Irgafos 168 0.2%	**191**	-	**2.95**	-	**253**	-	**52.8**	-
#3 Irganox 1098 0.2%+HALS 944 0.3%	**181**	-	**2.85**	-	**256**	-	**55.9**	-
#4 Irganox 1098 0.2%+Irgafos 168 0.2%+HALS 944 0.3%	**207**	-	**3.05**	-	**278**	-	**52.1**	-
#5 Na hypophosphiote 0.2%+HALS944 0.3%	**193**	-	**2.85**	-	**281**	-	**63.1**	-
150°C								
#1	138	69.9	2.5	87.7	200	71.9	26.2	45.6
#2	137	71.7	2.65	93.0	143	56.5	28.6	54.2
#3	127	67.9	2.7	98.0	124	48.4	27.2	48.7

#4	139	67.1	2.8	90.3	156	56.1	23.8	45.7
#5	149	80.1	2.85	99.1	148	52.7	31.1	49.3
175°C								
#1 Cu/l 0.4%	140	67.0	2.5	87.7	183	65.8	25.4	44.2
#2 Zn acetate 0.1%+Irgafos 168 0.2%	115	60.2	2.65	93.0	130	51.4	27.3	51.7
#3 Irganox 1098 0.2%+HALS 944 0.3%	116	62.0	2.5	95.0	135	52.7	26.0	46.5
#4 Irganox 1098 0.2%+Irgafos 168 0.2%+HALS 944 0.3%	129	62.3	2.65	85.5	125	45.0	24.9	47.8
#5 Na hypophosphite 0.2%+HALS 944 0.3%	141	75.8	2.75	98.2	144	51.2	31.0	49.1
200°C								
#1	85	50.2	1.6	56.1	98	35.3	8.4	14.6
#2	91	47.6	2.1	73.7	70	27.7	10.0	18.9
#3	103	55.1	1.95	75.0	76	29.7	9.6	17.1
#4	98	47.3	1.90	61.2	72	25.8	8.4	16.1
#5	105	56.5	2.2	81.5	86	30.6	13.6	21.6

Current investigations allow optimization of PPA stabilization compounding as a mixture of copper compounds with phosphorus-containing antioxidant and phenol or HALS. The use of such compounding causes the following effects:

- PPA processing becomes easier due to the melt index increase;
- The obtained polymer possesses higher physicomechanical properties;
- Strength properties are preserved at quite high level during aging in the temperature range of 150 - 200°C.

Glass-filled composite materials derived from poly(alkane imide)

Thermal stabilization of fatty-aromatic polyimides at operation temperatures with the help of additives is suggested in patents [38, 53] on materials derived from PAI. The use of transition metal compounds as additives to PAI, to some extent based on the analogy to aliphatic PA, is not confirmed in the literature, i.e. it falls apart from traditional antioxidant stabilization and, therefore, requires additional study.

As shown above, thermal oxidation of PAI at moderate temperatures, close to the operation range, possesses some signs of usual radical-chain process with branchings on hydroperoxides. After the specific act of initiation, thermal oxidation continues developing in fatty chain by the well-known radical-chain scheme with the known approaches to inhibition. Similar to additive screening in PPA, it is shown that classical antioxidants of phenol and amine types are not effective enough, though they slow down the low-temperature oxidation. Organic phosphites, both mixed with phenols and individual, are quite effective in hydroperoxide degradation reactions [110, p. 202]. However, by effectiveness in PAI all studied phosphites abate phosphate – diphenyl ether of anilidophosphoric acid (*BT5*), which is the high-temperature stabilizer for polyheteroarylenes [35]. As used in quite high concentrations (up to 2 wt.%), *BT5* effectively inhibits O_2 absorption (more than two-fold) during PAI oxidation in the solid phase and in melt. Antioxidant action of *BT5* is displayed in elimination of exothermal peak on the DTA curve. A mixture of *BT5* with phenol antioxidant gives a synergic effect for solid-phase oxidation of PAI. This blend possesses the highest stabilizing activity among all organic additives to PAI: the initial rate of O_2 absorption is more than 3-fold reduced. The action of

Table 43

PAI-S-EK-1 properties

Sample	Maximum squeezing effort, kgf	*MFI*, g/10 min, at 10 kg load		Physicomechanical properties		Dielectric properties	
		10 min	30 min	Blow viscosity, kJ/m^2	Tensile strength, MPa	Dielectric constant at 10^6 Hz	Breakdown voltage, kV/mm
Without additives	40-45	10.0	Cross-linking	13.0	85.5	3.2	24.5
$CuSO_4$ (0.1%) + *BT5* (2%)	18-20	10.7	9.5	20.0	93.5	3.4	24.9
Irganox 1010 (0.2%) + *Stafor 11* (0.5%)	36-39	24.2	23.3	19.0	92.0	3.4	28.3
$CuSO_4$ (0.1%) + *BT5* (2%) + *HALS 944* (0.2%)	18-20	15.3	14.4	22.0	95.0	3.4	25.7

BT5 and other PCA in heat resistant polymers will be discussed below. Similar to PPA, good thermostabilizing efficiency in PAI is displayed by transition metal compounds, specifically, mixed with PCA.

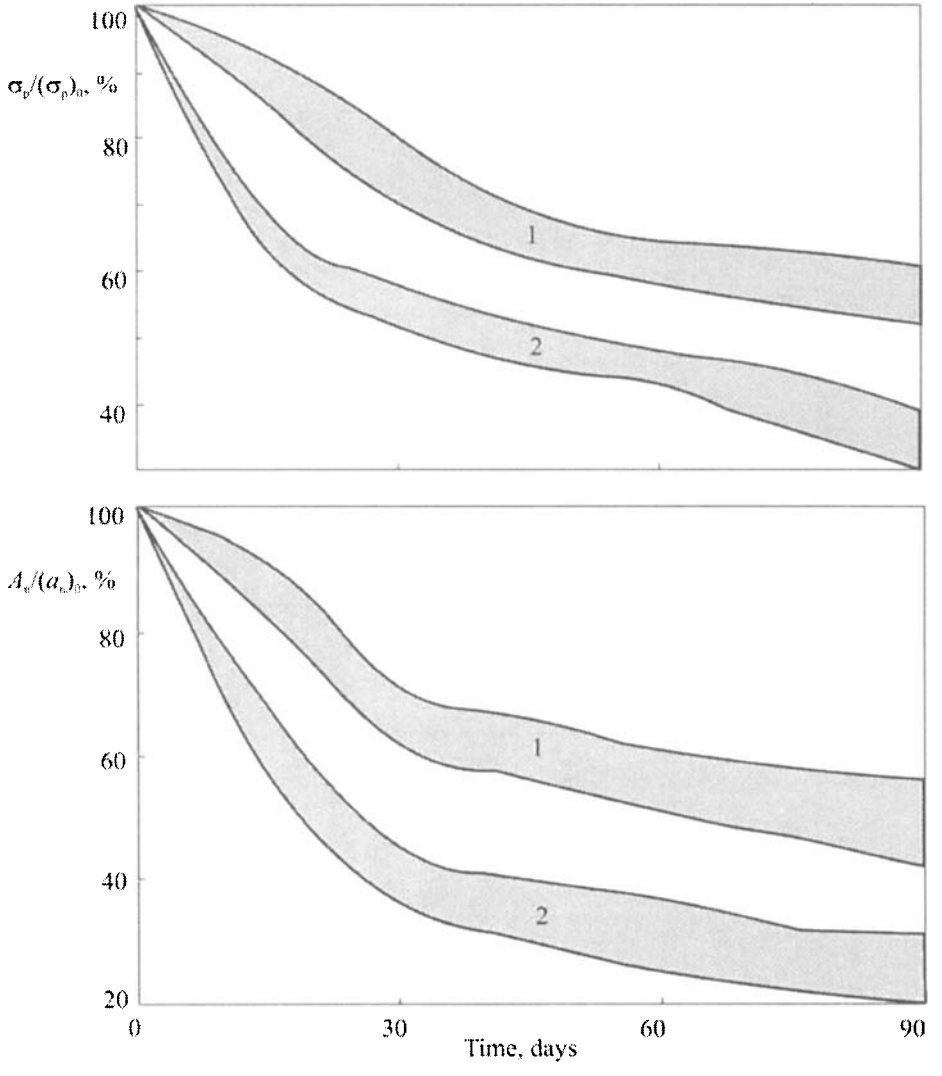

Figure 89. Relative changes of strength (a) and blow viscosity (b) of stabilized (1) and nonstabilized (2) PAI-S-EK during heat aging in air at 200°C

The difficulty in PAI processing is associated with branching and crosslinking processes, intensively proceeding at high temperature. Under real conditions without stabilization, total presence of the material in melt during 30 min (total effect of extrusion and molding of articles) may cause full crosslinking. Table 43 shows properties of stabilized and nonstabilized composite, glass-filled PAI.

At long-term thermal aging in air in the temperature range of 200 - 250°C, stabilized materials preserve higher strength properties longer than nonstabilized ones (Figure 89). Therefore, effective thermostabilizing systems were determined, which improve quality of composite materials derived from PAI simultaneously with endurance of the articles.

On the mechanism of transition metal compounds

Inorganic and organic alternate valence metal salts and their complexes inhibit O_2 absorption and mass loss in PAI at heating in the presence of O_2 at high temperature (for example, Figure 90). Under these conditions, non-transition metal compounds are inert. The effect of 0.05 – 1.0 wt.% additions of transition metal compounds on PAI thermal oxidation is also traced by heat patterns as full elimination of exothermal DTA peak corresponded to oxidation. The origin of this peak is discussed in detail in the previous Section. The gross effect of molecular-mass characteristic stabilization in PAI under conditions that simulate processing may be assessed using the melt flow index (*MFI*). This parameter is more stable in the presence of additives and shows no tendency of the polymer to crosslinking, which is specifically typical of PAI and makes the processing more difficult (Figure 91). In case, if an additive is colorless, stabilization is observed by PAI yellowing decrease after tests in IIRT device.

Addition of transition metal compounds reduces the rate of carbon oxides and heavy product release during PAI thermal oxidation (Figure 92), and, as shown by IR-spectra, increase of C=O and OH-group contents in the polymer residue. Stabilizing activity of additives is preserved after simulation of PAI processing and manifests itself in mass loss and O_2 absorption kinetics during accelerated thermal oxidation.

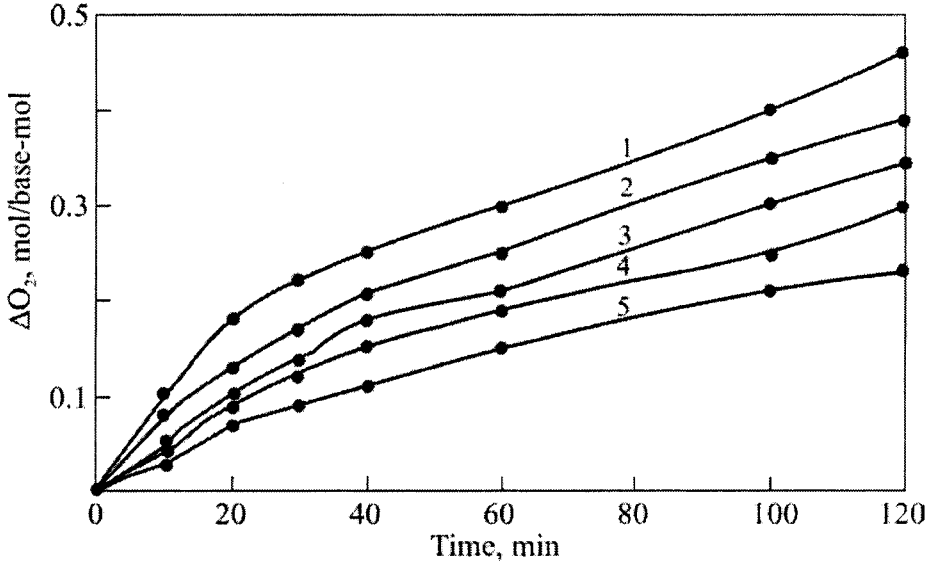

Figure 90. Kinetic curves of O_2 absorption by pure PAI (1) and PAI stabilized by 0.05 wt.% $CoCl_2$ (2), $FeSO_4$ (3) *MKS-21* (4), and copper acetate (5) ($T = 250°C$; $P(O_2) = 266.6$ kPa)

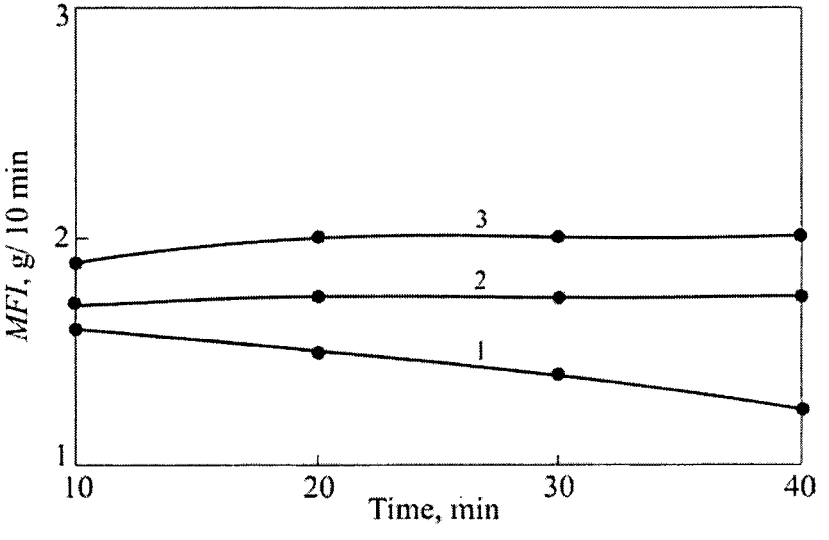

Figure 91. *MFI* change for PAI at 320°C: initial (1) and stabilized by 0.05 wt.% $FeSO_4$ (2) and copper acetate (3)

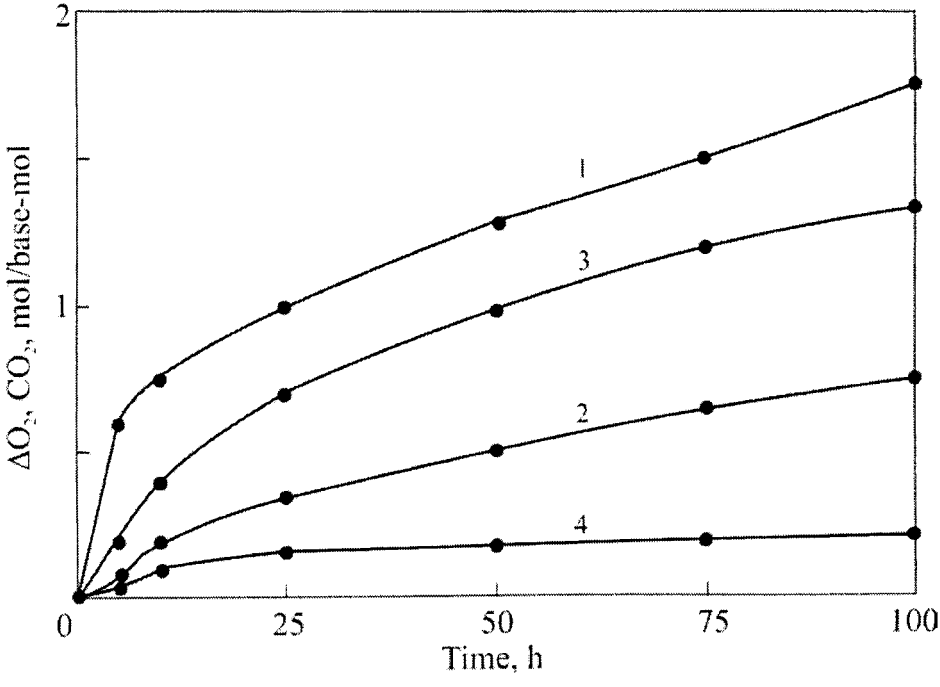

Figure 92. Oxygen absorption (1, 3) and CO_2 release (2, 4) in thermal oxidation of PAI: initial (1, 2) and $CuSO_4$ (0.05 wt.%) stabilized (3, 4); T = 200°C, in air

Generally, transition metal compounds display clear antioxidant effect, inhibiting PAI degradation in the whole processing and operation temperature range. Usually, inorganic salts are less effective than organic salts. The effect of cation on organic salt effectiveness is traced on the example of bivalent copper, nickel, chromium and tin diphenylphosphonium salts. As shown by mass loss (Figure 93) and O_2 absorption (Figure 94), the additive effectiveness reduces in the sequence as follows:

$$Cu^{2+} > Ni^{2+} > Co^{2+} > Cr^{2+} > Sn^{2+}.$$

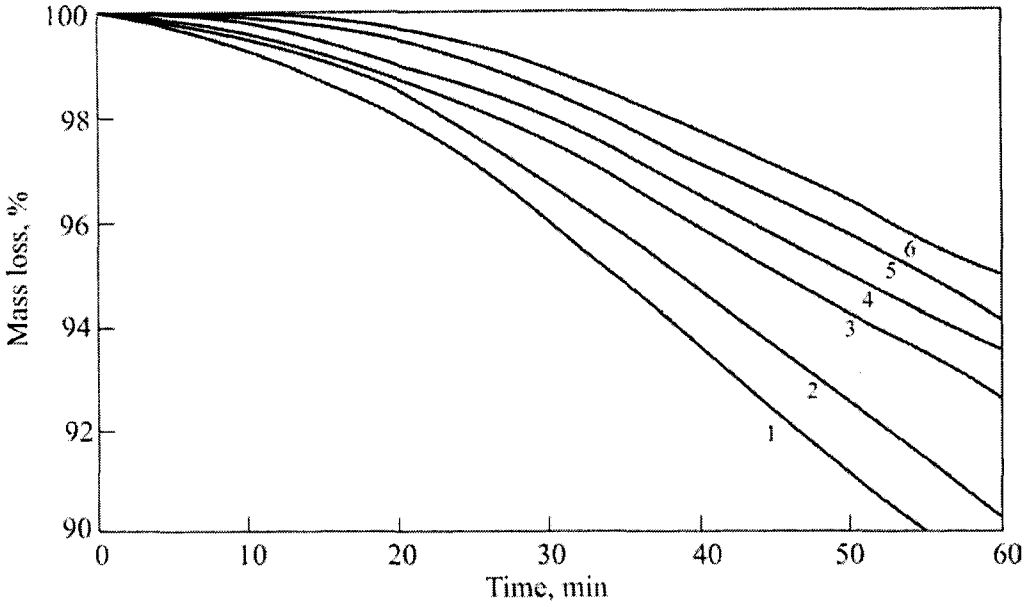

Figure 93. TGA patterns for PAI: pure (1) and stabilized by 0.05 wt.% portions of Sn-X (2), Cr-X (3), Co-X (4), Ni-X (5), and Cu-X (6), where X is diphenylphosphonic acid residue; $T = 350°C$, in air

Similar sequence may be composed for metal phthalocyanines. The effectiveness of additives also depends on the valence state of metal. As shown on the example of copper, metals in the highest valence state are more effective, e.g. $C^{2+} > Cu^{+}$. The effectiveness sequences of transition metal additives generally correlate with the sequence of their electronegativity values [159]: Cu^{+2} – 2.1; Cu^{+} - 1.8; Ni^{+2} – 1.9; Co^{+2} – 1.9; Cr^{+2} – 1.6; Sn^{+2} – 1.6, which is reverse to the sequence of effective ion and covalent radii. For example, covalent radii increase in the sequence from Cu^{+2} (1.25) to Sn^{+2} (1.4). The effect of anion on the additive effectiveness is relatively low, and no regularities (acetate, sulfate, silicate) are observed in it (acetate, sulfate, silicate), except for anions with suggested self reactivity in degradation reactions. For example, *MFI* data show that Ni^{+2} salt effectiveness changes in the following sequence:

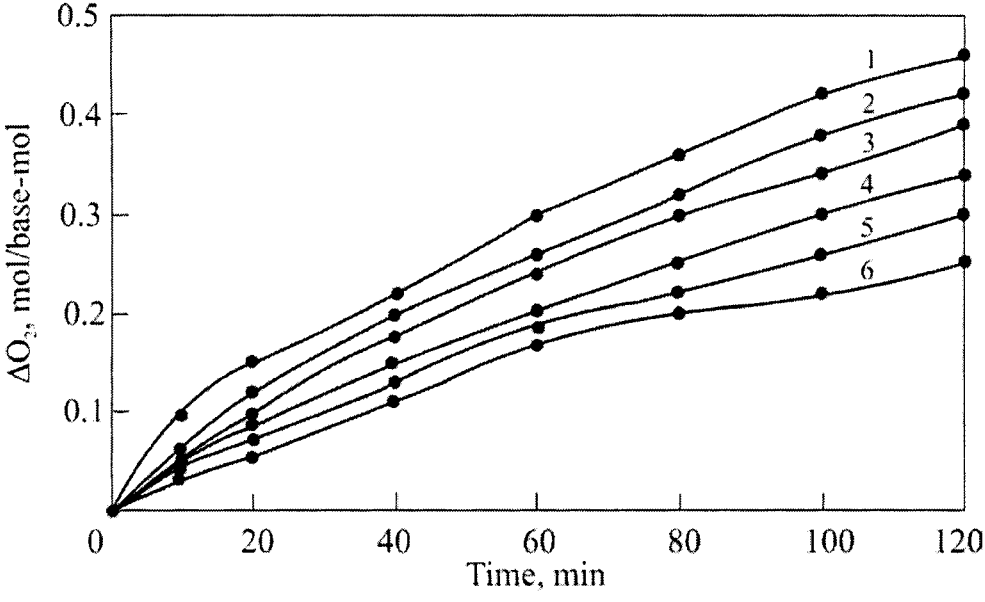

Figure 94. Oxygen absorption kinetics for PAI: pure (1) and added by 0.05 wt.% portions of Sn-X (2), Cr-X (3), Co-X (4), Ni-X (5), and Cu-X (6), where X is diphenylphosphonic acid residue; $T = 250°C$, $P(O_2) = 266.6$ kPa

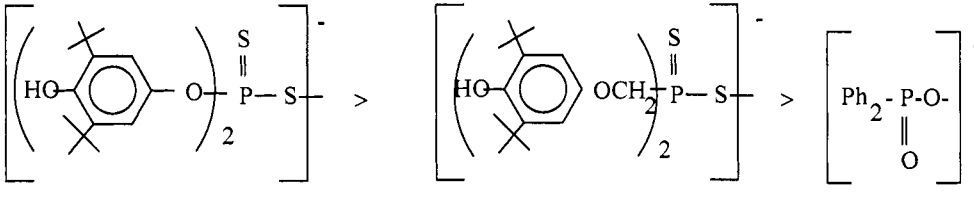

whereas mass losses at 350°C indicate equal average effectiveness for all three additives, despite the presence of a hindered phenol fragment in two of them. Nevertheless, a combination of elements in the mentioned phosphonic and dithiophosphonic acids provide for self stabilizing activity, displayed in O_2 absorption and mass loss of both acids themselves and their salts of non-transition (inactive) metals, zinc, for example.

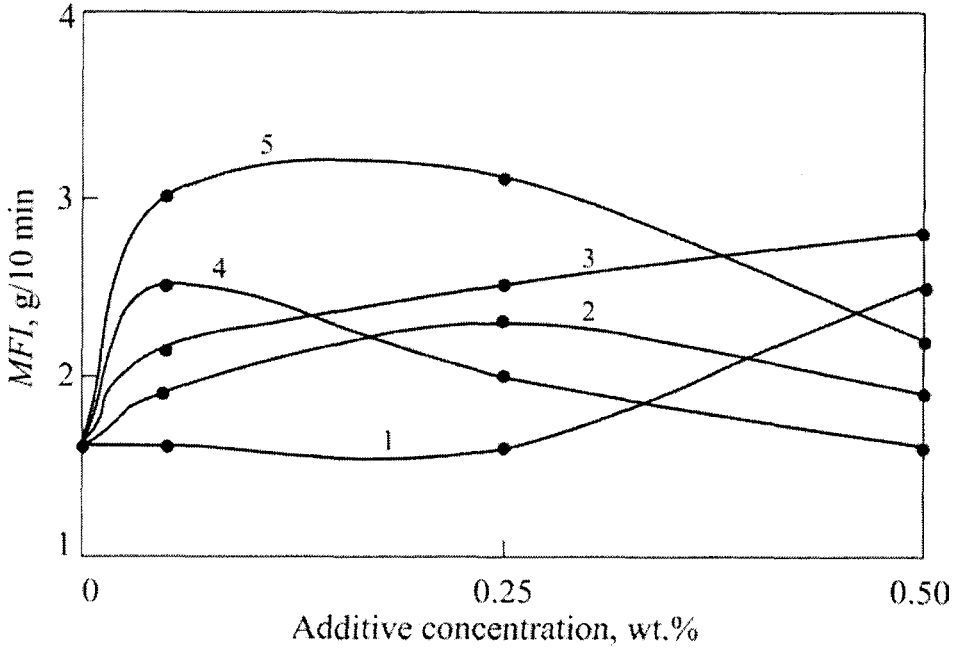

Figure 95. Concentration dependence of diphenylphosphonic acid salts (X) additions on $MFI_{10\ min}$ for: Sn-X (1), Co-X (2), Cr-X (3), Ni-X (4), and Cu-X (5)

The presence of additions of phosphorus or combinations of phosphorus with sulfur, shaped as salts, acids or even sulfides, in the structure causes an original placticizing effect on PAI, *MFI* of which increases by 50 – 500% and reaches (for example, in the case of Ni dithiophosphate addition) 8 g/10 min, whereas *MFI* of pure PAI equals 1.62 g/10 min. However, the whole stabilizing effect and its universality for different temperature ranges is only realized in phosphorus (or phosphorus and sulfur) combination with alternate valence metals, shaped as compounds and, apparently, admixtures.

Concentration dependencies of the additive stabilization effect possess peaks at 0.001 – 0.005 g-atom/base-mol cation content in PAI (Figures 95 and 96).

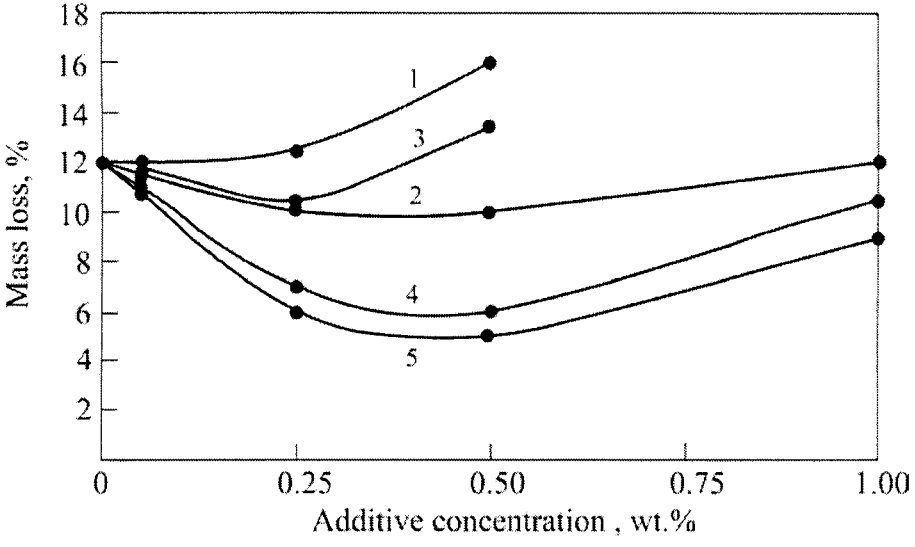

Figure 96. Concentration dependence of diphenylphosphonic acid salts (X) additions on mass losses in PAI with additions: Sn-X (1), Co-X (2), Cr-X (3), Ni-X (4), and Cu-X (5); T = 350°C, in air

Therefore, additions of transition metals display the antioxidant activity in PAI in concentrations approximately equal one metal ion per one macromolecule. Stabilizing efficiency of metal ions in PAI correlates with their electronegativity, ionic and covalent radii, soft-hard interaction type [160], i.e. the complex forming parameters of these ions.

As mentioned in the literature, transition metals may form complexes with polypyromellitamido acids (PAA) as a stage of obtaining metal-containing polyimides, which are polymers with specific properties [161]. In particular, solid-phase complex formation between PAA and disperse transitions metals (Cu, Fe, Ni, Co) is detected in the X-ray analysis by elimination of the metal phase [162]. Using the ESR method, changes in the polymeric complex ($PAA{\cdot}Cu^{+2}$) were traced. These changes happen at PAA heating up and its transformation to polyimide. Simultaneously, Cu^{+2} is restored to Cu^{+} or even to pure metal [161]. Besides existence of the complex, changes in ESR spectra with respect to copper compound concentration indicate the existence of exchange copper clusters. It is believed [161] that the polymer complex is formed due to ionic exchange by ligands and valent bond formation between

copper and PAA acid groups. Hence, the complex is thermally decomposed and, therefore, polyimide contains metal and metal oxides heterophase.

A suggestion about complex formation is also confirmed by the following reasons. The well-known is the problem of deactivation of transition metal admixtures, specifically copper, in polyolefin materials used in production of cable insulation [21]. Admixtures abruptly decrease thermal and weather resistance of polyolefins. Thermal stability and weather resistance of polyolefins, especially polypropylene, are increased by adding up to 0.5 wt.% chelating agents, therefore, the thermal stabilization effect correlates with the stability constant of forming copper complex, for example, by the induction period of O_2 absorption [163]. Among copper deactivators, aromatic amides and imides are the strongest. Marketable deactivators, produced by Van-der-Bilt, Monsanto, and American Cyanamide companies, contain mentioned groups in their structure [163]. Thus, the current question appears somewhat turned inside out but, nevertheless, the complex formation is quite strictly proved. It is believed that a complex is formed during processing, e.g. it resists high temperatures up to 240°C (polypropylene extrusion, for example).

The PAI-copper compound system (or a model) was studied by ESR and magnetic susceptibility methods. The model – didodecylpyromellitimide has no ESR signal, and another model – Dodecane diphathalimide and PAI, is paramagnetic and display singlets with $g_{av} = 2.183$.

The effective thermal stabilizer of PAI, which is $CuSO_4$, is characterized by the effective signal of mixed shape (Figure 97) with $g_n = 2.077$ and $g_l = 2.27$. This indicates the presence of crystal-hydrate water in the additive ($CuSO_4 \cdot nH_2O$). The signal intensity, its shape and value are preserved in the additive subject to thermal processing in air at 300°C. Thermal processing in vacuum and, apparently, crystal-hydrate decomposition change the signal shape, which now represents a wide distorted singlet with $g_{ave} = 2.208$. Mechanical mixing of PAI or models with $CuSO_4$ specifically changes the copper signal shape (Figure 97). Thermal processing of PAI or models mixtures with $CuSO_4$ at 300°C in air most abruptly reduces the intensity (down to its absolute absence). Note that analogous thermal processing of $CuSO_4$ without PAI causes no changes in spectra, e.g. Cu^{+2} is spent in thermally oxidizing PAI.

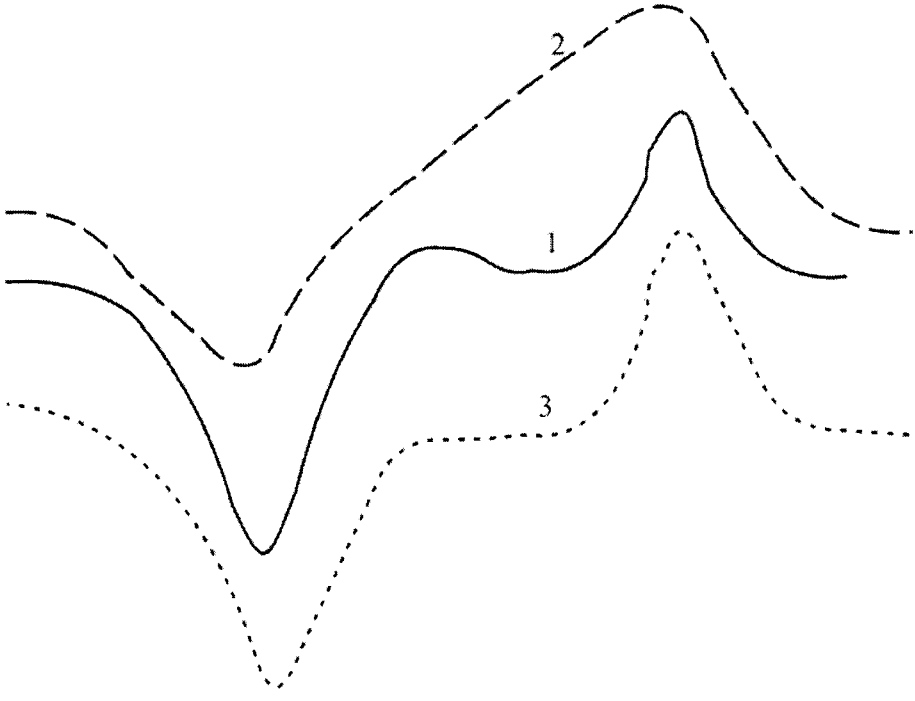

Figure 97. ESR spectra for $CuSO_4$ before (1) and after (2) thermal treatment (T = 320°C, 30 min, in vacuum) and $CuSO_4$ mixture with dodecamethylene diphthalimide (3)

Magnetic susceptibility measurements performed by the Faraday relative method on the device, constructed by specialists of IONCh, AS USSR, indicated paramagnetic properties of PAI. Hence, the effective magnetic moment, μ_{eff}, equals 0.77 – 0.94 B.M. (Bor magneton) at 287 K. As temperature decreased to 79 K, the value monotonously decreased to 0.39 - 0.63 M.B. (the whole massif of serial and laboratory samples was analyzed). Such behavior is typical of the so-called cluster states, in which paramagnetic centers realize exchange interactions, described by the Haisenberg-Dirac-Van Flick Hamiltonian (the HDVF model):

$$H = -2\sum_{i,j} J_{ij} S_i S_j ,$$

where S_i and S_j are spin operators; J_{ij} are exchange parameters. Computer calculation of exchange parameters by dimer, trimer and polymer cluster software [164] shows that magnetic susceptibility of PAI is described well within the framework of HDVF antiferromagnetic linear model with the exchange parameter J_{ij} = 226 cm^{-1}, which corresponds to high conjugation degree, usually, along the polymeric chain by the π-system or between chains, for example, by defect structures. Chemical structure of PAI, in which pyromellitic fragments are separated by long methylene chains, does not provide such type of conjugation. The unique possibility to realize conjugation is formation of intramolecular (A) or intermolecular (B) complexes:

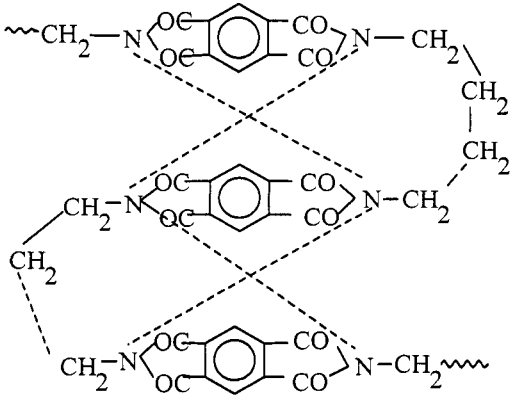

A

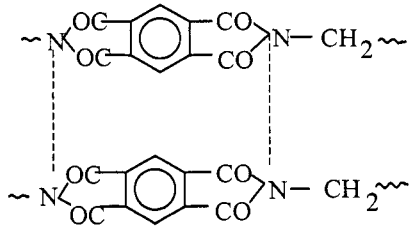

B

Intramolecular conjugation similar to complex A, may be hardly realized for PAI, because in this case, the distance between conjugation centers must not exceed 4 Å, and the identity period for PAI (X-ray analysis data) [47] equals 18 Å, which is much above the maximum value [164]. At thermal processing of PAI in air at 320°C, the its magnetic behavior does not generally change, however, exchange parameters decrease to -110 and -150 cm^{-1}, respectively, that may happen with the conjugation decrease. As a result of thermal processing at 320°C during 0.5 h and even in the presence of oxygen, degradation changes in PAI are insignificant. X-ray structural analysis data [47] testify that the initial powder-like PAI, synthesized in solution, is characterized by methylene-chain convolved conformation of macrochains. As annealed at temperatures 10 - 15°C below the melting point, the period along PAI chain axis changes jump-like, and convolved conformation changes to stretched one. This

is irreversible change – the reverse phase change is not observed. After phase transition, the initial monoclinic crystallite structure transforms to a new monoclinic structure of higher density, crystal density in which increases from 1.302 to 1.398 g/cm^3. Temperature dependence of PAI conformation correlates well with that of exchange interactions in PAI clusters. Since an increase of intermolecular interaction and, consequently, contribution increase of hypothetic intermolecular π-complexes into conjugation with the packing density might be expected, the experiment displays the inverse effect – it is desirable to interpret the conjugation decrease caused by thermal processing and associated stretching of macrochains as a result of intramolecular complex degradation. Thus, PAI is the example of yet unknown realization of polymer conjugation not by the chain, but in the cluster.

The study of copper sulfate magnetic susceptibility shows the island structure of this complex. The effective magnetic moment μ_{eff} equals 1.86 B.M. does not vary with temperature in the range of 78 – 291 K. Thermal processing of the additive without polymer at 320°C in air and in vacuum causes partial loss if combined water, and μ_{eff} value increases to 1.87 – 1.88 B.M. The values of μ_{eff} for initial and thermally processed sulfate are somewhat higher than μ_{eff} spin values (1.73 B.M.). It is typical of copper complexes and is explained by the contribution of spin-orbital component.

Magnetic susceptibility of non-reacting mechanical admixtures is the additive value, i.e. molar magnetic susceptibility of polymers with inclusion of any coordination compound equals:

$$\psi_{mix} = \alpha\psi_n + (1 - \alpha)\psi_c,$$

where ψ_n and ψ_c are molar susceptibilities of polymeric matrix and complex compound incorporated in this matrix; α is the molar part of the polymeric matrix. If the immediate surrounding of paramagnetic center is restructured chemically or even sterically, the additivity rule is disturbed. For equimolar mixtures of PAI and copper sulfate, the additivity rule is not observed: ψ_r values of initial complexes and the mixture equal 5.78×10^{-6}; 6.43×10^{-7} and 6.86×10^{-7}, respectively. Deviation from additivity is much clearer for thermal processed mixture, for example, magnetic susceptibility of the mixture, heated in air at 320°C during 0.5 h, equals 1.05×10^{-5}. This significantly exceeds the totality of parts of similarly processed copper sulfate and PAI: 8.78×10^{-6} and 1.46×10^{-6}, respectively. Thermal processing in any atmosphere leads to a significant increase of magnetic susceptibility and effective magnetic moment of PAI and

PAI mixtures with copper sulfate, and the effect is higher for thermal processing in air (Figure 98).

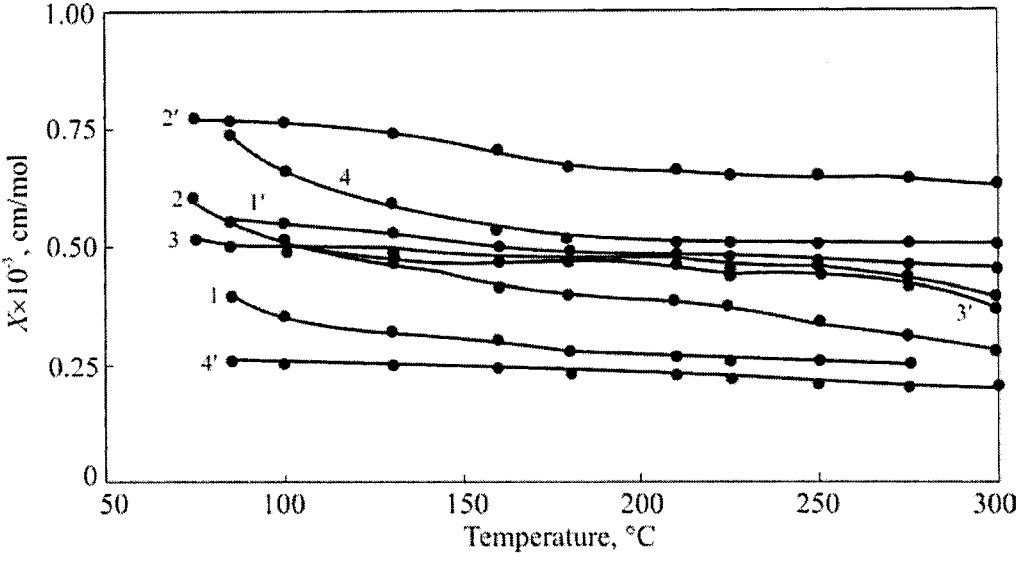

Figure 98. Changes in molar magnetic susceptibility (X) of samples before (1 – 4) and after (1' – 4') heating of pure PAI (1, 1'), PAI added by $CuSO_4$ (2, 2'), *BT-5* (3, 3'), and $CuSO_4$ and *BT-5* blend (4, 4')

Thus, studies of magnetic properties clearly indicate the interaction of PAI macromolecules and a transition metal compound even at mixing. This interaction restructures the coordination additive sphere, apparently, by means of the ligand exchange. At high temperatures, especially in the presence of oxygen, the system remains labile. As a result of all transformations, apparently, Cu^{+2} is reduced to Cu^{+}.

The reduced results of magnetic property study of the system and correlation of the stabilizing efficiency with electronegativity of additives do not counter the hypothesis of complex formation as the stabilization mechanism. If we base on the competition between the additive and O_2 in the complex formation with pyromellitic fragment structure elements, even at maximal coordination numbers 6 – 8 (unreal for PAI with respect to bulkiness of pyromellitic fragment, interlocking of all pyromellitic fragments requires 0.1 – 0.2 g-atom of metal/base-mol of additive. One may assume that thermal oxidation develops in the amorphous phase of the polymer only, and regular and

O_2 hardly accessible structures in the melt are preserved, and other, various assumptions can be made, but this mechanistic way does not allow approaching the empirical concentration of the additive to experimental optimal values (0.001 – 0.005 g-atom of metal/ base-mol) even by an order of magnitude. Therefore, the model of stabilization act must be replaced.

Two alternatives are possible:

- The first alternative represents an old idea [155] about chain inhibition in additive reaction with peroxy-radical, but with participation in the complex of peroxy oxygen and neighboring imide fragment of pyromellitimide residue simultaneously:

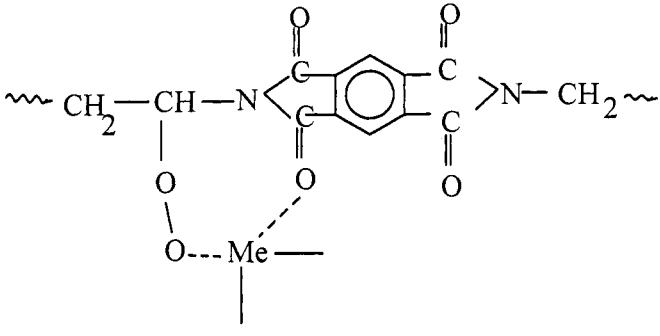

otherwise ineffectiveness, for example, of copper compounds at thermal oxidation of PE methylene chain at any temperatures may not be explained. For example, at 130°C the addition of 0.05 wt.% $CuSO_4$ almost two-fold speeds up oxygen absorption. Basically, such inhibition mechanism assumes low concentrations of additives. For example, classical antioxidant concentrations in hydrocarbon polymers by the order of magnitude correspond to effective concentrations of transition metal compounds in PAI. However, the mechanism of oxidation chain inhibition suggests sufficient migration ability of the additive and synchronization of complex formation with two ligands - peroxide oxygen and, for example, carbonyl group in the neighbor imide cycle. Two facts contradict to this condition. Firstly, inorganic salts insoluble and, consequently, non-migrating in the polymer are effective in PAI. Secondly, if an imide group plays the role of the partner-ligand, the first alternative about imide cycle interlocking by the complex formation, i.e. about high additive concentrations, becomes actual. Thus, the first version of the stabilization mechanism

insufficiently conforms to the experiment. Apparently, even if this mechanism is realized, it is not important for PAI stabilization.

- The second alternative suggests existence of any labile structures in PAI, at which thermal oxidation is initiated. The role of labile structures, or "defects", or variety of units in determination of polymer thermal stability is known well [165]. For example, common PE possesses much lower thermal oxidative stability compared with polymethylene due to the presence of unsaturated internal and end groups and branchings in macromolecules. Another known example is PVC, in which labile structures define both hydrochlorination and development of the thermal oxidation process [13]. In PAI, the polymer of the polycondensation type, labile structures are amidoacid units and, possibly, salt end groups [54].

The dependence of thermal oxidative stability on the end group origin was traced by O_2 absorption kinetics and mass loss in PAI, synthesized with 5% excess of diamine or dianhydride, or with addition of an interlocking agent – phthalic anhydride (Figures 92 and 93). Degradation transformations proceed more intensively in the sample, synthesized with diamine excess. High thermal stability was observed in PAI with pyromellitic dianhydride excess and added interlocking agent. Therefore, experimental concentration dependence of additive efficiency may be explained, if it is believed that complex forming action of transition metal additives is realized via deactivation of defect structures, which content in PAI equals several percents.

Generally, shortly studied phenomenon of thermal oxidation stabilization of amide polymers by transition metal compounds may not be unambiguously interpreted. The authors were lucky showing that the present stabilization method falls outside the framework of aliphatic polyamide class, for which it is already known, and may also be used for other polymers, for fatty-aromatic polymellitimide, in particular. Mechanical transfer of classical radical-chain oxidation scheme gives no explanation to some sufficient features of polyamide and polyimide thermal behavior and their thermal stabilization. Apparently, new models are required, which would include acts with participation of amide or imide groups. Studies of magnetic and paramagnetic properties indicate the interaction of transition metal additive with PAI, initiated already during mixing. Moreover, is degradation is intensive, this interaction is also intensified. Even at dry mixing and milling of absolutely diamagnetic polymer (PA-6) with a paramagnetic complex Cu^{+2} (compound *MKS-21*)

changes in ESR spectra are observed. These changes may only be caused by the interaction between amide groups and additives, must likely by the ligand exchange mechanism. Apparently, the complex formation (or the ligand exchange) of macromolecule or its fragment with transition metal additive is the necessary prerequisite for performance of the antioxidant action. The role of this reaction in the general mechanism of inhibited thermal oxidation may not yet be shown, though different models, mentioned above, for example, may be suggested: labile group interlocking, prevention of molecular complex formation with O_2, and, possibly, some new reactions with peroxy-radicals. This new area of stabilization (to be called high-temperature stabilization) requires further study and development, as well as the classical mechanism of hydrocarbon polymer inhibited oxidation. Studies of the latter were initiated in early 2000's and are intensively developed still.

On the mechanism of degradation transformations in heat-resistant heterochain polymers in the presence of stabilizers – phosphorus-containing compounds

Analysis of data from the literature and the authors' investigations indicate injection of phosphorus-containing additives (PCA) in polymers as the most perspective way of heat-resistant polymer thermal stabilization [26, 31, 32, 168, 169, 201-207, 211-216, 226, 254]. Tests of a wide PCA range in different polymer structures (aromatic and fatty-aromatic polyamides and polyimides, polyesterimides, polyamidoimides, polysulfones, liquid-crystal copolyesters, ets.) allowed selection of optimal thermostabilizing additives: aromatic esters and phosphorous and prosphoric esteramides. For pure aromatic polyimides, polyimidophenylquinoxalines and polybenzoxazoles, optimal concentrations are 3 wt.% PCA. At equal heat loads, properties of stabilized samples are 1.5 – 2.5 times higher compared with non-stabilized polymers. For aliphatic-aromatic polymers (bisphenol A-derived polysulfone and polyesterimide, polyalkane imide, and polyphthalimides), PCA optimal concentrations are two times lower: 0.3 – 1.0 wt.%. This is caused by lower temperature impacts during processing and operation of materials and articles.

To develop the idea of heat resistant polymer stabilization, one must understand the mechanism of PCA stabilizing action in them. Simultaneously with applied stabilization, some studies were performed before on the example of aromatic polyimides. The inhibiting action of PCA on oxidation branch of degradation and pre-polymer cyclization rate increase in PCA presence were

detected. It was also found that crosslinking processes are intensified on the initial stages of thermal oxidation.

Experimental data indicate a complex mechanism of PCA action in heat-resistant polymers, which includes inhibition of radical chain reactions and catalysis of cyclization and crosslinking processes.

The comparison data on kinetics of inhibited and non-inhibited oxidation of polypyromellitimide, PAI, PPA, PEI and PSF at high processing temperature and in solid oxidation show general tendencies. In both cases, kinetic curves of oxygen absorption and main oxidation products release (carbon oxides) may be conditionally divided into two stages: the initial stage obeying kinetic order one and the constant rate stage. Inhibition of thermal oxidation is observed at the first stage of heat-resistant polymer degradation. For example, rate constants of oxygen absorption by PI equal 7.5×10^{-7} - 1.6×10^{-8} and 1.9×10^{-6} - 7.4×10^{-8} s^{-1} for non-stabilized and stabilized PI, respectively. Gas products release demonstrates similar relations. A decrease of thermal oxidation solid product (pyromellitdiimide, PDI) yield was also observed – by 2.5 times for PI and 5 times for PAI:

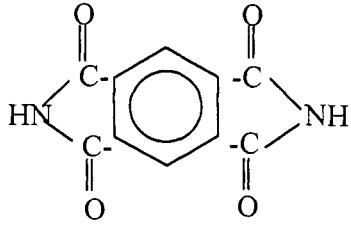

Injection of PCA to polyphenylquinoxalines significantly decreases the yield of analogous (in relation to the polymer structure) product, which is N-phenylpyrazine:

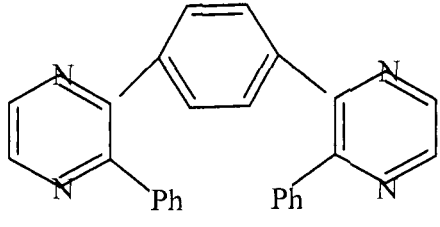

Correspondingly, in PPA [254] the yield of tetraphthalic amide

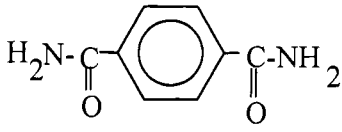

is almost eliminated (during the studied time period up to 5,000 h).

The amounts of PDI and analogous products (relative to polymer structures) [32, 226] indicate the conversion degree in oxidation transformations. The absence of these compounds in degradation products after reaction without oxygen testifies about exclusively thermal oxidation origin of their formation. Therefore, stabilization of heat-resistant polymers (HRP) displays clear antioxidant type, i.e. an additive is capable of interacting with radicals and other labile products of HRP thermal oxidation.

High-temperature activity of PCA in radical reactions is additionally confirmed by stabilizing effect of anilidophenylphosphate (*BT-5*) on PE degradation at 300°C. Application of such a model system to this particular case is desirable, because the radical-chain type of PE thermal oxidation at 200 - 250°C is well-known. It is also forecasted well for higher temperatures and, therefore, at some chain branching degree is forecasted well for carbonyl structures.

A significant contribution of the branching degree to polymer properties, including thermal stability, was shown by Korshak [228]. Non-cyclic units represent the main element of branching [2, 32]. The PCA effect on the cycle formation process was assessed using gas-chromatographic analysis of water release from polyamidoacid films – PI and PEI pre-polymers. Intensive water release was observed at initial cyclization stages at 150 - 200°C. Total water amount released from stabilized and non-stabilized PI and PEI at 250 - 300°C are nearly the same, i.e. in both cases, cyclization degrees are close. The PCA effectiveness for polyphenylquinoxaline – the polymer, in which cyclization proceeds easily, without any additional heat treatment – indicates that cyclization process acceleration in heat-resistant polymers (PI, for example) may not explain the protective action of PCA.

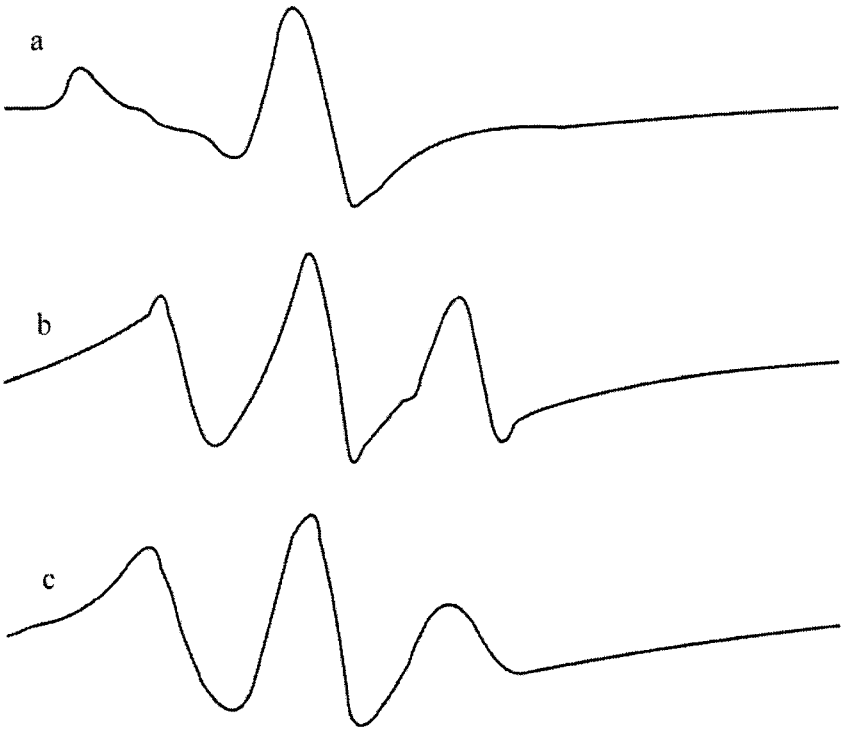

Figure 99. ESR spectra of spin probe in PI film without additives (a, c) and added by *BT-5* (b); a, b – prior to thermal aging; c – after thermal aging at 300°C during 500 h in air

Another possible stabilization mechanism – the formation of more stable network polymer structure in the presence of PCA with hindered oxygen access – was checked using the spin probe technique [9]. The probe (nitroxyl radical) diffusion into PI matrix was traced by changes in ESR spectra from classical triplet of freely isotropic-rotating, stable nitroxyl radical to a triplet degenerate by boundary components, typical of a probe rotating in a viscous medium. The spectrum (Figure 99) is of superposition type and indicates the presence of slow (main) and fast probe motion zones in the polymeric matrix. Relaxation times for non-stabilized and stabilized PI films were determined from graphic charts [229] as follows: $\tau_1 = 2\times10^{-8}$, τ_2 (~5%) = 10^{-9} s and $\tau_1 = (2 \div 5)\times10^{-8}$, τ_2 (~10 ÷ 15%) = 10^{-10} s, respectively. These values indicate a definite plasticizing effect of the additive on PI film properties. After thermal aging of films at 300°C during 500 h, τ_1 does not increase. Vice versa, for non-stabilized sample it

decreases to 10^{-9} s, whereas for stabilized sample it remained practically unchanged. Apparently, the decrease of τ_1 in non-stabilized film is associated with probe fixing on structure defects (various microcracks), but not with molecular mobility increase.

Degraded non-stabilized PI possesses self paramagnetic properties (a singlet with $\Delta H \approx 10$ E), which superimposes on the central component of ESR spectrum of the probe. This contribution is negligible for stabilized sample. The behavior of paramagnetic probe definitely reflects molecular mobility of the solid. Moreover, rotational and translational diffusion of the probe correlates with behavior of other "small" molecules (oxygen, for example) in the solid matrix. As observed in the experiment, additional crosslinking does not cause a noticeable change in molecular mobility of the polymer and hindrance of O_2 diffusion inside the sample.

The effective method for increasing thermal oxidation stability of polymers is control of the physical structure [9]. The additive effect on the physical structure of PI film was studied with the help of X-ray structural analysis. The film possesses mesomorphous regularity, of which the presence of an intrachain order in the absence of interchain packing regulation is typical. As shown on the diffraction pattern, such structure manifests itself by a single narrow peak of the intrachain order (5 – 6 deg) and wide amorphous halo (Figure 100). Diffraction patterns show high intrachain orderliness of the stabilized sample. This difference is preserved still after 1,000 h of aging at 300°C at total reduction of the intrachain order. Similar situation is observed on diffraction patterns for liquid-crystal polymers (Figure 103), stabilized by cyclic phosphites derived from pentaerythtitol *Irgafos 126*. However, stabilization may just partly be associated with the intrachain order increase in the presence of PCA. PCA are also effective in amorphous polymers, such as PSF and PPQ (refer to Chapter 4) [32].

As shown by the experiment, crosslinking proceeding during aging of PI films, both stabilized and non-stabilized, does not cause any significant change in molecular mobility of the polymer and hindrance of oxygen diffusion deep in the sample. Crosslinking intensification by PCA injection is disproved by the data on PAI and PPA melt viscosity decrease in the presence of PCA.

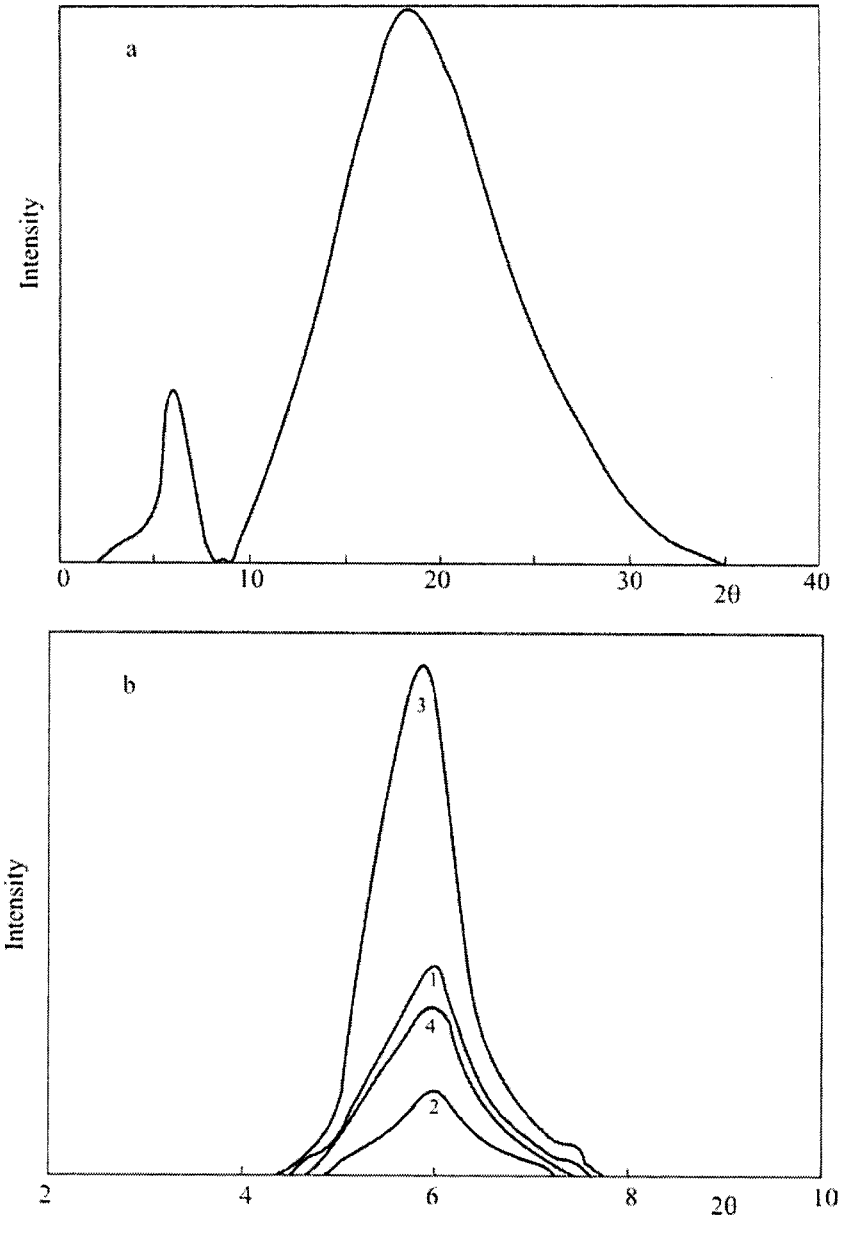

Figure 100. Diffraction patterns for PI films without additives (1, b; 1, 2) and added by 2 wt.% *BT-5* (b; 3, 4) prior to heat aging (a, b; 1, 3) and after thermal oxidation (b; 2, 4); $T = 300°C$; 700 h in air

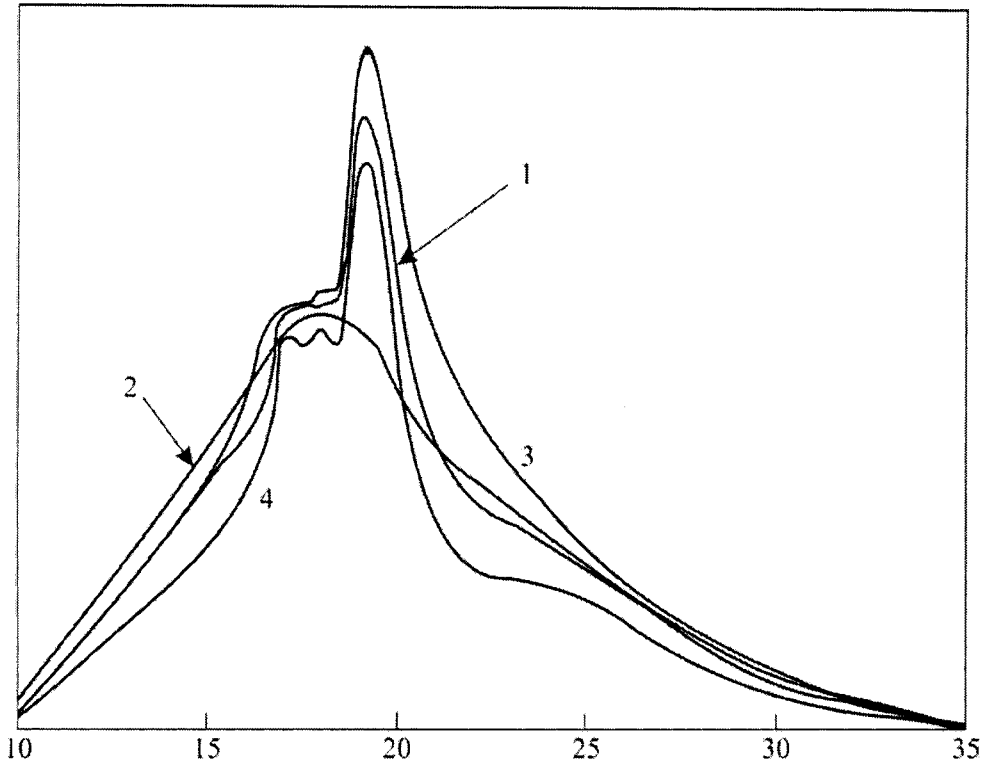

Figure 101. Diffraction pattern for LCP derived from TPA, IPA, *p*-OBA and DODP without additives (1, 2) and added by 0.5% *Irgafos 126* (3, 4): (1, 3) prior to heat treatment and (2, 4) after thermal processing; $T = 300°C$; 5 h in air

The studies performed with industrial and model PAI, PPA, PEI and PSF samples, aimed at determination of PCA action as deactivators of admixtures in heat-resistant polymers gained positive results.

PSF high-temperature oxidation is slowed down by low PCA additions. Though organic phosphites, specifically SHP, are of the highest efficiency and their stabilizing action is spread upon the whole complex of degradation manifestations, other PCA classes, even red phosphorus, are positively active, mostly stabilizing color.

Analysis of the literature data [192 – 218] concerning phosphite activity at low-temperature oxidation (initiated self-induced oxidation of hydrocarbons and polyolefins) and behavior of polymers with phosphorus-containing

additives at pyrolysis in the sub-flame zone indicates possible mechanisms of phosphorus stabilizing activity. These mechanisms are taken into consideration in the analysis of PSF stabilization during processing:

- phosphorylation or other chemical interactions between SHP and PSF macromolecules or labile and oxidized structures;
- inhibition of high-temperature oxidation radical reactions;
- transition metal admixture deactivation;
- other mechanisms, for example, deactivation of electron-excited states.

Feasibility of the stabilization molecular mechanism was estimated by NMR analysis of AO-118 mixtures with oligosulfones (the polymerization degree 5 – 7), 4,4'-dichlorodiphenylsulfone, or bisphenol A at 280 - 300°C in vacuum and in air. Under the condition of interaction with phosphite, high content of end OH- and Cl-groups in the oligomer and monomers provides for high resolution observation of phosphorylation by spectral methods. ^{13}C NMR spectra of heat treated mixtures preserve substrate reflexes and their relations that testify about the absence of molecular interactions. On the other hand, heating leads to phosphite decomposition, e.g. hydrolysis to corresponded monophenol and acid pentaerythritol diphosphite, signals from which at 64.5 and 63.4 ppm indicate dominance of tautomeric, four-coordinated shape:

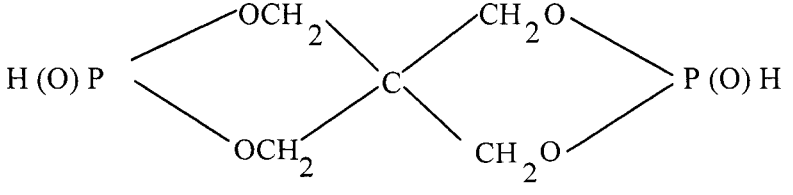

Phosphite additives to preliminarily degraded PSF and further heat treatment do not make the polymer color lighter and, according to IR spectra, have no effect on intensity of absorption bands associated with oxidized structures, for example, carbonyl groups. To put it differently, phosphorylation, noticeable, as the heat stabilization mechanism in other systems, for example, at PET and PMMA combustion and pyrolysis inhibition [199] or thermal oxidation of synthetic rubbers and vinylchloride polymers [216], is not observed during inhibited high-temperature PSF degradation.

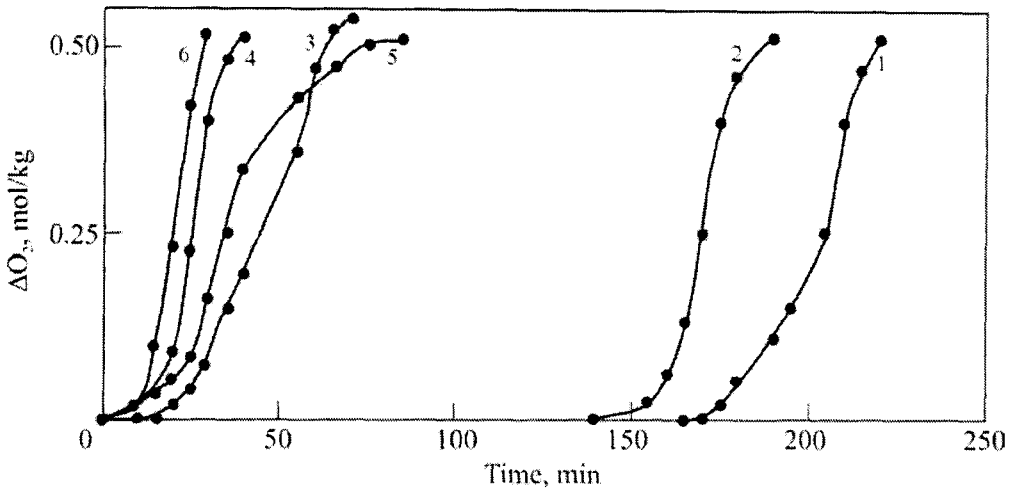

Figure 102. PE oxidation kinetics in the presence of SHP: *AO-118* (1, 2), *Stafor 11* (3, 4) and its acid ester (5, 6) without water absorption (1, 3, 5) and with water absorption (2, 4, 6); T = 200°C, $P(O_2)$ = 399.9 kPa

SHP high-temperature stabilization by additives show signs of radical inhibition: low effective concentrations (optimally, 1 – 1.5 mmol/kg), the efficiency O_2 pressure (in the absence of O_2 the efficiency is negligibly low). SHP decelerate the homolytical process of PSF macromolecule branching during thermal oxidation. Higher efficiency of cyclic SHP, compared with open ones, in the high-temperature oxidation process is, apparently, the general rule, because analogous dependence is displayed at PE high-temperature oxidation (Figure 102). This may be considered as the model of really radical, high-temperature process.

The increase of SHP effectiveness with hydrolysis probability (see Figure 97), shown in experiments with water linking, indicate the significant role of acid esters in inhibition of SHP hydrolysis products. Cycl;ic SHP of *AO118* type possess chemical shift on ^{31}P nuclei equal 115 – 120 ppm, whereas low-effective SHP of tris-(2,4-di-*tert*-butylphenol)phosphite and common triarylphosphites possess chemical shifts of about 130 ppm, and trialkylphosphites – 137 – 139 ppm. Since in all cases P-O bond is observed, i.e. at the first glance any change in electronegativity of the partner is absent and changes in SHP chemical shifts (at obvious absence of steric hindrances effect on the chemical shift) are associated with the differences in values of O-P-O-

bond valent angles in cyclic and open SHP, in accordance with the definition of ^{31}P chemical shift [217]:

$$\Delta\delta = -c\Delta\chi_\alpha + k\Delta n_\pi + A\Delta Q,$$

where $\Delta\chi_\alpha$ is the difference in electronegativity values of P-X-bonds; Δn_π is the change in π-electron overlapping; ΔQ is the change of σ valent angles. The change of valent angles causes changes in configuration of the electron cloud around phosphorus nucleus, i.e. the nucleus screening is changed. Formally, the effect is adequate to the change in electronegativity of partners bonded with phosphorus. Chemical shifts on ^1H, ^{13}C and, apparently, ^{31}P nuclei is inversely proportional to electronegativity of the partner nucleus [121], i.e. electronegativity of P is somehow reduced in the phosphite sequence:

cyclic alkylene-aromatic > aromatic > aliphatic.

Poling's electronegativity of atoms P, C and O equals 2.1, 2.5 and 3.5, respectively [83], e.g. P-C-bond is possesses much higher polarity than C-O-bond and is hydrolytically sensitive. Bulky groups of the *tert*-butyl type in the *ortho*-position at the ester bond makes steric hindrances to hydrolysis (kinetic mechanism). Changes in valent angles in the six-term steric phosphites reduce polarity of the ester bond and, as a consequence, its hydrolyzing ability (thermodynamic mechanism). For cyclic SHP, both mechanisms of hydrolytic stabilization are realized. Therefore, it is proved experimentally that these phosphites, for example, *AO118* and *Ultranox 626*, are most resistant to hydrolysis [218]. Finally, hydrolysis of open phosphites, including open SHP, leads to H_3PO_3, which is low-effective high-temperature stabilizer. At hyfrolysis of cyclic SHP alkylene-ester structure is preserved (NMR data), and the final product (acid cyclic phosphite) is the effective high-temperature stabilizer. This was shown by direct comparison of effectiveness of *Stafor 11* and its acid analogue, specially synthesized for tests. For example, tests performed on IIRT device at 320°C, *Stafor 11* makes PSF color lighter, increasing the light transmittance index by 3 – 5 units. For PSF acid ester, this index is increased by 10 – 12 units, though differences in other indices are not so great.

Indirectly, the radical mechanism of SHP stabilizing activity is confirmed by additive elimination of active degrading effect on PSF from the side DMSO. As shown by the strength of C-S-bonds in $(CH_3)_2SO_2$, equal 264 kJ/mol [78], and higher total reactivity of sulfoxides compared with sulfones

[219], DMSO is not heat resistant compound. At low temperature (about 100°C) molecular thermal cis-splitting happens with an olefin formation, though at higher temperatures homolytical C-S-bond break is suggested [219, p. 261]. Actually, over sixteen main products of DMSO degradation at PSF processing temperature (the ampoule technique) were detected by the mass-spectrometric method. The highest yields are observed for dimethyl disulfide, methyl ethyl sulfide, methyl and ethyl mercuptanes, 3-hydroxypropyl methyl sulfide, methylethoxymethylsulfide, and similar substances, which formation may be explained with respect to alkyl and alkylthio-radical recombination, as well as labile oxygen exchange reactions in semipolar sulfoxide group. As PSF is processed, DMSO residues play the role of an original radical initiator of degradation, and SHP addition eliminates this effect.

The idea to deactivate metal admixtures, first of all, iron compounds by SHP additives follows from extremely much higher efficiency of SHP in "impure" samples compared with almost pure ones (Table 44).

Table 44

The dependence of SHP effectiveness on polysulfone purity

Sample	$MFI_{10\ min}$ (320°C), g/10 min	$MFI_{10\ min}/MFI_{20\ min}$	Light transmittance at 425 nm, %	$M_z \times 10^3$
PSF with [Fe] = 5×10^{-5} wt.%	-	-	73.0	99.5
The same sample after IIRT	3.5	1.02	78.0	94.0
The same added by 0.3 wt.% *AO118*	4.3	1.01	73.0	98.0
PSF with [Fe] = 5×10^{-5} wt.%	-	-	60.0	87.0
The same sample after IIRT	3.7	1.5	68.0	58.0
The same added by 0.3 wt.% *AO118*	4.2	1.05	63.0	80.0

If an iron compound (up to 0.005 wt.%) is injected to "pure" PSF, light transmittance will be decreased by 20 – 30 units, whereas subsequent injection of SHP reduces this effect significantly. On the other hand, PSF color may be stabilized in tests simulating processing of phosphorus-containing transition metal complexes by additives.

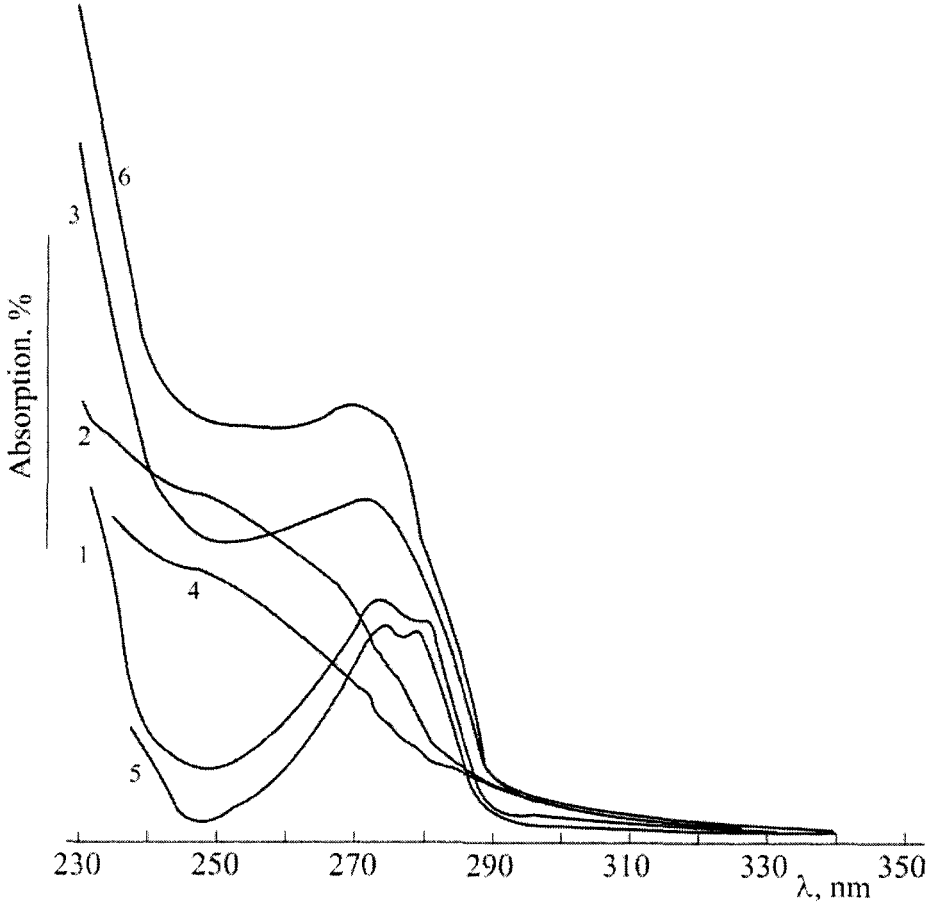

Figure 103. UV-spectra for chloroform solutions of *AO-118* (1), ferrocene (2), and their mixture (3). Differential spectra: mixture – *AO-118* (4), mixture-ferrocene (5); calculated additive *AO-118*-ferrocene spectrum (6)

Diphenylphosphonic salt additions (cations Co, Cr, Ni, Cu) up to 0.1 wt.% stabilize PSF similar to polyalkane imide, though these effects in PSF are not so high as in case of SHP use. The simplicity of phosphite interaction (*AO-118*, in particular) with transition metal compounds is shown by UV-spectra of *AO-118* and model substance (ferrocene), and their mixture chloroform solutions (Figure 103). At room temperature phosphite and iron-containing model interact at once, which causes a noticeable deviation of experimental UV-spectrum from calculated (additive) one.

This interaction represents an example of common complex-forming function of phosphorus compounds. With respect to the type of substitutes and coordination degree, phosphorus atom or phosphoryl oxygen is electron donor. The electron lone pairs of these atoms is transferred to empty or partly filled α-orbitals of neighboring atom of metal. Phosphorus-metal complexes are strongly bound due to relatively low potentials of phosphorus compound ionization and additional linking of π-electrons because of donor and acceptor (metal) vacant α-orbital overlapping [220].

The donor-acceptor interaction is one of the main mechanisms for metal compound extraction. The extraction ability correlates with the distribution of electron density in extracting agents, including phosphorus-organic compounds [221]. Correlations between effective extraction parameters defined by thermodynamics of the donor-acceptor bond and the so-called "effective charge" at phosphorus by which electron density distribution in molecule is described, and associated parameters of substitute electronegativity with ^{31}P NMR chemical shift as well. Generally, dependencies of the extraction effective constant (K) logarithm are linear:

$$\lg K = A - Bf,$$

where A and B are constants defined by the metal type and parameter f; f is the parameter characterizing electron density, for example, by the sum of electronegativity values of substitutes at phosphorus atom. There are data [221] on effective charges on phosphorus atoms in many phosphorus-containing compounds. Effective charges are determined from X-ray diffraction patterns by the energetic shift of phosphorus absorption range boundaries.

Iron admixtures significantly speed up thermal oxidation of all studied heat-resistant polymers. PCA injection fully eliminates this acceleration. Therefore, PCA stabilizing effect in heat-resistant polymers may be explained by metal admixture binding.

The products of "model + stabilized" system (equimolar mixture of N-phenylphthalimide and *BT-5*) thermal transformation were analyzed with the help of NMR-spectroscopy technique. It is shown that at 250 - 300°C the model does not transform, and the stabilizer partly degrades forming diphenylamine, phenol, phosphoric acid and its condensation products. All these compounds are not stabilizers of PI, PAI, PPA and other compounds or display much lower stabilizing action than initial *BT-5*. As a consequence, the stabilizing action is defined by either the initial PCA structure or intermediate products of stabilizer transformation. The occurrence of ESR signal (a singlet with ΔH = 9.1 E and g = 2.0003) allows a suggestion that stabilizer thermal transformation products are of the radical origin.

Emission extinguishing in PI film is observed by fluorescence spectra at 520 – 530 nm under the effect of BT-5 additive. The paramagnetism increase as a result of degradation in stabilized samples is much lower than in non-stabilized polymers. This is reproduced both in PI and PAI. Therefore, if electron excitation is considered as the oxidation initiation, endoperoxide formation, etc., thermal activation of the imide structure transfer to the electron-excited state in stabilized samples is hindered.

Thus, the investigation performed allowed the exclusion from consideration unreliazable or weakly realizable PCA effect on heat-resistant polymer cyclization and crosslinking and detection of the most probable stabilization mechanisms – admixture bonding and inhibition of radical-chain oxidation processes.

Optimal PCA concentrations of 2 – 5 wt.% in PI, PPQ, and PBO and 0.5 – 1.0 wt.% in PEI, PPA, PSF, and PAI, e.g. ~0.02 – 0.05 or 0.005 – 0.01 mol/base-mol, respectively. If one considers that the rate of translational diffusion of low-molecular substances in the rigid structure of heat-resistant polymers is low and may not provide the additive transport to the oxidation focus, it may be concluded that inhibition is possible only in the additive interaction with macromolecule and changes of its reactivity. Experiments with models did not display phosphorylation, i.e. direct interaction between the additive and aromatic heterocyclic structure. In this case, apparently, a polymer-additive complex is formed, which changes the macromolecule reactivity in relation to oxygen. The complex formation may change the electron state of the whole macromolecule or a large part of it, i.e. change the reactivity of it. Clearly, conjugation blocks (refer to Chapter 1) are present in the macrochain: PDI in PI and PAI, PPP in PPQ and CPIPQ, amide-TPA in PPA, i.e. the products characterizing chain conjugation. Their output at thermal oxidation is

decreased by PCA injection, whereas carbon oxides yields are reduced by 1.5-2 times only.

Thus, basing on the totality of experimental data on PCA stabilization one may conclude that the most probable stabilization mechanisms are additive deactivation, inhibition of radical oxidation processes and deactivation of electron-excited states.

Chapter 8. Conclusion

Here we considered degradation and stabilization of PAI, PPA, PSF PEL, LCP, etc. At the beginning of this investigation, these materials were united due to their functional similarity – heterochain heat-resistant polymer (HRP) processed at 280 - 400°C with operation temperatures up to 250°C according to the known engineering index for plastics UL 746. Now we also have other grounds to unite them. The phenomenology of degradation and its inhibition indicates similar reflexes of alkanimide or amide and arylene sulfone, or ester macrostructure to the external impact, as well as the presence of other substances in the system. Let us designate these substances as additives.

Additives distinguish real polymers from idealized models, the study of degradation of which must determine real reflexes of high-molecular compounds to heat impact. It is impossible to synthesize a polymer absolutely free from admixtures. Apparently, we should speak about their maximum content, above which their effect on the degradation kinetics becomes noticeable. All studied polymers are sensitive to additives, primarily, due to high processing temperature. Impurity of raw materials, low-quality equipment for synthesis and processing, and disturbances of production process increase the content of admixtures up to hundred (sometimes thousand) ppm that immediately decrease of the marketable product quality. Even without thermal stabilization the process measures aimed at purification of heat-resistant polymers to the minimal residual content of additives represent the most efficient way of thermal stability increase and, consequently, their quality.

As pure monomers are used, the content of defect structures in macromolecules synthesized by polycondensation is usually lower compared with polymers, obtained by radical polymerization, though the so-called different unit property[223]: for example, amidoacid structures in aromatic PI are the wide-spread phenomenon in polycondensation polymers. In the borders of sensitivity of spectral and chromatographic methods, elemental and chemical analysis no defect structures in the chain were observed. Thermal stability may be caused by labile end groups only.

Similar end groups are also observed in other heat-resistant polymers, for example, polyesterimide, PES. Interlocking of labile end groups is the second method of thermal stability increase.

At any purity degree (including interlocking of ends) of HRP, their structure is reactive at heat impact and O_2 attack. The only question is how quickly degradation reactions will induce the material quality loss. Autooxidation dormancy in the solid phase is general for semi-crystalline PAI and PPA, liquid-crystal polymers and, apparently, other HRP with no respect to their crystallinity degree. Judging by ESR chemical shifts (1.24 ppm), even PAI with long methylene chain (with, at least, 10 methylene groups of adequate PE methylene chain) is resistant to oxidation in the solid phase (O_2 absorption by PAI at 200°C exposure during 200 h equals only 2.4 mol/base-mol, whereas PE absorbs 7.6 mol/base-mol during the same length of exposure at 110°C in the solid phase [28]).

In chemical physics of polymer aging and stabilization [9] the effects of this type are associated with solid-phase autooxidation kinetics dependence on intensity of molecular movements in macromolecules.

Degradation of studied polymers in melt at processing temperature is caused by autooxidation. Though in vacuum-extrusion and press molding there is no direct contact between polymers and atmospheric air (residual O_2 pressure is 20 – 50 mmHg), high processing temperatures stimulate oxidation even at such insignificant concentration of O_2. Formally, studied polymers are related to different chemical classes of polymers. Actually, these are polymers of similar structure: aliphatic-aromatic polymers with strong electro-acceptor groups – sulfonyl, amide or imide. It is found experimentally [219, 224] that sulfonyl and amide groups activate methylene groups located nearby. The analogous effect of electron-acceptor groups on the methylene chain in PAI and dislocation of electron density on PSF aromatic rings was also determined. If at low temperatures corresponded to HRP operation, on the background of low degradation gross-rates, oxidation of aromatic fragments is not observed, and high-temperature oxidation affects aliphatic and aromatic parts of the macrochain, simultaneously. The typical feature of aromatic structure oxidation in studied polymers and, apparently, other HRP containing aromatic rings in the structure, is structuring and crosslinking of macrochains. This makes processing difficult because of melt viscosity increase and causes loss of strength and elastic properties. Moreover, occurrence of aromatic C=O-groups possessing high extinction coefficients, as a result of oxidation, intensifies electron conjugations of the aromatic structure. This is shown up in UV-absorption shift to the visible region and is visually perceived as the typical feature of degradation – the polymer yellowing.

The phenomenology of heat-resistant polymer high-temperature oxidation is explained from positions of the radical-chain mechanism.

Participating in the conjugation with electron pulling, strong electron-acceptor groups stabilize macroradicals and, therefore, provide for their low reactivity and, correspondingly, the decrease of degradation effective rates compared with carbochain structures. All known HRP always have electron-acceptor heterogroups in the structure (or a combination of strong electron-acceptor groups with donors).

Sulfonyl group in PSF participates in electron conjugation [219, p. 21] in the manner that even at interlocking influence of isopropylidene group The PSF structure is characterized by conjugation blocks. Contrary to diamagnetic PSF, PAI-12, described in Chapter 1, is paramagnetic and possesses high magnetic susceptibility, which may not be explained by paramagnetic admixtures, but only by interchain conjugation by pyromellitic residues. Conjugation or realization of molecular orbitals of valent electrons by the macrochain reduces electron excitation energy down to a possibility of purely thermal excitation. Some features of degradation of the studied polymers are explained from this very position. The contribution of electron excitation is displayed clearer at higher temperatures, which are processing temperatures (320 - 380°C) of polyestersulfones, polyesterimide, PPQ, SPIPQ, LCP, or polyester ketones.

Thermal stability of heat-resistant polymers is increased during processing with the help of additives. All polymers are effectively stabilized by PCA or their blends. Classical antioxidants of amine and phenol types are ineffective at high-temperature degradation. Low values of effective concentrations, the presence of optimal concentration dependence and other features of stabilizing PCA, discussed in the book, indicate high probability of chain inhibition, the more so that PCA were also found effective for deceleration of PE high-temperature oxidation, which may be considered as a "test field" for radical-chain, branched oxidation process. Moreover, the important PCA function is deactivation of admixtures, especially iron compounds. The less pure the polymer is, the higher is necessity of thermal stabilization and effects of PCA additives are relatively higher.

Similarity of studied polymer degradation and stabilization processes and their structural similarity to other HRP (alkyl-aromatic and aromatic structures with highly electron-acceptor heterogroups) also allow forecasting thermal behavior and efficiency of PCA for other heat-resistant polymers. Actually, all signs of high-temperature oxidation were observed, typical of PAI and PSF, and in tests of PES, copolymeric polysulfones, polyester ester ketones. As shown by mass loss, O_2 absorption, MFI stability, and color stability data, low increments of PCA slow down degradation of these HRP also effectively at 340 - 400°C. For example, the rate of O_2 absorption by polyester ester ketones

is twice reduced at addition of 0.5 wt.% phosphites derived from pentaerythritol.

To conclude the discussion, let us note that the problem of high-temperature degradation and stabilization should also be comprehensively investigated, similar to the attention paid in 1960 - 1970's to degradation and stabilization of polyolefins and vinyl polymers. Besides the study of reactivity of aromatic structures and polar effects at thermal reactions, and other fundamental aspects, these investigations would also promote applied development of HRP. This is of high importance for future technologies in electron, electrotechnical, automobile and aerospace engineering.

ABBREVIATIONS

Methods:

IRS – IR-spectroscopy
MINRM – multiple internal non-full reflection method
^{13}C, ^{1}H, ^{31}P NMR – NMR spectroscopy on carbon nuclei, protons (PMR) and phosphorus, respectively
GLC – gas-liquid chromatography
MS – mass-spectrometry
ESR – electron spin resonance
CMS – chromato-mass-spectrometry
DSC – differential scanning calorimetry
DTA – differential thermal analysis
GC - gas chromatography
GPC – gel-penetrating chromatography
MMD – molecular-mass distribution
M_w, M_n, M_z – molecular masses
YI – yellowing index
IIRT – a test device for melt flow index of thermoplastic polymers
MFI – melt flow index of polymers
TS – thermal stability of polymer melt
G – the amount of gel fraction
ΔH – polymer melting (crystallization) enthalpy
$[\eta]$ – characteristic viscosity
T_g – glass transition temperature
T_m – melting temperature
E_a – effective activation energy
CTC – charge transfer complex

Polymers:

HRP – heat-resistant polymers
PAI – polyalkanimide

PAI-6 ... PAI-13 – polyalkanimides derived from diamines, possessing 6 to 1
methylene groups, respectively
PE - polyethylene
PVC - polyvinylchloride
PI, PM-1, Kapton – aromatic polyimide
PA – aliphatic polyamides, PA-6, PA-66 and PA-12, respectively
PET – poly(ethylene terephthalate)
PBT – poly(butylene terephthalate)
PPP – 2,2'-1,4-phenylene)-bis-(3-phenylpyrazine)
PDI – pyromellite diimide
PPA – aliphatic-aromatic polyamides
PES – aromatic polyester sulfone
PSF – polysulfone derived from bisphenol A
PEI – polyester imide
PC - polycarbonate
PPQ – polyphenylene quinoxaline
CPIPQ – copolyimidophenyl quinoxaline
PBO - polybenzoxazole
LCP – liquid-crystal copolyesters
CP - copolymers
PAA – poly(amido acid)
TPA – terephthalic acid
IPA – isophthalic acid
p-OBA – *para*-oxybenzoic acid
h-MDA – hexamethylene diamine

Stabilizers:

HALS – sterically hindered amines
PCA – phosphorus-containing additives
CCC – complex copper compounds

Trademarks of industrial antioxidants::

Phenols – *Irganox 1010*, *Irganox 1098* (Ciba)
Phosphites – *AO-118* (Czeck Republic), *Iltranox 626* (Borge Worner)
Stafor 11 (Russia), *Irgafos 126* and *Irgafos 168* (Ciba)

Irganox B1171 – a mixture of *Irganox 1098* and *Irgafos 168*

REFERENCES

1. Semenov N.N., *On Some Problems of Chemical Kinetics and Reactivity (Free Radicals and Chain Reactions)*, 2nd Ed., Moscow, AN SSSR, 1958, 686 p. (Rus)
2. Kandratiev V.N. and Nikitin E.E., *Chemical Processes in Gases*, Moscow, Nauka, 1981, 262 p. (Rus)
3. Voevodsky V.V., *Physics and Chemistry of Elementary Chemical Processes*, Moscow, Nauka, 1969, 414 p. (Rus)
4. Neiman M.B., *Aging and Stabilization of Polymers*, Moscow, Nauka, 1964, 332 p. (Rus)
5. Kuz'minsky A.S., *Oxidation of Caoutchoucs and Rubbers*, Moscow, Goschimizdat, 1957, 319 p. (Rus)
6. Grassi N., *Chemistry of Polymer Degradation Processes*, Moscow, Inostrannaya Literatura, 1959, 252 p. (Rus)
7. Madorsky S., *Thermal Degradation of Organic Polymers*, Moscow, Mir, 1967, 320 p. (Rus)
8. Emanuel N.M., Denisov E.T., and Maizus Z.K., *Chain Reactions of Hydrocarbons Oxidation in the Liquid Phase*, Moscow, Nauka, 1965, 375 p. (Rus)
9. Emanuel N.M. and Buchachenko A.L., *Chemical Physics of Polymer Aging and Stabilization*, Moscow, Nauka, 1982, 359 p. (Rus)
10. Shlyapnikov Yu.A., Kiryushkin S.G., and Mar'in A.P., *Antioxidant Stabilization of Polymers*, Moscow, Khimia, 1986, 252 p. (Rus)
11. Popov V.A., Rapoport N.Ya., and Zaikov G.E., *Oxidation of Oriented and Stressed Polymers*, Moscow, Khimia, 1987, 232 p. (Rus)
12. Zaikov G.E. and Moiseev V.V., *Chemical Resistance of Polymers in Aggressive Media*, Moscow, Khimia, 1979, 216 p. (Rus)
13. Minsker K.E. and Fedoseeva G.T., *Degradation and Stabilization of Polyvinylchloride*, 2nd Ed., Moscow, Khimia, 1979, 272 p. (Rus)
14. *Degradation and Stabilization of Polymers*, Ed. G. Genskens, London: Appl. Sci. Publ., 1975, 201 p.
15. *Comprehensive Chemical Kinetics*, Ed. C.H. Baneford and C.F. Tipper, Amsterdam: Elsevier Publ., 1975, vol. **4**, 162 p.
16. *Aspects of Degradation and Stabilization of Polymers*, Ed. H.H. Jellinek, Amsterdam: Elsevier Publ., 1978, 112 p.

17. *Developments in Polymer Degradation*, Ed. G. Scott, London: Appl. Sci. Publ., 1979, vol. **1**, 198 p.
18. *Antioxidation and Antioxidants*, Ed. W.O. Lundberg, N.Y.: Intercience, 1961, 120 p.
19. Scott G., *Atmospheric Oxidation and Antioxidants*, Amsterdam: Elsevier Publ., 1965, 112 p.
20. Denisov E.T., Mitskevich N.Y., and Agabekov V.E., *Liquid–Phase Oxidation of Oxygen-Containing Compounds*, N.Y.: Consultants Bevican, 1977, 126 p.
21. *Polymer Stabilization*, Ed. W.L. Hewkins, N.Y.: Wiley, 1972, 201 p.
22. Pospisil J., *Antioxidanty*, Praha: Academia, 1968, vol. **75**, p. 23.
23. Comprehensive Chemical Kinetics, Ed. C.H. Baneford, Amsterdam: Elsevier Publ., 1980, vol. **16**, 264 p.
24. 'Resin Sales by Market 85-86', *Mod. Plast. Int.*, 1987, No. 1, pp. 20 - 34.
25. *Modern Plastics Encyclopedia*, N.Y.: McGraw-Hill. Inc., 1980, pp. 160 - 189.
26. Kovarskaya B.M., Blyumenfeld A.B., and Levantovskaya I.I., *Thermal Stability of Heterochain Polymers*, Moscow, Khimia, 1977, 263 p. (Rus)
27. Koton M.M., *New Polymers in National Economy*, Kiev, Izd. AN UkrSSR, 1959, 37 p. (Rus)
28. Thermal Stability of Polymers, Ed. R.T. Conley, vol. **1**, N.Y.: Marcel Dekker, 1970, 347 p.
29. Bessonov M.I., Koton M.M., Kudryavtsev V.V., and Laius L.A., *Polyimides – the Class of Heat-Resistant Polymers*, Leningrad, Nauka, 1983, 328 p. (Rus)
30. Annenkova N.G., 'The Study of Thermal Stability of Aromatic Polyimides', *Candidate Dissertation Thesis*, Moscow, 1973. (Rus)
31. Novotortseva T.N., 'High-Temperature Stabilization of Polybenzoxazole', *Candidate Dissertation Thesis*, Moscow, 1987. (Rus)
32. Vdovina A.L., 'Thermal Transformations and Stabilization of Polypyromellitimide, Polyphenylquinoxaline and Copolyimidophenyl-quinoxalines', *Candidate Dissertation Thesis*, Moscow, 1988. (Rus)
33. Gladyishev G.P., Ershov Yu.A., and Shustova O.A., *Stabilization of Heat-Resistant Polymers*, Moscow, Khimia, 1979.
34. Wood S., 'There good reason for all the action aromatic sulfone polymers', *Mod. Plast. Int.*, 1987, No. 3, pp. 32 - 34.
35. Blyumenfeld A.B., Levantovskaya I.I., and Annenkova N.G., 'Problems of thermal stability and stabilization of heterochain polymers', In Coll.:

Progress in Science and Technology, Ser. Navy Chem. Technol., vol. **20**, Moscow, VINITI, 1985, pp. 143 – 211. (Rus)

36. *US Patent No. 2,760,835*, Fatty-aromatic Polyimides, Publ. June 18, 1955.
37. Vinogradova S.V., Churochkina N.A., and Vyigodsky Ya.S., 'Synthesis and properties of some fatty-aromatic polyimides', *Vysokomol. Soed.*, 1971, vol. **A13**(3), pp. 1146 – 1150. (Rus)
38. *US Patent No. 3,551,200*, 'Wire insulation derived from poly-1,12-dodecamethylene-1,13-tridecamethylene pyromellitimide, Publ. December 29, 1968 (cl. 117-232).
39. *US Patent No. 2,019,457*, Electroinsulating materials, Publ. Sept. 18, 1969 (cl. 20100 CO8g).
40. *US Patent No. 3,677,921*, Poly-1,12-dodecamethylene and poly-1,13-tridecamethylene pyromellitimide and their degradation and crosslinking products, Publ. Oct. 29, 1970 (cl. 204-159/g).
41. Lava V.L. and Halperin R.M., 'A new extruded alkanimide wise', *Technical paper for presentation on the 18th International Cable Symp.*, Atlantic City, New Jersey, Dec. 3-5, 1968.
42. *US Patent No. 2,944,993*, Glass-filled thermoplastic composites derived from linear polypyromellitimides, Publ. Jun. 14, 1955 (cl. 260-37).
43. Vohninkel E., *Neue Polumere Werkstoffe fur die Industrielle Andwendung*, Munhen: Carl Hauser Verlag, 1983, S. 257.
44. Tuichiev Sh., Kuznetsova A.M., and Mukhametdieva A.M., 'Temperature changes of molecular and permolecular structure of polyalkanimide', *Vysokomol. Soed.*, 1987, vol. **A29**(8), pp. 1756 – 1760. (Rus)
45. Vigodsky J.S., Vinogradova S.V., Nagiev S.T., and Korschak V.V., 'A study of copolyimide synthesis, structure and properties', *Acta Polymerica*, vol. **33**(2), pp. 131 - 137.
46. Kazaryan L.G., Azriel A.E., and Vasil'ev V.A., 'Phase transitions in polyalkanimide', *Vysokomol. Soed.*,1979, vol. **B21**(9), pp. 644 – 645. (Rus)
47. Kazaryan L.G., Azriel A.E., Vasil'ev V.A., Annenkova N.G., Pinaeva N.K., and Chernova A.G., "Structure and properties of polyalkanimide', *Vysokomol. Soed.*,1988, vol. **A30**(3), pp. 644 – 647. (Rus)
48. Hummel D.O., In: *Analytical Pyrolysis*, Ed. C.S.R. Jenes and C.A. Cramers, Amsterdam: Elsevier Publ., 1977, p. 177.

49. Dussel H.J., Rosen H., and Hummel D.O., ‚Feldionen- und Elektronenstos- Massenspektrometrie von Polymeren und Copolymeren', *Die Macromolekulare Chemie*, 1976, Bd. **177**(8), S. 2343 – 2368.
50. Soboleva L.I., Matevosyan Ts.M., Chernova A.G., and Pinaeva N.K., 'Hydrolytic properties of polyalkanimide', In Coll.: *Production and Processing of Plastics and Synthetic Resins*, Moscow, NIITEKhim, 1976, No. 9, pp. 34 – 36. (Rus)
51. Chernova A.G., Lebedinskaya M.L., Pinaeva N.K., and Nekrasova L.N., 'Deformation and strength properties of poly(1,12-dodecamethylene pyromellit)imide', In Coll.: *Production and Processing of Plastics and Synthetic Resins*, Moscow, NIITEKhim, 1977, No. 7, pp. 20 – 23. (Rus)
52. Chernova A.G., Sedyikh V.M., Lushcheikin G.A., Pinaeva N.K., and Nekrasova L.P., 'Electrical properties of polyalkanimide *AI-1G*', In Coll.: *Production and Processing of Plastics and Synthetic Resins*, Moscow, NIITEKhim, 1979, No. 2, pp. 15 – 17. (Rus)
53. *US Patent No. 3,714,116*, Polyimide composite, Publ Aug. 30, 1970 (cl. 121-232).
54. Sekacheva I.V., Solyankin I.N., Pinaeva N.K., Koshel' G.N., Kryukova G.G., Kozlova O.S., and Smirnova O.M., 'Synthesis and identification of salts from pyromellitic acid and 1,12-dodecamethylene diamine, *Sb. Yaroslavskogo Politekhnicheskogo Instituta*, 1990. (Rus)
55. Adorova I.V., Chernova A.G., Bulgakova M.A., Pinaeva N.K., and Siling M.I., 'Chromatographic analysis of monomers in polycondensation products of pyromellitic dianhydride and dodecamethylene diamine', In Coll.: *Production and Processing of Plastics and Synthetic Resins*, Moscow, NIITEKhim, 1979, No. 2, pp. 18 – 21. (Rus)
56. Abramova I.M., Azriel A.E., Vatagina V.A.,Zezina L.A., Zyisk K.Yu., Kazaryan L.G., Pinaeva N.N., Savina M.E., Sade A.G., and Chernova A.G., 'The effect of aging conditions on the structure and properties of polyalkanimide *AI-1G*', In Coll.: *Heat-Resistant Materials*, Moscow, NIITEKhim, 1985, pp. 162 – 167. (Rus)
57. *Engineering Thermoplastics: Properties and Application*, Ed. J.M. Margolis, N.Y.: Marcel Dekker, 1985, 385 p.
58. Ballintyn N.J., *Encyclopedia of Chemical Technology*, vol. **18**. N.Y.: Wiley, pp. 832 - 848.
59. *Encyclopedia of Polymer Science and Technology*, vol. **2**, pp. 503 – 665; vol.**3**, pp. 144 - 180, 692 - 700.

60. Storozhuk E.P. and Valetsky P.M., 'Formation regularities and properties of polyarylene sulfonoxides', In Coll.: *The Results of Science and Technology, Ser. Chemistry and Technology of High-molecular Compounds*, Moscow, VINITI, 1978, vol. 12. pp. 127 – 176. (Rus)
61. Militskova E.A. and Andrianova N.V., 'Aromatic polysulfones', In Coll.: *Modern Problems of Chemistry and Chemical Industry*, Moscow, NIITEKhim, 1977, Iss. 3, vol. **42**, pp. 78 – 82. (Rus)
62. Lancaster T.M. and Wright W.W., 'Thermal degradation of polymer with aromatic rings in the chain', *J. Appl. Polymer Sci.*, 1965, vol. **9**, pp. 1955 - 1971.
63. Hale W.F., Farnham A.G., Johnson R.N., and Cledinning R.A., 'Polyarylethers by nucleophilic aromatics', *J. Polymer Sci.*, 1967, Part A1, vol. **5**, pp. 2399 - 2414.
64. Grossland B., Knight G.J., and Wright W.W., 'A comparative study of the thermal stability and mechanism of degradation of poly(arylene sulphones)', *Brit. Polymer J.*, 1986, vol. **18**(3), pp. 156 - 160.
65. Danilina L.I., Teleshov E.N., and Provednikov A.N., 'Thermal degradation of aromatic polysulfones', *Vysokomol. Soed.*, 1974, vol. **A16**(3), pp. 581 – 587. (Rus)
66. Davis A., 'Thermal stability of polysulphone', *Macromolek. Chemie*, 1968, vol. **28**, p. 242 - 251.
67. Kuroda S.I., Terarechi K., Negani K., and Mita I., 'Degradation of aromatic polymers. 1. Rates of crosslinking and chain scission during thermal degradation of several soluble aromatic polymers', *Eur. Polym. J.*, 1989, vol. **25**(1), pp. 1 - 7.
68. Danilina L.I., Muromtsev V.I., and Pravednikov A.N., 'The mechanism of phenol formation in thermal degradation of aromatic polysulfones', *Vysokomol. Soed.*, 1975, vol. **A17**(11), pp. 2592 – 2596. (Rus)
69. Perkins M., *Free Radicals*, N.Y.: Wiley, 1973, 231 p.
70. Levantovskaya I.I., Dralyuk G.V., Mochalova O.A., Yurkova I.A., Akutin M.S., and Kovarskaya B.M., 'Polysulfone degradation', *Vysokomol. Soed.*, 1971, vol. **A13**(1), pp. 8 – 15. (Rus)
71. Laktionov V.M., Zhuravleva I.V., and Pavlova S.A., 'Thermal stability of poly(sulfone arylates) and poly(sulfone arylenoxides), *Vysokomol. Soed.*, 1976, vol. **A18**(2), pp. 330 – 338. (Rus)
72. Laktionov V.M. and Zhuravleva I.V., 'Chromatographic kinetic study of aromatic polysulfone degradation in vacuum', *Vysokomol. Soed.*, 1975, vol. **A17**(12), pp. 2813 – 2814. (Rus)

73. Danilina L.I., Teleshov E.N., and Pravednikov A.N., 'About the mechanism of polysulfone thermal degradation', *Doklady AN SSSR*, 1972, vol. **207**(5), pp. 1121 – 1124.. (Rus)
74. Bansal R.K., Agarval R., and Keshow K., 'Epoxy resins 8. Thermal-properties of 4,4'- sulfonyldiphenol and bisphenol A epoxy resins', *Angew. Macromol. Chem*, 1983, vol. **117**, pp. 211 - 217.
75. Sotnikov E.E. and Rastyannikov E.I., 'Identification of volatile products at direct vapor-phase pyrolysis of polymers', *Plastmassy*, 1989, No. 2, pp. 71 – 74. (Rus)
76. Tarnowiecki H.M., Das Verhalten von Thermoplasten unter Warmbeanspruchung. 2. Uber den thermischen Abbau von Polysulfon, *Mitt. Chem. Forschungsinst. Wirt Osterr.*, 1970, Bd. **24**(6), S. 296 - 298.
77. Munro H.S. and Clark D.T., 'The surface photodegradation of bisphenol A polysulphone', *Polym. Degrad. Stability*, 1987, vol. **17**(4), pp. 319 - 325.
78. *Energies of Chemical Bond Break, Ionization Potentials and Affinity to Electron*, Moscow, Nauka, 1974, 351 p. (Rus)
79. Kondratiev V.N., *Rate Constants of Gas-Phase Reactions*, Reference Book, Moscow, Nauka, 1971, 351 p. (Rus)
80. Denisov E.T., *Rate Constants of Homolytical Liquid-Phase Reactions*, Moscow, Nauka, 1972, 712 p. (Rus)
81. Roberts J.T., Ritterberg B., and Kovacic P., 'Pyrolysis of N,N'-dihalo derivatives of amides and sulfonamides', *J. Org. Chem.*, 1981, vol. **46**(20), pp. 3988 - 3996.
82. Magaril R.Z., *The Mechanism and Kinetics of Homogeneous Thermal Transformations of Hydrocarbons*, Moscow, Khimia, 1970, 224 p. (Rus)
83. Gordon A. and Ford R, *Chemist Companion*, Moscow, Mir, 1976, 541 p. (Rus)
84. Chemical Encyclopedia, vol. **2**, Moscow, Izd. Sovetskaya Entsiklopediya, 1990, pp. 447. (Rus)
85. Jaffe H.H., 'A re-examination of the Hammett equation', *Chem. Rev.*, 1953, vol. **53**, pp. 191 - 254.
86. Buchachenko A.L., Complexes of Radicals and Molecular Oxygen with Organic Molecules, Moscow, Nauka, 1970, 489 p. (Rus)
87. Gesner B.D. and Kelleher P.G., 'Thermal and photooxidation of polysulfone', *J. Appl. Polym. Sci.*, 1968, vol. **12**(5), pp. 1199 - 1208.
88. Glasser H., 'Polysulfonfolie, eine Warmebestendige Folie mit einer Gunstigen Eigenschafts-Kombination' *Kunstoffe*, 1971, Bd. **61**(4), S. 232 - 234.

89. Dilks A. and Clark D.T., 'ESCA studies of natural weathering-phenomena at selected polymer surface', *J. Polymer Sci.: Polym. Chem. Ed.*, 1981, vol. **19**, pp. 2847 - 2860.
90. Gesner B.D. and Kelleher P.G., 'Oxidation of bisphenol A polymers', *J. Appl. Polym. Sci.*, 1969, vol. **13**(10), pp. 2183 - 2191.
91. Khukhreva I.I., Derevyagina S.V., and Barkov A.S., 'Light resistance of polysulfone', *Vysokomol. Soed.*, 1972, vol. **A14**(5), pp. 1122 – 1126. (Rus)
92. Ranby B. and Rabek J.F., *Photodegradation and Photostabilization of Polymers*, London: Wiley, 1975.
93. Davis A.G., *Organic Peroxides*, London: Butterworths, 1962.
94. Levantovskaya I.I., Narkon A.L., Ershov O.V. et al., 'The study of some regularities of polysulfone high-temperature oxidation', *Vysokomol. Soed.*, 1985, vol. **A27**(2), pp. 362 – 368. (Rus)
95. Vogel H., 'Polyarylsulfones. Synthesis and properties', *J. Polym. Sci.*, 1970, vol. **A18**, pp. 2035 - 2047.
96. Dashevskaya S.S., Akutin M.S., and Shlyapnikov Yu.A., 'High-temperature oxidation of polysulfone', *Vysokomol. Soed.*, 1974, vol. **B16**(5),pp. 353 – 356. (Rus)
97. Dashevskaya S.S., Shlyapnikov Yu.A., and Akutin M.S., 'High-temperature oxidation of polysulfone containing no aliphatic groups', *Vysokomol. Soed.*, 1974, vol. **B16**(10),pp. 761 – 763. (Rus)
98. Narkon A.L., Levantovskaya I.I., Gur'yanova V.V. *et al.*, 'The effect of molecular-mass distribution on thermal stability of polysulfone', *Vysokomol. Soed.*, 1986, vol. **A28**(3), pp. 505 – 509. (Rus)
99. Badikova N.D., Militskova E.A., and Andrianova N.V., 'Technological factors for obtaining optical polysulfone', In Coll.: *Production and Processing of Plastics and Synthetic Resins*, Moscow, NIITEKhim, 1974, No. 10, pp. 54 – 57. (Rus)
100. Badikova N.D., Militskova E.A., and Zelenina E.N., 'The effect of precipitation method on light and technical properties of polysulfone', In Coll.: *Production and Processing of Plastics and Synthetic Resins*, Moscow, NIITEKhim, 1977, No. 1, pp. 22 – 25. (Rus)
101. Badikova N.D., Militskova E.A., and Andrianova N.V., 'The effect of various end groups on light and heat resistance of polysulfone', *Plastmassy*, 1976, No. 1, pp. 72 – 73. (Rus)
102. Jonson R.S., Farnham A.G., Clendinning R.A., Hale W.F., and Merriam C.N., 'Poly(arylethers) by nucleophilic aromatic substitution 1.

Synthesis and properties', *J. Polym. Sci.*, 1967, Part A1, vol. **5**(9), pp. 2375 - 2398.

103. Badikova N.D., Militskova E.A., and Gur'yanova V.V., 'Polysulfone light stabilization', *Plastmassy*, 1976, No. 9, pp. 70 – 72. (Rus)
104. Narkon A.L., Levantovskaya I.I., Kotov Yu.I., Konovalova B.E., Reiburd L.I., Bolotina L.M., and Blyumenfeld A.B., 'The studies of admixture effect on polysulfone degradation and structuring processes', *Vysokomol. Soed.*, 1984, vol. **A26**(8), pp. 1712 – 1717. (Rus)
105. Gur'yanov V.V., Alkaeva O.F., Melamid S.E., Reiburd L.I., Narkon A.L., Arshava B.M., Pavlov A.V., and Novikov D.D., 'The study of polysulfone molecular-mass characteristics by gel-penetrating chromatography method', *Vysokomol. Soed.*, 1983, vol. **A25**(2), pp. 375 – 380. (Rus)
106. Devis A., Cleaves H., and Golden J.H., 'The electron irradiation stability of polysulfone', *Macromol. Chemie*, 1969, vol. **129**, pp. 63 - 72.
107. Susuda T., Hayakawa N., and Joshida K., 'Electron beam irradiation effects on mechanical relaxation of aromatic polysulphones', *Polymer*, 1987, vol. **28**(2), pp. 236 - 241.
108. Shut N.I., Klimenko N.V., Blotina L.M., and Gordienko V.P., 'Heat-physical properties of irradiated polysulfones', *Plastmassy*, 1987, No. 4, pp. 25 – 28. (Rus)
109. Sasuga T. and Hagiwera M., 'Radiation deterioration of several aromatic polymers under oxidative conditions, *Polymer*, 1987, vol. **28**(1), pp. 1915 - 1922.
110. Denisov E.T., *Oxidation and Degradation of Carbochain Polymers*, Moscow, Khimia, 1990, 286 p. (Rus)
111. Verkhovskaya Z.N., *Diphenylol Propane*, Moscow, Khimia, 1971, 196 p. (Rus)
112. Narkon A.L., Levantovskaya I.I., Siling M.I., Ruiburd L.I., and Lutsic V.V., 'The effect of admixtures on polysulfone thermal stability', *Plastmassy*, 1983, No. 11, pp. 20 – 23. (Rus)
113. Wasserman A.M. and Buchachenko, *Izv. AN SSSR, Ser. Khim.*, 1967, No. 9, pp. 1947 – 1952. (Rus)
114. Bagdasar'yan Kh.S., *The Theory of Radical Polymerization*, Moscow, Nauka, 1966, 252 p. (Rus)
115. Buchachenko A.L. and Wasserman A.M., *Stable Radicals*, Moscow, Khimia, 1973, 407 p. (Rus)
116. Ito R., Migita T., Morikawa N., and Simamura O., 'Influence of substituent groups in arylation of substituted benzenes by aryl-radicals

derived from p-substituted N-nitrosoacetanilides, *Tetrahedron*, 1965, vol. **21**, pp. 955 - 961.

117. *Catalogue of NMR spectra by Variant Co.* (Rus)
118. Williams G.H., *Homolytical Aromatic Substitution*, Oxford: Pergamon Press, 1960.
119. Palm V.A., *Fundamentals of Quantitative Theory of Organic Reactions*, Leningrad, Khimia, 1967, 285 p. (Rus)
120. Alger J.D., Grant D.M., and Paul E., 'Carbon-13 magnetic resonance. 6. Theory of ^{13}C magnetic resonance shifts in aromatic molecules, *J. Amer. Chem. Soc*, 1966, vol. **88**(23), pp. 5391 - 5406.
121. Ionin B.I., Ershov B.A., and Kol'tsov A.I., *NMR-Spectroscopy in Organic Chemistry*, Leningrad, Khimia, 1983, 269 p. (Rus)
122. Lanterbur P.S., '^{13}C NMR-spectroscopy. 1. Aromatic hydrocarbons', *J. Amer. Chem. Soc.*, 1961, vol. **83**(8), pp. 1839 - 1852.
123. Jones A., Alger T., Grant D., and Litchman W.M., 'Carbon-13 magnetic resonance. 15. Nonalternaut hydrocarbons', *J. Amer. Chem. Soc.*, 1970, vol. **92**(8), pp. 2386 - 2395.
124. Adam H. and Grimison A., *Tetrahedron*, 1967, vol. **23**, pp. 2513 - 2518.
125. Duddeck H. and Kaiser M., *J. Org. Magnetic Res.*, 1982, vol. **20**(2), pp. 55 - 72.
126. Launterbur P., In: *Determination of Organic Structures by Physical Methods*, Ed. F.C. Nachod, N.Y.: Academic Press, 1962, vol. **2**, p. 7.
127. Borchardt J.K., 'Calculation of reactivity ratios and sequence distributions in copolymers from monomers ^{13}C-NMR data, *J. Macromol. Sci.*, 1985, vol. **A22**(12), pp. 1711 - 1737.
128. Spieskei H. and Schneider W., *J. Chem. Phys.*, 1961, vol. **35**, pp. 731 - 735.
129. Klein J., 'Directive effects in allylic and benzylic polymetalations - the question of u-stabilization, Y-aromaticity and cross-conjugation', *Tetrahedron*, 1983, vol. **39**(17), pp. 2733 - 2759.
130. Denisov E.T., Uspekhi Khimii, 1973, vol. **42**(3), pp. 361 – 390. (Rus)
131. Rafikov S.R., Laktionov V.M., and Zhuravleva I.V., 'The effect of sulfur-containing groups of the acid fragment on thermal stability of polyarylates', Vysokomol. Soed., 1977, vol. **B19**(10), pp. 795 - 798. (Rus)
132. Kovarskaya B.M. and Levantovskaya I.I., 'Assessment of polymer thermal stability', In Coll.: *Test, Control and Investigation Methods for Mechanical Engineering Materials*, Moscow, Mashinostroenie, 1973, vol. **3**, pp. 242 – 249. (Rus)

133. Murav'eva S.I., *Sanitary-Chemical Air Monitoring at Industrial Facilities*, Moscow, Meditsina, 1982, pp. 272 – 280. (Rus)
134. Kalinina L.S., Motorina M.A., Nikitina N.I., and Khachapuridze N.A., *Analysis of Condensed Polymers*, Moscow, Khimia, 1984, 296 p. (Rus)
135. Antonovsky V.L. and Buslaeva M.M., *Analytical Chemistry of Organic Peroxide Compounds*, Moscow, Khimia, 1978, pp. 23 - 25. (Rus)
136. *The Library of IR-spectra for Perkin-Elmer Device* (USA), N.Y., 1981.
137. Laius L.A. 'The study of PI-film structures by IR-spectroscopy method', Vysokomol. Soed., 1974, vol. **A16**(9), pp. 2101 - 2107. (Rus)
138. Nakanisi K., *IR-Spectra and Structure of Organic Compounds*, Moscow, Mir, 1965, 215 p. (Rus)
139. Blumenfeld A.B., Goglev R.S., Kovarskaya B.M., and Heiman M.B., 'About strength of chemical bonds in polyethers', *Vysokomol. Soed.*, 1972, vol. **A14**(10), pp. 2215 – 2220. (Rus)
140. Bulgarovskaya I.V., Smelyanskaya E.M., Fedorov Yu.G., and Zvonkova Z.V., 'Crystalline structure of 1:1 pyromellitic N,N-dimethyldiimide – anthracene complex', *Kristallografia*, 1977, vol. **22**(1), pp. 184 - 187. (Rus)
141. Mortimer C., *Reaction Heats and Bond Strengths*, Moscow, Mir, 1964, 287 p. (Rus)
142. Annenkova N.G., Kovarskaya B.M., Gur'yanova V.V., Pshenitsyna V.P., and Molotkova N.N., 'High-temperature oxidation of polyimide', *Vysokomol. Soed.*, 1975, vol. **A17**(1), pp. 134 - 138. (Rus)
143. Encyclopedia of Polymers, vol. **3**, Moscow, Sovetskaya Encyclopedia, 1977. (Rus)
144. Sklyarova A.G., Branzali F., and Wasserman A.M., 'Comparison of C-H-bond reactivity in polyethylene and low-molecular hydrocarbons', *Vysokomol. Soed.*, vol. **B16**(1), 1972, pp. 72 - 78. (Rus)
145. Tager A.A., *Physical Chemistry of Polymers*, Moscow, Gosizdat, 1963, 528 p. (Rus)
146. Shlensky O.F., Vainstein E.F., and Matyukhin A.A., 'Dynamic thermal decomposition of linear polymers and its study by thermoanalytical methods', *J. Thermal Anal.*, 1988, vol. **34**(3), pp. 645 - 655.
147. Edemskaya V.V., 'The study of high-temperature oxidation of polyethylene and polypropylene', *Candidate Dissertation Thesis*, Moscow, 1973. (Rus)
148. Serenkova I.A., Kulagin V.N., Tseitlin G.M., Shlyapnikov Yu.A., and Korshak V.V., 'Kinetics and mechanism of polybenzoxazole thermal oxidation', *Vysokomol. Soed.*, 1974, vol. **B16**(7), pp. 493 - 496. (Rus)

149. Kovarskaya B.M., Annenkova N.G., Gur'yanova V.V., and Blumenfeld A.B., 'On the mechanism of polyimide oxidation', *Vysokomol. Soed.*, 1973, vol. **A15**(11), pp. 2458 - 2464. (Rus)
150. Do C.H., Pearce E.M., Bulkin B.J., and Reinschulssel H.K., 'FI-IR-Spectroscopic study on the thermal and thermal oxidative degradation of Nylons', *J. Polym. Sci.: Polym. Chem. Ed.*, 1987, vol. **A25**(9), pp. 2409 - 2424.
151. Goldenberg A.L., 'The study of structural changes in polyethylene during oxidation using infrared absorption spectra', In Coll.: *Application of Spectroscopy Methods in Food Industry and Agriculture*, Leningrad, Leningrad University, 1957, pp. 79 - 86. (Rus)
152. Chien J.C.W. and Wang D.S.T., 'The thermal and thermal oxidative of polyolefines', *Macromolecules*, 1976, vol. **8**, pp. 920 - 929.
153. Blyumenfeld A.B., Vdovina A.L., Pleshkova A.P., and Annenkova N.G., 'About polypyromellitimide and polyphenylquinoxaline thermal oxidation products', *Vysokomol. Soed.*, 1986, vol. **B28**(7), pp. 500 - 503. (Rus)
154. Bolland J.L. and Ten Have P., Molecular Complex-O_2 with oxidative *ot* polyolefins, *Trans. Faraday Soc.*, 1947, vol. **43**, pp. 201 - 205.
155. Smirnov L.A., 'Increasing heat and light resistance of caproic fiber with the help of polymer stabilization by metal-containing organic compounds', *Candidate Dissertation Thesis*, Moscow, 1969. (Rus)
156. Voevodsky V.V. and Nalbandyan A.B., *Hydrogen Oxidation and Combustion Mechanism*, Moscow-Leningrad, AN SSSR, 1949, Chap. 3. (Rus)
157. Yakimansky A.V., Milevskaya I.S., Zubkov V.A., and El'yashevich A.M., 'Quantum-chemical analysis of crosslinked system and volatile product formation at thermolysis of polyimides', *Vysokomol. Soed.*, 1989, vol. **A32**(11), pp. 2318 – 2326. (Rus)
158. Kosobutsky V.A., 'Electron composition and some physical and chemical properties of aromatic polyamides and polyheteroarylenes', *Candidate Dissertation Thesis*, Rostov-na-Donu, 1973. (Rus)
159. Batsanov S.S., *Electronegativity of Elements and Chemical Bonding*, Novosibirsk, Izd. Sib. AN SSSR, 1962, 195 p. (Rus)
160. Garnovsky A.D., Sandimenko A.P., Osipov O.A., and Tsinisadze G.V., *Soft-Strong Interactions in Coordination Chemistry*, Rostov-na-Donu, Izd. Rostov University, 1986, 257 p. (Rus)
161. Volozhin A.I., Prokopchuk N.R., Yakimtsova A.B., Krut'ko E.T., and Solntsev A.P., 'Thermal stability of poly(4,4'-

diphenyloxide)pyromellitimide of bicycle-(2,2',1)-hept-5-ene-2,3-dicarboxylic acid', *Vestsi AN BSSR, Ser. Khim. Nauk*, 1988, No. 5, pp. 109 - 111. (Rus)

162. Bryik M.T. and Danilenko E.E., 'Complex formation in synthesis of metal-containing polyimides', *Ukr. Khim. Zhurnal*, 1988, vol. 54(4), pp. 355 - 358. (Rus)
163. Osawa L., The role of metals and metal-deactivators in polymer degradation, *Polym. Stab.*, 1988, vol. **20**(3-4), pp. 203 - 236.
164. Larin G.M., Umarov B.B., Minin V.V., Rakitin Yu.V., Yusupov V.G., Parshev N.A., and Buslaev Yu.A., 'Anti-ferromagnetic exchange by O-bond chain in binuclear copper(II) complexes', *Doklady AN SSSR*, 1988, vol. **303**(1), pp. 139 - 143. (Rus)
165. Korshak V.V., *Chemical Structure and Temperature Characteristics of Polymers*, Moscow, Nauka, 1970, 419 p. (Rus)
166. Kirpichnikov P.A, Mukmenyova N.A., and Cherkasova O.A., 'Efficiency and mechanism of stabilizing effect of organic phosphorous acids in polymers', *Intern. J. Polym. Mater.*, 1990, vol. **14**, pp. 41 - 52.
167. Van Krevelen D.V., *Properties and Chemical Structure of Polymers*, Moscow, Khimia, 1976, 415 p. (Rus)
168. Mukmeneva N.A., Akhmadulina A.G., Sabirova L.Kh., and Kirpichnikov P.A., 'Intensification of the stabilizing efficiency of phosphoric ethers by four-valent titanium compounds during low density polyethylene oxidation', *Vysokomol. Soed.*, 1976, vol. **B18**, pp. 108 - 115. (Rus)
169. Pobedimsky D.G., Grossman G., Kondratyeva T.N., Cherkasova O.A., Scheller D., Mukmeneva N.A., and Kirpichnikov P.A., In: *Proc. 4th International Symposium on Homogeneous Catalysis*, Leningrad, 1984. (Rus)
170. Chamberlain N.F., *The Practice of NMR Spectroscopy, with Spectra-Structure Correlation for Hydrogen – 1*, N.Y.: Plenum Press, 1974, 424 p.
171. Bazilevsky M.V. and Piskun N.I., 'The effect of substituents in radical hydrogen detachment in methyl group', *Zh. Fiz. Khim.*, 1965, vol. 39, pp. 762 - 770. (Rus)
172. Balyakov V.A., Shanina E.L., Roginsky V.A., and Miller V.B., 'O-H-Bond energies and inhibiting ability of spatially hindered phenols', *Izv. AN SSSR, Ser. Khim.*, 1975, No. 12, pp. 2685 - 2691. (Rus)
173. Militskova E.A., 'New modifications and application of poly(arylene ether sulfones)', In Coll.: *Chem. Ind., Ser. Production and Processing of*

Plastics and Synthetic Resins, Moscow, NNITEKhim, 1990, Iss. 2, pp. 45 - 52. (Rus)

174. Blyumenfeld A.B., 'The study of thermal and thermal oxidative degradation of some polyethers', *Candidate Dissertation Thesis*, Moscow, 1970. (Rus)
175. Narkon A.L., 'The study of admixture, end group and molecular-mass characteristic effects on thermal stability of polysulfone', *Candidate Dissertation Thesis*, Moscow, 1984. (Rus)
176. Vinogradov R.V. and Malkin A.Ya., Rheology of Polymers, Moscow, Khimia, 1977, 438 p. (Rus)
177. Edemskaya V.V., Miller V.B., and SHlyapnikov Yu.A., 'Kinetic regularities and mechanisms of high-temperature oxidation of polyethylene', *Doklady AN SSSR*, 1971, vol. **196**(5), pp. 1121 - 1124. (Rus)
178. Saito O., 'Thermal degradation of aromatic polyethers', J. *Phys. Soc. Jap.*, 1974, vol. **13**, pp. 198 - 208.
179. Dashevskaya S.S., 'Polysulfone oxidation', *Candidate Dissertation Thesis*, Moscow, MkhTI, 1974. (Rus)
180. Serenkova I.A. and SHlyapnikov Yu.A., 'Kinetics of poly(dimethyl phenylene oxide) thermal oxidation', *Vysokomol. Soed.*, 1982, vol. **A24**(4), pp. 808 - 813. (Rus)
181. Ioffe I.I., 'About the mechanism of incomplete benzene oxidation', *Zh. Fiz. Khim.*, 1954, vol. **28**(2), pp. 1555 – 1561. (Rus)
182. Evans D.F., 'Molecular complex with oxygen', *J. Chem. Soc.*, 1953, pp. 345 - 352.
183. Tsubomura H. and Milliken R.S., 'Molecular complexes and theirspectra. 12. Ultraviolet absorbtions spectra caused by interaction of oxygen', *J. Amer. Chem. Soc.*, 1960, vol. **82**(23), pp. 5906 - 5974.
184. Alexandrov J., Figurova G.N., and Razuvaev G., 'The formation of a reversible complex between diethyl cadmium and oxygen', *J. Organomet. Chem.*, 1973, vol. **57**(1), pp. 71 - 75.
185. Belyakov V.K., Belyakova I.V., Kosobutsky V.A., Savinov V.M., Medved' S.S., Erin A.F., and Sokolov L.B., 'On heat resistance of polyheteroarylenes', *Vysokomol. Soed.*, 1971, vol. **A13**(8), pp. 1739 - 1747. (Rus)
186. Pokhodenko V.D., *Phenoxyl Radicals*, Kiev, Naukova Dumka, 1969, 190 p. (Rus)
187. Matsuoka S., *Failure of Plastics*, Ed. Broetow, N.Y.: SPE and Hausor, 1986, Ch. 3.

188. *Patent No. 976680 (USSR)*, 'Polysulfone-derived composite', Publ. Jul. 21, 1980. (Rus)
189. *US Patent No. 379,615*, 'Polysulfones stabilized by phosphoric compounds', Publ. Feb. 22, 1972.
190. *UK Patent No. 1,365,503*, 'Aromatic polymers', Publ. Sept. 04, 1974.
191. Voigt I., *Polymer Stabilization Against Light and Heat Impacts*, Leningrad, Khimia, 1972, 544 p. (Rus)
192. Gamino G., Martinasso G., and Costa L., 'Thermal degradation of pentaeritritol diphosphat model compound for fire retardant intumescent systems. 1. Overall thermal degradation, *Polym. Degrad. Stab.*, 1990, vol. **27**(2), pp. 285 - 269.
193. Suebsaeng T., Wilkie C.A., Burger V.T., Carter J., and Brown C.E., 'Solid products from thermal decomposition of polyethylenterephtalate of investigation by CP/Mass, ^{13}C-NMR and Fourier transform IR-spectroscopy', *Eur. Polym. J.*, 1981, vol. **17**(2), pp. 1259 - 1263.
194. Becher C.H., Troer K., and Croleva A., 'Thermal properties P-contents PETF', *Eur. Polym. J.*, 1981, vol. **17**(2), pp. 1259 - 1263.
195. Troer K., Grozeva A., and Borisov G., 'Introduction of phosphorus into the PET-molecule via 1,2-dicarbomethoxyethyl phosphate', *J. Appl. Polym. Sci.*, 1981, vol. **17**(1), pp. 27 - 33.
196. Wilkie C., Pettegrew J., and Brown C., 'Pyrolysis reactions of poly(methyl methacrylate) and red phosphorus: an investigation with cross-polarization, magic angle NMR-spectroscopy' *J. Polym. Sci.: Polym. Lett. Ed.*, 1981, vol. **19**, pp. 409 - 414.
197. Day M. and Wiles D., 'Temperature influence on thermal degradation of fiber PETF, one fire retardant tris(2,3-dibromopropyl)-phosphate', *J. Anal. and Appl. Pyrol.*, 1984, No. 7, pp. 65 - 82.
198. Inagaku N., Sakurai S., and Katsuura K., 'Affect tris(2,3-bromo-propyl) phosphate with flame retardant of polystyrene', *J. Appl. Polym. Sci.*, 1979, vol. **23**, pp. 2023 - 2030.
199. Brown C., Wilkie C., Smukalla J., and Cody B., 'Inhibition by red phosphorus of unimolecular thermal chain scission in poly(methyl methacrylate): investigation by NMR, FT-IR and laser decomposition/ Fourier transform mass spectroscopy, *J. Polym. Sci.: Polym. Chem. Ed.*, 1986, vol. **24**, pp. 1297 - 1311.
200. Day M. and Willes D., 'Combustion and pyrolysis of poly(ethylene terephthalate). 1. The role of flame retardants in products pyrolysis', *J. Appl. Polym. Sci.*, 1981, vol. **26**, pp. 3085 - 3091.

201. Arbuzov B.V., Polezhaeva N.A., Vinogradova V.S., Polozova G.I., and Musina A.A., 'Structure and properties of interaction products of benzylidene benzoyl acetate with trimethylphosphite and dimethylphosphoric acid, *Izv. AN SSSR, Ser. Khim.*, 1974, No. 9, pp. 2071 – 2075. (Rus)
202. Pobedimsky D.G., Mukmeneva N.A., and Kirpichnikov P.A., In: *Developments in Polymer Stabilization*, Ed. Scott G., London.: Appl. Sci. Publ., 1980, vol. **2**, 125 p.
203. Mukmeneva N.A., Minsker K.S., Kolesov S.V., and Kirpichnikov P.A., *Doklady AN SSSR*, 1984, vol. **274**(6), pp. 1393 – 1396. (Rus)
204. Kirpichnikov P.A., Mukmeneva N.A., and Pobedimsky D.G., 'Phosphorus-organic stabilizers of polymers – efficiency and mechanism', *Uspekhi Khimii*, 1983, vol. **52**(11), pp. 1831 – 1851. (Rus)
205. Mukmeneva N.A., Gol'denberg A.L., and Lazareva N.P., 'Interaction between phosphoric acid ethers and carboxylic groups in polyethylene', *Vysokomol. Soed.*, 1983, vol. **A25**(6),pp. 1302 – 1306. (Rus)
206. Pobedimsky D.G., Kirpichnikov P.A., and Denisov E.T., 'About reactions of phosphorus-organic inhibitors with hydroperoxide groups and polyethylene peroxide radicals', *Vysokomol. Soed.*, 1976, vol. **A18**, pp. 2650 - 2658. (Rus)
207. Hudson R., *Structure and Mechanism of Reactions with Phosphorus-Organic Compounds*, Moscow, Mir, 1967, 361 p. (Rus)
208. Kibrey A. and Warren S., *Organic Chemistry of Phosphorus*, Moscow, Mir, 1967, Ch. 4. (Rus)
209. Bentrude W.G., In: *Free Radicals*, Ed. Kochi J., N.Y.: Wiley, 1973, p. 22.
210. Ingold K. and Roberts B., Free-radical Substitution Reactions, Moscow, Mir, 1974, pp. 133 - 149. (Rus)
211. Mukmeneva N.A., Sharifulin A.Sh., Eliseeva L.A., and Iskhakov O.A., 'Phosphorus-organic inhibitors of polymeric material combustion', *Proc. 6th All-Union Conf. Combustion of Polymeric Materials*, Suzdal', Nov. 29 – Dec. 01, 1988, *Rep. Thes.*, Moscow, 1988, pp. 156 - 157. (Rus)
212. Ruger C., Konig T., and Schwetlick. K., 'Phosphororganische Antioxidatien. 6. Einflus Cyclischer Phosphite auf die Radikalisch initierte Oxidation von Kolenwasserstoffen und Polymeren', *Acta Polymerica*,1986.-Bd. **37**(7), S. 435 - 438.

213. Schwetlick K., Konig T., Ruger C., Pionteck J., and Habicher W.D., 'Chain-breaking antioxidant activity of phosphite ester', *Polym. Degrad. Stability*, 1986, vol. **15**, p. 97 - 108.
214. Schwetlick K., Konig T., Pionteck J., Sasse D., and Habicher W.D., 'Organophosphorus antioxidants. 9. Inhibition of the oxidation of hydrocarbons by hindered aryl phosphites', *Polym. Degrad. Stability*, 1988, vol. **22**(4), pp. 357 - 373.
215. Lebedeva L.P. and Levin P.I., 'Antioxidant efficiency of phosphites and their mixtures', *Vysokomol. Soed.*, 1982, vol. **B24**(5), pp. 379 – 383. (Rus)
216. Mukmeneva N.A., 'Phosphorylation as the way of increasing stability of polymers', *Proc. 8th All-Union School-Seminar on Organoelement Compounds*, Moscow, INEOS AN SSSR, 1984, 22 p. (Rus)
217. Gorestein D., Phosphorus-31 NMR- Principles and Applications, N.Y.: Academic Press, 1984, 14 p.
218. Spivack J., Pastor S., and Patrl A., *Polym. St. J.*, 1984, pp. 247 - 257.
219. Sigeru Oae, *Chemistry of Sulfur Organic Compounds*, Moscow, Khimia, 1975, Ch. 6. (Rus)
220. Gur'yanova E.N., Gol'dstein I.P., and Romm I.P., *The Donor-Acceptor Bond*, Moscow, Khimia, 1973, 338 p. (Rus)
221. Mazalov L.N. and Dyumatov V.D., *Electronic Structure of Extragents*, Novosibirsk, Nauka, 1984, 196 p. (Rus)
222. *Patent No. 45-29392 (Japan)*, 'PSF composition', Publ. Aug. 25, 1970.
223. Korshak V.V., *Different Unit Composition of Polymers*, Moscow, Nauka, 1977, 301 p. (Rus)
224. Sharkey W.H. and Mocher W.E., 'Mechanism of the Photooxidation of Amides', *J. Amer. Chem. Soc.*, 1959, vol. **81**, pp. 3000 - 3011.
225. Paul D.R. and Newman S., *Polymer Blends*, vol. **1**, N.Y., Academic Press, 1997, 452 p.
226. Kalugina E.V., 'Thermal transformations and stabilization of some heat-resistant heterochain polymers', *Candidate Dissertation Thesis*, Moscow, 1992.
227. Kalugina E.V., Novotortseva T.N., Andreeva M.B., Blyumenfeld A.B., Urman Ya.G., and Gur'yanova V.V., 'Thermal transformations and stabilization of aliphatic-aromatic polyamide', *Plastmassy*, 2001, No. 2, pp. 11 - 16. (Rus)
228. Korshak V.V., *Different Unit Composition of Polymers*, Moscow, Nauka, 1977, 302 p. (Rus)

229. Atlas of ESR Spectra – Spin Labels and Probes, Ed. A.L. Buchachenko, Moscow, Nauka, 1977, 159 p. (Rus)
230. Pravednikov A.N., 'Thermal degradation of polymers with rings in the cycle', *A Report at the 5th Polymeric School Devoted to Methods of Synthesis and Study of Heat-Resistant Polymers*, Gomel', 1972, 12 p. (Rus)
231. Annenkova N.G., Kovarskaya B.N., and Gur'yanova V.V., 'High-temperature oxidation of polyimides', *Vysokomol. Soed.*, 1975, vol. **A17**(1), pp. 134 - 142. (Rus)
232. Gaudiana R.A. and Conley R.T., 'Weak-link versus active carbon degradation of aromatic heterocyclic systems', *J. Polym. Sci.*, 1969, vol. 7(11), pp. 793 – 801.
233. Gaudiana R.A. and Conley R.T., 'Weak-link versus active carbon degradation of aromatic heterocyclic systems', *J. Macromol. Sci.*, 1970, vol. **4**(2), pp. 441 – 480.
234. Buchachenko A.L., Galimov E.M., Ershov V.V., Nikiforov G.A., and Pershin A.D., 'Isotope enrichment, induced by magnetic interactionsin chemical reactions', *Doklady AN SSSR*, 1976, vol. **228**(2), pp. 379 – 381. (Rus)
235. Buchachenko A.L., Yasina L.L., Makhov S.V., and Galimov E.M., 'Magnetic isotope effect and ^{17}O enrichment at polypropylene oxidation', *Doklady AN SSSR*, 1981, vol. **260**(5), pp. 1143 – 1145. (Rus)
236. Belikov V.K., Belyakova I.V., Kozlova M.V., Okunev P.A., and Tarakanov O.G., 'The effect of chemical structure of polyheteroarylenes on resistance to thermal oxidation', *Vysokomol. Soed.*, 1973, vol. **A15**(12), pp. 2635 – 2642. (Rus)
237. Bazilevsky M.B., *The Method of Molecular Orbitals and Reactivity of Organic Molecules*, Moscow, Khimia, 1969, 303 p. (Rus)
238. Straightwiser E., *The Theory of Molecular Orbitals*, Moscow, Mir, 1965, 435 p. (Rus)
239. Waters W., Oxidation Mechanism of Organic Compounds, Moscow, Mir, 1966, 175 p. (Rus)
240. Parr R.G., *Quantum Theory of Molecular Electronic Structure A. Lecture – note and reprint volume*, N.Y., W.A. Benjamin Inc. Publ., 1964, p. 510.
241. White E.N. and Harding M.J.C., 'Chemiluminescence in liquid sols. – Chemiluminescence of laphine and its derives', *J. Am. Chem. Soc.*, 1964, vol. **86**, pp. 5686 – 5698.

242. Kurtz D.W. and Shetcher H., 'Photooxidation of tryphenyl oxazole', *J. Chem. Soc. Ser. D. Chem. Commun.*, 1966, No. 7, pp. 689 – 698.
243. Matsuuta T. and Saito J., 'Photosensitized oxidation of hydroxylated purines', *Tetrahedron Letters*, 1968, vol. **29**, pp. 3273 – 3281.
244. Kuthan J., Danihel J., and Skala V., 'Quantum chemical study of dissociation of *meta*- and *para*-substituted benzoic acids in π-electron approximation', *Collect Czechosl. Chem. Commun.*, 1978, vol. **43**(2), pp. 447 – 462.
245. Slonim I.Ya. and Urman Ya.G., *NMR-Spectroscopy of Heterochain Polymers*, Moscow, Khimia, 1982, 232 p. (Rus)
246. Johnson L.F., *Carbon-13 NMR Spectra*, N.Y., Wiley, 1972.
247. Breitmaier E., Haas G., and Voelter W., *Atlas of Carbon-13 NMR Data*, Heyden, London, 1979.
248. Formacek V., Desnoyer L., Kellerhals H.P., Keller T., Clerc J.T., *^{13}C Data Bank*, Bruker Physik, Karlsruhe, 1976.
249. Hummel/Scholl, Atlas of Polymer and Plastics Analysis.
250. Dekhant I., Danu V., Cimmer V., and Schmolke R., *Infrared Spectroscopy of Polymers*, Moscow, Khimia, 1976. (Rus)
251. *Liquid-Crystal Polymers*, Ed. N.A. Plate, Moscow, Khimia, 1988. (Rus)
252. Kalugina E.V., NovoTortseva T.N., and Andreeva M.B., 'Thermal Oxidation Features of Heat-Resistant Heterochain Polymers', *Obzor Polim. Mater.*, 2001, No. 6, pp. 29 - 37. (Rus)
253. Sing K., and Dreg S., *Absorption, Surface, Porosimetry*, Moscow, 1984.
254. Andreeva M.B., 'Thermal transformations and stabilization of aliphatic-aromatic polyamides and derived mixtures', *Candidate Dissertation Thesis*, Moscow, 2002. (Rus)
255. Fedotova O.Ya, Kerber M.L., and Losev I.P., 'On some properties of aromatic, arylaliphatic polyamides, obtained by polycondensation at the interface', *Vysokomol. Soed.*, 1960, vol. **A**(2), p 1020. (Rus)
256. Mark H., Atlas S.M., and Ogata N., *J. Polym. Sci.*, 1962, vol. **61**, p. 849.
257. Patent No. 637,257 (Belgium), 1964.
258. Patent No. 637,258 (Belgium), 1964.
259. Preston J. and Dobinson F., 'New high-temperature aromatic polyamides', *J. Polym. Sci.*, 1964, vol. **B2**, p. 1171.
260. Weiss L.O. and Morgan H.S., 'Thermal behavior of aromatic polyamides', *J. Polym. Sci.*, 1967, vol. **4**, p. 19 – 26.
261. Krasnov E.P., Savinov V.M., Sokolov L.B., Logunova V.I., Belyakov V.K., and Polyakova T.A., 'Thermal degradation of isomeric aromatic polyamides', *Vysokomol. Soed.*, 1966, vol. **A**(8), p. 380. (Rus)

262. Kuznetsov G.A., Gerasimov V.D., Fomenko L.N., Maklakov A.M., Pimenov G.G., and Sokolov L.B., 'The study of poly(methaphenylene isophthalamide) transition origin', *Vysokomol. Soed.*, 1965, vol. **A**(7), p. 1592. (Rus)
263. Krasnov E.P., Aksenov V.P., and Kharkov S.N., 'Thermal degradation of polyamides of various structure', *Vysokomol. Soed.*, 1969, vol. **A**(11), p. 1930. (Rus)
264. Kolesnikov G.S., 'The study of aryl-aliphatic polyamide degradation processes', *Vysokomol. Soed.*, 1970, vol. **12**(1), pp. 177 - 181. (Rus)
265. Kalugina E.V., 'Thermal transformations and stabilization of some heat-resistant heterochain polymers', *Doctoral Dissertation Thesis*, Moscow, 2003. (Rus)
266. Eareckson W., *J. Polym. Sci.*, 1959, vol. **40**, pp. 343 – 358.
267. Rafikov S.R., V.P. Budtov, and Yu.B. Monakov, *Introduction to Physical Chemistry of Polymer Solutions*, Moscow, Nauka, 1978, 328 p. (Rus)
268. Kalugina E.V., Blyumenfeld A.B., Annenkova N.G., Gvozdev D.V., Savina M.E., and Pinaeva N.K., 'Thermal oxidative stability of polyalkanimide', *Polim. Mater.*, 1988, No. 7, p. 26. (Rus)
269. Gur'yanova V.V., Ershov O.V., Mednikova G.S., Sharyigina I.A., Kalugina E.V., Reiburd L.I., and Kozhina V.A., 'The relationship between molecular-mass characteristics and rheological properties of polysulfone-derived mixtures', *Polim. Mater.*, 1990, No. 6, p. 82. (Rus)
270. Kalugina E.B., Blyumenfeld A.B., Annenkova N.G., Arshava B.M., Kotov Yu.I., Savina M.E., and Pleshkova A.P., 'Thermal stability and heat transformations of polyalkanimide', *Polim. Mater.*, 1991, No. 7, pp. 48 - 51. (Rus)
271. Kalugina E.V., Blyumenfeld A.B., Annenkova N.G., Volkov M.A., and Savina M.E., 'Stabilization of aliphatic-aromatic poluimide', *Polim. Mater.*, 1993, No. 1, pp. 30 - 32. (Rus)
272. Blyumenfeld A.B., Kalugina E.V., Annenkova N.G., Volkov M.A., and Savina M.E., 'Heat effects in aliphatic-aromatic poluimide', *Polim. Mater.*, 1993, No. 1, pp. 24 - 27. (Rus)
273. Blyumenfeld A.B., Kalugina E.V., Bolotina L.M., and Savina M.E., 'The problem of thermal stability of high-temperature engineering thermoplasts', *Polim. Mater.*, 1993, No. 2, pp. 21 - 24. (Rus)
274. Kalugina E.V., Blyumenfeld A.B., Annenkova N.G., Volkov M.A., Savina M.E., Rafieva S.R., Markova E.I., and Janibekov N.F.,

'Increasing polyalkanimide thermal stability by specific admixtures', *Polim. Mater.*, 1993, No. 3, pp. 30 - 32. (Rus)

275. Kalugina E.V., Blyumenfeld A.B., Savina M.E., and Novotortsev V.M., 'Thermal stabilization of aliphatic-aromatic polyimide in the processing and during long-term heat aging', *Polim. Mater.*, 1996, No. 1. (Rus)
276. Narkon A.L., Kalugina E.V., Volkov M.A., and Astakhov P.A., 'New super-engineering plastics derived from heat-resistant liquid-crystal polyesters', *Plastmassy*, 1996, No. 3, pp. 4 – 6. (Rus)
277. Andreeva M.B., Novotortseva T.N., Kalugina E.V., Tochin V.A., Gurinovich L.N., Andreeva T.I., and Kalinina I.G., 'The improvement of compatibility in glass reinforced PA6/PP composites', *Polim. Mater.*, 1998, No. 2, pp. 18 - 22. (Rus)
278. Blumenfeld A.B., Kalugina E.V., Zaikov G.E., 'Structure. Impurities. Thermal stability and thermal stabilization of the engineering thermostable resins polyimide and polysulfone types', *Intern. J. Polym. Mater.*, 1999, vol. **44**, pp. 95 – 105.
279. Andreeva M.B., Novotortzeva T.N., Kalugina E.V., Tochin V.A., Gurinovich L.N., Andreeva T.I., Kalinina I.G., Gumargalieva K.Z., and Zaikov G.E., 'The improvement of compatibility in glass reinforced PA6/PP blends', *Polymer & Polymer Composites*, 1999, vol. 7(7), pp. 491 – 499.
280. Andreeva M.B., Novotortzeva T.N., Kalugina E.V., Tochin V.A., Gurinovich L.N., Andreeva T.I., Kalinina I.G., Gumargalieva K.Z., and Zaikov G.E., 'The improvement of compatibility in glass reinforced PA6/PP blends', *Intern. J. Polym. Mater.*, 2000, vol. **46**,pp. 641 – 654.
281. Novotortzeva T.N., Kulachinskaja O.B., Andreeva M.B., Kalugina E.V., Aizinson I.L., Lunin A.S., Tochin V.A., Urman Ja.G., Kalinina I.G., Gumargalieva K.Z., and Zaikov G.E., 'The aging of modified glass-reinforced polypropylene in air and antifreeze', *J. Appl. Polym. Sci.*, 2000, vol. **76**, pp. 807 – 813.
282. Novotortzeva T.N., Kulachinskaja O.B., Andreeva M.B., Kalugina E.V., Aizinson I.L., Lunin A.S., Tochin V.A., Urman Ja.G., Kalinina I.G., Gumargalieva K.Z., and Zaikov G.E., 'The aging of modified glass-reinforced polypropylene in air and antifreeze', *Polym. Degrad. Stab.*, vol. **69**, pp. 17 - 22.
283. Novotortzeva T.N., Kulachinskaja O.B., Andreeva M.B., Kalugina E.V., Aizinson I.L., Lunin A.S., Tochin V.A., Urman Ja.G., Kalinina I.G., Gumargalieva K.Z., and Zaikov G.E., 'The aging of modified glass-

reinforced polypropylene in air and antifreeze', *Intern. J. Polym. Mater.*, 2000, vol. **46**, pp. 617 – 627.

284. Blumenfeld A.B., Kalugina E.V., and Zaikov G.E., 'Structure, impurities, thermal stability and thermal stabilization of the engineering thermostable resins of polyimide and polysulfone types', In: *Polymer Yearbook*, Ed. R.A. Pethrick, vol. **17**, Harwood Academic Publishers, 2000, pp. 275 – 285.
285. Smirnova N.M., Novikova D.K., Kalugina E.V., and Dreval' V.E., 'Modification of polyamides and polypropylene by "PEBAK S" thermoplasts', *Polim. Mater.*, 2000, No. 8, pp. 34 – 41. (Rus)
286. Blyumenfeld A.B., Kalugina E.V., and Zaikov G.E., 'Structure, impurities, thermal stability and thermal stabilization of the engineering thermostable resins polyimide and polysulfone types', In: *Polymer Yearbook*, Ed. R.A. Pethrick, Harwood Academic Publishers, vol. **17**, 2000, pp. 275 – 283.
287. Kalugina E.V., Novotortseva T.N., Andreeva M.B., Blyumenfeld A.B., Urman Ya.G., and Gur'yanov V.V., 'Thermal transformations and stabilization of aliphatic-aromatic polyamide', Polim. Mater., 2001, No. 2, pp. 11 – 16. (Rus)
288. Kalugina E.V., Novotortseva T.N., and Andreeva M.B., 'The features of thermal oxidation of heat-resistant heterochain polymers', *Polim. Mater.*, 2001, No. 6, pp. 29 – 31. (Rus)
289. Kalugina E.V., Novotortseva T.N., Andreeva M.B., Saratovskaya N.V., Blyumenfeld A.B., and Urman Ya.G., 'Degradation and stabilization of liquid-crystal polymers', *Polim. Mater.*, 2001, No. 6, pp. 41 – 45. (Rus)
290. Kalugina E.V., Novotortseva T.N., Andreeva M.B., Saratovskaya N.V., Blyumenfeld A.B., and Narkon A.L., 'Liquid-crystal copolyesters as modifiers for thermoplasts', Polim. Mater., 2001, No. 6, pp. 38 - 41. (Rus)
291. Samoryadov A.V., Kalinina I.G., Andreeva M.B., Tochin V.A., and Kalugina E.V., 'The study of porous structure of polyamide 6 glass-reinforced composites', Polim. Mater., 2001, No. 6, pp. 21 – 24. (Rus)
292. Kalugina E.V., Novotortzeva T.N., Gumargalieva K.Z., and Zaikov G.E., 'Specific features of thermooxidation of thermoresistant heterochain polymers', *Oxidation Communication*, 2002, vol. **25**(2), pp. 214 – 231.
293. Kalugina E.V., Novotorzeva T.N., Andreeva M.B. *et al.*, 'Liquid crystalline copolymers as modifiers for some thermoplastics', In: *Aging of Polymers, Polymer Blends and Polymer Composites*, Eds. G.E.

Zaikov, A.L. Buchachenko, V.B. Ivanov, vol. **1**, Nova Science Publishers, NY, 2002, pp. 192 – 199.

294. Kalugina E.V., Novotorzeva T.N., Andreeva M.B. et al., 'Thermal behavior and stabilization of aryl-aliphatic polyamide', In: *Aging of Polymers, Polymer Blends and Polymer Composites*, Eds. G.E. Zaikov, A.L. Buchachenko, V.B. Ivanov, vol. **1**, Nova Science Publishers, NY, 2002, pp. 175 – 190.
295. Kalugina E.V., Gvozdev D.V., Vakhtinskaya, Andreeva T.I., and Tochin V.A., 'Thermal stabilization of poly(butylene terephthalate', *Polim. Mater.*, 2003, No. 10. (Rus)
296. Kalugina E.V., Novotortzeva T.N., Gumargalieva K.Z., and Zaikov G.E., 'Specific features of thermooxidation of thermoresistant heterochain polymers', In: *Reaction in Condensed Phases: Kinetics and Thermodynamics*, Eds. G.E. Zaikov and V.M.M. Lobo, Nova Science Publishers, NY, 2003, pp. 101 - 121.
297. Kalugina E.V., Novotortzeva T.N., Gumargalieva K.Z., and Zaikov G.E., 'Specific features of thermooxidation of thermoresistant heterochain polymers', (Chapter 7), In: *Polymer Yearbook*, Ed. R.A. Pethrick, Harwood Academic Publishers, vol. 20, 2003. (in press)
298. *Patent No. 1,550,913 (USSR)*, 'The method for extracting polysulfone', Appl. Jul. 04, 1988 (No. 4454478/05). (Rus)
299. *Application No. 3190367/05 (USSR)*, Jan. 28, 1988. (Rus)
300. *Patent No. 2,028,337 (Russian Federation)*, 'Polymeric composite', Publ. Jun. 24, 1992. (Rus)
301. *Patent No. 2,069,670 (Russian Federation)*, 'The method for obtaining fatty-aromatic polyimide', Publ. Feb. 24, 1993. (Rus)
302. *Patent No. 2,115,672 (Russian Federation)*, 'Polymeric thermoplast', Publ. Jun. 20, 1998. (Rus)
303. *Patent No. 2,174,526 (Russian Federation)*, 'A polymeric composite material', Publ. Oct. 10, 2001. (Rus)
304. *Patent No. 2,144,050 (Russian Federation)*, 'A polymeric composite material', Publ. Jan. 10, 2000. (Rus)
305. Blyumenfeld A.B., Vdovina A.L., Voloshchuk K.A., Zabel'nikov N.S., and Tseitlin G.M., 'Thermal aging of heat-resistant polymer polyphenylquinoxaline', *XV Colloquium of Danube Countries on Problems of Natural and Artificial Aging of Polymers*, Sept. 27 – 30, 1982, Moscow, p. 4142. (Rus)

306. Vdovina A.L., Blyumenfeld A.B., Zabel'nikov N.S., and Annenkova N.G., 'On thermal stability of phenylquinoxaline copolymers', *VMS*, 1984, vol. *B XXVI*(3), pp. 223 - 227. (Rus)
307. Vdovina A.L., Blyumenfeld A.B., Annenkova N.G. *et al.*, 'The laws of thermal oxidative transformations of polypyromellitimide and polyphenylquinoxaline', *Proc. XXII All-Union Conference on High-Molecular Compounds*, Oct. 15 – 19, 1985, Alma-Ata. (Rus)
308. Vdovina A.L., Ryaboi V.M., and Blyumenfeld A.B., 'Quantum-chemical criterion of thermal oxidative stability of polyheteroarylenes', *VMS*, 1985, vol. **B27**(11), pp. 808 - 811. (Rus)
309. Blyumenfeld A.B., Vdovina A.L., Pleshkova A.P., and Annenkova N.G., 'About thermal oxidation products of polypyromellitimide and polyphenylquinoxaline', *VMS*, vol. **B28**(7), pp. 500 - 503. (Rus)
310. Tseitling G.M., Voloshchuk K.A., and Blyumenfeld A.B., 'Thermal degradation of polyphenylquinoxaline', *VMS*, 1989, vol. **A31**(2), pp. 295 - 297. (Rus)
311. Blumenfeld A.B., Vdovina A.L., and Annenkova N.G., 'Thermal behavior and heat stabilization of polyimide and related polymers', In: *Polyimides and Other High-Temperature Polymers*, Eds. M.J.M. Abadie and B.Sillon, Elsevier, 1991, pp. 183 - 189.
312. Buchachenko A.L., Yasina L.L., Vdovina A.L., and Blyumenfeld A.B., 'New nuclear-spin selective reaction of molecular oxygen', *Izv. AN, Ser. Khim.*, 1994, No. 8, pp. 1402 - 1404. (Rus)